The interaction of focal adhesion kinase with apoptotic regulators underpins anoikis resistance in human oesophageal carcinoma

Stephanie Fanucchi

A thesis submitted to the Faculty of Science, University of the Witwatersrand, in fulfillment of the requirements for the degree of Doctor of Philosophy
Johannesburg, 2011

Declaration

I declare that this thesis is my own, unaided work. It is being submitted for the Degree of Doctor of Philosophy at the University of the Witwatersrand, Johannesburg. It has not been submitted before for any degree or examination in any other University.

_____

Stephanie Fanucchi

_____day of _____ 2011

"Nobody trips over mountains. It is the small pebble that causes you to stumble. Pass all the pebbles in your path and you will find you have crossed the mountain."

~Author Unknown

Abstract

Aberrant communication between survival signalling- and cell death pathways enables tumour cells to resist anoikis - the subset of apoptosis triggered by loss of cell-extracellular matrix (ECM) contact. Focal adhesion kinase (FAK) has been implicated as the key intermediate in the acquisition of anoikis resistance, as constitutively active FAK rescues epithelial cells from anoikis. Pertinent to anoikis-related regulation, enhanced FAK-dependent signalling has been demonstrated to repress p53- and Fas-mediated apoptosis. Elevated expression of FAK correlates with increased metastasis of human oesophageal squamous cell carcinoma (HOSCC). Furthermore, downregulation of Fas as well as a loss of p53 tumour suppressor function are early events in HOSCC progression. In this study, staurosporine (STS) was used to experimentally induce apoptosis in HOSCC cell lines harbouring either wild type (wt) or mutant (mt) p53-R175H. Dephosphorylation of FAK accompanied STS-mediated FAK cleavage and caspase-3 activation in the wt p53 cell lines. Consistent with the lack of FAK cleavage observed post STS treatment, the mt p53-R175H cell line displayed sustained FAK Tyr397 phosphorylation and persistent integrin β1-activated FAK. However, although the survival signals transduced by integrin-activated FAK are attributed to protein kinase B (PKB) activation, fibronectin-mediated protection to STS-mediated detachment demonstrated in the wt p53 cells lines was independent of pPKB Ser473 phosphorylation. Moreover, the altered regulation of FAK in the mt p53-R175H cell line is not due to the inability of mt p53-R175H to associate with FAK. Constitutive activation of FAK has been previously shown to protect cells from anoikis-mediated activation of caspase-8. Correspondingly, in the mt p53-R175H cell line, delayed caspase-8 activation was accompanied by the maintenance of FAK Tyr397 phosphorylation, integrin β1-associated FAK and a Fas/FAK complex. Thus, the data presented highlight that, by interacting with both major apoptotic regulators, FAK is central to anoikis-related regulation. Moreover, through maintained FAK phosphorylation, the “hot spot” mt p53-R175H may have a significant impact on the survival of tumor cells post cell detachment, by opposing the induction of anoikis.

List of associated publications and presentations

Published manuscripts

Fanucchi, S. and Veale, R.B. (2009) Role of p53/FAK association and p53Ser46 phosphorylation in staurosporine-mediated apoptosis: Wild-type versus mutant p53-R175H. *Febs Lett.* **583**: 3557-3562.

Fanucchi, S. and Veale, R.B. (2011) Delayed caspase-8 activation and enhanced integrin β1-activated FAK underpins anoikis in oesophageal carcinoma cells harbouring mt p53-R175H. *Cell Biol. Int. Manuscript in Press.*

Local conference(s)

Fanucchi, S. and Veale, R.B. (2010). Is focal adhesion kinase at the crossroads of apoptotic regulation in human oesophageal squamous cell carcinoma? SASBMB 22nd Congress, Bloemfontein, 18-20 Feb 2010.

Acknowledgements

First and foremost, I would like to extend my sincere gratitude to my supervisor, Professor Rob Veale, for his invaluable advice, assistance and direction throughout this PhD. In spite of his very busy schedule, he was always available for consultation and his enthusiasm for my work has been an inspiration to me.

I would also like to thank Mrs. Elsabé Scott for all her assistance. Without her expertise in cell culture, as well as her continuous supply of cells, this research would not have been possible.

To my fellow colleagues Nicolene, Cass, Yael, Ari, David and Sandile. Thank-you for your encouragement and for always making me smile, especially when I had to repeat an experiment for the umpteenth time.

Personal thanks also go to my parents. Mom and Dad, thank-you for your endless supply of love and support. In addition, my heartfelt thanks to Ant, for always encouraging me and believing in me.

Finally, my sincere appreciation to the Council of Scientific and Industrial Research, the Deutscher Akademischer Austausch Dienst, and the University of the Witwatersrand. Without your funding this PhD would not have been possible.

Table of Contents

List of figures

List of Tables

Abbreviations

ANOVA:	analysis of variance
Apaf-1:	Apoptotic protease activation factor-1
APS:	ammonium persulphate
ATCC:	American Type Tissue Collection
ATP:	adenosine triphosphate
Bcl-2:	B cell lymphoma 2
BH:	Bcl-2 homology domain
bp:	base pair
BSA:	bovine serum albumin
CAD:	caspase-activated DNase
cDNA:	copy deoxyribonucleic acid
CHO:	Chinese hamster ovary
DAB:	3.3'-diaminobenzidine tetrahydrochloride
DBD:	DNA binding domain
DFF45:	DNA fragmentation factor 45 kDa
dH_2O:	distilled water
DIABLO:	direct IAP binding protein with low pI
DISC:	death-inducing signalling complex
DMEM:	Dulbecco's Modified Eagles Medium
DMSO:	dimethyl sulfoxide
DRM:	detergent-resistant microdomain
DN:	dominant negative
DNA:	deoxyribonucleic acid
dUTP:	dioxyuridine
ECM:	extracellular matrix
EDTA:	ethylenediamine tetraacetic acid
EGFR:	epidermal growth factor receptor
ERK:	extracellular regulated kinase
FADD:	Fas associated death ligand
FAK:	focal adhesion kinase

FasL:	Fas ligand
FAT:	focal adhesion targeting
FCS:	fetal calf serum
FERM:	erythrocyte band four.1exrin-radixin-moesin
FN:	fibronectin
FRNK:	FAK related non-kinase
GEM:	glycosphingolipid-enriched membrane
GOF:	gain of function
HOSCC:	human oesophageal squamous cell carcinoma
HRP:	horseradish peroxidise
HUVEC:	human umbilical vein endothelial cells
IAP:	inhibitor of apoptosis protein
ILK:	integrin-linked kinase
IB:	immunoblot
ICAD:	IAP inhibitor of CAD
ICE:	interleukin-1β converting enzyme
IP:	immunoprecipation
JNK:	c-Jun NH2-terminal kinase
kDa:	kilodalton
L/C:	loading control
LOF:	loss of function
MAPK:	mitogen activated protein kinase
MDCK:	Madin-Darby canine kidney
MEKK:	MAP/ERK kinase kinase
mt:	mutant
MMLV:	Moloney Murine Leukemia Virus
mTOR:	mammalian target of rapamycin
MWM:	molecular weight marker
NF-γB:	nuclear factor of kappa light chain gene enhancer in B-cells
Numa:	Nuclear mitotic apparatus protein
PAGE:	polyacrylamide gel electrophoresis
PARP:	Poly (ADP-ribose) polymerase

PBS:	phosphate buffered saline
PCR:	polymerase chain reaction
PEG:	polyethylene glycol
pFAKTyr397:	Tyr397 phosphorylation of FAK
PH:	pleckstrin homology
PI3K:	phosphoinositide-3 kinase
PKB:	protein kinase B
PMSF:	phenyl-methyl-sulphonyl fluoride
POD:	conjugated with horse-radish peroxidase
pPBKSer473:	Ser473 phosphorylation of PKB
PTEN:	phosphatase and tensin homologue deleted on chromosome
PYK2:	proline-rich tyrosine kinase 2
RGD:	arginine-glycine-aspartic acid
RIP:	receptor-interacting protein
RNA:	ribonucleic acid
SCC:	squamous cell carcinoma
SD:	standard deviation
SDS:	sodium dodecyl sulphate
SH2:	Src homology domain 2
Smac:	second mitochondria-derived activator of caspase
SS:	serum starve
STS:	staurosporine
TBS:	tris buffered saline
TCA:	tricholoracetic acid
TdT:	terminal deoxynucleotidyl transferase
TE:	Trypsin/EDTA
TEMED:	N,N,N',N'-Tetramethylethylenediamine
Tris:	tris(hydroxymethyl)aminomethane
TUNEL:	TdT-mediated dUTP-biotin nick end labelling
W/C:	whole cell
WHCO-:	Wits Human Carcinoma of the Oesophagus-
wt:	wild type

Chapter 1

General Introduction

Central role of focal adhesion kinase in anoikis resistance

1.1 Aberrant adhesion-mediated signalling is fundamental to the metastatic progression of tumour cells

Multicellular organisms require efficient mechanisms of intercellular communication to maintain normal tissue homeostasis (Hynes and Zhao, 2000). These requirements are largely met by adhesion receptors that establish transmembrane connections, thereby, linking cells to components of the extracellular matrix (ECM) and adjacent cells. In addition to providing mechanical support, these molecules significantly influence cell behavior, through the activation of intracellular signalling pathways. As these pathways regulate diverse cellular process including cell survival, proliferation and migration, cell adhesion is vital to development and differentiation (De Arcangelis and Georges-Labouesse, 2000; Bill *et al*., 2004). Consequently, aberrant regulation of adhesion-based signalling is prevalent in many pathological conditions such as psoriasis, inflammation and neoplasia, and is central to tumour invasion and metastasis (Hanahan and Weinberg, 2000).

Although the mechanism whereby tumours escape normal cellular control remains an enigma, decades of research have indicated that it is metastasis that causes approximately 90 % of deaths from solid tumours (Gupta and Massague, 2006). To achieve metastasis, cancer cells need to evade multiple levels of tissue regulation to bypass stringent cellular restraints. Evasion of these cellular barriers is fueled by genomic and epigenomic instabilities (Gorgoulis *et al*., 2005; Gupta and Massague, 2006). Thus, metastasis has been described as an evolutionary process as it involves the selection of a genetically diverse subpopulation of cells (Gupta and Massague, 2006). Within the metastatic cascade several discrete steps are discernable: loss of cell adhesion from the primary tumour, invasion of

surrounding tissue, entry in the circulatory system and eventual colonization of a secondary site (*Figure 1.1;* Fidler, 2003). However, since detachment from the primary tumour is an initial step in the metastatic cascade, the molecular basis for inappropriate cell adhesion-mediated signaling has become an area of intense research. Moreover, in addition to facilitating metastasis, the resultant aberrant activation of cell survival pathways may reduce the sensitivity of cancer cells to the apoptosis-inducing capacity of chemotherapeutic treatment (Leu *et al*., 2000; Westhoff and Fulda, 2009). Consequently, exploring the relationship between cell adhesion and cell death pathways is imperative, as it reveals the mechanism used by tumours to overcome normal tissue restraints, facilitating their metastatic progression.

1.2 The concepts of anoikis and apoptosis-related death

A remarkable aspect of adhesion-mediated signaling is anchorage-dependent survival. The survival of many normal cell types, particularly epithelial cells, is dependent on cellular adhesion to a substratum (Aoudjit and Vuori, 2001; Bozzo *et al*., 2006; Kamarajan and Kapila, 2007). Subsequent loss of contact to the ECM triggers the cells to undergo "apoptosis-like" death. This subset of cell death is referred to as anoikis (Frisch and Francis, 1994). Malignant tumour cells have reduced requirements for surface adhesion due to the evasion of anoikis-related apoptotic pathways (Frisch and Screaton, 2001; Kupferman *et al*., 2007; Cao *et al*., 2009). However, the underlying molecular events rendering tumour cells resistant to anoikis are cryptic. Do cancer cells possess the inherent ability to constitutively activate signalling pathways, thereby abrogating substratum-dependent survival signalling? And if so, which apoptotic and cell adhesion intermediates are fundamental to substratum-deprived survival? Knowledge of this nature may allow the manipulation of anoikis-related intermediates, thereby enhancing the susceptibility of tumour cells to anoikis-inducing chemotherapeutic agents.

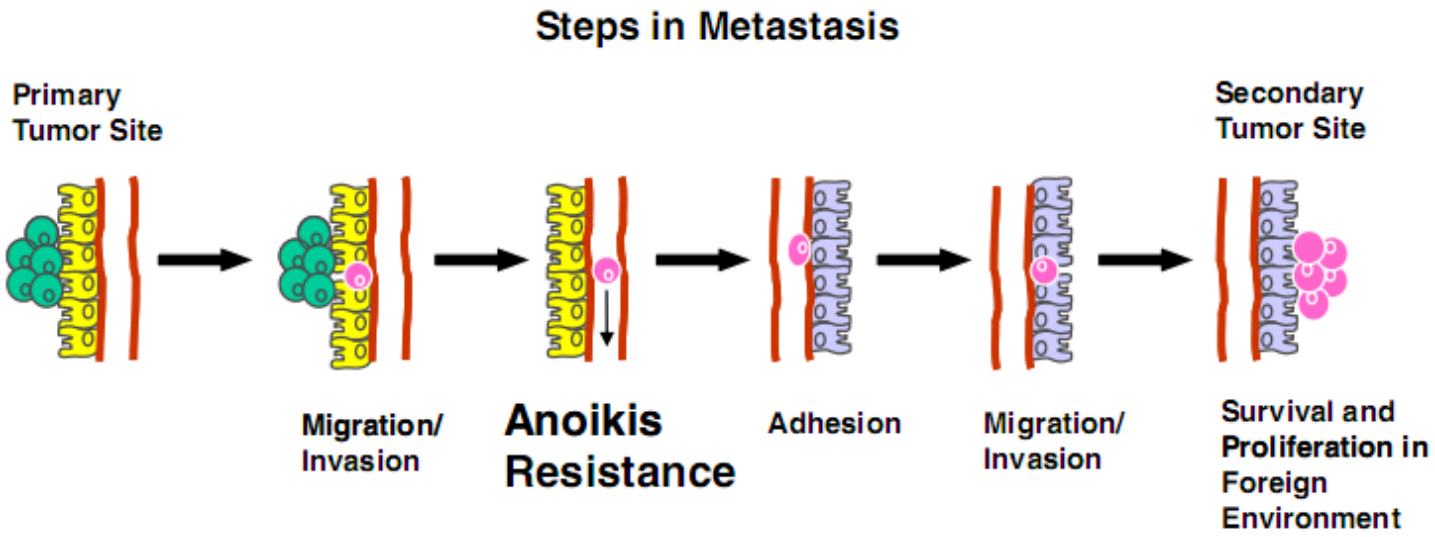

Figure 1.1: Tumour cells bypass numerous tissue-dependent barriers to achieve metastasis. Firstly, tumour cells acquire a migratory phenotype that allows them to invade through the basement membrane. Upon entering the circulatory or lymphatic system, cancer cells acquire the ability to survive in the absence of adhesion to the ECM (referred to as anoikis resistance). Tumour cells must then adhere to the walls of a blood or lymphatic vessel at a secondary site and invade the surrounding tissue. Finally to complete the metastatic cascade, cancer cells have to survive in the foreign environment and grow to form secondary tumour masses. © Simpson *et al*. (2008)

Anoikis was first identified in endothelial (Meredith *et al*., 1993) and epithelial cells (Frisch and Francis, 1994) that were experimentally dissociated from the ECM. The resultant death that ensued was accompanied by characteristic apoptotic features. Apoptosis is the physiological pathway that describes the mechanism of programmed cell death (Kerr *et al*., 1972; Jin and El-Deiry, 2005). During apoptosis, a specific series of events lead to the organized dismantling of the cellular components. The cell acquires distinct morphological features that include; condensation of the chromatin, apoptotic body formation, cell shrinkage and blebbing of membrane prior to cell lysis (Kerr *et al*., 1972; Kaufman and Hengartner, 2001). With regard to the modification in biochemical parameters, there is also intranucleosomal DNA cleavage, phosphatidylserine translocation to the external membrane and the inactivation by cleavage of several DNA repair enzymes and cellular substrates (Riedl and Shi, 2004).

1.2.1 Caspases - executioners of anoikis

Although the exact mechanism whereby cells undergo anoikis is poorly understood, both the intrinsic or mitochondrial pathway and the extrinsic or death receptor pathway have been implicated (*Figure 1.2;* Lui *et al*., 2006; Kamarajan and Kapila, 2007; Kamarajan *et al*., 2010). Both apoptotic pathways are dependent on the activation of caspases, a family of aspartate-specific cysteine proteases (Stennicke and Salvesen, 1998; Riedl and Shi, 2004). Caspases are synthesized as inactive zymogens that become autoactivated by proteolytic processing in an amplified cascade (Nicholson *et al*., 1995). Apoptotic stimuli mediated via both extrinsic and intrinsic death cascades converge on caspase-3 (CPP32, YAMA or apopain) (Riedl and Shi, 2004). Activated caspase-3 is responsible for the cleavage and disassembly of approximately 100 proteins that participate in survival signalling, structural and cell adhesion events (Wen *et al*., 1997; Kivinen *et al*., 2005). Consequently, caspase activation abrogates survival signalling and dismantles sites of focal contact, facilitating the apoptotic death process.

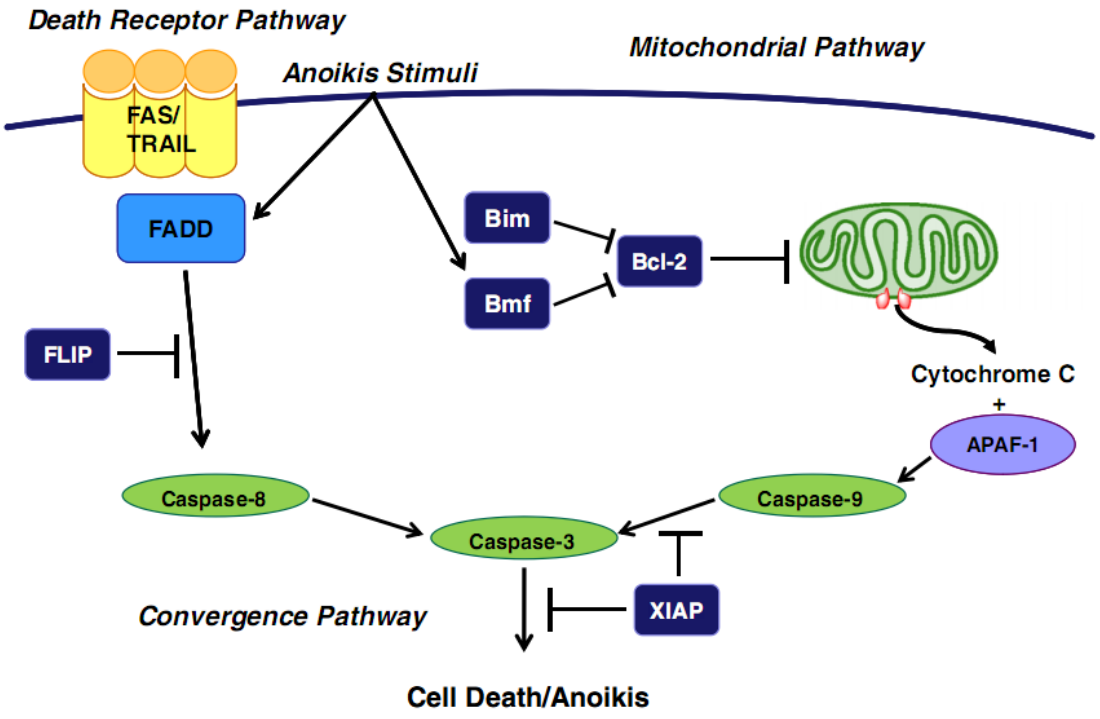

Figure 1.2: Anoikis-related stimuli converge on the activation of caspase-3. The mitochondrial or intrinsic death pathway is initiated by p53 in response to oxidative stress and DNA damage. Both caspase-dependent and -independent apoptotic substrates are released from the inner membrane space of the mitochondrion and lead to the ultimate activation of caspase-3. The death receptor or extrinsic pathway leads to the sequential activation of caspase-8 and -3. Hence, both the extrinsic and intrinsic apoptotic pathways converge on the activation of caspase-3. Importantly, defects in either death cascade render tumour cells resistant to anoikis. © Simpson *et al*., (2008)

1.2.2 The mitochondrial death cascade and anoikis

Aberrant regulation of the mitochondrial apoptotic pathway is implicated as a major contributor to anoikis resistance (Frisch and Francis, 1994; Ilic *et al*., 1998; Rytomaa *et al*., 2000; Zhang *et al*., 2004 (b); Lui *et al*., 2006). The intrinsic apoptotic pathway involves the altered permeability of the mitochondrial membrane, and the release of apoptotic proteins from the intermembrane space into the cytoplasm (*Figure 1.2*; Wang, 2001). The Bcl-2 family of proteins controls the release of mitochondrial proteins. This family is divided into three categories depending on the possession of at least one of the four highly conserved Bcl-2 homology domains (BH1 – BH4). (1) The anti-apoptotic factors; Bcl-2 and Bcl-xl, (2) the pro-apoptotic factors; Bax and Bak and (3) the 'BH3-only' pro-apoptotic factors which includes Bid (Zimmerman *et al*., 2001). In viable cells, both Bax and Bak are the major initiators of the intrinsic apoptotic pathway and reside in the cytoplasm and outer mitochondrial membrane respectively (Wei *et al*., 2001). In response to a death signal, Bax undergoes a conformational change that enables its insertion into the mitochondrial outer membrane, and the formation of pores. Bak monomers also undergo conformational changes and oligomerization, facilitating the permeablisation of the mitochondrial membrane (Willis *et al*., 2005).

Upon oligomerization of Bax or Bak, the mitochondrial outer membrane is permeabilized resulting in the release of proteins from the intermembrane space of the mitochondria into the cytoplasm (Willis *et al*., 2005). *Cytochrome c* is one of the key small molecules released from the mitochondrion and results in the activation of the cytoplasmic protein, apoptotic protease activation factor-1 (Apaf-1) (Li *et al*., 1997; Riedl and Shi, 2004). The binding of cytochrome c to the adapter molecule apaf-1 induces a conformational change in apaf-1, facilitating the formation of the apoptosome and the recruitment of procaspase-9 (Li *et al*., 1997; Jiang and Wang, 2000). Procaspase-9 is not activated by simple cleavage, but rather by binding to apaf-1 (Stennicke and Salvesen, 1998). The apoptosome then activates the effector caspase, caspase-3, which is cleaved by activated

caspase-9. Other small molecules released from the mitochondrion are second mitochondria-derived activator of caspase/direct IAP binding protein with low pI (Smac/ DIABLO) and Omi/HrtA2 (Riedl and Shi, 2004). Both factors indirectly contribute to caspase activation by inhibiting members of the inhibitor of apoptotic protein (IAP) family (Liu *et al*., 2000).

Members of the Bcl-2 family of proteins have been implicated in reducing the susceptibility of tumour cells to anoikis. Overexpression of the anti-apoptotic protein, Bcl-2 has been shown to protect epithelial cells from anchorage-dependent cell death (Frisch and Francis, 1994). In Madin-Darby canine kidney (MDCK) cells and primary mouse mammary epithelial cells, detachment from the ECM induces rapid mitochondrial translocation of Bax (Rytomaa *et al*., 2000). Moreover, in non-transformed intestinal cells, the release of Omi/HtrA2 and was associated with detachment-induced down-regulation of Bcl-XL (Lui *et al*., 2006). However, in these cells, anoikis did not involve activation of caspase-9 (Lui *et al*., 2006).

The p53 tumour suppressor protein controls the balance between pro-apoptotic and anti-apoptotic proteins (Rotter *et al*., 1983; Brosh and Rotter, 2009). As the anti-apoptotic factors are proposed to inhibit the pro-apoptotic proteins through the sequestration of their BH3 domains, the ratio between the two groups determines the susceptibility of cells to the intrinsic death pathway. Thus, by redistributing pro-apoptotic factors at the mitochondrial membrane, p53 initiates the intrinsic apoptotic pathway (Miyashita and Reed, 1995; Rodier *et al*., 2007). Anoikis has been demonstrated to be p53-dependent, as anchorage-deprived death was suppressed in fibroblasts transfected with dominant-negative p53 (Ilic *et al*., 1998). Consistent with this observation, inhibition of endogenous p53 activity in thyroid epithelial cells inhibited anoikis and transformed fibroblasts underwent detachment-induced apoptosis only when intact p53 is present (Vitale *et al*., 1999). Thus, in several cell types, substrate-deprived death is regulated by the Bcl-2 family of apoptotic protein and central to this regulation is the tumour suppressor protein, p53.

1.2.3 Anoikis and the death receptor pathway

Studies in non-malignant epithelial and endothelial cells, and recently, in malignant cancer cell lines implicate the death receptor pathway in anoikis induction (Frisch, 1999; Marconi *et al*., 2004; Bozzo *et al*., 2006; Mawji *et al*., 2007; Kamarajan *et al*., 2010). The extrinsic pathway is initiated by the binding of the Fas death ligand (FasL), to its corresponding death receptor, Fas (synonyms: Apo-1, CD95, and TNFRSF6) (*Figure 1.2;* Nagata, 1999; Aoudjit and Vuori, 2001). The binding of the death stimulus results in the recruitment of the adaptor protein Fas associated death domain (FADD) as well as the initiator procaspase-8, to form a death-inducing signalling complex (DISC) (Peter and Krammer, 2003). Procaspase-8 generally has low activity in the cell, however, upon formation of the DISC, procaspase-8 molecules aggregate and autoactivate one another to form active caspase-8 (Barnhart *et al*., 2003). Activated caspase-8 then cleaves the effector caspases; procaspase-3, -6 and -7 which are cleaved into their active forms (Barnhart *et al*., 2003; Westhoff and Fulda, 2009). Thus, the effector caspases become catalytically activated and commit the cell to death by the concomitant cleavage of structural and repair enzymes.

With respect to Fas-mediated apoptosis, cells are classified as either type I or type II (Scaffidi *et al*., 1998). In type I cells, Fas activation results in the efficient assembly of the DISC and processing of downstream effector caspases. In contrast, in type II cells, the formation of the DISC is impaired and the Fas-mediated death signal is transmitted via the mitochondrial apoptotic cascade. More recently, this hypothesis has been refined by the 'lipid raft theory' (Simons and Ikonen, 1997; Chaigne-Delalande *et al*., 2008). The original view that the lipid bilayer is a dynamic entity (Singer and Nicolson, 1972) has been revised to include ordered lipid assemblies that reside within the fluid membrane (Chaigne-Delalande *et al*., 2008). As these subdomains are enriched with sphingolipids and cholesterols they have been described as lipid rafts, detergent-resistant microdomains (DRMs) or glycosphingolipid-enriched microdomains (GEMs) (Chaigne-Delalande *et al*., 2008). Subsequently, the classification of cells as

either type I or type II has been attributed to the localisation of Fas within or outside the DRMs respectively (Muppidi and Siegel, 2004). Hence, the transmission of Fas-dependent death signals is reliant on the level of Fas residing within the lipid rafts (Legembre *et al*., 2006).

Aberrant regulation of the death receptor signalling pathway is implicated in the resistance of anoikis in tumour cells and subsequently, chemotherapeutic therapies (Frisch, 1999; Rytoma *et al*., 1999; Marconi *et al*., 2004; Mawji *et al*., 2007). Importantly, the detachment of non-malignant cells from the ECM induces anoikis through activation of the Fas-mediated apoptosis (Aoudjit and Vuori, 2001). Both Fas and FasL levels are upregulated, whilst FLIP levels are reduced in HUVEC cells post detachment (Aoudjit and Vuori, 2001; Kamarajan *et al*., 2010). Moreover, these alterations in the extrinsic death intermediates were associated with the induction of Fas-mediated apoptosis (Aoudjit and Vuori, 2001). In MDCK cells, detachment-induced apoptosis occurs via the death receptor pathways, as overexpression of a dominant negative FADD blocked anoikis, and led to the activation of caspase-8 and -3 (Rytomaa *et al*., 1999). Consistent with the previous study, both Fas and FasL expression was up-regulated post detachment. However, the functional significance of these events is uncertain, as the soluble extracellular domains of the death receptors were not able to protect against anoikis, even though caspase-8 was activated in a FADD-dependent manner (Rytomaa *et al*., 1999). Moreover, lack of reliance on the death receptors was demonstrated in a study by Stupack *et al*., (2001), where the integrin β subunit was shown to recruit caspase-8 to the membrane, and activate caspase-8 in a death receptor-independent manner (Stupack *et al*., 2001). Hence, although the mechanism underlying anoikis appears to be cell-type specific, conditions that trigger anoikis converge on the activation of caspase-8 (Kamarajan *et al*., 2010). In contrast to normal cells, malignant cells fail to activate the death receptor pathway upon loss of ECM contact, despite up-regulating Fas and FasL (Mawji *et al*., 2007). Hence, due to aberrant regulation of Fas-mediated apoptosis, tumour cells resist anchorage-independent death, facilitating their metastatic progression.

1.3 Influence of tumour microenvironment on anoikis regulation

In normal tissue, adhesion to appropriate extracellular matrix proteins is essential for survival, and loss of this adhesion induces anoikis via intrinsic or extrinsic apoptotic pathways (Ilic *et al*., 1998; Kurenova *et al*., 2004; Kamarajan *et al*., 2010). However, tumour cells are able to overcome this regulation and survive in the absence of cell adhesion. Cell anchorage is a multifaceted process involving adhesion molecules that interact with different structural components referred to as the ECM and neighboring homotypic or heterotypic cells (Grossman, 2002). Thus, anchorage-deprived death is associated with the loss of many different kinds of cell-cell/cell-matrix interactions. Hence, the tumour microenvironment comprising of non-cancerous cells and the protein network surrounding the cancerous mass, is a key regulator of tumour biology.

1.3.1 Cell-cell survival signalling

Signals mediated via direct cell-cell contact of tumour cells may aid survival, as ECM-deprived squamous cell carcinoma cells resist anoikis (Kantak and Kramer, 1998; Zhang *et al*., 2004 (a)). At sites of adherens junctions the cell-cell connections are mediated by cadherins, transmembrane glycoproteins that maintain cell-cell adhesion via a calcium-dependent mechanism (Takeichi *et al*, 1990; Yagi and Takeichi, 2000). Of the 10 subclasses of cadherins that have been identified, E-cadherin/ uvomorulin, P-cadherin and N-cadherin are the most common and have a unique tissue-specific distribution. E-cadherin is well characterized and its expression is limited to normal epithelial tissue. As cadherins interact homophilically, E-cadherins only interact selectively with other E-cadherins and so forth (Shapiro *et al*., 1995).

The adhesive function of cadherins is dependent on their interaction with cytoplasmic proteins. In the cytoplasm, either α- or β-catenin bind to the cadherin to form a link between the adjacent cell and the actin cytoskeleton, thereby influencing structural organization as well as development of cells (Takeichi,

1990; De Arcangelis and Georges-Labouesse, 2000). Consequently, altered cadherin expression has been reported in many tumours. Reduced E-cadherin expression is associated with an increase in epithelial cell invasiveness and dedifferentiation that accompanies the development of various carcinomas (Van Aken *et al*., 2001). Moreover, blockage of E-cadherin interactions induces anoikis (Kantak and Kramer, 1998), whilst overexpression of β-catenin, facilitates anchorage-independent growth in epithelial cells (Orford *et al*., 1999).

1.3.2 Cell-substrate interactions: ultimate regulator of anoikis?

Normal cells introduced into the incorrect microenvironment, due to inappropriate cell-substrate engagement, will be driven towards anoikis-dependent death. Hence, these cell-ECM connections profoundly regulate cell fate decisions as they suppress the proliferation of cells existing outside their appropriate environment (Badylak *et al*., 2009). Conversely, cancer cells that overcome anoikis regulatory mechanisms may populate locations that would normally be incompatible to non-transformed cells. Thus, interactions between the ECM and the tumour cell are believed to be a main determinant in anoikis resistance (Zhang *et al*., 2004 (a); Kamarajan and Kapila, 2007). The ECM is composed of a complex network of fibrous proteins and glycosaminoglycans that are produced locally and secreted via exocytosis. This extracellular microenvironment functions as a scaffold to maintain tissue integrity (Badylak *et al*., 2009). In addition, cells directly interact with the ECM via surface receptors, such as the integrins, which upon engagement with the ECM activate a broad range of signalling cascades that regulate apoptosis, cell survival and migration. The integrins are a family of transmembrane glycoproteins that exist as α/β heterodimers (Gilcrease, 2007). At present, 18 α subunits and 8 β subunits have been identified (Nagaprashantha *et al*., 2010). Both subunits associate at cell adhesion sites known as focal adhesions. The extracellular domains of integrins interact with components of the extracellular matrix, including fibronectin, collagen and laminin (Gilcrease, 2007). The specificity of these interactions is determined the subunit combinations of the integrins as well as the cell type.

In Chinese Hamster ovary (CHO) cells and human umbilical vein endothelial cells (HUVEC), anoikis is suppressed through interactions between fibronectin and the α5β1 integrin (Zhang *et al*., 1995; Fukai, *et al*., 1998). Consistent with these reports, survival signals mediated via collagen I/α5β1 interactions protected the rat intestinal epithelial cell line (RIE1) from apoptotic stimuli (Lee *et al*., 2000). Mammary epithelial cells derive survival signals from a laminin-rich basement membrane or collagen I, utilizing α1, α2, α3 and β1-integrin chain ligation (Howlett *et al*., 1995). In addition, by blocking the binding of α5β1 integrins to collagen, MDCK cells undergo anoikis (Lui *et al*., 2000). In the MDA-MB-435 breast cancer cell line, disrupting survival signals mediated via the α6β1 integrin increased apoptotic induction and repressed metastatic growth *in vivo*, whilst, blockage of αvβ3 integrin-mediated signals induced anoikis in breast cancer and melanoma (Fukai, *et al*., 1998; Lui *et al*., 2000). Hence, it is evident that aberrant integrin/ECM signalling disrupts normal cellular regulation and facilitates the metastatic progression of cells.

1.4 Signalling pathways relevant to anoikis converge on key cell adhesion intermediates

Due to the crucial role of ECM-integrin signalling in regulating cell survival, the signal transduction cascades activated by cell adhesion molecules are central to anoikis resistance (Attwell *et al*., 2000; Kamarajan and Kapila, 2007). Key players in integrin-mediated signal transduction are the integrin-associated non-receptor kinases, focal adhesion kinase (FAK) and integrin-linked kinase (ILK). Upon integrin-ECM engagement, both ILK and FAK activate various signaling pathways involved in cell survival and proliferation (*Figure 1.3;* Sonoda *et al*., 1999; van Nimwegen and van der Water, 2007) including the mitogen activated protein kinase (MAPK)/extracellular regulated kinase (ERK) pathway and the phosphatidylinositol 3′kinase (PI3K) pathway with its downstream target protein kinase B (PKB/AKT) (Gilcrease, 2007). Unlike FAK, ILK may activate PKB directly or indirectly via the PI3K cascade (Attwell *et al*., 2000).

The Jun amino-terminal kinases (JNKs) are a family of MAP kinase related serine/threonine kinases. Early studies indicated that activation of the JNK-pathway and MAP/ERK Kinase Kinase 1 (MEKK-1) pathway was critical to anoikis resistance, as the dissociation of epithelial cells from the extracellular matrix induced a substantial increase in JNK activity (Frisch *et al*., 1996). Furthermore, the blockage of the JNK pathway by a dominant-negative form of JNK kinase partially inhibited anoikis (Xia *et al*., 1995). However, a recent study demonstrated that the level of JNK activation decreased following detachment of A549 cells from the ECM, indicating that the role of JNK signalling in anoikis resistance may be not be as important as originally believed (Liu *et al*., 2008).

Alternatively, activation of the PI3K-PKB cascade has been shown to be central to anoikis resistance, as enhanced PKB activation is associated with substrate-deprived survival (Díaz-Montero *et al*., 2006). Upon activation, PI3K phosphorylates PIP_2 on the 3'OH position to produce $PI(3,4,5)P_3$ (PIP_3). The tumour suppressor phosphatase and tensin homolog deleted on chromosome 10 (PTEN) opposes PI3K-dependent signalling by dephosphorylating PIP_3 to PIP_2. In order for PKB to achieve full activation, phosphorylation at both serine 473 (Ser473) of the hydrophobic tail and threonine 308 (Thr308) of the activation motif is required (Majumder and Sellers, 2005). To date, several candidate kinases are implicated in the regulation of PKB Ser473 phosphorylation including the second mammalian target of rapamycin (mTOR)-containing protein complex mTORC2 (Sarbassov *et al*., 2006), choline kinase (Chua *et al*., 2009) and ILK (Attwell *et al*., 2000). Acting as a second messenger, PIP_3 recruits PKB via its pleckstrin homology (PH) domain to the peripheral membrane. Similarly, PDK1 is also recruited via its PH domain to phosphorylate Thr308 residue of PKB (Majumder and Sellers, 2005).

The serine-threonine kinase PKB is a central to cell survival, as anchorage-mediated signal transduction from FAK and ILK converge on the activation of this kinase (Sonoda *et al*., 1999; Attwell *et al*., 2000). Activation of PKB negatively regulates apoptotic processes by inhibiting caspase-9 activation,

inactivating the proapoptotic proteins bad and bax, (Datta *et al*., 1997; Cantley, 2002) and impeding the negative regulation of NF-κB, thus, enhancing the transcription of antiapoptotic and prosurvival genes (Duronio, 2008). Consequently, reduced PKB-mediated signalling induces the mitochondrial translocation of Bad and Bax, thereby altering the Bad/Bcl-2 ratio and increasing permeability of the outer mitochondrial membrane (Datta *et al*., 1997). In addition, PKB activation reduces the transcription of proapoptotic molecules by negatively regulating the Forkhead family transcription factors (Brunet *et al*., 2001). Furthermore, by enhancing p53 ubiquitination, phosphorylation of Mdm2 by PKB antagonizes p53-mediated apoptosis (Duronio, 2008). PKB activation abrogates the activity of the TSC1/TSC2 dimer, by inhibiting the rheb GTPase (Sarbassov *et al*., 2005). Activated rheb stimulates mTORC1, leading to increased protein synthesis via p70 S6 kinase-mediated phosphorylation of eukaryotic initiation factor 4E and the ribosomal S6 protein (Sarbassov *et al*., 2005). As previously mentioned, the complete activation of PKB is achieved through the second mTOR complex, mTORC2, which phosphorylates PKB on serine 473 (Sarbassov *et al*., 2006). Thus, it is apparent that based on its central role in coordinating cell adhesion-mediated signalling, a particular threshold level of PKB-mediated survival signalling is required to oppose substrate-deprived death (Ilic *et al*., 1998; Frisch *et al*., 1999; Attwell *et al*., 2000).

As both FAK and ILK suppress anoikis via PKB activation (Sonoda *et al*., 1999; Attwell *et al*., 2000), it is difficult to discern which kinase is central to anoikis resistance. Furthermore, anoikis induced by ILK inactivation is not rescued by FAK, suggesting that the two kinases affect anoikis in different and parallel pathways (Attwell *et al*., 2000). Consequently, several studies have been undertaken to determine which survival signaling molecule is the most important to anoikis resistance (Guan and Shalloway, 1992; Ilic *et al*., 1998; Attwell *et al*., 2000; Zhang *et al*., 2004 (a); Kamarajan and Kapila, 2007). Although ILK has been shown to suppress anoikis, this protection is restricted to PKB-mediated survival signalling (Attwell *et al*., 2000). In contrast, numerous reports have demonstrated that FAK offers protection from anoikis by enhanced activation of

PKB-mediated survival as well as directly suppressing apoptotic pathways (Sonoda *et al*., 1999; Kurenova *et al*., 2004; Golubovskaya *et al*.. 2005; Lim *et al*., 2008). Accordingly, due to its central role in integrating signals between extracellular and intracellular events FAK has been implicated as the key intermediate in the acquisition of anoikis resistance (Frisch *et al*., 1996; Duxbury *et al*., 2004; Zhang *et al*., 2004 (a); Kamarajan and Kapila, 2007).

1.4.1 Focal adhesion kinase (FAK) is at the hub of cell adhesion events

FAK is a 125 kDa non-receptor protein tyrosine kinase localized to sites of focal contact (*Figure 1.4*; Parsons, 2003; Kamarajan and Kapila, 2007). The catalytic core of FAK is flanked by C- and N-terminal domains. FAK is directed to focal adhesion sites by protein-protein interactions with the C-terminal region, which contains the focal adhesion targeting (FAT) sequence (Martin *et al*., 2002). This region is also critical for interactions with paxillin, a scaffolding protein that mediates interactions with integrins (Schaller *et al*., 1995; Crowe and Ohannessian 2004). The N-terminal region comprises of a sequence with high homology to the FERM (erythrocyte band four.1-exrin-radixin-moesin) family of proteins (van Nimwegen and van der Water, 2007). The N-terminal domain of FAK associates with the cytoplasmic region of the β subunits of integrins (Schaller *et al*., 1995), the death-receptor complex binding protein RIP (receptor-interacting protein) (Kurenova *et al*., 2004) as well as epidermal growth factor receptor (EGFR) (Sieg *et al*., 2000).

Recent studies show the FERM domain directly interacts with the central region of FAK, thereby inhibiting its kinase activity (Cooper *et al*., 2003; Cohen and Guan, 2005). In response to the clustering of integrins at sites of cell contact, the FERM domain is proposed to release its autoinhibition of FAK through the formation of higher affinity associations with the integrin cytoplasmic tails or other integrin-associated proteins (Cooper *et al*., 2003). Consequently, FAK is activated by autophosphorylation at tyrosine 397 (pFAKTyr397) (Parsons, 2003). Tyr397, the main phosphorylation site of FAK both *in vitro* and *in vivo*, lies in the

linker region between the FERM and kinase domains (Schaller *et al*., 1994; van Nimwegen and van der Water, 2007). The activation by autophosphorylation of FAK, results in the recruitment of proteins with Src homology 2 (SH2) and Src homology 3 domains (SH3). An important SH2 containing protein that interacts with FAK at the phosphorylated Tyr397 residue is Src (Mitra and Schlaefper, 2006). The crystal structure of the FAK N-terminal region suggests that Src binding may also contribute to FAK activation by promoting release of the FERM domain from its binding sites on FAK (Ceccarelli *et al*., 2006). In addition, two residues within the catalytic core, Tyr576 and Tyr577 are phosphorylated in response to Src binding (Calalb *et al*., 1995; Owen *et al*., 1999; Mitra and Schlaefper, 2006). Thus, Src plays an integral role in FAK regulation, as full activation of the FAK kinase domain requires phosphorylation of all three tyrosine residues. The formation of the FAK-Src complex facilitates the phosphorylation of Tyr925, allowing Grb2 to bind and activate the MAP kinase pathway (Schleapfer *et al*., 1994; van Nimwegen and van der Water, 2007). Moreover, given its location in the focal adhesion targeting domain, Tyr925 phosphorylation may also negatively affect focal adhesion targeting (van Nimwegen and van der Water, 2007).

In addition to Src family kinases, Tyr397-phosphorylated FAK can mediate interactions with SH2 domains of several other signaling proteins, including PLC-γ1, and adaptor proteins, such as Src homology and collagen protein (SHC), Grb7, Nck-2, and the p85 subunit of PI3K (Sonoda *et al*.,1999; Parsons, 2003; Mitra *et al*., 2005; Siesser and Hanks, 2006). Consequently, FAK activation at sites of cell contact increases activation of PKB, the downstream effector of the PI3K cascade (Majumder and Sellers, 2005). Thus, through phosphorylation, FAK activates numerous downstream signalling pathways that regulate proliferation, survival and migration (van Nimwegen and van der Water, 2007).

A.

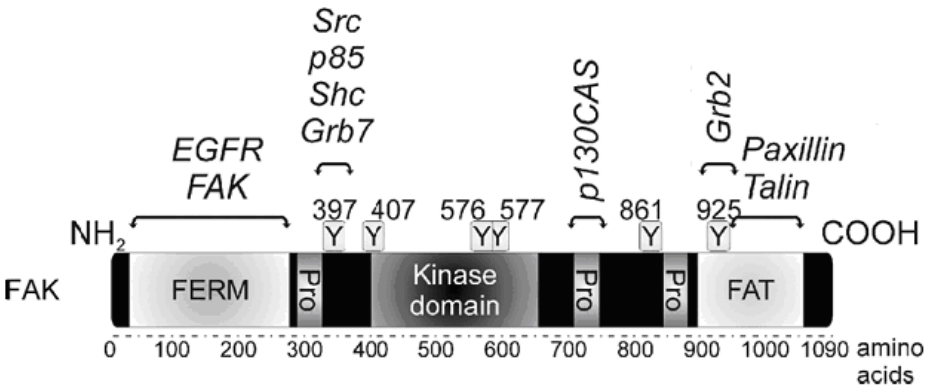

B.

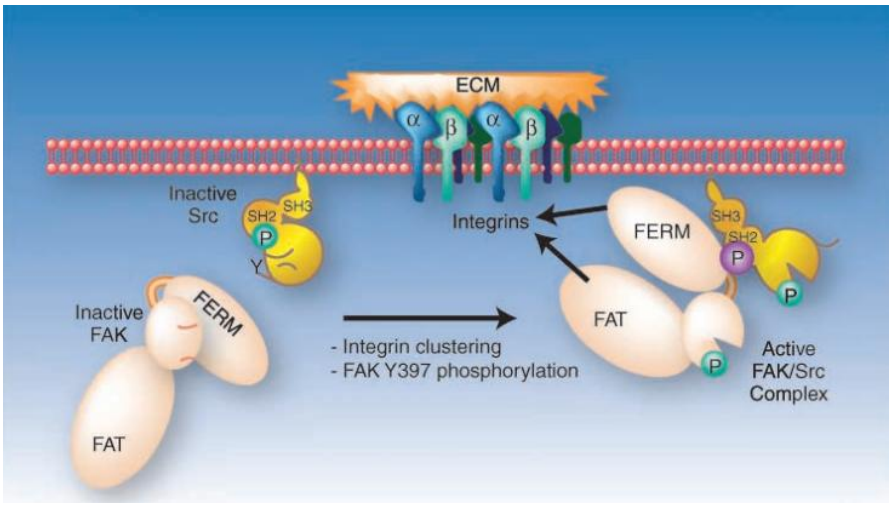

Figure 1.3: Schematic representation of FAK. A) The kinase domain of FAK is flanked by C- and N-terminal domains. The main phosphorylation site, Tyr397, lies in the linker region between the FERM and kinase domains. Upon Tyr397 autophosphorylation, Src, Grb7 and the p85 subunit of PI3K are recruited and Tyr576 and Tyr577 are phosphorylated in the catalytic core. The C-terminal region contains the FAT sequence, which localizes FAK to focal adhesion sites and interacts with the scaffolding proteins, talin and paxillin. © van Nimwegen and van der Water, 2007 B) During attachment of cells, the clustering of integrins facilitates the binding of the FERM domain of FAK to the cytoplasmic tail of the β subunit of the integrins. Consequently, FAK is unfolded and releases the FERM-dependent autoinhibition of FAK, allowing its activation by autophosphorylation at Tyr397. © Siesser and Hanks, 2006

1.5 FAK: the key player in anoikis resistance

The underlying mechanism enabling tumour cells to bypass stringent anoikis-related regulation appears to rely on constitutive activation of survival signalling and the repression of apoptotic pathways (Ilic *et al*., 1998; Kamarajan *et al*., 2010). Accordingly, studies have demonstrated that constitutive activation of FAK is associated with the repression of apoptotic pathways and maintained cell survival in the absence of cell contact (Frisch and Francis, 1994; Frisch *et al*., 1996; Zhang *et al*., 2004 (a); Golubovskaya *et al*., 2005). Increased Tyr397 phosphorylation of FAK is associated with enhanced cell adhesion (Guan and Shalloway, 1992; Zhang *et al*., 2004 (a); Kamarajan and Kapila, 2007). Correspondingly, constitutively active FAK rescues epithelial cells from anoikis and loss of substrate adhesion reduces FAK activation (Frisch and Francis, 1994). In addition, a crucial role of FAK in anoikis resistance has been demonstrated as expression of CD2-FAK, a fusion protein that retains a high level of Tyr397 phosphorylation when cells are held in suspension, dramatically opposed anoikis (Frisch *et al*., 1996). Moreover, knockdown of FAK expression in oral squamous cell carcinoma (Zhang *et al*., 2004 (a)) and pancreatic adenocarcinoma (Duxbury *et al*., 2004) promotes anoikis in these cells.

Enhanced activation of FAK transmits survival signals via the PI3K pathway, as phosphorylation of Tyr397 results in PI3K activation by phosphorylation (*Figure 1.4;* Sonoda *et al*., 1999). However, as previously mentioned, the PI3K cascade is not exclusively regulated by FAK (Attwell *et al*., 2000). Furthermore, a definitive role of aberrant FAK activity in the progression of most tumours has been reported (Miyazaki *et al*., 2003; Lark *et al*., 2005; Watermann *et al*., 2005; Jiang *et al*., 2010). Thus, an alternative survival role of FAK in the regulation of anoikis-related events has been proposed. Although the details of this regulation are enigmatic, both the extrinsic and intrinsic apoptotic pathways have been implicated in the FAK-dependent suppression of anoikis (Kurenova *et al*., 2004; Golubovskaya *et al*., 2008; Lim *et al*., 2008).

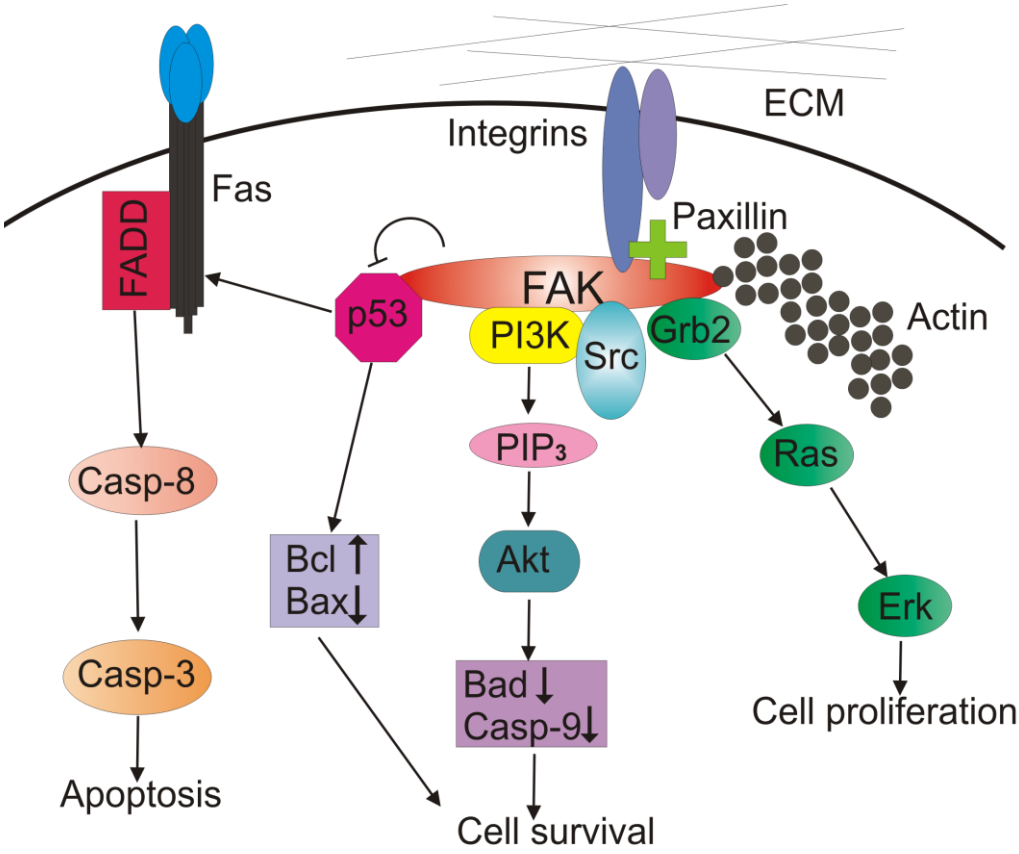

Figure 1.4: FAK-mediated signalling pathways. FAK localizes to integrins via interactions with its C-terminal domain. As a consequence of FAK-integrin engagement, FAK is autophosphorylated at Tyr397 providing a binding site for Src. Src further phosphorylates FAK, increasing FAK's kinase activity. Consequently, PI3K is recruited to FAK and activates PKB. Once activated by phosphorylation, PKB initiates downstream survival events. Interaction of the N-terminal domain of FAK with p53 inhibits the transcriptional activity of p53, thereby also enhancing survival signalling. An important transcriptional target of p53 is the death receptor, Fas. Binding of Grb2 to phosphorylated Tyr 925 results in the activation of the Grb2/Ras/ERK pathway which enhances survival signalling. Therefore, FAK is at the hub of survival, proliferation, adhesion and migration signalling.

1.5.1 FAK represses p53-mediated apoptosis

In the absence of cell-ECM interactions, p53 has been implicated in the regulation of FAK-dependent anoikis (*Figure 1.4;* Golubovskaya *et al*., 2005). Under conditions of ECM deprivation, thyroid epithelial cells undergo anoikis through a p53-dependent pathway (Vitale *et al*., 1998). A study by Golubovskaya *et al*. (2005) showed that the N-terminal FERM domain of FAK specifically interacts with the N-terminal domain of p53. The p53/FAK has been proposed to inhibit p53 activity by enhancing Mdm-2 dependent ubiquitination of p53, or alternatively, reducing the transcriptional activity and therefore pro-apoptotic effect of p53 (Golubovskaya *et al*., 2008; Lim *et al*., 2008). In another study, survival signals mediated by fibronectin and integrin alpha v were shown to affect FAK phosphorylation and prevent p53-mediated apoptosis (Zhang *et al*., 2004 (a)). Moreover, loss of cell adhesion increased FAK nuclear localisation, enhanced p53 degradation and promoted cell survival (Ilic *et al*., 1995). Therefore, although considerable evidence points to a crucial role of p53 in FAK-mediated repression of anoikis, the exact function of interplay of FAK and p53 in cell function remains to be clarified.

1.5.2 Association between FAK and Fas-mediated apoptosis

Intriguingly, in addition to the mitochondrial-mediated apoptotic pathway, FAK has also been implicated in the suppression of the death-receptor pathway (*Figure 1.4*). A functional link between FAK and the death receptors has been demonstrated (Kurenova *et al*., 2004; Kamarajan *et al*., 2010). Furthermore, a Fas antagonistic antibody was shown to rescue SCC from FAK-mediated anoikis (Kamarajan and Kapila, 2007) and abrogation of FAK expression has been shown to be associated with enhanced caspase-8 activation and the induction of anoikis (Kurenova *et al*., 2004; Kamarajan *et al*., 2010). Therefore, although the details of crosstalk between Fas and FAK still need to be elucidated, the role of Fas in anchorage-dependent survival represents a fascinating step in anoikis control.

1.6 Aberrant FAK signalling in tumour progression

Advances in the molecular profiling of primary tumours have revealed genes the expression of which correlate with the reoccurrence of metastatic cancer (Weigelt *et al*., 2005). To date, numerous reports have implicated aberrant expression and regulation of FAK in facilitating the metastatic progression of tumour cells (Miyazaki *et al*., 2003; Lark *et al*., 2005; Watermann *et al*., 2005; Gabriel *et al*., 2006; Jiang *et al*., 2010). Accordingly, inappropriate expression of FAK has been reported in human tumours including oral carcinoma (Schnieder *et al*., 2002), breast cancer (Lark *et al*., 2005), colorectal carcinoma (Lark *et al*., 2003), oesophageal carcinoma (Miyazaki *et al*., 2003) and tongue cancer (Jiang *et al*., 2010). In a study of 55 matched pairs of breast cancer and corresponding normal tissue, a significant increase in FAK expression was observed by immunoblot analysis in the tumour cells with respect to normal tissue (Watermann *et al*., 2005). Analysis of matched normal tissue and primary human colorectal adenocarcinomas revealed higher levels of FAK in tumours, whereas reduced expression of FAK was found in liver metastases compared with the matched primary tumours (Ayaki *et al*., 2001). Consistent with this study, reduced FAK expression is associated with the progression of cervical cancer and pelvic lymph node metastasis (Gabriel *et al*., 2006). In contrast to these reports, elevated expression of FAK was shown to correlate with increased invasiveness and metastasis of HOSCC (Miyazaki *et al*., 2003). However, despite these disparities, all studies provide compelling evidence for an important role of FAK in tumour formation through the aberrant regulation of apoptotic events.

In addition to establishing the role of FAK in the different stages of metastatic progression, several reports have highlighted the important role of FAK as a mediator of tumourigenesis *in vivo* (Mclean *et al*., 2001; Mclean *et al*., 2004). A study examining malignant papillomas showed that the amounts of FAK were similar in the $fak^{+/-}$ and $fak^{+/+}$ mice, suggesting that despite the presence of only a single operational *fak* allele in the *fak* heterozygous mice, FAK protein expression was elevated during tumour progression (Mclean *et al*., 2001). Skin-specific

deletion of *fak* after formation of papillomas revealed that FAK is directly required for tumorigensis *in vivo* (Mclean *et al*., 2004). As the resultant reduced tumour progression is attributed to increased apoptosis after deletion of FAK (Mclean *et al*., 2004), these models support the prominent role of FAK in tumourigenesis.

Although a correlation between FAK mRNA levels and protein expression has been demonstrated (Golubovskaya *et al*., 2005), very few studies have examined the molecular events that lead to enhanced FAK expression. Analysis of the FAK promoter region revealed binding sites for NF-kappa β and p53 (Golubovskaya *et al*., 2004). Importantly, NF-kappa β induces, whilst, p53 inhibits transcription of FAK (Golubovskaya *et al*., 2004). Thus, as aberrant regulation of both these proteins is associated with tumourigenesis, it is not surprising that numerous reports have linked inappropriate expression and/or activity of FAK to the metastatic progression of cancer cells.

1.7 Human oesophageal squamous cell carcinoma (HOSCC) is a highly metastatic tumour

Under normal physiological conditions, the oesophagus is lined by stratified squamous epithelium (Katada *et al*., 1997). These epithelial cells are constantly exposed to a fluctuating environment that compromises both the chemical and physical integrity of the surface oesophageal keratinocytes. Consequently, the remodelling and turnover of oesophageal epithelial cells is a finely regulated mechanism. As apoptosis is fundamental to normal epithelial cell turnover (DeNardi and Riddell, 1991), the modulation of cell death in oesophageal squamous epithelium is of particular importance. Accordingly, the balance between cell proliferation and survival becomes disrupted in HOSCC, enabling oesophageal tumour cells to escape anoikis-mediated death and metastasize (Lin *et al*., 2009). Therefore, elucidating the molecular events that facilitate anoikis resistance in HOSCC is of particular importance, as HOSCC is a highly metastatic

tumour, which evades tissue-dependent restraints through multiple mechanisms (*Figure 1.5;* Tew *et al*., 2005).

HOSCC is a cancer of variable geographical distribution and is currently ranked the sixth most common cause of cancer death worldwide (McCabe and Dlamini, 2005). Due to insensitivity to the apoptosis-inducing ability of chemotherapeutic reagents, prognosis remains poor with the survival rate over 5 years just under 10% (Lerut, 1999; Shibakita *et al*., 2000; Tew *et al*., 2005). The highest mortality rates of the disease are in China, with an elevated occurrence of the disease in Western Europe, Japan, South America, South Africa and the former Soviet Union (Pickens and Orringer, 2003). Universally oesophageal cancer is more common in men and is currently the second most common cancer in the South African male population, and the most common cancer in the South African black male population (McCabe and Dlamini, 2005). Its prevalence also increases with age with a peak in incidence between 65 to 70 years of age (Lerut, 1999).

A multistage process has been proposed for the evolution of HOSCC, in which normal squamous epithelia progress from non-invasive precursor lesions, towards invasive cancer that metastasizes to the lymph nodes and other organs (Bird-Lieberman and Fitzgerald, 2009). With respect to diagnosis and prognosis, HOSCC tumours are placed into three categories based on their morphological appearance and tissue architecture. Briefly, well-differentiated tumours have a high level of keratinisation whilst, poorly-differentiated tumours have reduced keratin levels and pleomorphic nuclei (Grace *et al*., 1985). Tumours intermediate to the well- and poorly differentiated categories are classified as moderately-differentiated. Consequently, these clinicopathological categories are extremely broad, especially the moderately-differentiated category, into which many borderline cases are placed. However, the visual classification of oesophageal tumours may not reflect their metastatic potential, as *in vitro* studies show that oesophageal tumour cells from all three categories achieve metastasis (Robinson *et al*., 1982). Hence, it is evident that the visual classification of oesophageal tumours alone is not sufficient to predict oesophageal tumour prognosis.

Consequently, the molecular analysis of the protein alterations accompanying HOSCC progression is critical to provide a more consistent method of detecting and diagnosing this cancer.

1.7.1 Molecular events underlying anoikis resistance in HOSCC

HOSCC is highly resistant to apoptotic stimuli due the upregulation of anti-apoptotic proteins including Bcl-2, Bcl-x, and survivin, and the suppression of proapoptotic proteins including p53, BAX, Fas and FasL (Chang *et al*., 2005; Takikita *et al*., 2009). The loss of the tumour suppressor function of p53 is proposed to be an early event in the development of oesophageal carcinoma (Stoner and Gupta, 2001). Mutations between exon 5 and exon 8 are common in HOSCC (Gamieldien *et al*., 1998; Li *et al*., 2004), with 85% of the p53 mutations being GC to AT transitions and 69% located in CpG dinucleotides (Wang *et al*., 2003). In particular, mutations in codons 175, 248, and 273 of p53 facilitate the progression of HOSCC (Wang *et al*., 2003; Vrba *et al*., 2008). These single base mutations abolish the ability of p53 to transcriptionally activate apoptotic proteins, thereby, altering cell cycle control and suppressing apoptosis (Robert *et al*., 2000). Consequently, due to the reduced sensitivity to apoptotic stimuli, HOSCC tumours harbouring a "hot spot" p53 mutant are highly resistant to conventional chemotherapy (Inaba *et al*., 1986; Robert *et al*., 2000).

HOSCC has been shown to be nonresponsive to Fas-mediated apoptosis (Rigberg *et al*., 1999). Both Fas and FasL have been demonstrated to be downregulated at early stages during the development of HOSCC (Xue *et al*., 2006). FADD, on the other hand, was shown to be overexpressed in oesophageal carcinoma, whilst caspase-8 was strongly downregulated (Xue *et al*., 2006). In addition, Hughes and colleagues demonstrated that wt Fas was retained in cytoplasm and did not translocate to membrane (Hughes *et al*., 1997). Thus, perturbations in the Fas-mediated death cascade are pivotal to HOSCC progression.

In addition to deregulation of both intrinsic and extrinsic cell death pathways, aberrant regulation of cell adhesion-mediated signalling pathways is implicated in tumour development and metastasis of oesophageal cancer (Leu *et al*., 2000). HOSCC cell lines showed higher levels of αv integrin expression when compared to normal oesophageal tissue (Miller and Veale, 2001). In addition, expression of the α2 and β1 subunits was reduced (Miller and Veale, 2001). Moreover, overexpression of FAK has been shown to be correlated with increased invasiveness of HOSCC (Miyazaki *et al*., 2003). Hence, as FAK coordinates p53 and Fas-dependent death processes, these studies suggest that aberrant regulation of FAK may be central to anoikis resistance in HOSCC.

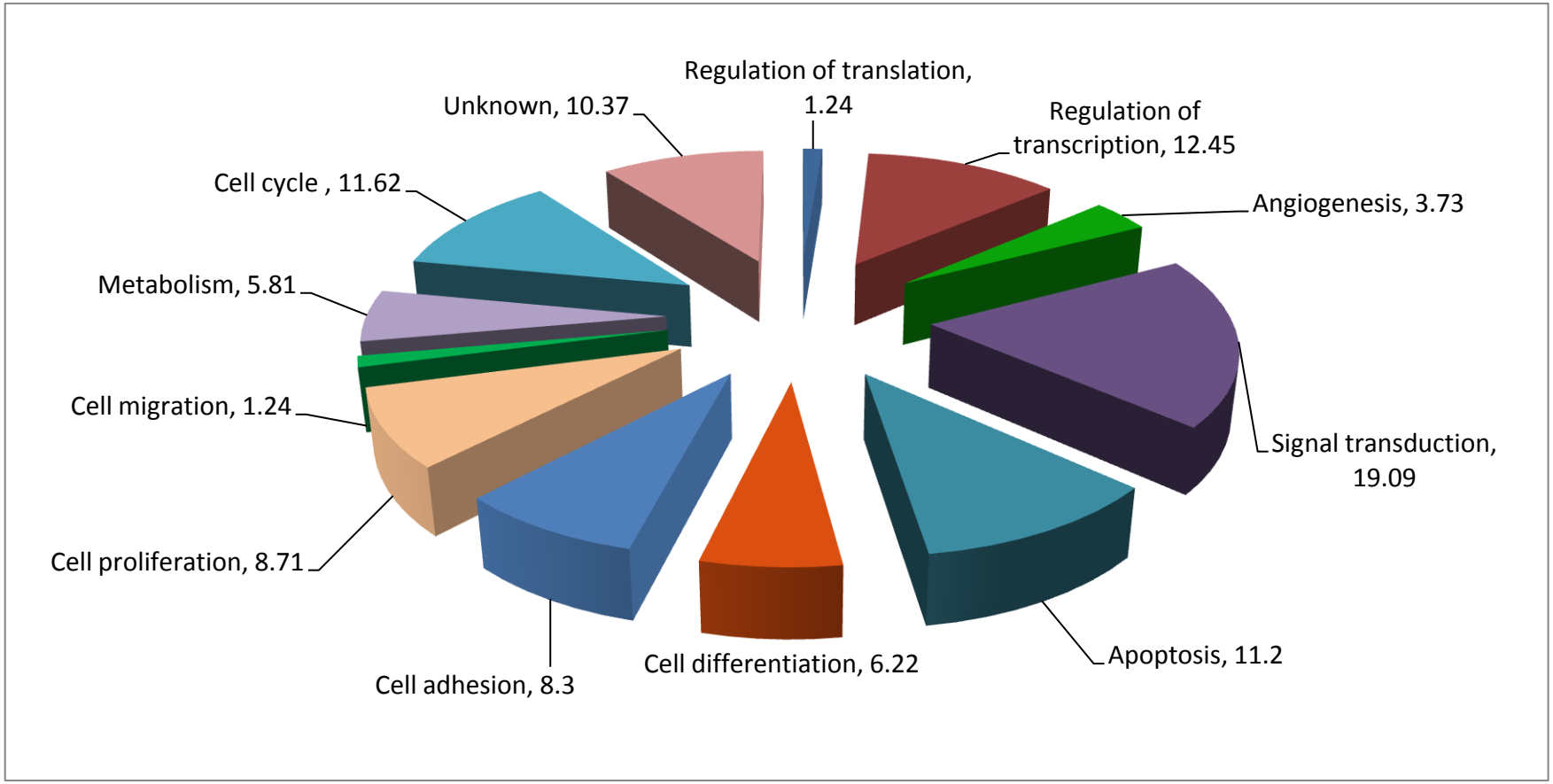

Figure 1.5: Biological functions of deregulated proteins in HOSCC. A large portion of deregulated proteins in HOSCC are involved in signal transduction, apoptosis and cell adhesion. Adapted from Lin *et al.*, (2009)

1.8 Aims

Although aberrant regulation of FAK has been implicated in anoikis resistance, the details of FAK-dependent anoikis regulation are cryptic. Pertinently, an important role of FAK in HOSCC metastasis has been demonstrated (Miyazaki *et al*., 2003). Thus, with the aim of characterising the molecular events that underpin anoikis resistance in HOSCC, we sought to:

i. Establish the relative expression and cellular distribution of the key anoikis-related intermediates, FAK, p53 and Fas in a system of moderately differentiated HOSCC cell lines.
ii. Ascertain whether a relationship exists between FAK-dependent signalling and apoptotic sensitivity in HOSCC.
iii. Establish whether the interaction between the major apoptotic constituents and FAK underlies anoikis resistance in HOSCC.

Chapter 2

Monitoring of typical anoikis-related intermediates in human oesophageal squamous cell carcinoma cell lines

2.1 Introduction

In the absence of cell-ECM contact, both the extrinsic and intrinsic apoptotic pathways have been implicated in the induction of anoikis (Kurenova *et al*., 2004; Golubovskaya *et al*., 2005). Fundamental to this anoikis-related regulation is FAK, a vital mediator of survival signalling at sites of cell contact (Schaller *et al*., 1992; van Nimwegen and van der Water, 2007). Adhesion to ECM components including fibronectin (Zhang *et al*., 2004 (a)) and collagen type IV (Sanders and Basson, 2000; Crowe and Ohannessian, 2004) increase activation of FAK by Tyr397 phosphorylation. Accordingly, increased Tyr397-phosphorylated FAK is associated with enhanced cell adhesion (Guan and Shalloway, 1992; Kamarajan and Kapila, 2007). In addition to regulating cell adhesion-mediated signalling, activation of FAK, through Tyr397 autophosphorylation, regulates processes critical to embryonic development including migration and proliferation. Consequently, FAK-null embryos die at day 8.5 and exhibit impaired vascular development, endothelial migration and tube formation, processes under stringent regulation by apoptosis (Ilic *et al*., 1995). Accordingly, the inhibition of FAK expression with oligonucleotides has been shown to induce cell rounding, detachment and apoptosis, whilst, constitutively active FAK suppresses anoikis and induces tumour formation in nude mice (Lim *et al*., 2008). Therefore, due to its central role in coordinating cell adhesion and apoptotic events, aberrant regulation of FAK is implicated as the key cell adhesion-related event involved in the acquisition of anoikis resistance (Frisch *et al*., 1996; Duxbury *et al*., 2004; Zhang *et al*., 2004 (a); Kamarajan and Kapila, 2007).

Survival signals transduced via ECM-activated FAK are reported to suppress apoptotic stimuli through the activation of the PI3K/PKB pathway (Sonoda *et al*., 1999). However, a report in a substrate-dependent squamous cell carcinoma cell

line revealed that ECM-mediated survival signals were independent of FAK-dependent activation of PKB (Zhang *et al*., 2004 (a)). Notably, increased activation of FAK by ECM influence, led to the suppression of p53-dependent apoptosis (Zhang *et al*., 2004 (a)). Furthermore, under conditions of ECM deprivation and reduced FAK-dependent signalling, cells undergo anoikis through a p53-mediated pathway (Ilic *et al*., 1998; Zhang *et al*., 2004 (a)). A specific interaction between the N-terminal of FAK and p53 has been demonstrated to inhibit p53 activity by enhancing Mdm-2-dependent ubiquitination of p53, or alternatively, inhibiting p53 transcriptional activity (Golubovskaya *et al*., 2008; Lim *et al*., 2008). Moreover, p53 regulates FAK at a transcriptional level, as p53 binding sites have been identified on the FAK promoter (Golubovskaya *et al*., 2005). Hence, the alternative survival role of FAK in the regulation of the p53-mediated intrinsic apoptotic pathway may facilitate the survival of tumour cells in the absence of cell contact.

In addition to the multiple levels of regulation identified between p53 and FAK, a functional link between FAK and Fas-mediated apoptosis has also been demonstrated (Kurenova *et al*., 2004; Kamarajan *et al*., 2010). The interaction between the Fas receptor and its associated ligand (FasL) initiates the death receptor pathway of apoptosis (Nagata, 1999; Aoudjit and Vuori, 2001). Both Fas and FasL were upregulated following detachment from the ECM and a Fas antagonistic antibody protects SCC cells from FAK-mediated anoikis (Ishida *et al*., 2003; Kamarajan *et al*., 2010). Moreover, recent studies have shown that caspase-8 inhibition abrogates anoikis, further implicating Fas-mediated apoptosis in anoikis induction (Kamarajan *et al*., 2010). In addition, p53 alters Fas expression by activating a p53-responsive region on the Fas promoter (Munsch *et al*., 2000; Zalcenstein *et al*., 2003). Consequently, interplay between the two major apoptotic constituents and FAK is critical to anoikis-related regulation.

Nonetheless, although these reports link aberrant regulation of FAK to anchorage-dependent survival, the mechanism underlying resistance to anoikis remains obscure. Moreover, while some information has been reported regarding the

prognostic significance of FAK, p53 and Fas in HOSCC progression (Miyazaki *et al*., 2003; Xue *et al*., 2006), there are no published reports on the role of these intermediates in anoikis-related signalling events. Furthermore, HOSCC progression is associated with constitutive activation of FAK, aberrations in the Fas-mediated death cascade and loss of the tumour suppressor function of p53 (Miyazaki *et al*., 2003; Xue *et al*., 2006). Thus, with the aim of characterising the molecular events that underpin anoikis resistance in HOSCC, the expression and localisation of the key anoikis-related intermediates was established in a series of moderately differentiated HOSCC cell lines.

2.2 Material and Methods

2.2.1 Cell lines

The five moderately differentiated human oesophageal squamous carcinoma cell lines; WHCO1, WHCO3, WHCO5, WHCO6 (Veale and Thornley, 1989) and SNO (Bey *et al*., 1976) were obtained from the Cell Biology Laboratory, School of Molecular and Cell Biology, University of the Witwatersrand. The HT29 cell line harbouring the mt p53-R273H (Bossi *et al*., 2006), derived from human colon adenocarcinoma and the caspase-3 null MCF7 cell line, derived from human breast carcinoma was supplied by The America Type Culture Collection (ATCC). Cell lines were cultured in 10 cm tissue culture dishes (Corning) and maintained in Dulbecco's Modified Eagles Medium (DMEM) (Appendix 1.1.1)/Hams F12 (3:1) (Appendix 1.1.1), supplemented with 10% Foetal Calf Serum (FCS) (Highveld Biologicals). Cultures were maintained in a humid, 37 °C incubator with 5% carbon dioxide atmosphere.

Once cells achieved a confluence of 80%, the medium was aspirated and the monolayer of cells washed with the sterile phosphate buffered saline (PBS) (Appendix 1.1.3). 2 ml of a trypsin (Gibco BRL) and ethylenediaminetetra-acetic acid (EDTA) (BDH Laboratory reagents) solution was then dispensed into the culture vessel and placed into an incubator at 37 °C for 5 min. Medium containing 10% FCS was then added to the cell suspension and grown as above.

2.2.2. Total RNA extraction

Total RNA was isolated from the HOSCC cell lines using the Trizol® reagent (GibcoBRL). Cells were grown to a confluence of 80%. Serum containing media was aspirated and the cells rinsed three times in PBS. Adhered cells were covered in a thin film of PBS, scraped from the culture dish and added to an Eppendorf. Excess PBS was removed by centrifugation at 1145 X *g* in a TOMY HF-120 centrifuge for 3 min. The supernatant was replaced with 1 ml Trizol reagent and vortexed briefly. The homogenized sample was incubated at room temperature for 5 min. 200 µl of chloroform was added, mixed well by vigorous shaking and incubated at room temperature for a further 3 min. Samples were centrifuged at 12

000 x *g* at 4 °C for 15 min to separate phases. The aqueous phase was transferred into a fresh Eppendorf. 500 µl of isopropyl alcohol was added to the aqueous phase, mixed thoroughly be shaking for 15 sec and incubated at room temperature for 10 min. Samples were centrifuged at 12 000 x *g* at 4 °C for 10 min to pellet RNA. The supernatant was removed, 1 ml 75% ethanol added to the Eppendorf and vortexed briefly to wash the pellet thoroughly. Samples were centrifuged at 12 000 x *g* at room temperature for 5 min to re-pellet RNA. The supernatant was removed and the pellet air-dried at room temperature for 10 min. The pellet was dissolved in dH_2O (30-100 µl, depending on yield) by gentle pipetting, incubated at 60 °C for 10 min and stored at -70 °C). Integrity of the RNA was established by electrophoresis of the RNA on a 1 % agarose gel (Appendix 1.4.1).

2.2.3 Reverse transcription

Once the integrity of the RNA was confirmed, the RNA was reversed transcribed into cDNA. 2 µl of random primers (Oligo T random hexamers) were added to 2 µl of RNA extracted from the HOSCC cell lines, and incubated at 60 °C for 10 min. Samples were placed on ice for 5 min and centrifuged at 1145 x *g* for 1 min. The following was then added to the Eppendorf: 5 µl 5X MMLV-RT buffer, 0.6 µl RNAsin, 1 µl MMLV-RT and 12.5 µl dH_2O. The samples were incubated at 37 °C for 1 hr and the reaction was terminated by incubation at 90 °C for 5 min. A phenol:chloroform (25:24) solution was added to the sample and vortexed briefly. The samples were centrifuged at 12 000 x *g* at room temperature for 5 min. The aqueous phase was then transferred into a fresh Eppendorf, 70 µl chloroform was added to the Eppendorf and centrifuged as above. The aqueous phase was transferred into a fresh Eppendorf and the volume measured by pipetting. Three times the volume of 100 % ethanol and 10 % sodium acetate was added. The sample was precipitated overnight at -20 °C. Samples were centrifuged at 12 000 x *g* at 4 °C for 20 min. The supernatant was removed and the pellet air-dried at room temperature for 1 hr and resuspended in 10 µl dH_2O or 1- 2 hr. Samples were stored at -70 °C. cDNA was visualized on a 1 % agarose gel (Appendix 1.4.1).

2.2.4 Polymerase chain reaction (PCR)

As interplay between FAK and the major apoptotic constituents is the primary focus of this study, primers were designed to amplify the FERM domain, the region of FAK involved in protein-protein interactions. Primers used to amplify the FERM domain were as follows:

Forward primer 5' GGACAGTCACAAAGTAAAGC 3'

Reverse primer 5' ATTGTCTAAATGTTTGTTGG 3'

Thermal cycle conditions included denaturation at 95 °C for 10 min and 32 cycles of denaturation at 95 °C for 0.5 - 1 min; annealing at 56 °C for 0.5 - 1min and extension at 72 °C for 1min with a final elongation at 72 °C for 10min. PCR products were visualized on a 1 % agarose gel following ethidium bromide staining. Fragments were sent to Inqaba Biotech for sequencing. A representative sequence trace is included in Appendix 3.1.

2.2.5 Antibodies

FAK, p53 and Fas were specifically detected with rabbit polyclonal antibodies obtained from SantaCruz Technology. Monoclonal mouse anti-pFAK(Tyr397) (Millipore) was used to detect Tyr397 autophosphorylation of FAK. Polyclonal horseradish peroxidase (HRP)-bound anti-rabbit secondary antibody (Separations, SA) and fluoroscine isothiocyanate (FITC)-conjugated anti-rabbit secondary antibody (Chappel, USA) were used in the immunoblot and immunofluorescence experiments respectively.

2.2.6 Protein estimation assay

A protein estimation assay was performed based on the protocol proposed by Bramhall *et al*. (1969). Cells were lysed in RIPA buffer (Appendix 1.3.2) for 30 min at 4 °C. 2 µl of the resultant lysate was spotted onto hydrated filter paper disks (Whatman) and allowed to dry. Bovine serum albumin (BSA) (BDH Laboratory reagents) was solubilized in single lysis buffer to create the protein standard concentrations; 1 µg, 3 µg, 6 µg, 12 µg, 16 µg and 20 µg. The protein standards were spotted onto the disk to create a standard curve. Paper disks were dried in the fume hood. Samples were fixed to the support medium with 7.5 % trichloroacetic acid (TCA) for 45 min. Excess acid was removed with 0.25 %

Coomasie Blue (Appendix 1.2.1) and then stained in Coomasie Blue for 1 hr. The filter paper was destained with a destain solution (Appendix 1.2.2) for 1 hr. Stained samples were cut out of the filter paper and incubated in elution solution (Appendix 1.2.3) overnight. The following day, the absorbance of the elution solution was determined at 596nm (Beckman Du®64 Spectrophotometer).

2.2.7 Immunoblot analysis

40 µg of protein per lane was separated on a 10% SDS-PAGE gel (Appendix 1.4.4) according to Laemmli (1970) at a constant current of 18 milliamperes (mA) with electrophoresis running buffer pH 8.3. Samples were electro-blotted onto a nitrocellulose membrane (Sartorius), using the Biorad mini trans-blot system at 400 mA for 3 hr (4 °C) in Western Blot Transfer Buffer (Appendix 1.5.1). After transfer was complete, the nitrocellulose membranes were rinsed twice with PBS (see Appendix 1.1.3), and stored overnight at 4 °C. Transfer efficiency was checked by staining the gel with Coomasie Blue (Appendix 1.2.1). Non-specific binding sites on the membrane were pre-blocked in blocking buffer (Appendix 1.5.2) for 1 hr. Blots were incubated with anti-FAK for 1 hr or overnight with p-FAK(Tyr397) in 1 % BSA. Washing was performed 6 times at 5-min intervals with PBS to remove any residual antibody. Following incubation in HRP-conjugated secondary membranes were washed 6 times at 5 min intervals with PBS before being exposed to the SuperSignal West Pico Chemiluminescent working solution (Appendix 1.5.3), from the West Pico Chemiluminescent Substrate Kit (Pierce, USA) for 5 min. Blots were sealed in polyethylene wrap and exposed to hyperfilm™ MP autoradiography film (Amersham, UK) for 10 min. Film was developed in developer (see Appendix 1.5.4) for 5 min, rinsed briefly in H_2O before fixing (see Appendix 1.5.5) for 5 min. Each immunoblot was repeated three times.

2.2.8 Indirect immunofluorescence

The visual determination of FAK, p53 and Fas was determined by indirect immunofluorescence. Cultured cells were washed four times with cold PBS, fixed with 4% paraformaldehyde (Appendix 1.6.1) for 30 min and washed twice with PBS. Following permeabilisation with 0.25 % Triton X-100 for 10 min, cells

were rinsed twice with PBS and allowed to dry partially. A fluid barrier created by the DAKO pen allowed the separate incubation of antibodies. Fixed cells were incubated with anti-FAK (1:250), anti-p53 (1:500) and anti-Fas (1:200) antibody for 1 hr at room temperature. Following incubation with the anti-rabbit fluoroscine isothiocyanate-conjugated secondary antibody (1:250) for 1 hr, Elvanol mounting agent (Dupont) was added to the wells and cells were viewed at 400 X magnification under a Zeiss LSM 410 confocal microscope (FITC excitation 490, emission 525). Immunofluorescence assays were repeated three times.

2.2.9 Co-immunoprecipitation

5 X 10^6 cells were lysed in RIPA buffer (Appendix 1.3.2) for 30 min at 4 °C. The lysates containing 350 µg protein were incubated with 3 µl of anti-integrin β1 at 4 °C for 6 hr. Then 20 µl of protein G-Sepharose beads were added to each lysate at 4 °C for overnight. The protein G-FAK-β1 complex was centrifuged at 3000 r.p.m. in a Sorvall® MC 12 V centrifuge for 2 min. The supernatant was decanted, and 800 µl Tris.HCl buffer pH 8.0 added. The supernatant was decanted and an equal volume (45 µl) of double lysis buffer (Appendix 1.3.1) was added to the pellet. The suspension was boiled for 5 min and centrifuged for 10 min at 12000 r.p.m. in a Sorvall® MC 12 V centrifuge. Samples were separated by SDS-PAGE and blotted onto nitrocellulose membranes (See 2.2.7). Blots were incubated in anti-FAK and anti-pFAKTyr397 to determine the relative association with integrin β1.

2.2.10 Densitometry

Labworks TM Image Acquisition and Analysis software (Labworks version 4.5) was used for densitometric analysis to semi-quantitatively determine the concentration level of protein in the western blots.

2.2.11 Image Capturing

Images were captured on a Hewlard Packard Scanjet 4400c series scanner. Brightness, contrast and magnification of all images were standardised using Corel Paint Shop Pro X.

2.3 Results

2.3.1 HOSCC cell lines express Tyr397-phosphorylated FAK

FAK was originally isolated as a highly tyrosine phosphorylated tyrosine kinase from v-Src transformed chicken embryo fibroblasts, and later in epithelial tissues, including oesophageal keratinocytes (Schaller *et al*., 1992; Whitney *et al*., 1993). Pertinent to anoikis-related events, overexpression of FAK correlates with enhanced invasiveness and metastasis of oesophageal cancer (Miyazaki *et al*., 2003). As anoikis-related signalling has never been investigated in HOSCC, two control cells with documented resistance to anoikis were included in the study. Specifically, the colon adenocarcinoma HT29 cell line as it is highly resistant to apoptotic stimuli due to harbouring the transcriptionally inactive p53 mutant R273H (Lin-Lee *et al*., 2001; Bossi *et al*., 2006), and the MCF-7 cell line as it lacks functional caspase-3 and is therefore nonresponsive to caspase-related apoptotic events (Jánicke *et al*., 1998; Mooney *et al*., 2002).

Transcription of the *fak* gene in the HOSCC and control cell lines was established by RT-PCR analyses. The success of the RNA extraction was confirmed by the presence of bands at 650bp and 1500bp resolved by agarose gel electrophoresis, representing the 18S and 28S subunits of ribosomal RNA subunits respectively (*Figure 2.1A*). Reverse transcription yielded a smear indicative of a broad range of different sized cDNA transcripts (*Figure 2.1B*). Sequence analysis of the resultant 476bp fragment confirmed the integrity of the FERM domain across the cell lines (*Figure 2.2*).

Consistent with previous studies (Schaller *et al*., 1992; Ilic *et al*., 1998; Golubovskaya *et al*., 2005), following detection with a polyclonal anti-rabbit FAK antibody, a band at 125 kDa was detected by immunoblot analysis across cell lines (*Figure 2.3A*). Despite standardised protein loading of 20 μg, densitometric analysis revealed differential FAK expression across the cell lines, with the WHCO6, SNO and WHCO5 cell lines having higher FAK expression relative to

the other four cell lines (*Figure 2.3B*). However, with respect to the seven cell lines, the WHCO6 cell line had the highest FAK expression overall. Both the WHCO1 and WHCO3 cell lines had the lowest FAK protein expression, at 5 and 4.5 fold less than the WHCO6 cell line respectively.

The structure of the FAK protein includes: the N-terminal domain with the primary autophosphorylation site, Tyr397, the central catalytic kinase domain and the C-terminal domain containing the focal adhesion targeting (FAT) subdomain (Parsons, 2003). The Tyr397 autophosphorylation site of FAK is critical to FAK-dependent survival signalling (Sonoda *et al*., 1999; Parsons, 2003). As FAK was differentially expressed across the seven cell lines (*Figure 2.3B*), we established whether there was a relationship between Tyr397 phosphorylated-FAK and FAK concentration in these cell lines. Using the same whole cell extracts as above, a monoclonal antibody specific for the Tyr397 autophosphorylation site was used to detect Tyr397-phosphorylated FAK across the cell lines (*Figure 2.3A*). Despite standardised loading of 80 μg, Tyr397-phosphorylated FAK was only detected in the cell lines with the highest FAK expression (WHCO6 and SNO) (*Figure 2.3C*). This raised the possibility that the other cell lines were resistant to FAK phosphorylation. Alternatively, due to the specificity of the antibody and lower level of FAK expression in the other cell lines, the level of pFAKTyr397 was below the detection level of the monoclonal antibody. Hence, to ascertain whether pFAKTyr397 was dependent on FAK concentration, we assessed if co-immunoprecipitation of FAK would enable the detection of the autophosphorylation site. Accordingly, pFAKTyr397 was detected in FAK-immunoprecipitated samples of the WHCO1, WHCO3, WHCO5, MCF7 and HT29 cell lines (*Figure 2.4*). Thus, the HOSCC, MCF7 and HT29 cell lines all express Tyr397-phosphorylated FAK. However, pFAKTyr397 was only detectable by immunoblot in the cell lines with the highest FAK expression (WHCO6 and SNO).

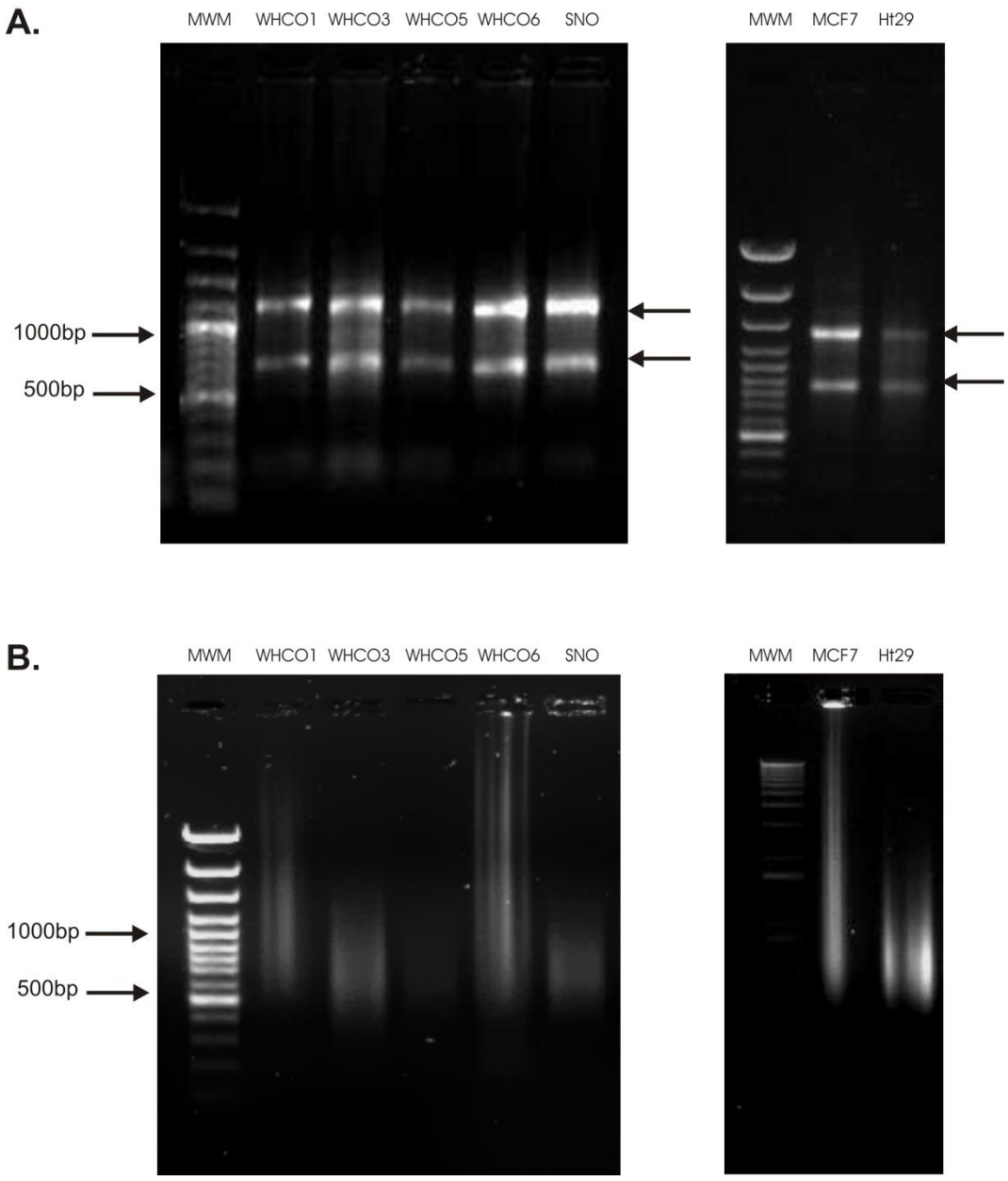

Figure 2.1: Efficacy of RNA extraction and reverse transcription reaction in the HOSCC, MCF-7 and HT29 cell lines. A) The integrity of the RNA was established by electrophoresis of the RNA on a 1% agarose gel. Two bands representing 28S and 18S (black arrows) RNA is clearly evident in the cell lines. B) The presence of cDNA was verified by the electrophoresis of the cDNA on a 1% agarose gel. The smear is indicative of cDNA. MWM – GeneRuler^{TM} 1kb DNA ladder

A.

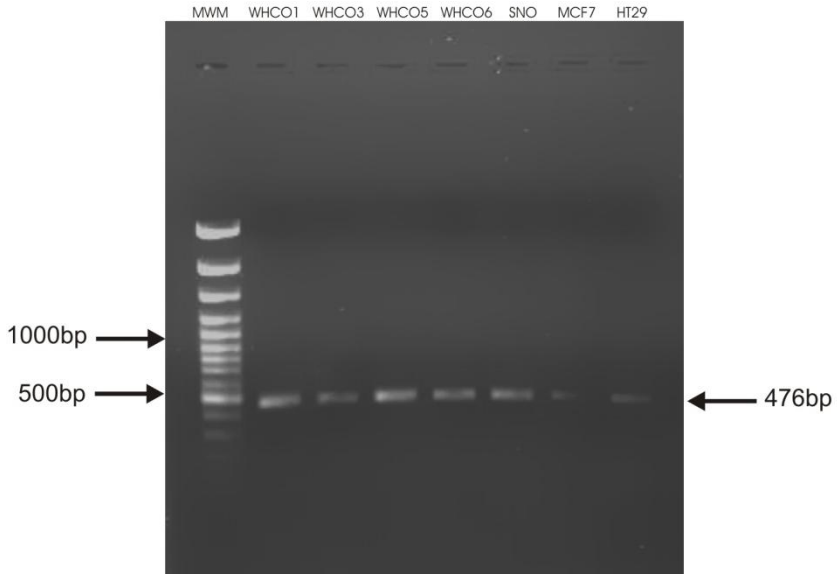

B.

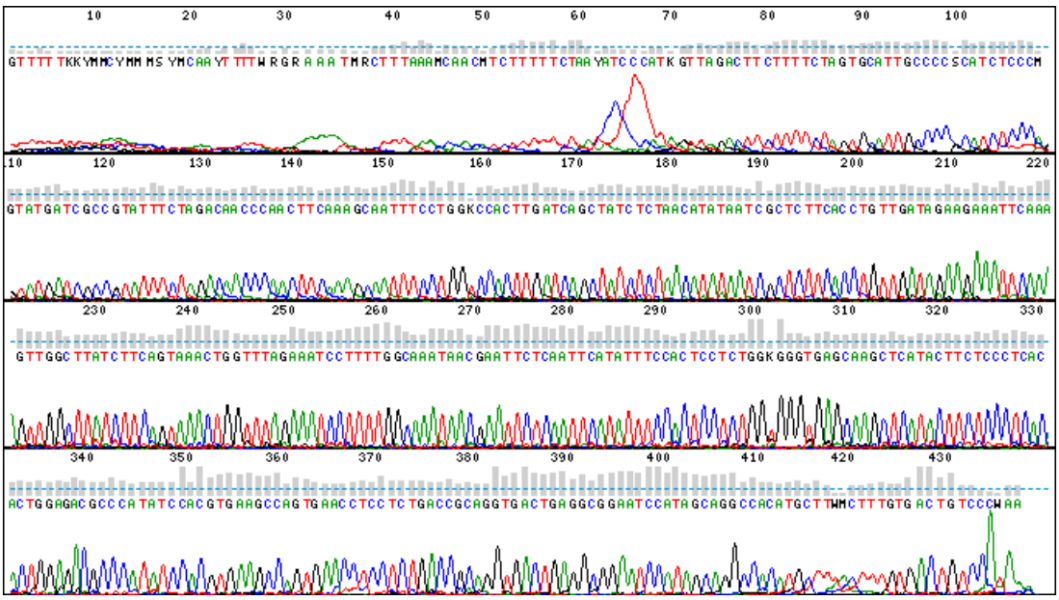

Figure 2.2: The FERM domain is intact in HOSCC cell lines. A) RT-PCR products were resolved by 2 % agarose gel electrophoresis following EtBr staining (10 µg/ml). A band of 476 bp was observed in HOSCC, MCF7 and HT29 cell lines. B) Sequence analysis of the FAK transcript revealed the FERM domain is intact in HOSCC, MCF7 and HT29 cell lines. MWM – GeneRuler^{TM} 1kb DNA ladder

A.

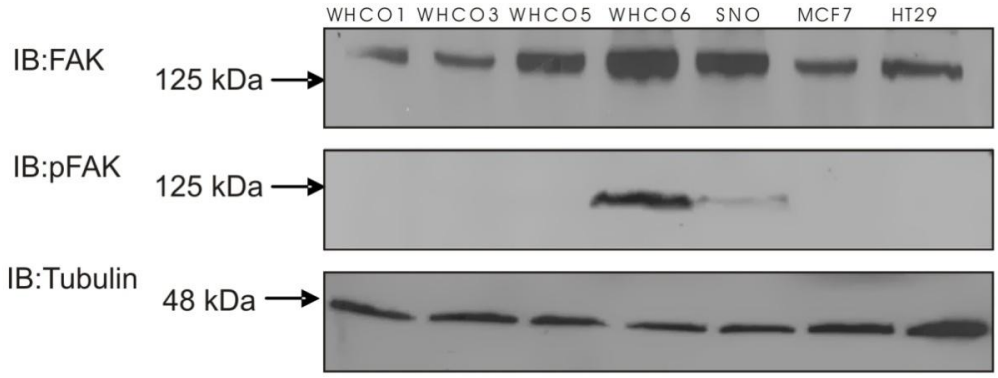

B.

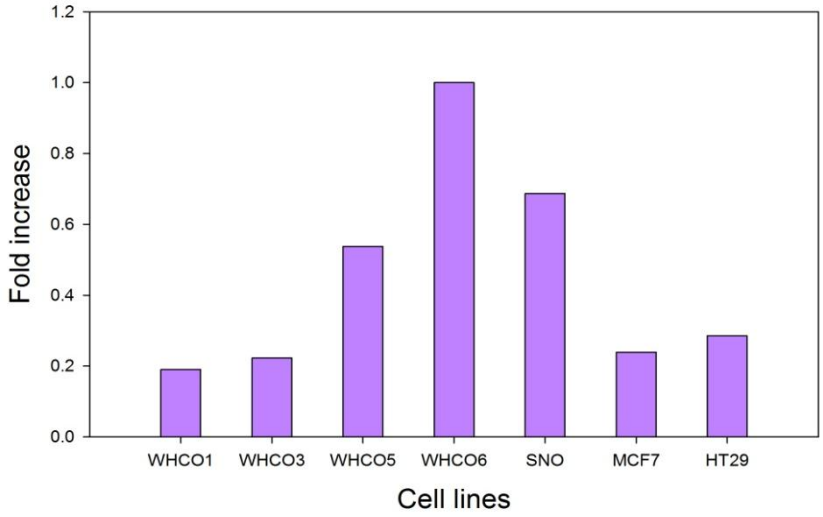

C.

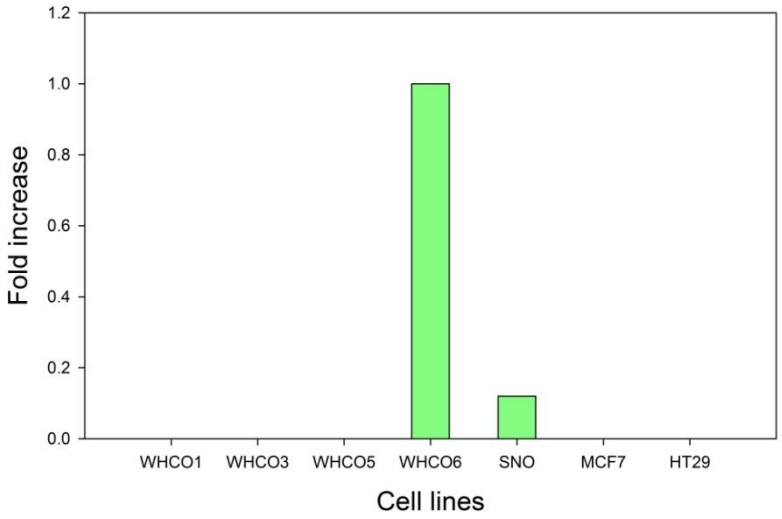

See next page for legend.

Figure 2.3: HOSCC cell lines differentially express Tyr397-phosphorylated FAK. A) FAK was detected at 125kDa in the HOSCC series of cell lines, as well as the MCF7 and HT29 control cell lines. A monoclonal anti-phosphoTyr397 antibody was used to detect autophosphorylation of FAK under normal tissue culture conditions. pFAKTyr397 was only detected in the WHCO6 and SNO cell lines by immunoblot. The tubulin loading control demonstrates equal protein loading of the whole cell extracts. B) Densitometric analysis revealed that the WHCO6 cell line expressed the highest level of FAK, whereas the lowest FAK expression was in the WHCO1 and WHCO3 cell lines respectively. C) The highest level of pFAKTyr397 was detected in the WHCO6 cell line. Note: the expression levels are relative to the maximum per 20µg (FAK) and 80µg (pFAKTyr397) of protein in the WHCO6 cell line. The western blots were repeated three times (*See Appendix 2 for representative western blot of entire gel*).

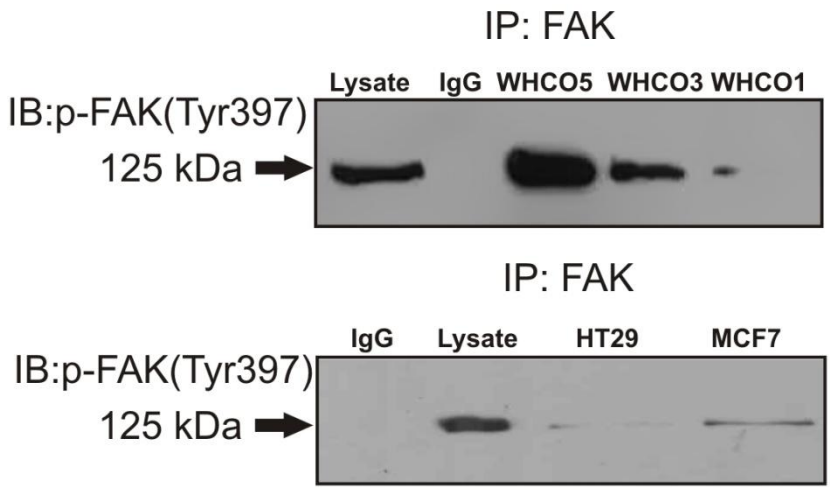

Figure 2.4: HOSCC, MCF7 and HT29 cell lines express Tyr397-phosphorylated FAK. pFAKTyr397 was detected in the FAK-immunoprecipitates in the WHCO1, WHCO3, WHCO5, MCF7 and HT29 cell lines. A whole cell lysate was included for each immunoblot to demonstrate the specificity of the immunoprecipitation reaction. A negative control (protein G sepharose + 2µl anti-FAK antibody) was included to demonstrate absence of IgG chains at the size of FAK (125kDa).

2.3.2 FAK localises to the cytoplasm in HOSCC cell lines

In other cell types, FAK is a cytoplasmic protein localised to sites of focal contact by integrin clustering (Schaller *et al*., 1994; Sonoda *et al*., 1999). In the HOSCC, MCF7 and HT29 cell lines under normal tissue culture conditions, FAK was localised primarily to the cytoplasm (*Figure 2.5*). However, even though FAK was named according to its localisation at focal adhesions, several reports have shown the accumulation of FAK in the nucleus (Levkau *et al*., 1998; Lobo and Zachary, 2000; Golubovskaya *et al*., 2005). Consistent with previous reports (Lobo and Zachary, 2000), nuclear localisation of FAK was evident in the WHCO1, WHCO3 and HT29 cell lines (*Figure 2.5*).

2.3.3 FAK and integrin β1 association in HOSCC cell lines

The direct interaction between the FERM domain of FAK and the cytoplasmic tail of the β1 integrin subunit is an important regulator of Tyr397 phosphorylation and localisation of FAK (Schaller *et al*., 1994). As we have shown that the protein-protein interacting domain of FAK is intact in the HOSCC cell lines (*Figure 2.2*), we assessed by co-immunoprecipitation whether a similar association is present in the HOSCC cell lines. We clearly show in the representative cell lines (WHCO6 and SNO) an association between FAK and integrin β1 (*Figure 2.6A*). The direct interaction between the FERM domain of FAK and the cytoplasmic tail of the β integrin subunit results in the rapid autophosphorylation of Tyr397 (Schaller *et al*., 1994). Accordingly, in the representative cell lines (WHCO6 and SNO), an interaction between integrin β1 and Tyr397-phosphorylated FAK was detected (*Figure 2.6B*).

WHCO1

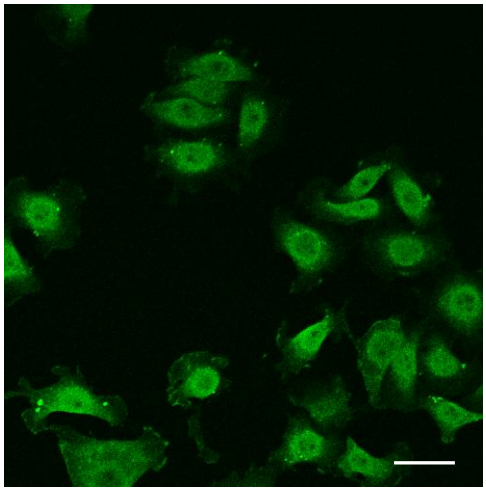

WHCO3

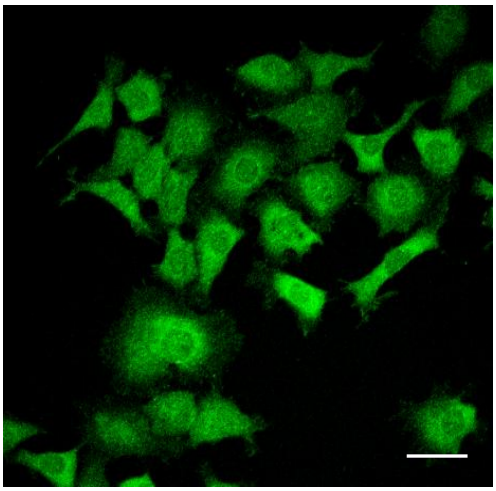

WHCO5

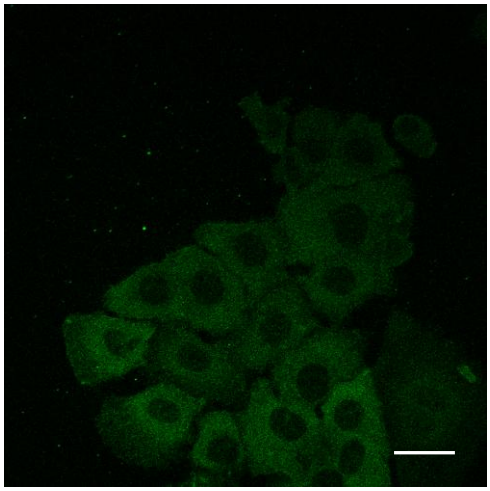

WHCO6

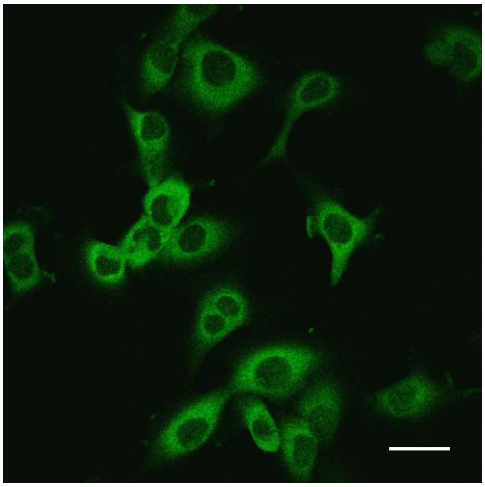

SNO

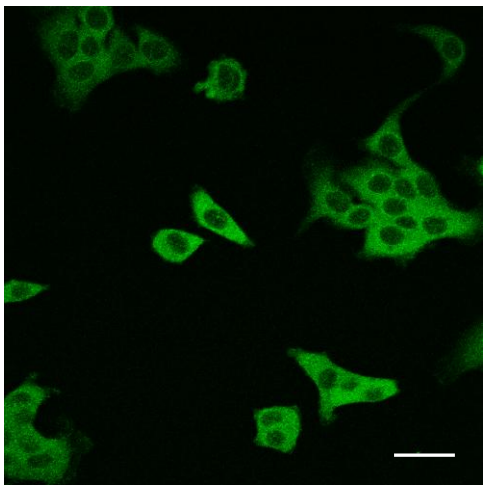

HT29

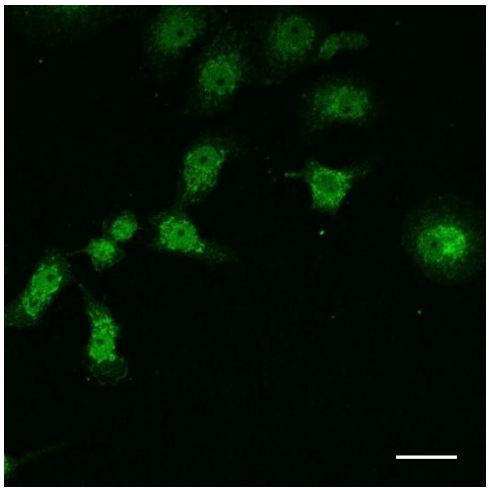

MCF7 Negative control

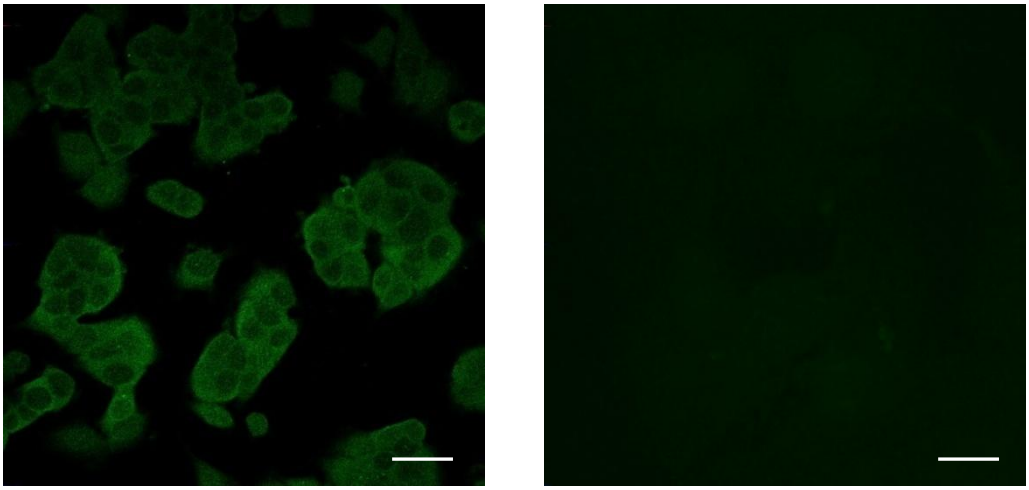

Figure 2.5: FAK localises primarily to the cytoplasm in the HOSCC, HT29 and MCF7 cell lines. Although FAK was primarily localised to the cytoplasm in HOSCC cell lines, a small proportion was detected in the nucleus in the WHCO1 and WHCO3 cell lines under normal tissue culture conditions, following immunofluorescent detection. Nuclear FAK was observed in the colon adenocarcinoma HT29 cell line harbouring mt p53-R273H. Negligible diffuse staining was observed in the negative control (excluding anti-FAK antibody). Scale bar = 25μm

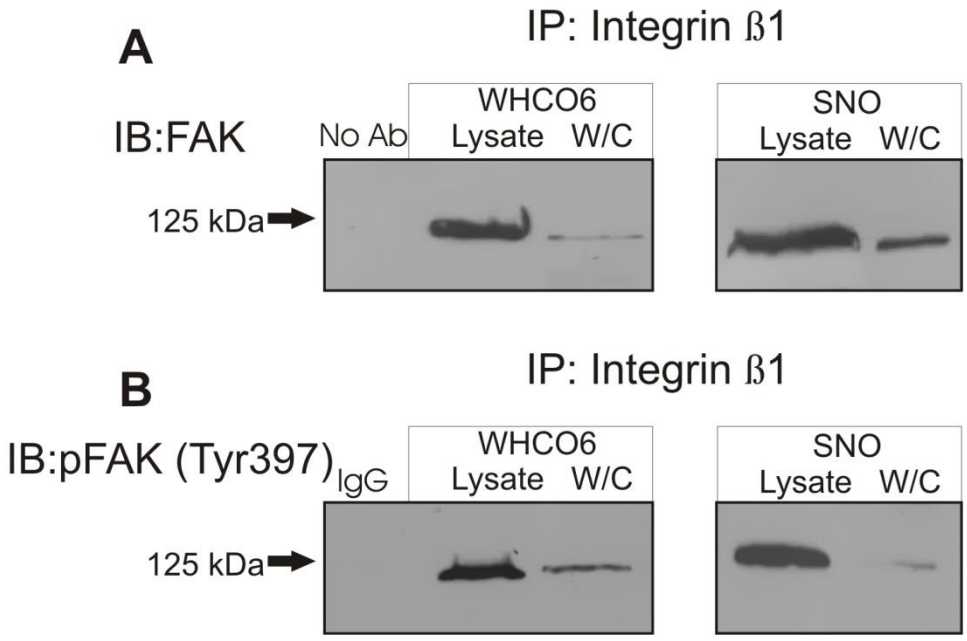

Figure 2.6: Integrin β1 associates with Tyr397-phosphorylated FAK in HOSCC cell lines. A) FAK was detected in complex with immunoprecipitated integrin β1 in the WHCO6 and SNO cell lines. B) Tyr397-phosphorylated was detected by immunoblot analyses in the anti-integrin β1 immunoprecipitates. A whole cell (W/C) WHCO6 loading control was included for each immunoblot to illustrate the specificity of the immunoprecipitation reaction. A negative control (protein G sepharose + 2µl anti-integrin β1 antibody) was included to demonstrate absence of IgG chains at the size of FAK (125kDa).

2.3.4 HOSCC cell lines express p53

In vitro, abrogation of FAK-dependent signalling induces p53-dependent apoptosis (Golubovskaya *et al*., 2005; Golubovskaya *et al*., 2008). Western blot analysis of untreated cell lysates revealed that all of the HOSCC cell lines express p53 (*Figure 2.7A*). Under standard tissue culture conditions, the WHCO6 cell line had the highest p53 expression, 1.2 fold higher than that of the SNO cell line and 1.3 fold higher than the HT29 cell line (*Figure 2.7B*). The lowest p53 expression was observed in the wt p53 MCF7 caspase-3 null control cell line, on average approximately 5 fold less than the WHCO6 and SNO cell lines (*Figure 2.7B*).

2.3.5 p53 is localised to the nucleus in HOSCC cell lines

Nuclear import or retention of p53 is critical for its ability to control growth inhibition or induction of apoptosis at a transcriptional level (Ryan *et al*., 1994; Knippschild *et al*., 1996; Moll *et al*., 1996; Golubovskaya *et al*., 2008). Immunofluorescence clearly revealed in all the HOSCC cell lines that p53 is localised to the nucleus (*Figure 2.8*), supporting the role of p53 as a transcription factor in these cell lines. Similar to the HOSCC cell lines, in the HT29 cell line harbouring the mt p53-R273H, p53 was localised to the nucleus. Studies in breast cancers have reported wild-type p53 being sequestered in the cytoplasm, suggesting that defects in the nucleocytoplasmic transport of p53 facilitates tumourigenesis in these cells (Ogretmen and Safa, 1997). Consistent with this previous report, p53 was localised primarily to the cytoplasm in the MCF7 cell line (*Figure 2.8*).

A.

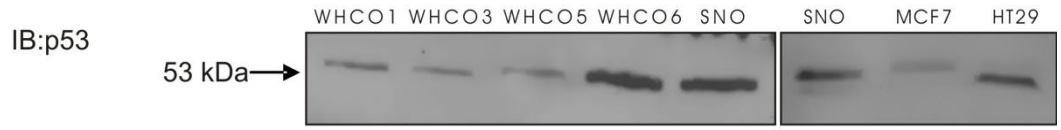

B.

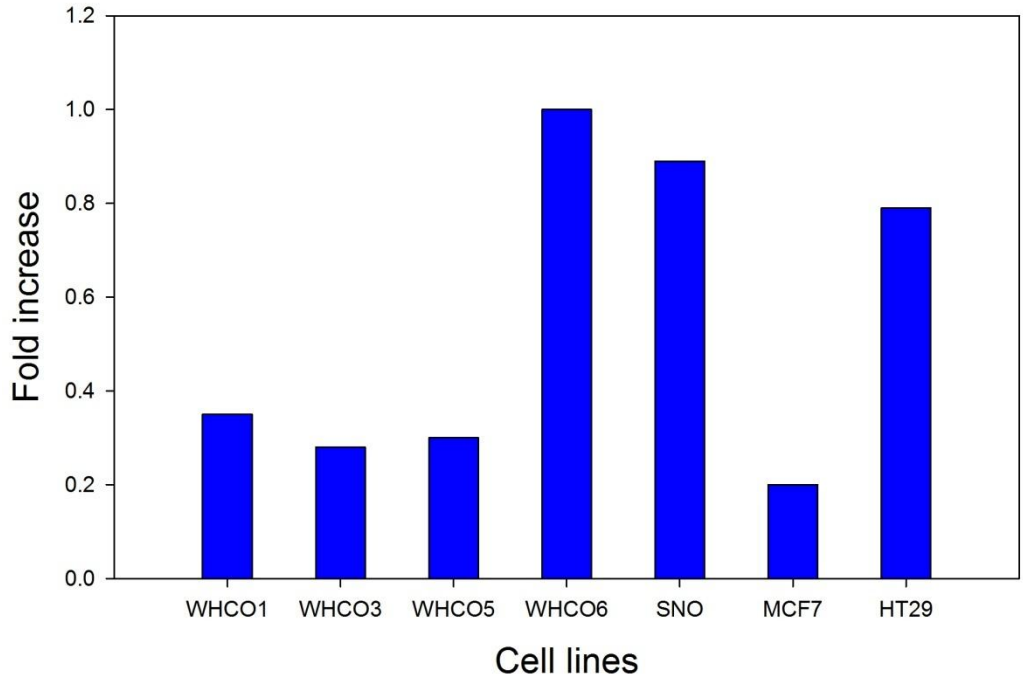

Figure 2.7: p53 is differentially expressed in the HOSCC, MCF-7 and HT29 cell lines under standard tissue culture conditions. A) Western blot analysis of the cell lysates using a polyclonal antibody against human p53. The highest level of p53 expression was observed in the WHCO6 and SNO cell lines. B) Densitometric analysis of the immunoblot was performed using Labworks™ Image Acquisition and Analysis software. Expression levels are relative to the maximum per 20µg of protein in the WHCO6 cell line. Note: the whole cell samples used to detect FAK in *Figure 2.3A* were the same samples used to detect p53, and therefore, the tubulin immunoblot also represents the loading control for the above immunoblot.

WHCO1

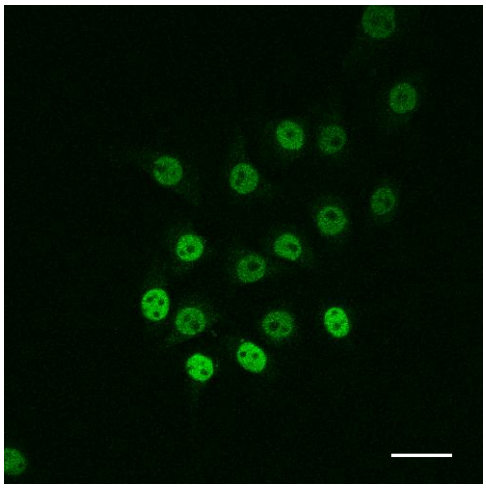

WHCO3

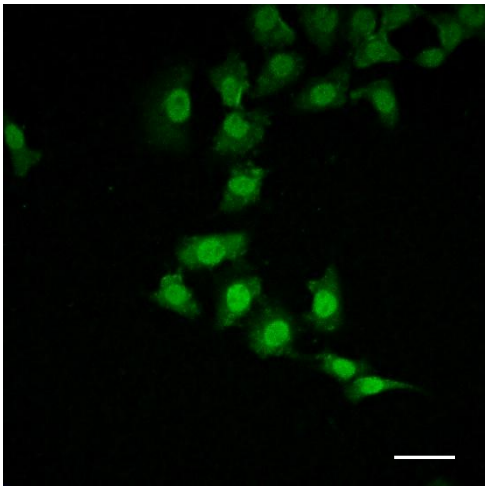

WHCO5

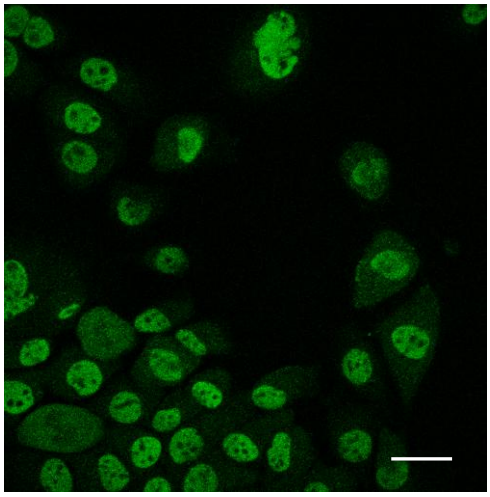

WHCO6

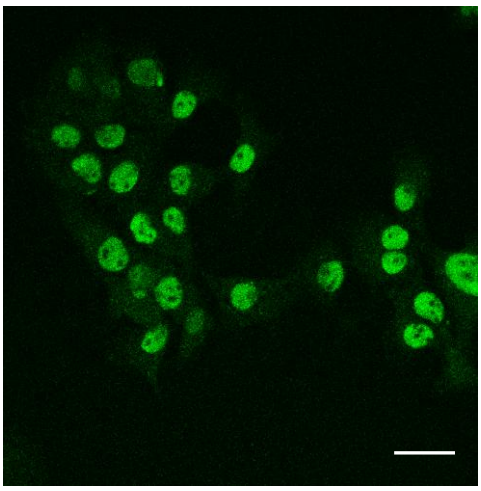

SNO

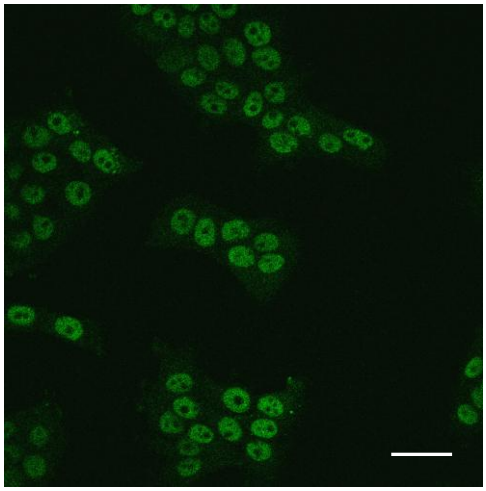

HT29

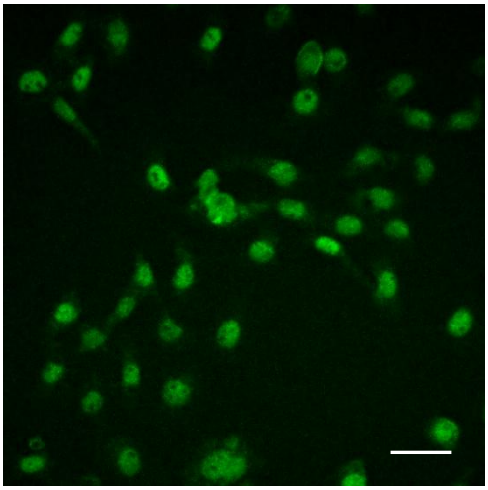

MCF7 Negative control

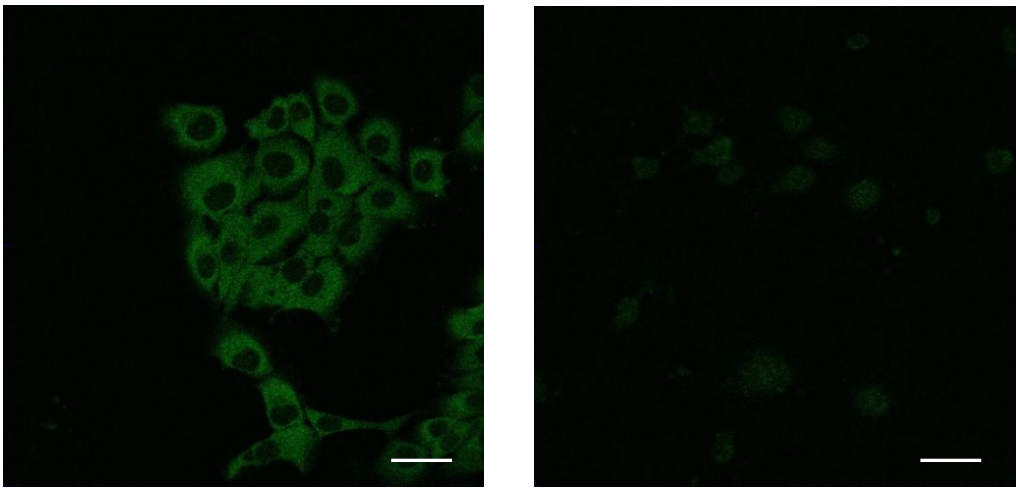

Figure 2.8: p53 is primarily localised to the nucleus in HOSCC cell lines. Nuclear localisation of p53 was observed in HOSCC and mt p53-R273H HT29 cell lines under normal tissue culture conditions, following immunofluorescent detection. Cytoplasmic localisation of p53 was observed in the caspase-3 null MCF7 breast carcinoma cell line. Negligible diffuse staining was observed in the negative control (excluding anti-p53 antibody). Scale bar = 25μm

2.3.6 HOSCC cell lines differentially express the death receptor, Fas

A functional link between FAK and the Fas has been demonstrated, implicating the death receptor pathway in the induction of anoikis (Kurenova *et al*., 2004; Kamarajan *et al*., 2010). In addition, p53 has been linked to the regulation of Fas-mediated apoptosis, as p53 response elements have been identified on the Fas promoter and wt p53 has been demonstrated to increase Fas membrane trafficking (Bennet *et al*., 1998; Zalcenstein *et al*., 2003). Western blot analysis of whole cell lysates from the HOSCC cell lines confirmed the presence of the Fas receptor protein (*Figure 2.9A*). The polyclonal antibody used in the western blot procedure was raised against the full length of the Fas receptor and, therefore, detected both the partially glycosylated Fas protein (48kDa) and the fully mature glycoprotein (52kDa). Under standard tissue culture conditions, the WHCO1, WHCO6 and SNO cell lines express both variants of Fas, with a higher proportion of the 52 kDa isoform (*Figure 2.9B).* Interestingly, the WHCO3 cell line only expresses the 52 kDa isoform of Fas and the WHCO5 and MCF-7 cell lines only express the 48 kDa isoform. The highest expression of Fas was observed in the 52 isoform in WHCO3, on average 1.5 fold higher than the WHCO1, WHCO5 and WHCO6 cell lines (*Figure 2.9B*). As consistent with the literature, due to the repression of the Fas promoter by the transcriptionally inactive mt p53-R273H (Zalcenstein *et al*., 2003), Fas was not detected in the HT29 cell line by immunoblot analysis (*Figure 2.9A*).

2.3.7 Peri-nuclear localisation of Fas was observed in HOSCC cell lines

The level of surface expression of Fas is one of the critical parameters in determining the ability of cells to undergo apoptosis, as the Fas expression on the cell surface transmits cell death signals via the ligation of FasL (Cahuzac *et al*., 2006). The observed variation in the glycosylation of Fas across the cell lines prompted the investigation of the cellular distribution of the protein. Consistent with previous reports of glycosylated proteins, peri-nuclear localisation of Fas in the vicinity of the golgi complex, was observed in the HOSCC and MCF7 cell

lines (*Figure 2.10*). Corresponding to the lack of Fas detection by immunoblot (*Figure 2.9A*), Fas was not detected by immunofluorescence in the HT29 cell line (*Figure 2.10*).

A.

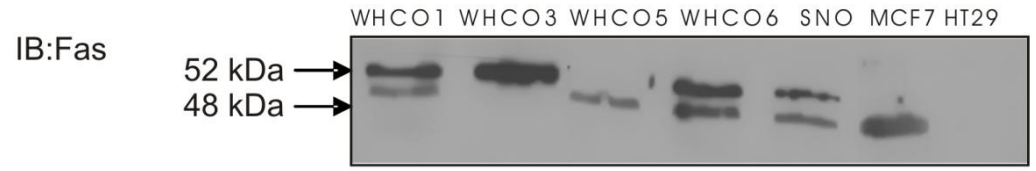

B.

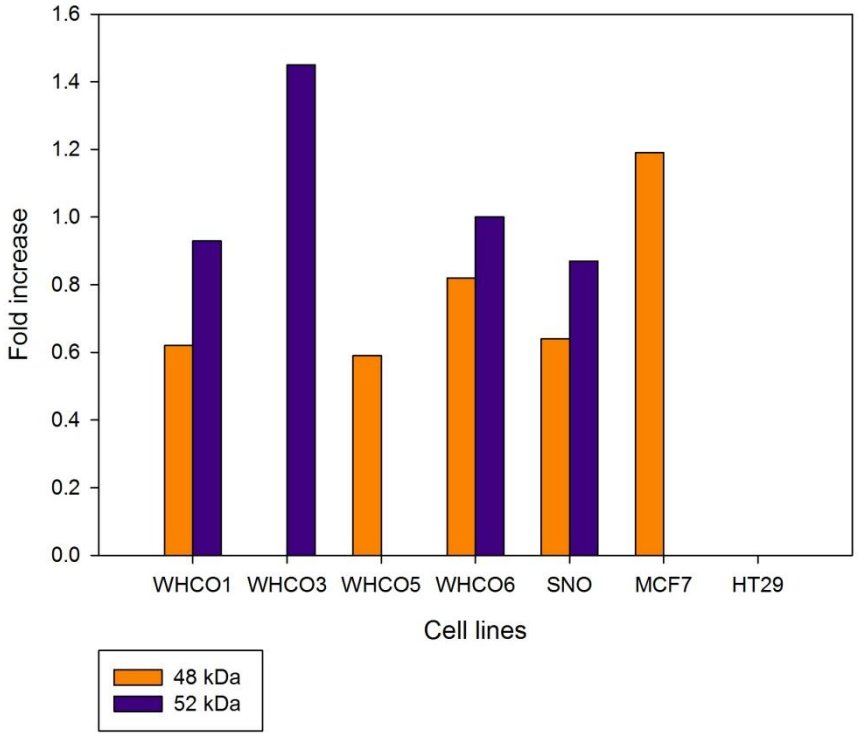

Figure 2.9: Fas was differentially expressed in the HOSCC, MCF-7 and HT29 cell lines under standard tissue culture conditions. (A) Western blot analysis of the cell lysates using a polyclonal antibody against human Fas receptor. Two bands of varying intensity represent the 52 kDa and 48 kDa isoforms of Fas. (B) Densitometric analysis of the immunoblot was performed using Labworks™ Image Acquisition and Analysis software. The relative difference in the 48kDa and 52kDa variants of Fas was assessed across all of the HOSCC cell lines. The expression levels are relative to the maximum per 20µg of protein in the WHCO6 cell line. Note: the whole cell samples used to detect FAK in *Figure 2.3A* we were the same samples used to detect Fas, and therefore, the tubulin immunoblot in *Figure 2.3A* also represents the loading control for the above immunoblot.

WHCO1

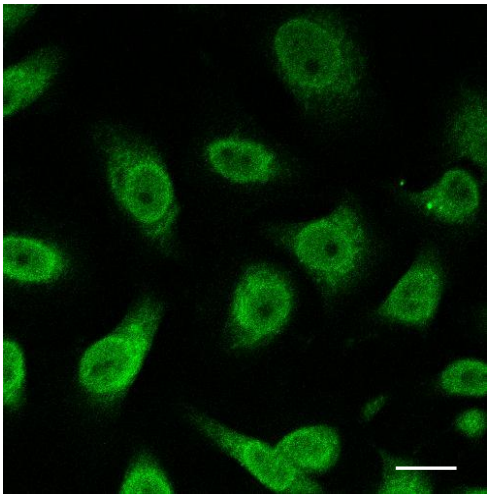

WHCO3

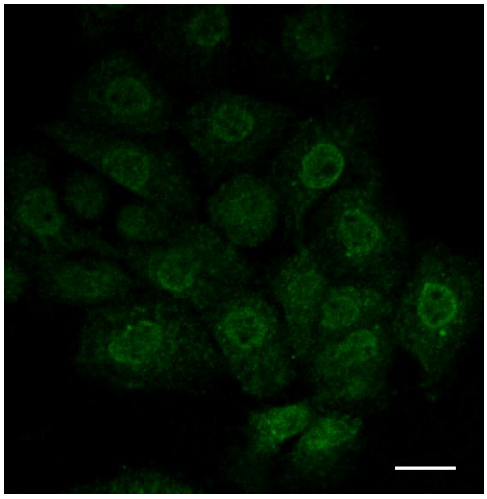

WHCO5

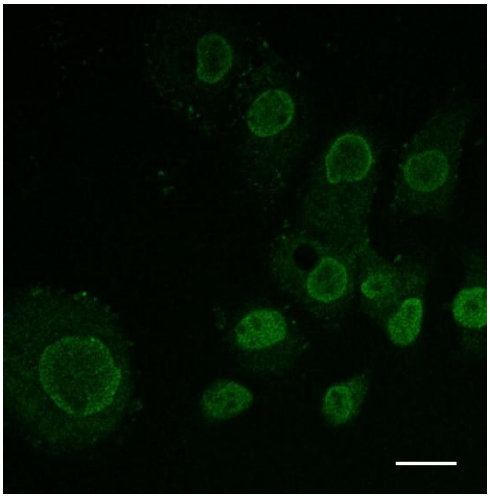

WHCO6

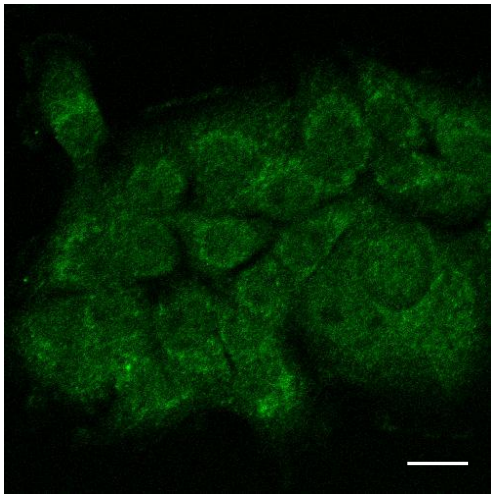

SNO

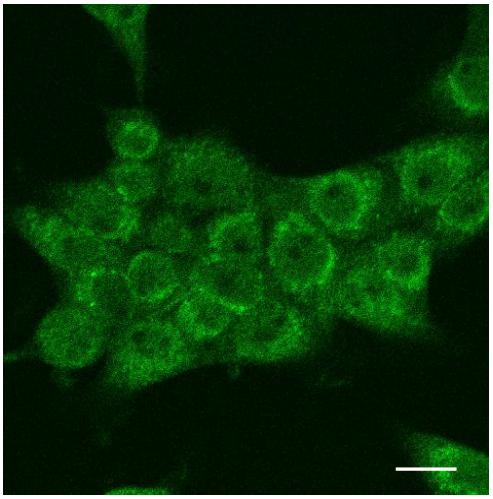

HT29

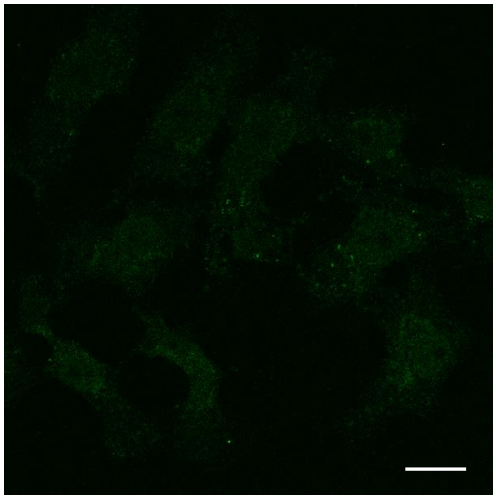

MCF7 Negative control

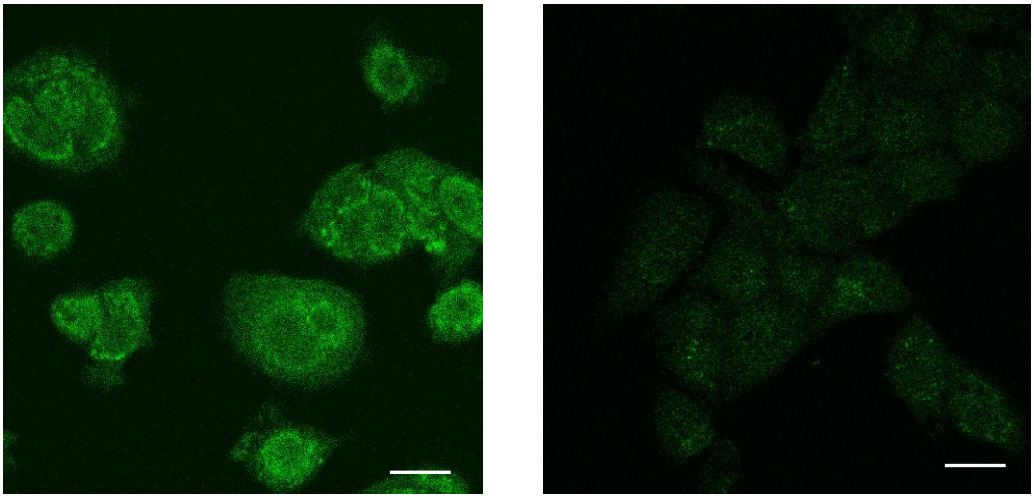

Figure 2.10: Peri-nuclear localisation of Fas was observed in the HOSCC cell lines. Under standard tissue culture condition, HOSCC cell lines show peri-nuclear localisation of Fas, with a smaller percentage being localised in the cytoplasm. Akin to the negative control (excluding anti-Fas antibody) negligible diffuse staining was observed in the HT29 cell line. Scale bar = 15 μm

2.4 Discussion

Interplay between FAK and apoptotic pathways has been shown to significantly influence cell fate decisions (Kurenova *et al*., 2004; Golubovskaya *et al*., 2008; Lim *et al*., 2008; Kamarajan *et al*., 2010). The *FAK* gene encodes a non-receptor tyrosine kinase that localizes at points of cell/ECM contact (Schaller *et al*., 1992; Luo and Guan, 2010). As a consequence of alternative splicing of the *FAK* gene, several isoforms exist. The non-catalytically active isoform originally isolated from chicken fibroblasts, FAK related non-kinase (FRNK), is the most characterised of these isoforms (van Nimwegen and van der Water, 2007). FRNK competes with FAK at sites of clustered β subunits of integrins, thereby acting as negative regulator of FAK-dependent signalling (Cooper *et al*., 2003). The only other closely related family member of FAK is the 112 kDa proline-rich tyrosine kinase 2 (PYK2). However, expression of PYK2 appears to be limited to cells of the nervous system, and cells of haematopoietic origin (van Nimwegen and van der Water, 2007). Hence, due to its integral role in cell adhesion signalling in epithelia, in this report we focus solely on interactions between FAK and key apoptotic regulators.

HOSCC is a highly metastatic cancer that presents symptomatically late in the course of the disease, therefore, the accurate diagnosis of this cancer is crucial to improve prognosis (Tew *et al*, 2005; Bird-Lieberman and Fitzgerald, 2009). Similar to other SCC tumours, HOSCC are histopathologically classified as poorly-, moderately- and well-differentiated tumours (Zhang *et al*., 2010). Although these categories reflect the differentiation status and morphology of oesophageal tumours, they provide limited molecular information – particularly in the moderately differentiated category. Consequently, in this study, the identification of similarities or disparities in anoikis-related signalling within a series of HOSCC cell lines traditionally classified as moderately differentiated, may aid in refining this broad category. Under standard tissue culture conditions, the WHCO6 and SNO cell lines expressed the highest level of FAK relative to the other moderately differentiated HOSCC cell lines, as well as the mt p53-R273H

HT29 and caspase-3-null MCF7 control cell lines (*Figure 2.3B*). Overexpression of FAK has been implicated in facilitating the metastatic progression of tumour cells (Schneider *et al*., 2002; Lark *et al*., 2005; Gabriel *et al*., 2006). Thus, as the moderately differentiated category is extremely broad, the WHCO6 and SNO cell lines may be derived from tumours that are closer to the poor end of the differentiation spectrum. However, a comparison to normal oesophageal epithelium would be required in order to firmly establish the relationship between elevated FAK expression in HOSCC and normal oesophageal tissue. Hence, due to the difficulty in obtaining and culturing normal oesophageal epithelium, this study focuses on the comparison of FAK-mediated signalling events between the moderately differentiated HOSCC cell lines displaying variable FAK expression (WHCO1, WHCO3, WHCO5, WHCO6 and SNO) and the HT29 and MCF7 control cell lines with documented resistance to anoikis. Specifically, the HT29 cell line is highly resistant to apoptotic stimuli as it harbours the transcriptionally inactive p53 mutant R273H (Lin-Lee *et al*., 2001), whilst the wt p53 MCF-7 cell line lacks functional caspase-3 and is therefore nonresponsive to caspase-related apoptotic events (Jánicke *et al*., 1998; Mooney *et al*., 2002).

Tyr397 autophosphorylation of FAK is critical to FAK-dependent survival signalling (Sonoda *et al*., 1999; Parsons, 2003). pFAKTyr397 was only detected by immunoblot analysis in the WHCO6 and SNO cell lines (*Figure 2.3A*). As these were the two cell lines displaying the highest FAK expression (*Figure 2.3B*) and pFAKTyr397 has previously been documented in the HT29 and MCF7 control cell lines (Beviglia *et al*., 2003), FAK protein levels were concentrated via co-immunoprecipitation in the other cell lines. Accordingly, pFAKTyr397 was detected in the FAK immunoprecipitates (*Figure 2.4*). Importantly, these data demonstrate a relationship between FAK expression and Tyr397 phosphorylation levels.

Overexpression of FAK and Tyr397-phosphorylated FAK are correlated with enhanced tumourigenesis and metastasis (Miyazaki *et al*., 2003; Lark *et al*., 2005; Jiang *et al*., 2010). However, in this study, the variation in FAK protein

expression and Tyr397 levels determined by semi-quantitative analyses (*Figure 2.3B & C*) excludes the possibility of using Tyr397-phosphorylated FAK as a molecular marker for this pathological grading of HOSCC. Nonetheless, due the high relative expression of FAK and detectable level of Tyr397-phosphorylated FAK by immunoblot (*See Figure 2.3A & B*), the WHCO6 and SNO cell lines represent an excellent model to examine the effect of FAK-dependent signalling on anoikis-related events in HOSCC.

Following attachment to the ECM, FAK is targeted to sites of focal contact, where it is autophosphorylated by integrin clustering (Owen *et al*., 1999). In particular, the direct interaction between the C-terminal of FAK with the cytoplasmic tail of the β1 integrin subunit facilitates the rapid Tyr397 autophosphorylation of FAK (Schaller *et al*., 1994). Importantly, β1 integrin was detected in complex with Tyr397-phosphoryated FAK (*Figure 2.6*). Hence, similar to other epithelial tumours (Crowe and Ohannessian, 2004; Thamilselvan *et al*., 2007), FAK is autophosphorylated at sites of focal contact. In combination with the observed cytoplasmic localisation of FAK (*Figure 2.5*), these data support an important role of Tyr397-phosphorylated FAK in cell adhesion signalling events in HOSCC.

Increased activation of FAK by ECM influence has been demonstrated to suppress p53-dependent apoptosis (Zhang *et al*., 2004 (a)). Corresponding to the elevated expression of Tyr397-phosphorylated FAK (*Figure 2.3C*), high p53 expression was detected in the WHCO6 and SNO cell lines (*Figure 2.7*). Interestingly, despite the similar levels of p53 in the WHCO6 and SNO cell lines, there was much greater FAK expression in the WHCO6 cell line in comparison to the SNO cell line. In addition, consistent with previous reports in transformed cells (Rotter *et al*., 1983; Shaulsky *et al*., 1990), p53 was detected in the nucleus by immunofluorescence in the HOSCC cell lines and the mt p53-R273H HT29 cell line (*Figure 2.8*). Consequently, the mutational status of p53 does not influence p53 localisation, as nuclear localisation of mt p53-R273H was observed in the HT29 cell line (*Figure 2.8*).

Abrogation of FAK expression has been shown to trigger the Fas-mediated death cascade (Kurenova *et al*., 2004). Differential expression of the 48kDa and 52kDa isoforms of Fas was observed in the HOSCC, HT29 and MCF7 cell lines (*Figure 2.9*). Both variants 48 and 52 kDa Fas glycoproteins are known to be targeted to the membrane, and transduce FasL-mediated apoptotic signals (Cahuzac *et al*., 2006). Consequently, the variation in Fas expression did not influence Fas localisation, as predominantly peri-nuclear localisation of Fas was observed in the HOSCC and MCF7 cell lines (*Figure 2.10*). Thus, these data validate that both p53 and Fas are expressed by the HOSCC cell lines. Furthermore, no unusual cellular distribution of both of the major apoptotic constituents was observed in the HOSCC cell lines.

p53 binding sites have been reported on both FAK and Fas promoters (Zalcenstein *et al*., 2003; Golubovskaya *et al*., 2005). Accordingly, in the HT29 cell line harbouring the transcriptionally inactive mt p53-R273H, there is reduced FAK levels and repressed Fas expression (*Figure 2.3 & 2.9*). Despite the same cellular distribution of FAK, p53 and Fas as the HT29 cell line, the key anoikis-related intermediates were differentially expressed in the HOSCC cell lines (*Figure 2.3, 2.7 & 2.9*). In particular, the expression of Tyr397-phosphorylated FAK and p53 was elevated in the WHCO6 and SNO cell lines (*Figure 2.3C & 2.7B*). Moreover, comparable to the mt p53-R273H HT29 control cell line, nuclear p53 was detected in the HOSCC cell lines (*Figure 2.8*). As tumours expressing mutated p53 overexpress FAK (Golubovskaya *et al*., 2009), these observations suggest that the loss of tumour suppressor function of p53 may be responsible for the altered expression of the anoikis-related intermediates in the HOSCC cell lines. Furthermore, endogenous p53 and overexpression of wild type p53 have been shown to inhibit FAK mRNA and protein levels whilst, mutant p53 did bind to the FAK promoter (Golubovskaya *et al*., 2008). Therefore, the ability of cell line(s) harbouring mutant p53 to resist apoptotic stimuli and alter FAK-dependent signalling is reported in the subsequent chapter.

Chapter 3

Apoptotic events in wt p53 HOSCC cell lines are accompanied by caspase-3 activation and FAK cleavage: opposing role of mt p53-R175H

3.1 Introduction

Increased activation of FAK by ECM influence has been demonstrated to repress p53-dependent apoptosis (Zhang *et al*., 2004 (a)). In addition, mutant p53 has been reported to suppress FAK expression by disabling the FAK promoter (Golubovskaya *et al*., 2005), and, a positive correlation between FAK overexpression and mutant p53 has been shown (Golubovskaya *et al*., 2005; Golubovskaya *et al*., 2009). Therefore, although p53 mutants are well established to desensitize tumours to apoptotic stimuli (Blandino *et al*., 1999; Tsang *et al*., 2005), these studies point to mutant p53 as being intimately involved in FAK-dependent anoikis resistance.

Impairment of p53 function is attributed to mutations within the p53 coding domain, as well as, mutations in intermediates that regulate p53 expression and activity (Vousden, 2002). The p53 protein has been well characterised and consists of distinct functional domains (Pavletich *et al*., 1993). The N-terminal domain is involved in transactivation by co-activators or co-repressors, and the DNA-binding domain (DBD) is located within the core of the protein (Vrba *et al*., 2008). wt p53 binds to DNA as tetramers and the C-terminal is responsible for this tetramerisation. Intriguingly, a single point mutation in the DNA binding domain may completely inactivate p53, highlighting the significance of DNA binding for the tumour suppression function of p53. Common "hot-spot" mutations that alter the structure of p53 include codons R175, G245, R249 and R282 (Cho *et al*., 1994; Vrba *et al*., 2008). Mutations within the amino acid residues that make direct contact with the DNA include codons R248, R273 and R280 (Cho *et al*., 1994; Vrba *et al*., 2008). (Note, hereafter mutations that alter

the p53 conformation will be referred to as 'conformational mutants', whilst mutations that affect the DNA contact residues will be referred to as 'DNA contact mutants'.)

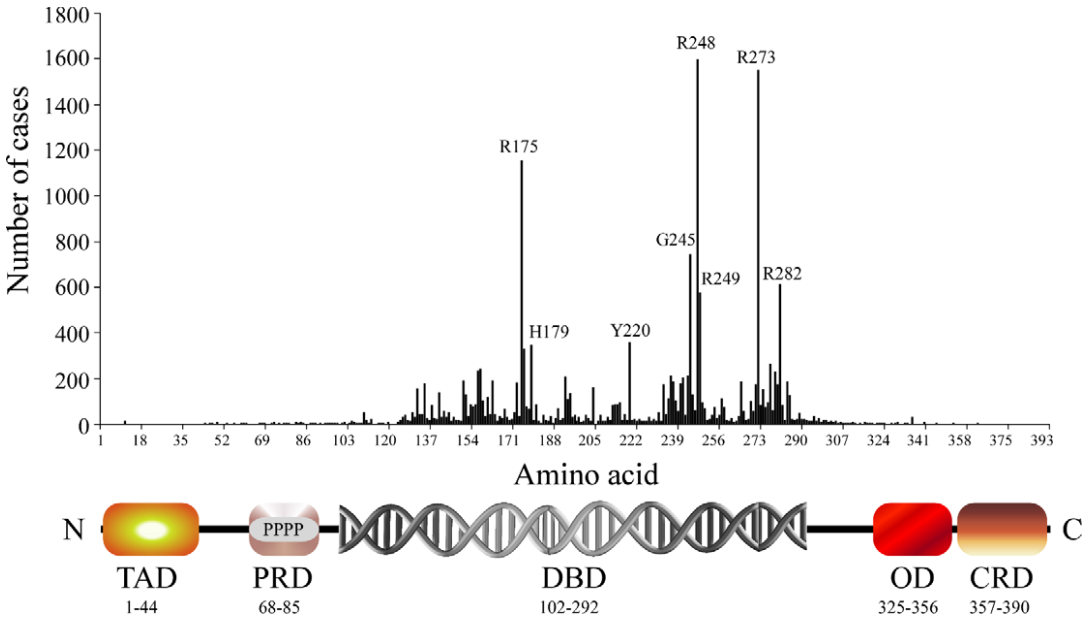

Figure 3.1: The distribution and frequency of p53 mutations in tumours. The vast majority of p53 mutations occur within the DNA binding domain. The three most prevalent p53 mutants, expressed in all cancers, are the conformational (R175H) and contact site (R248W and R273H) p53 mutants. © Buganim and Rotter, (2009) TAD, transactivation domain; PRD, proline-rich domain; OD, oligomerisation domain; DBD, DNA-binding domain; CRD, C-terminal domain.

Mutations within the DNA binding region of p53 located between exon 5 and exon 8 are common in HOSCC (*Figure 3.1;* Gamieldien *et al*., 1998; Li *et al*., 2004). However, Li and colleagues showed that in Chinese-derived HOSCC, 50.0% of point mutations occurred in exon 4 (Li *et al*., 2004). Furthermore, mutations within exon 4 were also observed in adjacent non-cancerous tissues. p53 mutational analysis of patients from the high risk Transkei region in South Africa, revealed that 17% of tumours contained a deletion, insertion or non-synonymous point mutation in exon 5 to 8 (Gamieldien *et al*., 1998). More recently, Vos and colleagues found that mutations were rarely observed in the regions flanking exon 5 and 8, however, polymorphisms were a frequent

occurrence in these flanking regions (Vos *et al*., 2003). The sequence polymorphism at codon 72 that encodes for either a proline or arginine was identified as one of the polymorphisms. Recent studies suggest that the Pro/Arg72 polymorphism may significantly contribute to the development of various cancers (Buyru *et al*., 2003; Pim and Banks, 2004). Interestingly, Yang and colleagues demonstrated that the p53 Arg/Arg72 genotype was significantly increased in HOSCC cases compared with control subjects (Yang *et al*., 2008). However, the functional significance of the Pro/Arg72 polymorphism with respect to p53 function in HOSCC is yet to be determined.

Irrespective of cell type, execution of anoikis ultimately converges on the activation of caspase-3 and as a consequence, initiates DNA fragmentation (Westhoff and Fulda, 2009). Hence, although anoikis is defined as the subset of cell death induced by loss of cell detachment, it is inherently an apoptotic process. Apoptotic stimuli mediated via both intrinsic and extrinsic apoptotic pathways converge on caspase-3 (Ilic *et al.*, 1998; Marconi *et al*., 2004; Mawji *et al*., 2007). Following activation, caspase-3 cleaves proteins within the focal adhesion, thereby, reducing cell attachment. FAK is an important target for caspase-3, as the C-terminal fragment generated by the caspase-dependent cleavage of FAK harbours the focal adhesion targeting (FAT) domain, which inhibits FAK Tyr397 phosphorylation (Gervais *et al*., 1998). In this way, activation of apoptotic death cascades effectively abrogates FAK phosphorylation and consequently, FAK-dependent survival signalling.

Oesophageal carcinoma is a highly malignant cancer that evades anoikis-related control via a possible FAK-dependent mechanism, as overexpression of FAK correlates with enhanced oesophageal tumor metastasis (Miyazaki *et al*., 2003) Moreover, HOSCC progression is associated with loss of tumour suppressor function of p53 (Xue *et al*., 2006). Therefore, as a direct correlation between FAK overexpression and mutant p53 has been demonstrated (Golubovskaya *et al*., 2009), the mutational status of the DNA binding domain of p53 was established in the HOSCC cell lines. In order to clarify the relationship between FAK-

dependent signalling and apoptotic regulation in HOSCC, the classic apoptotic markers, DNA fragmentation and caspase-3 activation were used to verify whether the apoptotic pathway is still intact in the HOSCC cell lines. The apoptotic-resistant HT29 cell line harbouring the transcriptionally inactive R273H DNA contact mutant p53 served as a mutant p53 control. Caspase-3 independent events were assessed using the caspase-3 null MCF7 cell line. Thereafter, the ability of mutant p53 to disrupt the caspase-3 associated cleavage of FAK, and as a consequence, maintain FAK dependent-signalling was determined. Pertinently, the data presented in this chapter provides evidence of a unique relationship between loss of p53 tumour suppressor function and enhanced cell adhesion-dependent signalling.

3.2 Material and Methods

3.2.1 Cell lines

As previously documented, see Chapter 2, Section 2.2.1

3.2.2 RNA extraction

As previously documented, see Chapter 2, Section 2.2.2

3.2.3 Reverse transcription

As previously documented, see Chapter 2, Section 2.2.3

3.2.4 PCR

The integrity of the DNA binding domain of p53 spanning exon 3 to 8 of the HOSCC cell lines was investigated by RT-PCR analysis. Primers used to amplify regions spanning exon 3-8 were as follows:

(exon3-5) Forward: 5' GAA ACA TTT TCA GAC CTA TGG 3'
Reverse: 5' TTC TGT CAT CCA AAT ACT CC 3'
(exon 6-8) Forward: 5' ATG ACA GAA ACA CTT TTC G 3'
Reverse: 5' GTA GAC TGA CCC TTT TTG G 3'.

Thermal cycle conditions for both primer sets included denaturation at 95 °C for 10 min and 32 cycles of denaturation at 95 °C for 0.5 - 1 min; annealing at 56 °C for 0.5 - 1 min and extension at 72 °C for 1 min with a final elongation at 72 °C for 10 min. PCR products were visualized on a 1% agarose gel following ethidium bromide staining. Fragments were sent to Inqaba Biotech for sequencing. A representative sequence trace is included in Appendix 3.2.

3.2.5 Genomic DNA PCR

Genomic DNA was extracted using the DNeasy kit (Promega) according to instructions by the manufacturer. The R175H mutation in exon 5 and the Pro/Arg72 polymorphism in exon 4 were confirmed by sequencing the respective exons from genomic DNA using the following primers:

(exon 4): Forward 5' CCT GGT CCT CTG ACT GCT CT 3'
Reverse 5' GCC AGG CAT TGA AGT CTC AT 3'

(exon 5) Forward 5’ GTT TCT TTG CTG CCG TCT TC 3’
Reverse 5’ CAA CCA GCC CTG TCG TCT CT 3’.

Thermal cycle conditions included denaturation at 95 °C for 10 min and 32 cycles of denaturation at 95 °C for 0.5 - 1 min; annealing at 56 °C for 0.5 - 1 min and extension at 72 °C for 1 min with a final elongation at 72 °C for 10 min. PCR products were visualized on a 1 % agarose gel following ethidium bromide staining.

3.2.6 Antibodies

FAK, integrin β1 and caspase-3 were specifically detected with rabbit polyclonal antibodies obtained from SantaCruz Technology. Monoclonal mouse anti-pFAK(Tyr397) (Millipore) and rabbit anti-cleaved caspase-3 (Cell Signaling Technology) were used to detect autophosphorylation of FAK and caspase-3 activation respectively. Polyclonal horseradish peroxidase (HRP)-bound anti-rabbit secondary antibody was used in (Separations, SA) was used in the immunoblot experiments.

3.2.7 Protein estimation

As previously documented, see Chapter 2, Section 2.2.6

3.2.8 Immunoblot analysis

40 µg of protein per lane was separated by 10% SDS-PAGE. Nonspecific binding sites on the membrane were pre-blocked in blocking buffer (Appendix 1.5.2) for 1 hr. Blots were incubated with anti-FAK for 1 hr or overnight with p-FAK(Tyr397) in 1% BSA. Washing was performed 6 times at 5 min intervals with PBS to remove any residual antibody. Following incubation in HRP-conjugated secondary membranes were washed 6 times at 5 min intervals with PBS before being exposed to the SuperSignal West Pico Chemiluminescent working solution (Appendix 1.5.3). Film was developed in developer (see Appendix 1.5.4) for 5 minutes, rinsed briefly in H_2O before fixing (see Appendix 1.5.5) for 5 minutes. Each immunoblot was repeated three times.

3.2.9 TUNEL

Apoptosis was induced by 30 nM of staurosporine (Sigma). Controls were incubated in vehicle (DMSO) only. In order to measure and quantitate cell death the cultured oesophageal cells were assayed with the *In situ* Cell Death Detection Kit, POD (Roche).

3.2.9a Preparation of sample material

5 X 10^6 HOSCC cells were fixed to the culture vessel with fixation solution (Appendix 1.7.1). The fixed cells were then rinsed three times in PBS and allowed to air dry for 5 min. A DAKO pen was used to draw circles to create wells on the dish. Fixed cells within the wells were then incubated with blocking solution (Appendix 1.7.1) for 10 min at 25 °C. After rinsing three times in PBS, the cells were incubated in permeabilisation solution (Appendix 1.7.2) for 5 min at room temperature.

3.2.9b Labelling protocol

5 µl of terminal deoxynucleotidyl transferase (TdT) was mixed with 45 µl of fluorescein-labeled deoxyuridine solution and added to each well. In negative controls, TdT was removed from the reaction mix. The culture vessel was incubated in a dark, humidified environment for 60 min at 37 °C. Samples were covered with parafilm to prevent evaporative loss. After the incubation, cells were rinsed six times in PBS.

3.2.9c Signal conversion

Incorporated flourescein-labeled nucleotides were detected by sheep anti-flourescein antibodies conjugated with horse-radish peroxidase. 15 µl of the converter-POD solution was added to each sample on the culture vessel and incubated in a humidified environment at 37 °C for 1 hr. The sample was covered with parafilm to prevent evaporative loss. After rinsing the sample 3 times in PBS, 20 µl of DAB peroxide working solution (Appendix 1.7.3) was added to the sample and incubated at 25 °C for 10 min. The samples were visualized by phase-contrast light microscopy.

The presence of standard morphological apoptotic features was confirmed in apoptotic cells, before evaluating apoptotic cell number. Five high powered fields (magnification X 100) with the most abundant distribution of TUNEL-positive cells were selected for counts in each of the cell lines. The percentage of apoptotic cells in relation to total number of cells was determined by counting 100 cells in each field. Mean $^{+}$/- SD was calculated from the five field views.

3.2.10 Cell detachment

Cells were plated at a concentration of 5×10^6 per 6cm tissue culture dish (Nunc). Following STS-treatment for 24hr, detached cells were collected, stained with 0.4% w/v Trypan Blue solution and transferred onto a haemocytometer (Fuchs-Rosenthal). The entire collection process was repeated five times and the average detached cells per total volume calculated. Attached cells were incubated in a Trypsin/EDTA solution for 5 min. Trypsinized cells were collected, transferred onto a haemocytometer and counted as described above. STS-induced detached cells were expressed as a percentage of total cells and mean $^{+}$/- SD was determined as above.

3.2.11 Statistics

A standard student's t test was used for comparative analyses (See Appendix 4.1 & 4.2). The level of significance was set at $p < 0.05$.

3.3 Results:

3.3.1 Mutational analysis of the DNA binding domain of p53 in HOSCC cell lines

In order to amplify the DNA binding domain of p53 spanning exon 4 to 8, the p53 RNA transcripts (*Figure 2.1A*) were reversed transcribed into cDNA (*Figure 2.1B*) and subject to PCR analysis. Sequence analysis of exon 3 through to 5 revealed that the SNO cell line harbours the conformational mt p53-R175H (G to A) (*Figure 3.2*). As consistent with findings by Vos *et al*. (2003), mutational analysis of exon 4 revealed no mutations in the HOSCC, HT29 or MCF-7 cell lines. However, the Pro/Arg 72 polymorphism on exon 4 was identified in the WHCO1 and SNO cell lines (*Figure 3.2*).

Primers specific for exon 5 through to exon 8 produced a 511 bp PCR product (*Figure 3.3*). Sequence analysis revealed no mutations in this region in the HOSCC cell lines. The previously described R273H mutation in the HT29 cell line is located in exon 8 (Bossi *et al*., 2006), whilst, the MCF7 cell line expresses wt p53 with respect to the DNA binding domain of p53.

Amplification of exon 4 from genomic DNA produced a fragment of 361bp in all cell lines (*Figure 3.4A*), whilst primers specific for exon 5 produced a fragment of 305 bp (*Figure 3.4B*). Both the Pro/Arg72 polymorphism located on exon 4 (*Figure 3.4C*) and the R175H mutation located on exon 5 (*Figure 3.4D*) were confirmed by sequence analysis of the respective exons of genomic DNA.

A.

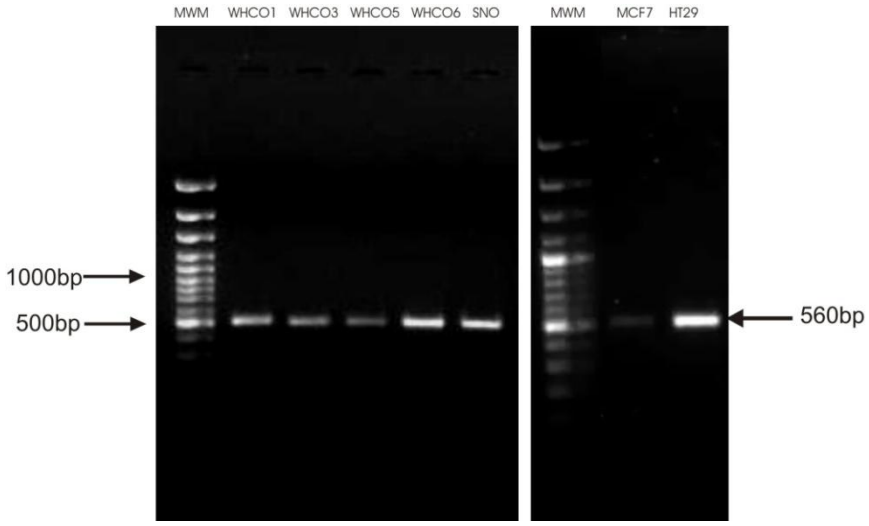

B.

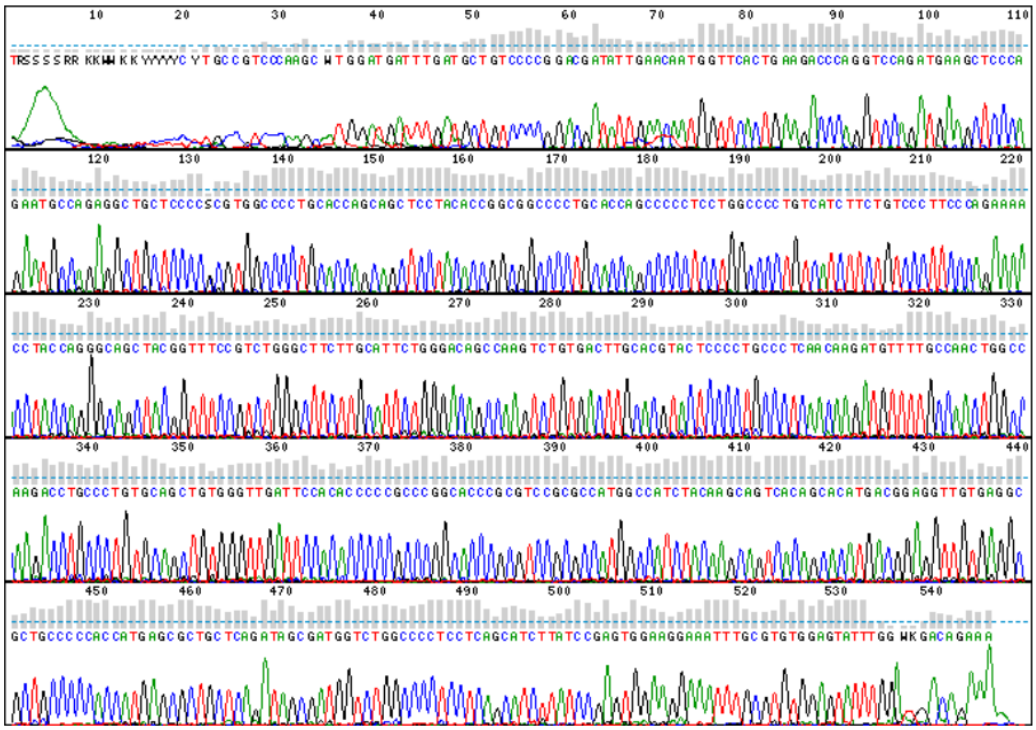

Figure 3.2: p53 mutational analysis of exon 3-5 of the HOSCC cell lines. A) RT-PCR products were resolved by 1 % agarose gel electrophoresis following EtBr staining (10 µg/ml). A band of 560 bp was observed in HOSCC, MCF7 and HT29 cell lines. B) Representative sequence trace of the 560 bp fragment. Sequence analyses revealed that the SNO cell line harbours mt p53-R175H and the Pro/Arg72 polymorphism was detected in the WHCO1 and SNO cell lines. MWM = GeneRuler^{TM} 100bp Plus DNA ladder

A.

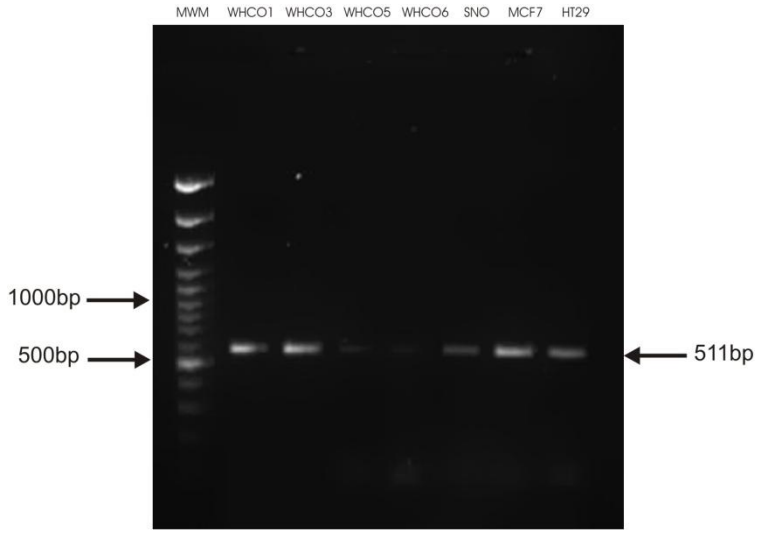

B.

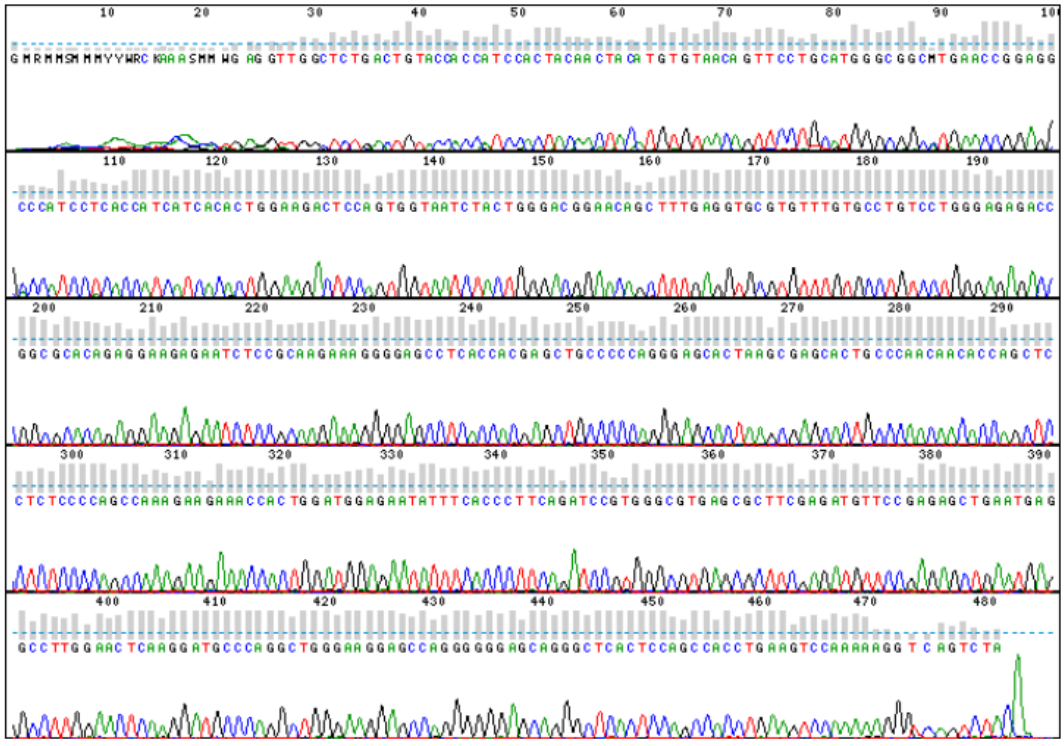

Figure 3.3: p53 mutational analysis of exon 6-8 of the HOSCC cell lines. A) RT-PCR products were resolved by 1 % agarose gel electrophoresis following EtBr staining (10 µg/ml). A band of 511 bp was observed in HOSCC, MCF7 and HT29 cell lines. B) Representative sequence trace of the 511 bp fragment. Sequence analyses revealed no mutations in this region of p53 in the HOSCC cell lines. MWM = GeneRuler^{TM} 100bp Plus DNA ladder

A.

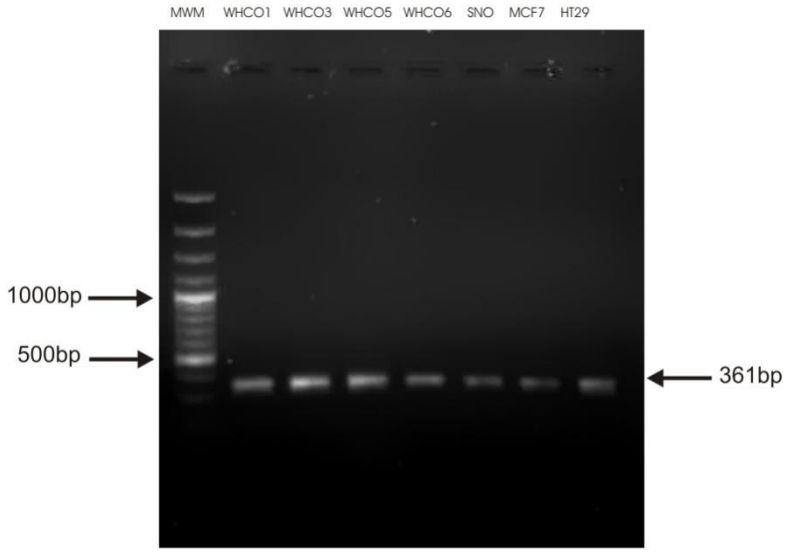
MWM
WHCO1
WHCO3
WHCO5
WHCO6
SNO
MCF7
HT29
1000bp
500bp
361bp

B.

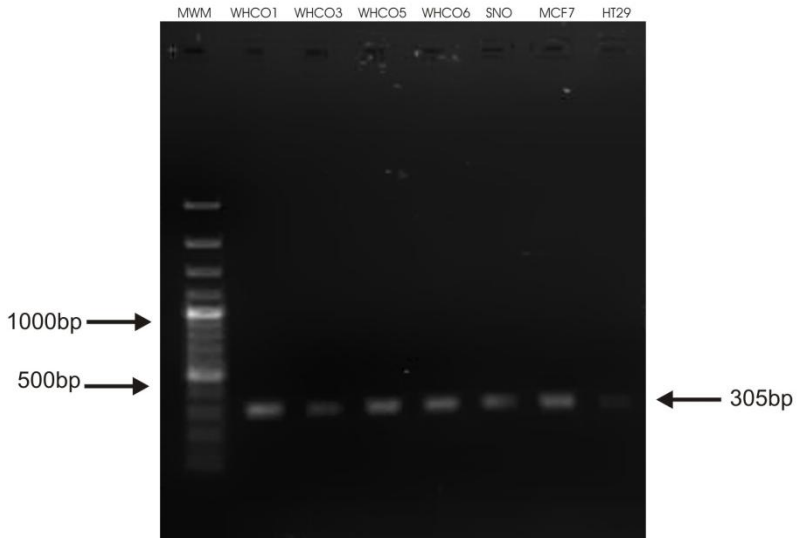
MWM
WHCO1
WHCO3
WHCO5
WHCO6
SNO
MCF7
HT29
1000bp
500bp
305bp

C.

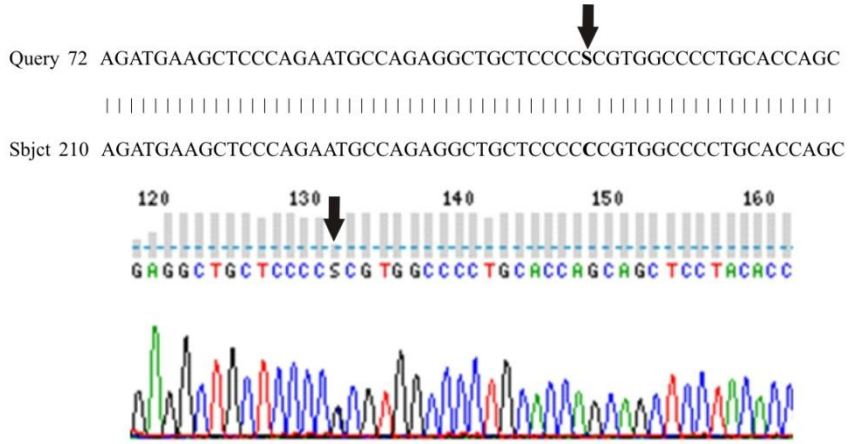

D.

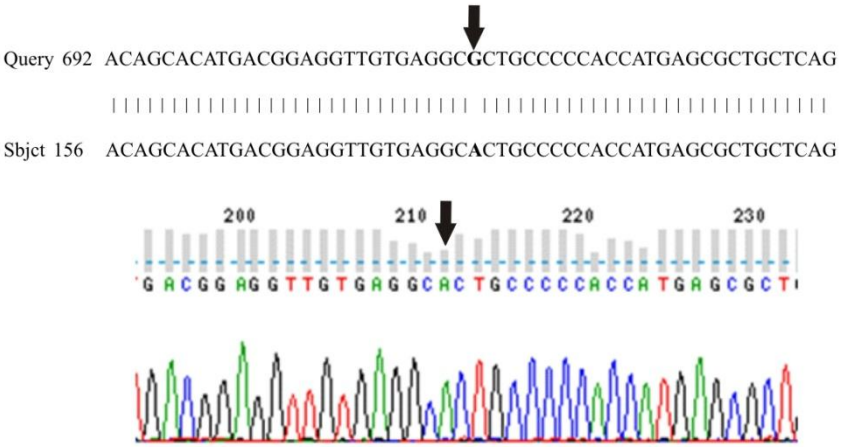

E. Cell lines	p53 mutations
MCF-7, WHCO3, WHCO5 and WHCO6	Wild type p53 (exon 4-8)
WHCO1	Heterozygous Pro/Arg 72
SNO	Heterozygous Pro/Arg 72 R175H mutation on exon 5
HT29	R273H mutation on exon 8 (Bossi *et al*., 2006)

Figure 3.4: p53 mutational status of HOSCC cell lines. A&B) PCR products were visualized on a 1 % agarose gel. A fragment corresponding to 361 bp for (A) exon 4 and 305 bp for (B) exon 5 was evident in the HOSCC, HT29 and MCF-7 cell lines. Fragments were sequenced to confirm the Pro/Arg72 polymorphism on (C) exon 4 and R175H mutation on (D) exon 5. E) Summary of the mutational analysis of exon 4 through to 8 of p53 in the HOSCC, MCF7 and HT29 cell lines.

3.3.2 STS induces apoptotic morphology in HOSCC cell lines

STS is a chemotherapeutic reagent commonly used to induce apoptotic death *in vitro*. The ability of STS to induce apoptosis in various squamous cell carcinomas is well documented (Qiao *et al*., 1996; Abiko *et al*., 1997; Mckeague *et al*., 2003; Zhang *et al*., 2004 (b); Yamagishi *et al*., 2006). Typical apoptotic morphology and oligonucleosomal cleavage has been shown to occur subsequent to STS treatment (Abiko *et al.,* 1997).

As the morphology of apoptotic cells is qualitatively different to cells in the process of necrotic cell death, cell morphology was examined very carefully. Typical apoptotic morphological signs were evident in both the wt p53 representative WHCO6 cell line and mt p53-R175H SNO cell line post STS treatment (*Figure 3.5B*). When compared to the untreated controls, a visible reduction in cell volume was evident in all cell lines. As apoptosis is asynchronous, various stages of apoptotic morphology were evident post STS-treatment in each cell culture. The small surface blebs that occur shortly after the onset of apoptosis, as well as large blisters are evident on the plasma membrane in STS-treated cells. Thin surface echinoid protrusions that follow membrane blebbing were also clearly visible (*black arrows; Figure 3.5B*).

A.

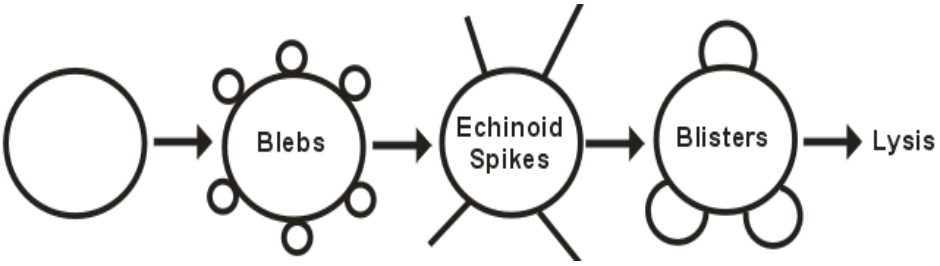

B.

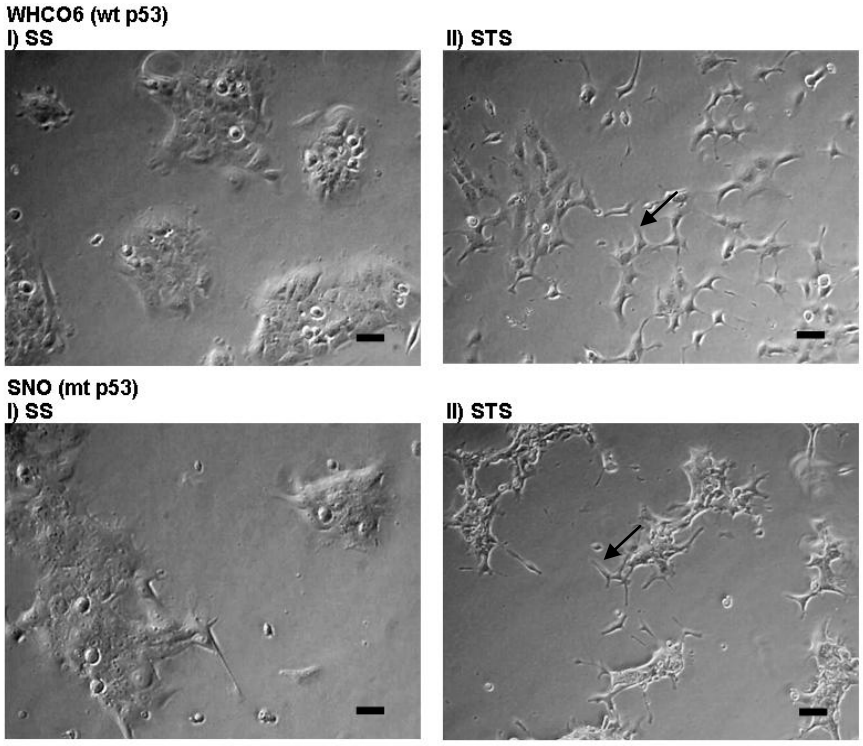

Figure 3.5: Morphology of STS-induced apoptotic HOSCC cells A) Schematic representation of the morphology of cells undergoing apoptosis. Initially cells undergoing apoptosis round up and acquire membrane ruffles. Then the cells become rigid; extending long, thin echinoid protrusions into the cytoplasm. The plasma membrane begins to blister and ultimately lyses committing the cell to death. © Adapted from Collins *et al.* (1997). B) STS induced recognisable apoptotic morphology in wt p53 and mt p53 HOSCC cells. Documented apoptotic morphology was observed in STS-treated HOSCC cells by phase-constrast microscopy. (I) Untreated HOSCC cells exhibit regular colony morphology with few cytoplasmic extensions. (II) STS-treated HOSCC cells show typical apoptotic morphology including reduction in cell volume and echinoid extensions of the plasma membrane (black arrow). Scale bar = 50μm.

3.3.3 Caspase-3 associated oligonucleosomal cleavage

Cells entering apoptotic death pathways display distinct nuclear and cytoplasmic morphology including oligonucleosomal cleavage. Nuclear disintegration was originally believed to be due to the activation of the endonuclease CAD/ DFF45, one of the major substrates of caspase-3 (Enari *et al*., 1998). Associated nuclear cleavage yields both double-stranded, low molecular weight DNA fragments, as well as single strand breaks in high molecular weight DNA. However, DFF45-independent cleavage of has also been observed in the caspase-3 null MCF7 cell line (Mooney *et al*., 2002), indicating the involvement of caspase-independent events in the DNA fragmentation process. Both the mitochondrial (intrinsic) and the death receptor (extrinsic) death pathways converge on the activation of caspase-3 (Wang, 2001; Aoudjit and Vuori, 2001). Upon activation, caspase-3 is proteolytically cleaved into a 19 kDa and 10 kDa subunit (*See Figure 3.6*).

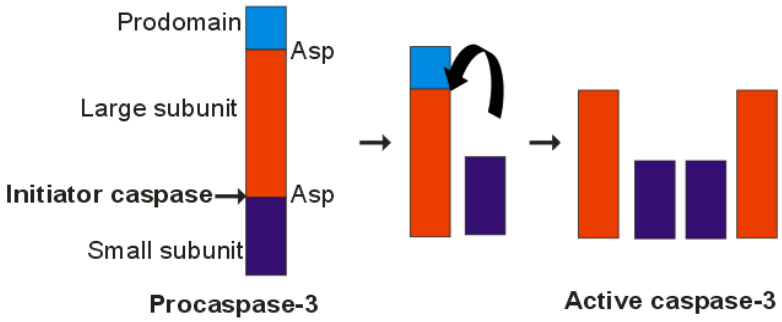

Figure 3.6: Proteolytic processing of procaspase-3. The 32 kDa inactive procaspase-3 protein contains three domains: the N-terminal prodomain (blue), a 20 kDa subunit (red) containing the catalytically active cysteine residue and a 10 kDa C-terminal subunit (purple). All caspases are activated to fully functional proteases by two separate events. The first is the proteolytic cleavage that divides the protein into a 10 kDa and 19 kDa subunit. This cleavage is initiated by an initiator caspase. The second is an autocleavage of the prodomain region. A fully functional caspase-3 is a heteroteterameric enzyme that consists of two 19 kDa and two 10 kDa subunits, with two active sites.

3.3.3a HOSCC cell lines express the caspase-3 precursor

Caspase-3 has been demonstrated to be a prognostic marker in HOSCC, as positive caspase-3 expression in HOSCC tumours was shown to correlate with increased lifespan (Hsia *et al*., 2003). Western blot analyses of whole cell lysates revealed that all of the HOSCC cell lines express the caspase-3 precursor (*Figure 3.7A*). Under standard tissue culture conditions, the WHCO6 cell line had the highest p32 expression (*Figure 3.7B*). In the MCF-7 breast carcinoma cell line, there is a loss of procaspase-3 expression due a functional deletion in exon 3 of the *CASP-3* gene (Jänicke *et al*., 1998; Mooney *et al*., 2002). Consistent with the literature, procaspase-3 protein was not detected in the MCF-7 cell line by immunoblot analysis (*Figure 3.7A*).

A.

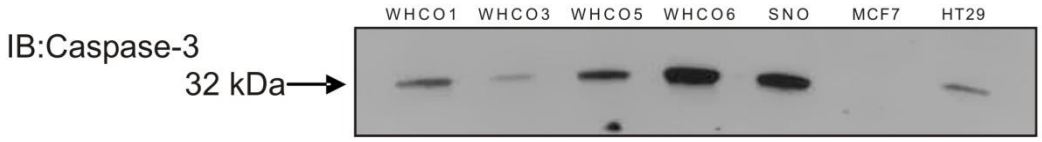

B.

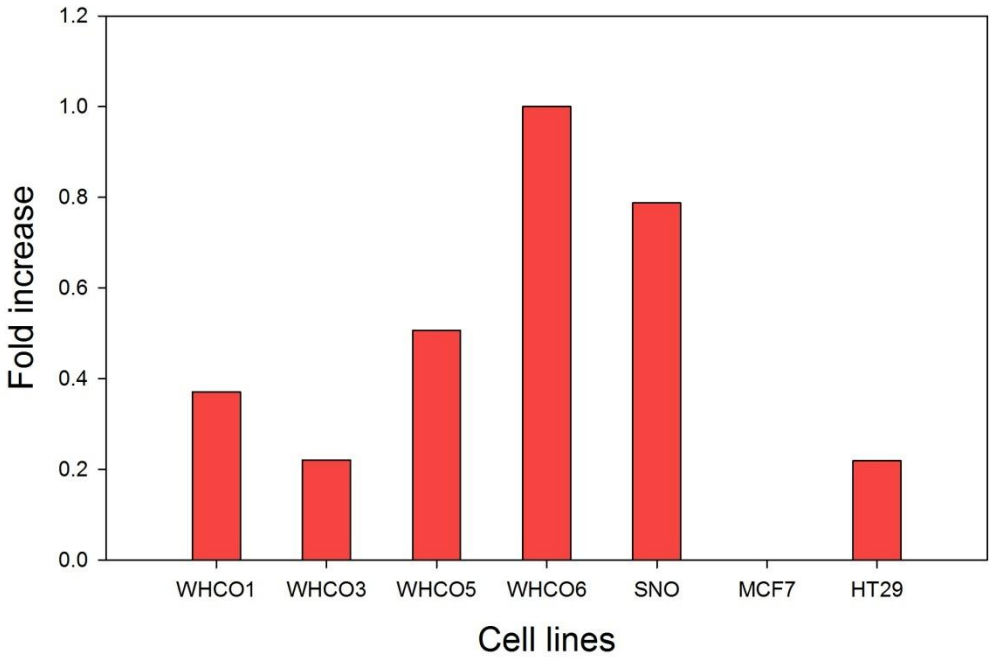

Figure 3.7: The HOSCC cell lines differentially express procaspase-3 under standard tissue culture conditions. (A) Western blot analysis of the cell lysates using a polyclonal antibody against human caspase-3. A single band of varying intensity, representing the 32 kDa caspase-3 precursor was apparent in all HOSCC cell lines. Due to a functional deletion in the *CASP-3* gene, the MCF-7 cell line does not express caspase-3. B) Semi-quantitative analyses of caspase-3 demonstrate that the WHCO6 cell line expresses the highest level of caspase-3 relative to the other cell lines. The expression levels are relative to the maximum per 20µg of protein in the WHCO6 cell line. Note: the whole cell samples used to detect FAK in *Figure 2.3A* we were the same samples used to detect caspase-3, and therefore, the tubulin immunoblot also represents the loading control for the above whole cell extracts.

3.3.4 Oligonucleosomal cleavage analysis in HOSCC cell lines

Oligonucleosomal cleavage was assessed by the standard methods; TUNEL assay and DNA laddering on an agarose gel. Both methods accurately identify the nuclear cleavage associated with apoptosis; however the laddering method requires the extraction of the entire cell and analysis of the pooled DNA extract whilst, the TUNEL method enables the identification *in situ* of the apoptotic nuclei allowing a quantitative comparative analysis.

3.3.4a DNA ladder analysis

Distinct oligonucleosomal cleavage was detected post STS treatment in the wt p53, mt p53-R175H and mt p53-R273H cell lines, as assessed by the laddering of DNA on an agarose gel (*Figure 3.8A*). In addition, caspase-3-independent DNA fragmentation was confirmed in the MCF7 cell line (*Figure 3.8A*).

3.3.4b TUNEL

TUNEL was performed under serum free conditions and following treatment with 30 nM STS. In each instance, the efficacy of the TUNEL assay was determined by pre-incubation with DNase I prior to the addition of the TUNEL reagents (*Figure 2.8B*). All HOSCC cell lines showed a significant increase in apoptotic positive nuclei post STS treatment (*Figure 3.8C*). The highest percentage of TUNEL positive nuclei was observed in the mt p53-R175H and mt p53-R273H cell lines. Whilst the lowest level of apoptotic nuclei was observed in the WHCO6 and WHCO5 cell lines respectively (*Figure 3.8C*).

3.3.5 STS induces cell detachment in HOSCC cell lines

Loss of cell-matrix contact in epithelial cells triggers cell death via anoikis-related apoptotic pathways (Frisch and Francis, 1994; Mawji *et al*., 2007). Hence, as TUNEL was performed *in situ* and apoptotic cells lose substrate contact, the presence of the apoptotic DNA ladder was confirmed in both attached and

detached cells (*Figure 3.9A*). Therefore, percentage detachment was used to compare STS-mediated apoptosis between wt and mt p53 cell lines (*Figure 3.9B*). Accordingly, in both the mt p53-R175H and mt p53-R273H cell lines, the highest levels of TUNEL positive nuclei corresponded to the lowest percentage of cell detachment. Conversely, the low level of TUNEL-positive nuclei in the wt p53 HOSCC cell lines, were associated with higher levels of cell detachment with respect to the mt p53 cell lines (*Figure 3.9B*).

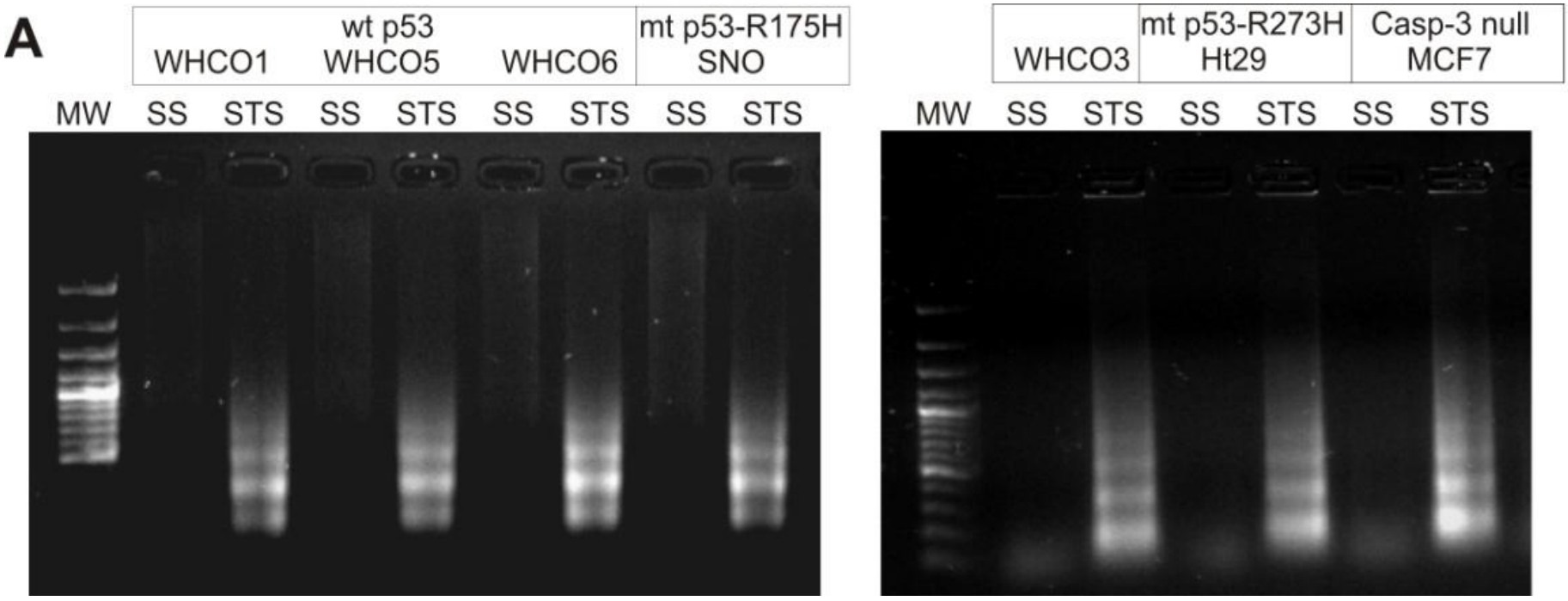

See next page for legend.

B.

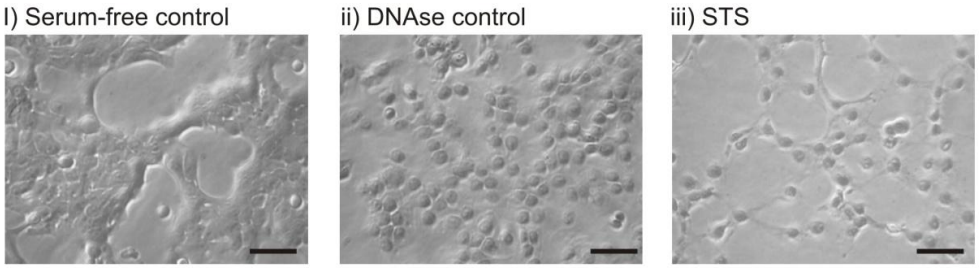

C.

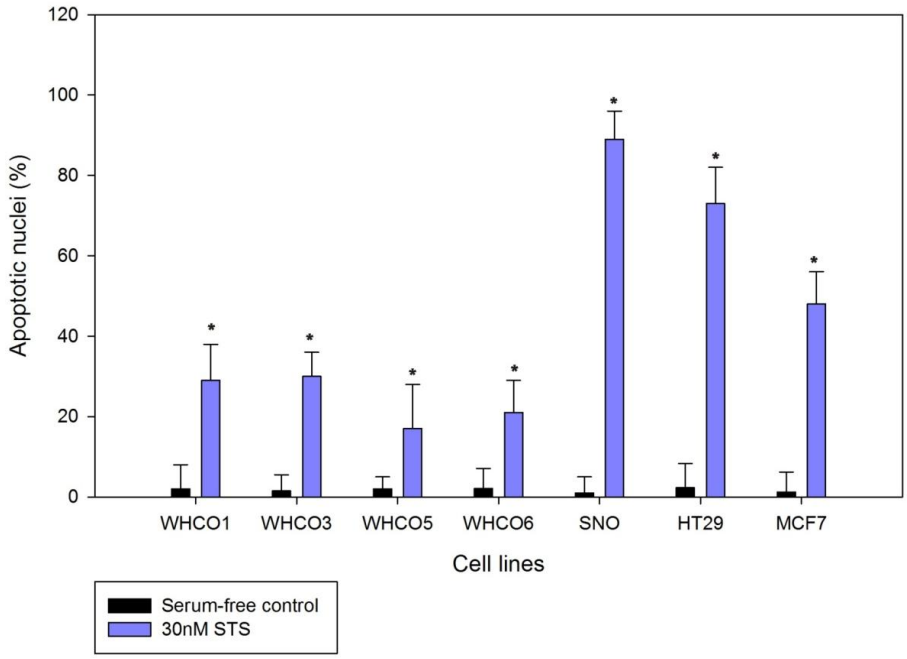

Figure 3.8: STS induction of internucleosomal DNA fragmentation in wt and mt p53 HOSCC cell lines. A) Apoptotic DNA ladder analysis in HOSCC cell lines under serum-free (SS) conditions and treated with 30 nM STS (STS). B) The SNO cell line was pre-incubated with 5 U/ml DNase I for 5 min prior to the addition of the TUNEL reagents, to determine the efficacy of the TUNEL assay. Pre-treatment with DNase I caused a distinct staining of all nuclei in the preparation as viewed by phase-contrast microscopy. Cells were unstained in the preparation. iii) TUNEL stained nuclei in the SNO cell lines. Dark nuclei, stained by DAB substrate are indicative of oligonucleosomal cleavage. C) The percentage of TUNEL-positive nuclei was determined in the wt, mt and caspase-3 null cell lines. The highest percentage of apoptotic nuclei was observed in the mt p53-R175H SNO cell line (89%). Bars represent standard deviation. MW = GeneRuler^{TM} 100bp Plus DNA ladder * $p < 0.05$

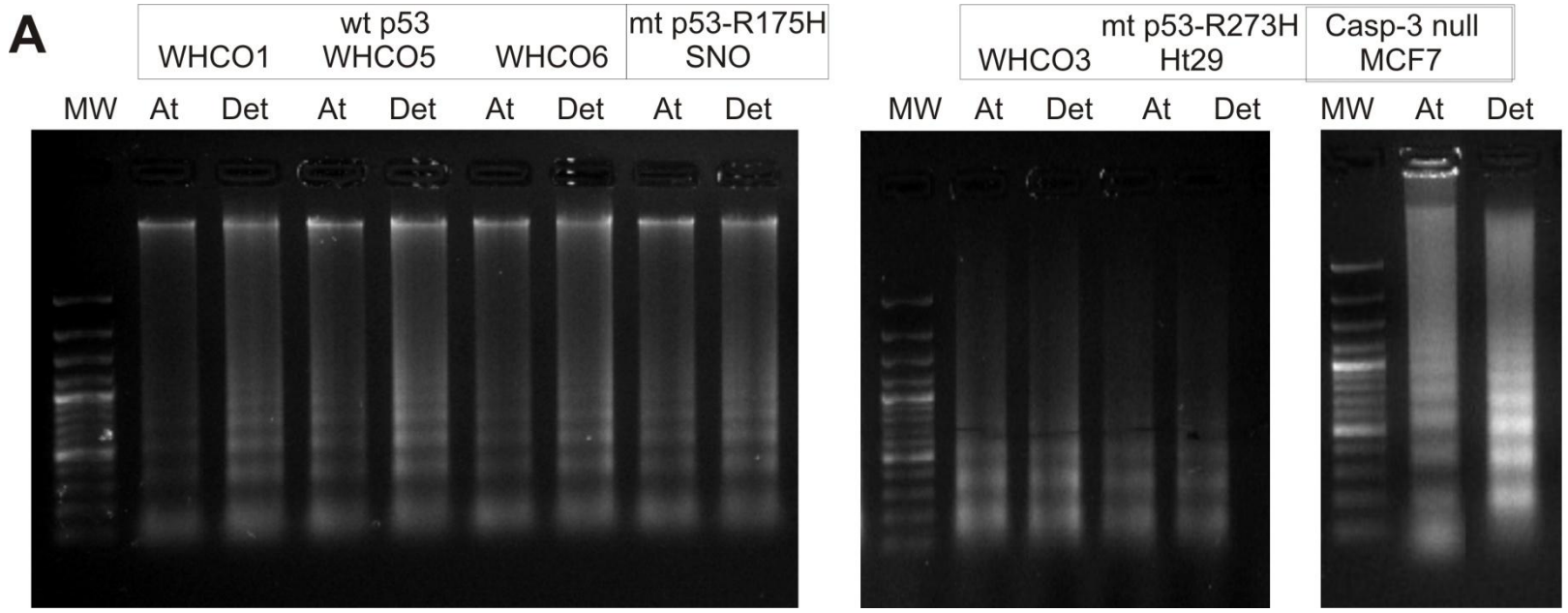

See next page for legend.

B.

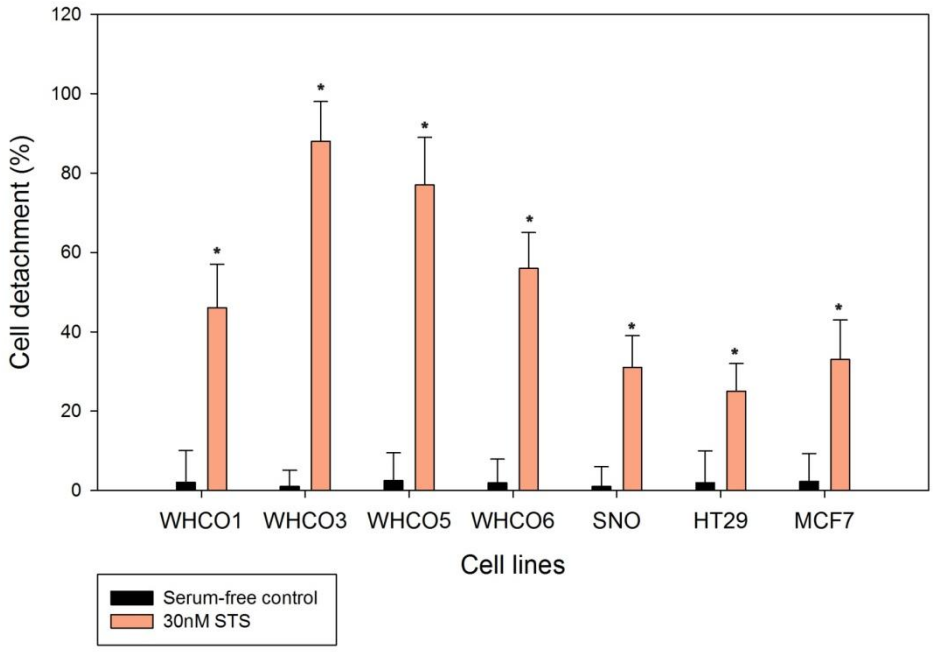

Figure 3.9: The p53-R175H and p53-R273H mt cell lines are resistant to STS-mediated detachment A) The apoptotic DNA ladder was evident in both the genomic DNA extracted from detached (Det) cells and attached (At) STS-treated HOSCC, HT29 and MCF7 cells. B) STS induced cell detachment in the HOSCC cell lines. The lowest percentage of cell detachment was observed in the mt p53 SNO cell line (28%), followed by the mt p53-R273H HT29 cell line (23%). Bars represent standard deviation. MW = GeneRulerTM 100bp Plus DNA ladder * $p < 0.05$

3.3.6 STS induces FAK cleavage and caspase-3 activation in HOSCC cell lines harbouring wt p53

Survival signals transduced by FAK are eliminated by caspase-dependent cleavage of the C-terminal portion of FAK harboring the focal adhesion targeting (FAT) domain (Cooper *et al*., 2003). In addition to abrogating integrin-associated FAK, this fragment inhibits FAK signalling, further enhancing the apoptotic effect of FAK cleavage (Gervais *et al*., 1998; Cooper *et al*., 2003).

The expression of FAK decreased in all the wt p53 HOSCC cell lines after 24 hours treatment with STS, which was associated with the formation of the double cleavage product, in the range of 85 kDa (*Figure 3.10*). Caspase-3 was activated in a similar time course to the formation of the cleavage product in the wt p53 HOSCC cell lines. No caspase-3 activation or FAK cleavage was observed post STS-treatment in the mt p53-R175H, mt p53-R273H or MCF7 cell lines (*Figure 3.10*).

3.3.7 The mt p53-R175H SNO cell line maintains integrin-associated FAK post STS treatment.

The release of the FAT domain of FAK post caspase-3 activation abrogates the association between FAK and integrin β1 (Gervais *et al*., 1998; van Nimwegen and van der Water, 2007). In contrast to the wt p53 WHCO6 cell line, the mt p53-R175H SNO cell line was resistant to FAK cleavage (*Figure 3.10*). Therefore, the possibility that the mt p53-R175H cell lines was maintaining cell adhesion-dependent signalling post STS treatment was explored. In the representative wt p53 WHCO6 cell line, caspase-3 activation and FAK cleavage (*Figure 3.10*) was accompanied by abrogation of the FAK/integrin β1 interaction (*Figure 3.11*). In contrast, corresponding to the lack of caspase-3 activation (*Figure 3.10*), the FAK/integrin β1 association was detected post STS treatment in the mt p53-R175H cell line (*Figure 3.11*).

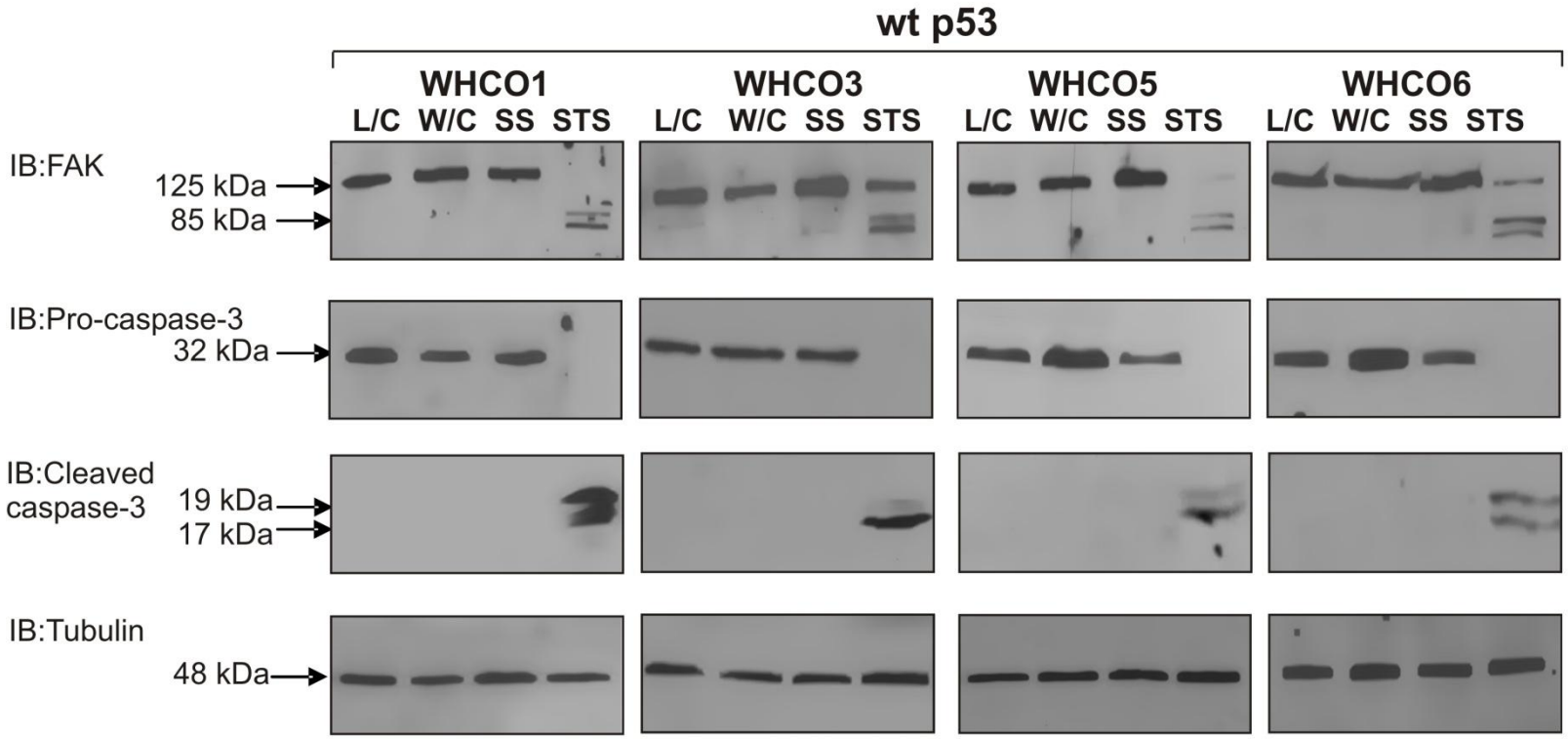

See next page for legend.

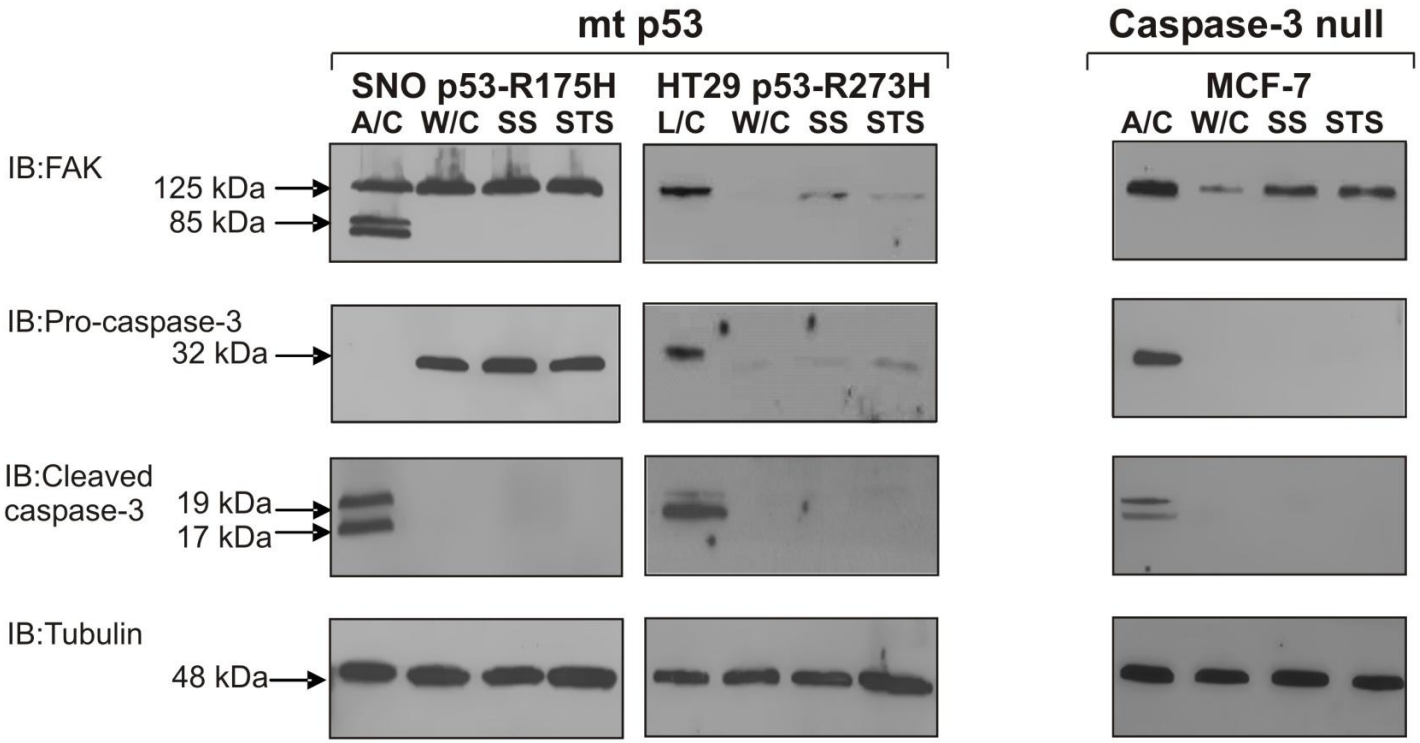

Figure 3.10: The p53-R175H and p53-R273H mt cell lines are resistant to FAK cleavage and caspase-3 activation. The expression of FAK decreased in WHCO1, WHCO3, WHCO5 and WHCO6 cell lines decreased after treatment with STS, which was associated with the formation of the double cleavage product, in the range of 85 kDa. Caspase-3 is activated with a time course corresponding to the formation of the cleavage product in the HOSCC cell lines. Note, in the mt p53 SNO and HT29 cell lines, neither FAK cleavage nor caspase-3 activation was detected. A standardized whole cell loading control from the SNO cell line (L/C) was included in the first lane of each immunoblot to allow for comparison of wt p53 cell lines. An apoptotic control (A/C) from the WHCO6 wt p53 cell line was included in the first lane of each immunoblot in the mt p53 and caspase-3 null cell lines. W/C = lysate from cell line SS = Serum-free conditions.

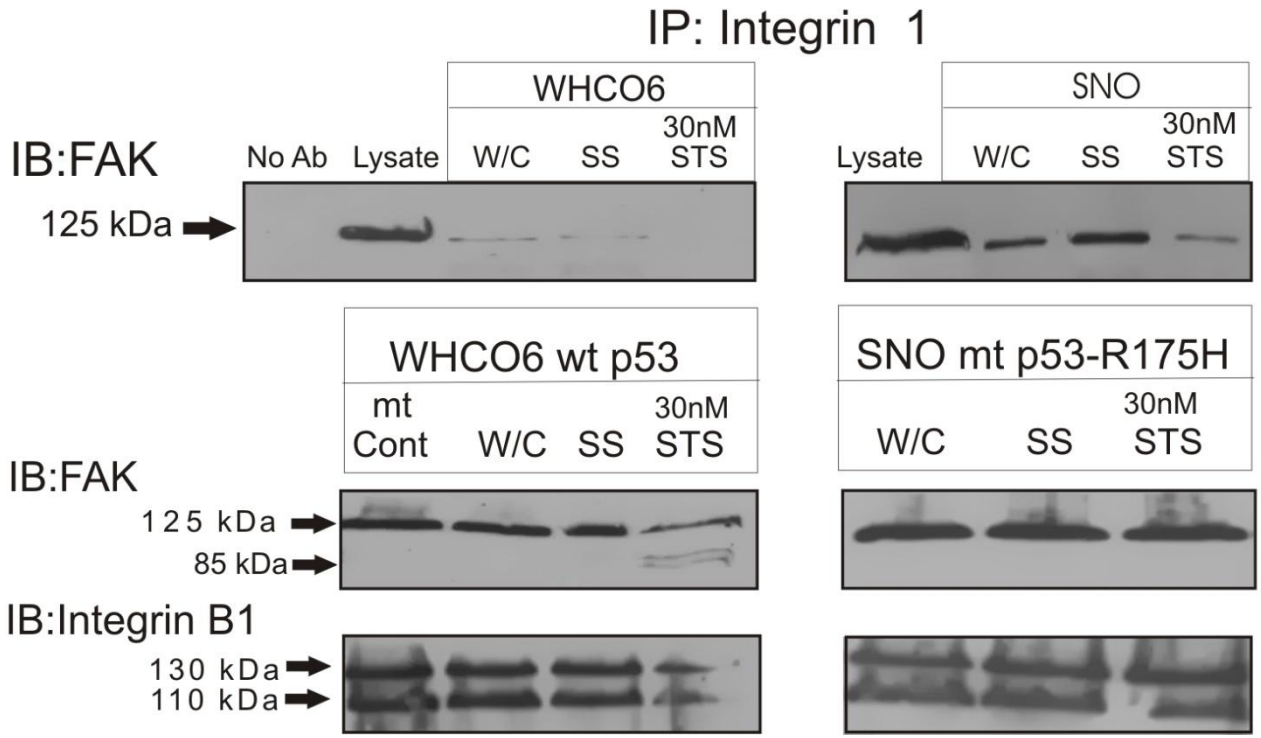

Figure 3.11: STS-mediated events do not abrogate the FAK/integrin β1 association in the mt p53-R175H cell line. FAK cleavage is associated with the complete abrogation of the FAK/integrin β1 interaction in the wt p53 WHCO6 cell line. However, in the mt p53-R175H SNO cell line, the complex between FAK and integrin β1 was still detected post STS treatment. Note: the samples used to detect FAK expression in *Figure 3.10* were the same samples used for immunoprecipitation, and therefore, also represent a loading control for the FAK/integrin β1 immunoprecipitation reaction. W/C = lysate from cell line SS = Serum-free conditions.

3.4 Discussion

Although the ability of mutant p53 to resist apoptotic stimuli is well established (Blandino *et al*., 1999; Zalcenstein *et al*., 2003; Golubovskaya *et al*., 2008 (a); Lim *et al*., 2008), the role of mt p53 in anoikis resistance has never been explored. In particular, the "hot-spot" conformation mt p53-R175H confers resistance to apoptosis by repressing key anoikis-related intermediates including the FAK promoter and caspase-3 levels (Tsang *et al*., 2005; Golubovskaya *et al*., 2008 (a)). Thus, with the aim of establishing the role of mt p53 in anoikis-related events, we made use of this unique model to compare STS-mediated apoptosis in HOSCC cell lines expressing wt p53 (WHCO1, WHCO3, WHCO5 and WHCO6) with the HOSCC cell line (SNO) harbouring the mt p53-R175H (*Figure 3.2*). In addition, the highly prevalent Pro/Arg72 polymorphism was detected in both the WHCO1 and SNO cell lines (*Figure 3.4*). The HT29 cell line harbouring the other prevalent DNA contact mutation, R273H was also included in the comparison, whilst, the caspase-3-null MCF7 cell line served as a negative control for caspase-independent apoptotic events (Jánicke *et al*., 1998; Lin-Lee *et al*., 2001; Mooney *et al*., 2002).

In the wt p53 HOSCC cell lines, definitive STS-induced apoptosis was evidenced by typical apoptotic morphology (*Figure 3.5*), oligonucleosomal cleavage (*Figure 3.8A*) and caspase-3 activation (*Figure 3.10*). Despite the Pro/Arg72 polymorphism, the WHCO1 cell line responded to STS in the same manner as the other wt p53 cell lines (*Figure 3.10*). Hence, for the rest of this report, the WHCO1 cell line is classified as a wt p53 cell line. Although, typical apoptotic morphology (*Figure 3.5*) and distinct oligonucleosomal cleavage was detected in the mt p53 cell lines (SNO and HT29) (*Figure 3.8A*) no caspase-3 activation was detected post STS-treatment (*Figure 3.10*). Interestingly, despite the lack of caspase-3 activation, the highest percentage of TUNEL-positive nuclei was observed in the mt p53 cell lines post STS-treatment (*Figure 3.8C*). The ability of STS to induce caspase-3 independent oligonucleosomal cleavage was demonstrated in the caspase-3 null MCF-7 cell line (*Figure 3.8A*).

As TUNEL was performed *in situ* and the apoptotic DNA ladder was detected in both adhered and detached cells (*Figure 3.9A*), percentage detachment was used to compare STS-mediated apoptosis between the wt and mt p53 cell lines. Accordingly, in the p53-R175H and p53-R273H cell lines, the high level of TUNEL-positive nuclei (*Figure 3.8C*) corresponded to the lowest percentage of cell detachment (*Figure 3.9B*). Thus, p53-R175H and p53-R273H do not protect the SNO and HT29 cell lines from STS-mediated oligonucleosomal cleavage. However, in comparison to the wt cell lines, the p53-R175H and p53-R273H cell lines were resistant to STS-mediated detachment and caspase-3 activation. Consequently, these data reveal a link between loss of tumour suppressor function of p53 and enhanced cell adhesion-dependent signalling.

Survival signals transduced by FAK are eliminated by caspase-dependent cleavage of FAK (Gervais *et al*., 1998; Cooper *et al*., 2003). We show distinct cleavage of FAK, which corresponded to caspase-3 activation, in the wt p53 HOSCC cell lines (*Figure 3.10*). The lack of caspase-3 expression in the MCF-7 emphasized the involvement of caspase activity in FAK cleavage, despite the presence of oligonucleosomal cleavage. Conversely, corresponding to resistance to STS-mediated detachment, no FAK cleavage was detected by immunoblot in the mt p53 cell lines (*Figure 3.10*). Consequently, FAK-dependent signalling is maintained in the mt p53 cell lines post oligonucleosomal cleavage.

Loss of cell-matrix contact in epithelial cells reduces integrin-mediated FAK survival signalling, thereby triggering anoikis (Frisch and Francis, 1994; Zhang *et al*., 2004 (a)). Importantly, the cleavage of FAK induces the loss of integrin-associated FAK at sites of focal contact (Schaller *et al*., 1994; van Nimwegen and van der Water, 2007). Accordingly, the absence of FAK cleavage in the SNO cell line was accompanied by the maintenance of the FAK/integrin β1 association (*Figure 3.11*). Importantly, these data strongly support the notion that mt p53-R175H facilitates anchorage-independent survival through the maintenance of FAK-dependent signalling.

In summary, even though HOSCC is highly resistant to the apoptosis-inducing ability of chemotherapeutic reagents (Leu *et al*., 2000; Lin *et al*., 2009), the data presented shows that oligonucleosomal cleavage was still inducible by the widely used apoptosis-inducing agent STS in the wt, mt and caspase-3 null cell lines (*Figure 3.8A*). However, both mt p53-R175H SNO and p53-R273H HT29 cell lines were resistant to STS-mediated detachment (*Figure 3.9B*). In addition, both mt p53 cell lines were resistant to caspase-3 activation and the cleavage of the C-terminal of FAK (*Figure 3.10*). Thus, sustained integrin β1-dependent activation of FAK (*Figure 3.11*) may be responsible for the resistance to STS-mediated detachment observed in the mt p53 cell lines. Survival signals mediated by ECM proteins are transmitted via the integrins, thereby activating FAK (Kamarajan and Kapila, 2007). Hence, due to the persistent activation of FAK observed in the mt p53-R175H cell line, these data strongly advocate a critical role of mt p53 in the maintenance of cell adhesion-dependent survival signalling. Consequently, the effect of p53 mutational status on the ECM/FAK-mediated suppression of apoptotic events forms the basis of the next chapter.

Chapter 4

The role of extracellular matrix-mediated activation of FAK in the suppression of apoptosis in HOSCC cell lines: wt vs. mt p53-R175H

4.1 Introduction

ECM-mediated signals play a particularly important role in the maintenance of normal tissue architecture, through the regulation of cell survival (Badylak *et al*., 2009). During metastatic progression, however, cells lose this anchorage dependence, allowing them to survive in inappropriate environments (Badylak *et al*., 2009). Consequently, loss of dependence on ECM-mediated signalling is a hallmark characteristic of tumour cells (Westhoff and Fulda, 2009). Therefore, the molecular analysis of ECM-mediated suppression of cell death is imperative as it reveals the underlying mechanism that enables tumour cells to evade these signals and escape anoikis.

Survival signals mediated by ECM proteins are transmitted via the integrins. Several factors, including tissue origin and matrix composition, determine which set of integrins transduce ECM-mediated survival signals. In an experimental setting, fibronectin (FN) has been demonstrated to be a potent inhibitor of anoikis via the activation of FAK-dependent survival signalling (Ilic *et al*., 1998; Zhang *et al*., 2004 (a)). FN is a large glycoprotein, found in soluble form in plasma and other body fluids as well as large cross-linked insoluble subunits in certain ECM (Parsons, 2003). Each fibronectin (FN) molecule consists of two 220 kDa chains joined together by disulfide bonds (Hynes and Yamada, 1982). There are several isoforms of FN, all of which arise from the alternative splicing of a single gene (Kamarajan and Kapila, 2007). Several cell adhesive sites are present on FN including the central arginine-glycine-aspartic acid (RGD) binding site, recognized by the $\alpha 5\beta 1$ integrin (Kamarajan and Kapila, 2007).

Early studies on an immortalized thyroid cell line, demonstrated that cells underwent apoptosis when the α5β1-FN interaction was blocked (Ilic *et al*., 1998). Moreover, apoptosis triggered by serum removal was prevented by coating culture plates with FN (Ilic *et al*., 1998). Importantly, an altered FN-matrix induced by inflammation has been shown to induce anoikis in human periodontal ligament cells (Dai *et al*., 2005). In addition, survival signals mediated by FN via the αvβ1 integrin subunit were sufficient to protect aggregated substrate-dependent SCC cells from detachment-induced death (Zhang *et al*., 2004 (a)). The survival signals transduced by FN-integrin engagement via FAK are attributed to activation of the growth factor-PI3K pathway, as phosphorylation of Tyr397 results in PI3K activation by phosphorylation (Sonoda *et al*., 1999). The PI3K pathway negatively regulates apoptosis, through direct phosphorylation by the serine/threonine protein kinase, PKB. Once activated by phosphorylation, PKB initiates downstream survival events. Among these are the inhibition of several pro-apoptotic proteins including Bad and caspase-9 (Datta *et al*., 1999).

In the previous chapter we reported that the cleavage of FAK corresponded to caspase-3 activation (*Figure 3.10*) and abrogation of the integrin β1/FAK association (*Figure 3.11*). Moreover, the mt p53-R175H and p53-R273H cell lines were resistant to STS-mediated detachment (*Figure 3.9B*) and FAK cleavage (*Figure 3.10*). Consequently, FAK-dependent signals were maintained post STS treatment in the mt p53 cell lines. Uniquely, by analyzing the influence of FN-mediated signalling on apoptotic events, the data presented in this chapter demonstrate that loss of the tumour suppressor function of p53 and maintained FAK-dependent signalling are critical factors underlying anoikis resistance.

4.2 Materials and Methods

4.2.1 Cell lines

As previously documented, see Chapter 2, Section 2.2.1

4.2.2 Antibodies

FAK and caspase-3 were specifically detected with rabbit polyclonal antibodies obtained from SantaCruz Technology. Monoclonal mouse anti-pFAK(Tyr397) (Millipore) and anti-PKBSer473 (Cell Signalling) were used to detect phosphorylation of FAK and PKB respectively. Polyclonal horseradish peroxidase (HRP)-bound anti-rabbit secondary antibody (Separations, SA) was used in the immunoblot experiments.

4.4.3 Protein estimation assay

As previously documented, see Chapter 2, Section 2.2.6

4.4.4 Immunoblot analysis

20 µg of protein per lane was separated by 10% SDS-PAGE. Nonspecific binding sites on the membrane were pre-blocked in blocking buffer for 1 hr. Blots were incubated with: anti-FAK (1:500) or anti-caspase-3 (1:750) for 1 hr; anti-pFAK(Tyr397) in 1% BSA (1:500) overnight or anti-pPKB(Ser473) (1:1000) in 5% BSA overnight. Following incubation in HRP-conjugated secondary membranes were exposed to the SuperSignal West Pico Chemiluminescent working solution, from the West Pico Chemiluminescent Substrate Kit (Pierce, USA) for 5 minutes. Blots were exposed to film and developed as documented in Chapter 2, Section, 2.2.7. Each immunoblot was repeated three times.

4.4.5 Cell detachment

As previously documented, see Chapter 3, Section 3.2.10

4.4.6 Densitometry

Labworks TM Image Acquisition and Analysis software (Labworks version 4.5) was used for densitometric analysis to quantitatively determine the concentration level of FAK in the Western blots.

4.4.7 Statistics

SigmaPlot (version 11.0) was used for statistical analyses. Statistical differences between untreated and treated cells within each cell line were determined by one way ANOVA analysis followed by a pair-wise comparison using the Holm-Sidak method (See Appendix 4.3). The level of significance was set at $p < 0.05$.

4.3 Results

4.3.1 FN increases Tyr397 phosphorylation of FAK

In order to assess whether FN-mediated signalling opposes apoptotic stimuli, the optimal FN concentration was first determined. As Tyr397 phosphorylation was clearly detected by immunoblot in the WHCO6 cell line (*Figure 2.3A*), WHCO6 cells were seeded onto tissue culture dishes, previously coated with 10 μg/ml and 20 μg/ml FN respectively. Following 24hr, the same time interval of STS-mediated apoptotic induction (*Figure 3.8*), cells were analysed for pFAKTyr397. Despite standard FAK expression, pFAKTyr397 increased 2.1 fold and 1.9 fold post FN treatments of 10 μg/ml and 20 μg/ml respectively (*Figure 4.1A*). Hence, these data demonstrate that all RGD sites are saturated at 10 μg/ml FN. Thus, 10 μg/ml was selected as the appropriate FN concentration to assess the opposing effect of increased FN-mediated FAK activation on apoptosis. Cells were seeded onto tissue culture dishes coated with FN, allowed to settle for 2hr, before the removal of serum and the addition of STS. Corresponding to increased pFAKTyr397, cells seeded onto 10 μg/ml FN demonstrated increased edge extension and a flattened morphology (*Figure 4.1B*).

4.3.2 FN treatment reduces STS-mediated detachment in wt p53 cell lines

Previous studies have reported reduced levels of apoptosis in non-transformed and transformed cells seeded onto dishes coated with FN (Ilic *et al*., 1998; Zhang *et al*., 2004 (a)). Due to the increased phosphorylation of FAK observed post FN treatment in the representative WHCO6 cell line, we examined whether FN would repress STS-mediated apoptosis via sustained activation of FAK in the HOSCC cell lines. As STS-mediated detachment was demonstrated to be a more accurate representation of apoptotic sensitivity than TUNEL (*Figure 3.9*), the ability of FN to oppose STS-mediated detachment was assessed across the cell lines. In comparison to serum-free conditions, FN treatment prior to STS treatment reduced STS-mediated detachment in the wt p53 cell lines (*Figure 4.2*). Moreover, with respect to three of four wt p53 cell lines (WHCO1, WHCO3 and

WHCO6) there was a significant reduction ($p < 0.05$) in STS-mediated detachment between the FN-pretreated and the STS control cells (*Figure 4.2*). In addition, corresponding to the resistance to detachment observed in the mt p53 cell lines, no appreciable difference between cell detachment post FN treatment was evident between cells seeded onto FN or control cells (*Figure 4.2*). The caspase-3 null MCF7 cell line showed a similar trend to the mt p53 cell lines.

A.

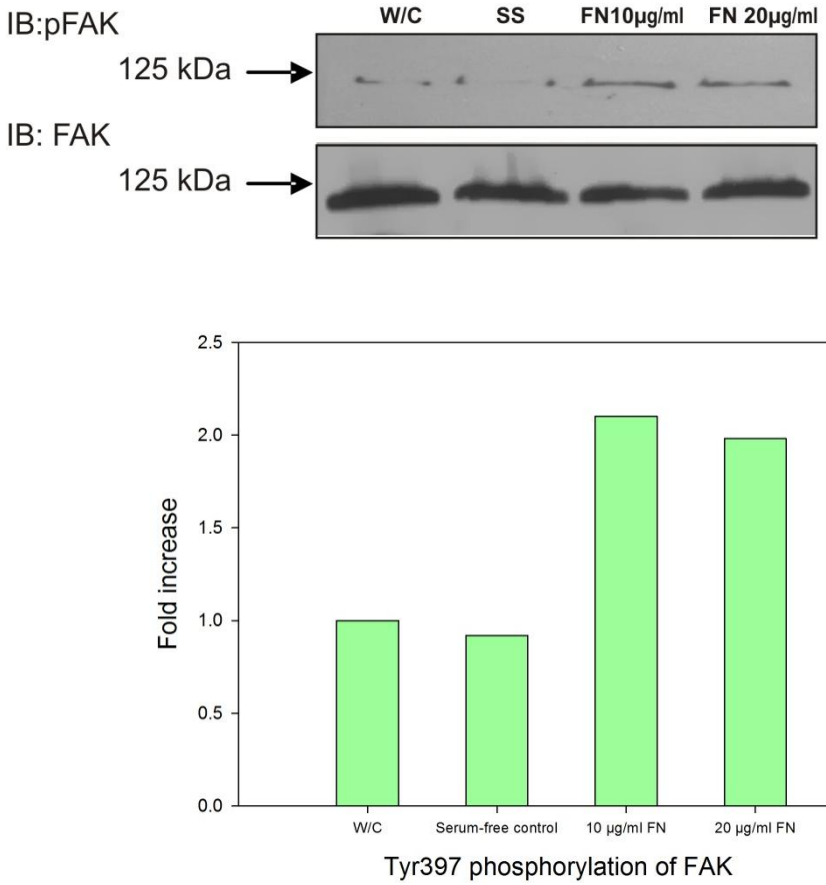

B.

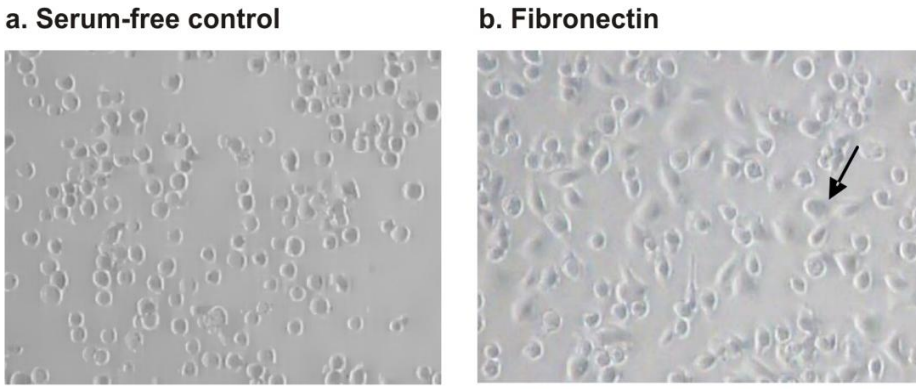

Figure 4.1: FN increases pFAKTyr397 in the WHCO6 cell line. A) FN treatment increased pFAKTyr397 2.1 fold at 10 µg/ml. No appreciable difference in pFAKTyr397 was observed between 10 µg/ml and 20 µg/ml FN. B) Increased edge extension was observed post FN treatment in the WHCO6 cell line, when compared to serum-free control. W/C = WHCO6 whole cell lysate. SS = serum free conditions

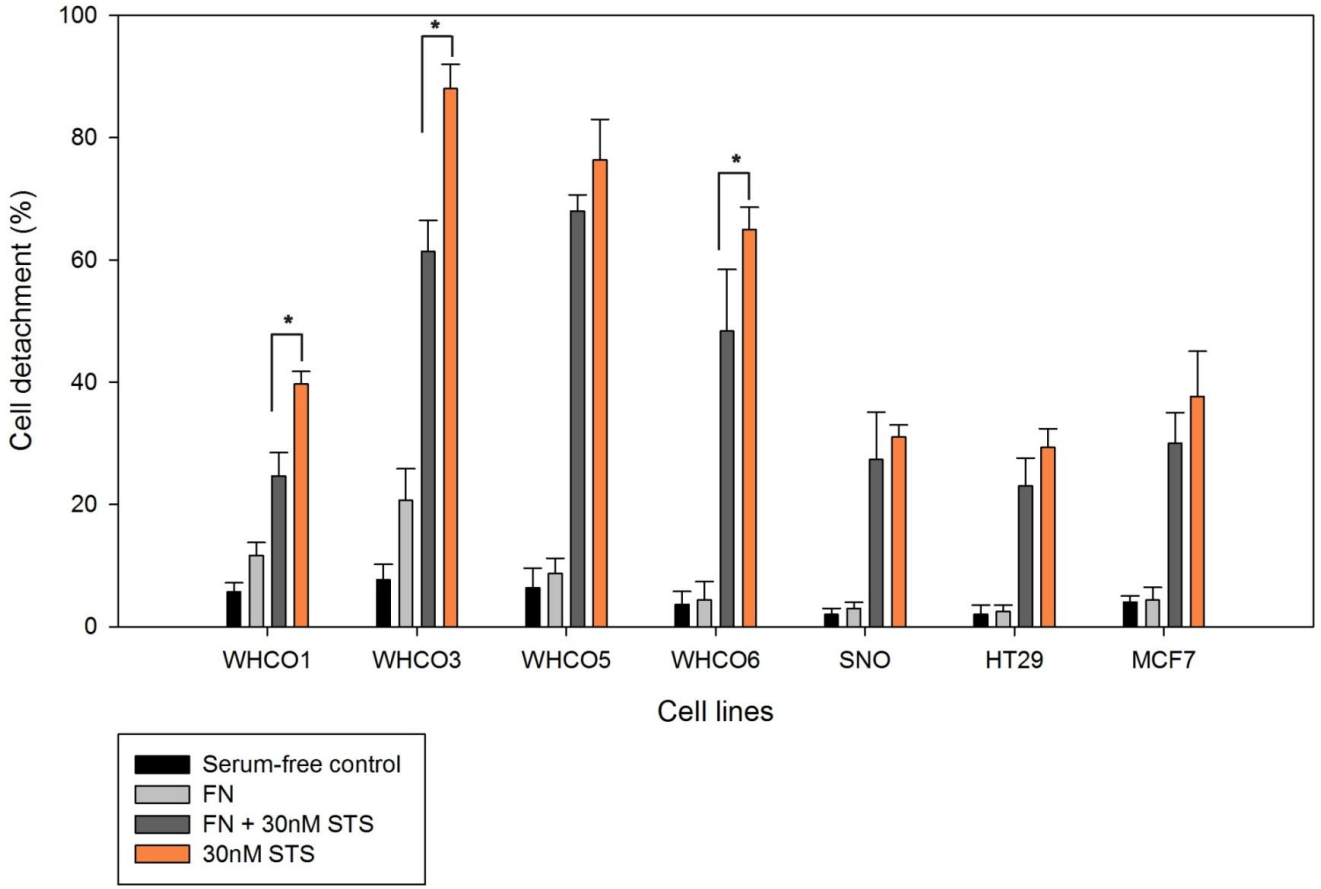

Figure 4.2: FN treatment reduces STS-mediated detachment in wt p53 cell lines. Wt p53 cells seeded onto FN prior to STS-treatment exhibit reduced detachment when compared to STS treated cells. No appreciable difference in detachment between FN and STS-treated cells was observed in the mt p53 and caspase-3 null cell lines. Results were analysed using one-way ANOVA with Holm-Sidak method. Bars represent standard deviation. *p <0.05

4.3.3 FAK cleavage is independent of cell detachment or FN-mediated signalling

We have clearly demonstrated that the cleavage of the C-terminal of FAK corresponded to caspase-3 activation (*See Figure 3.10*). In addition, FAK cleavage was only observed in the wt p53 HOSCC cell lines (WHCO1, WHCO3, WHCO5 and WHCO6). Hence, as these data demonstrates that the mt p53 cell lines may be maintaining FAK-dependent signalling, we examined whether cells seeded onto FN prior to STS treatment would demonstrate reduced FAK cleavage. Although FN offered protection to STS-mediated detachment in the wt p53 cell lines (*Figure 4.2*), there was no difference in FAK cleavage between FN-treated cells and control cells (*Figure 4.3*). Consistent with the previous demonstration (*Figure 3.10*), STS treatment was not accompanied by FAK cleavage in the mt p53-R175H, mt p53-R273H or caspase-3 null cell lines (*Figure 4.3*).

4.3.4 Survival signals transduced by FN are independent of FAK(Tyr397) or PKB(Ser473) phosphorylation

Survival signals transduced by FN-integrin engagement via FAK are attributed to activation of PKB-mediated signalling (Sonoda *et al*., 1999; Diaz-Montero *et al*., 2006). Hence, we examined whether increased PKB-dependent signalling was responsible for the FN-mediated reduction in cell detachment observed in the wt p53 cell lines (*Figure 4.2*). The wt p53 WHCO6 cell line, which showed a significant decrease in STS-mediated cell detachment post FN treatment, was compared to the mt p53-R175H SNO cell line that demonstrated no appreciable change in cell detachment. In order for PKB to achieve full activation, phosphorylation at the Ser473 site is required (Sarbassov *et al*., 2006). Although FN increased pFAKTyr397 in the WHCO6 cell line and reduced STS-mediated detachment, FN treatment did not maintain pFAKTyr397 or pPKBSer473 (*Figure 4.4*). Conversely, in the mt p53-R175H SNO cell line, pFAKTyr397 and pPKBSer473 were not influenced by STS treatment (*Figure 4.4*).

A.

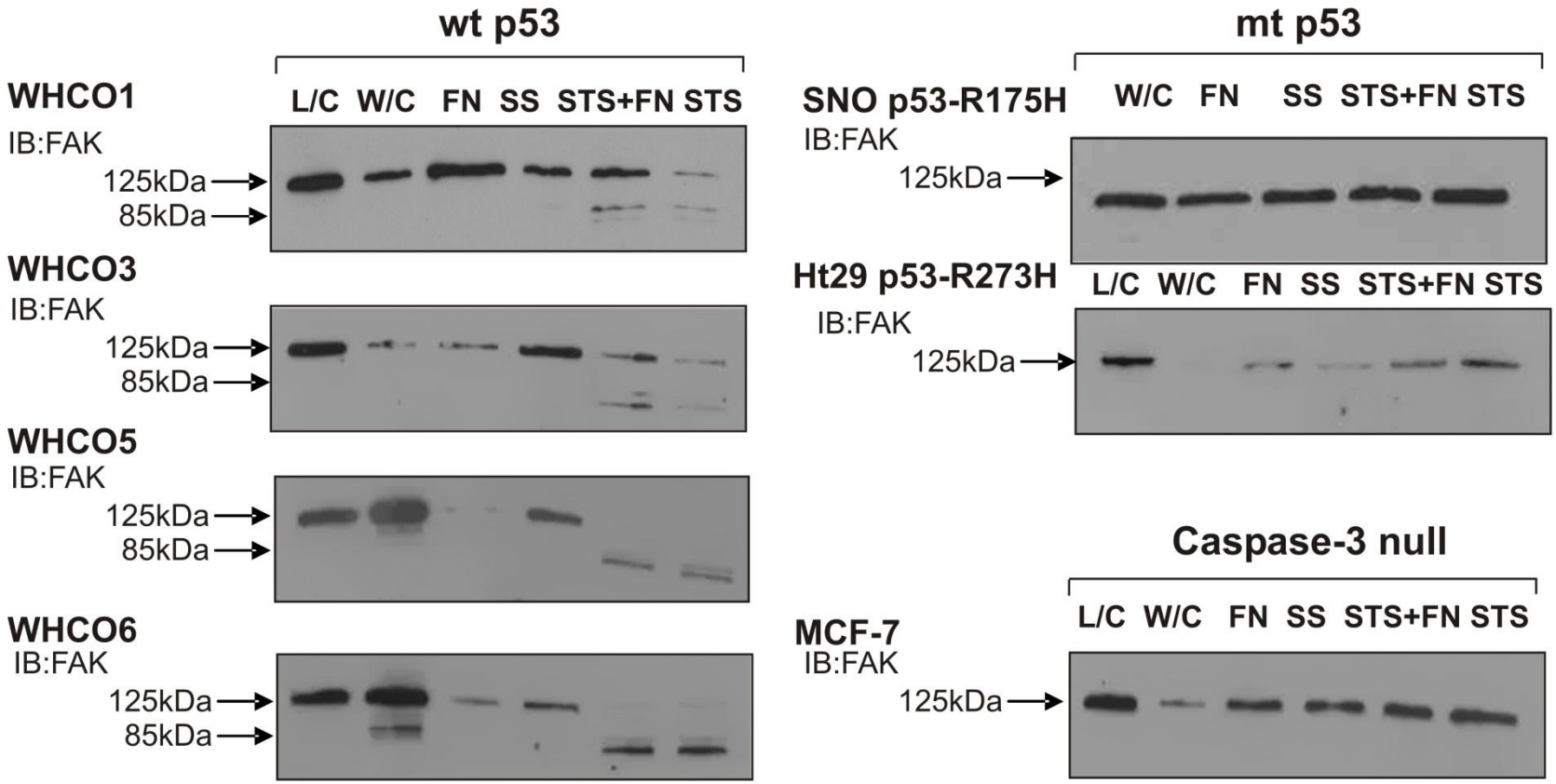

See next page for legend.

B.

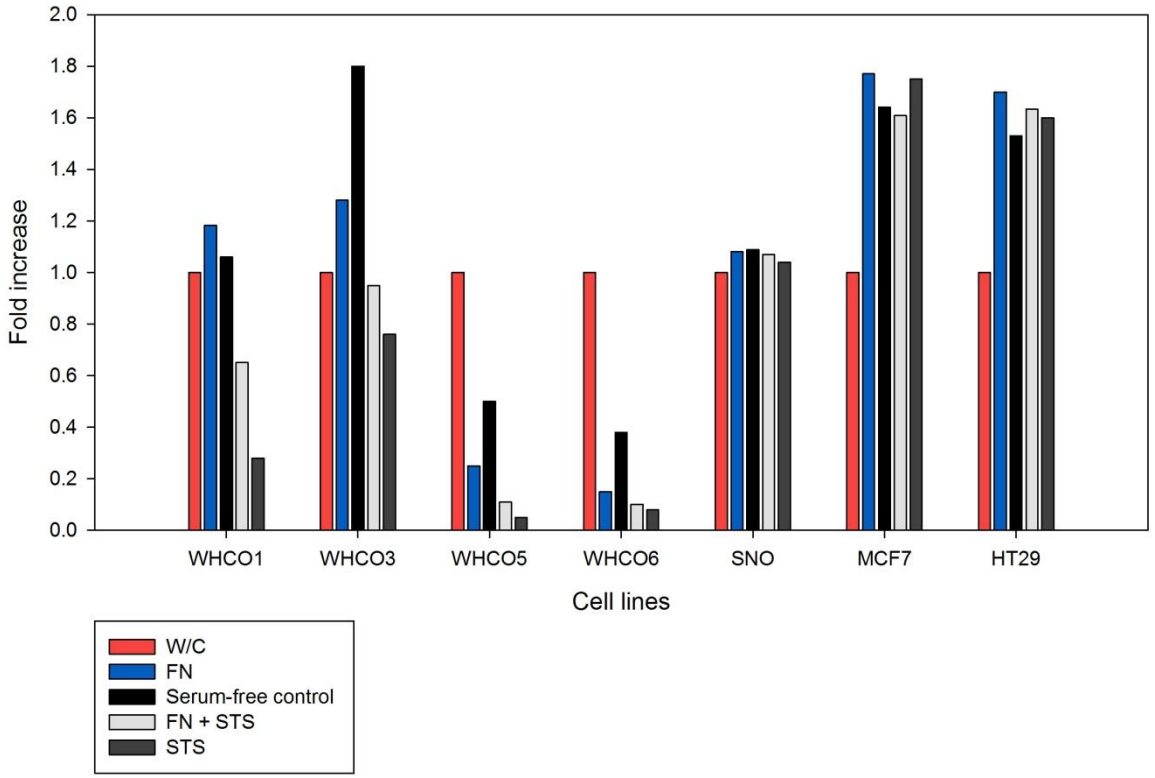

Figure 4.3: FN treatment does not alter FAK expression in HOSCC cell lines. A) FN treatment did not oppose FAK cleavage in wt p53 cell lines. FAK was not cleaved in mt p53-R175H, mt p53-R273H or caspase-3- null cell lines. B) Densitometric analyses of FAK expression post STS/FN treatment. FN did not appreciably influence the level of FAK expression post STS treatment in the wt or mt p53 cell lines. Note: A SNO loading control was included in the first lane of each immunoblot to normalise protein loading and allow for densitometric comparison between immunoblots.

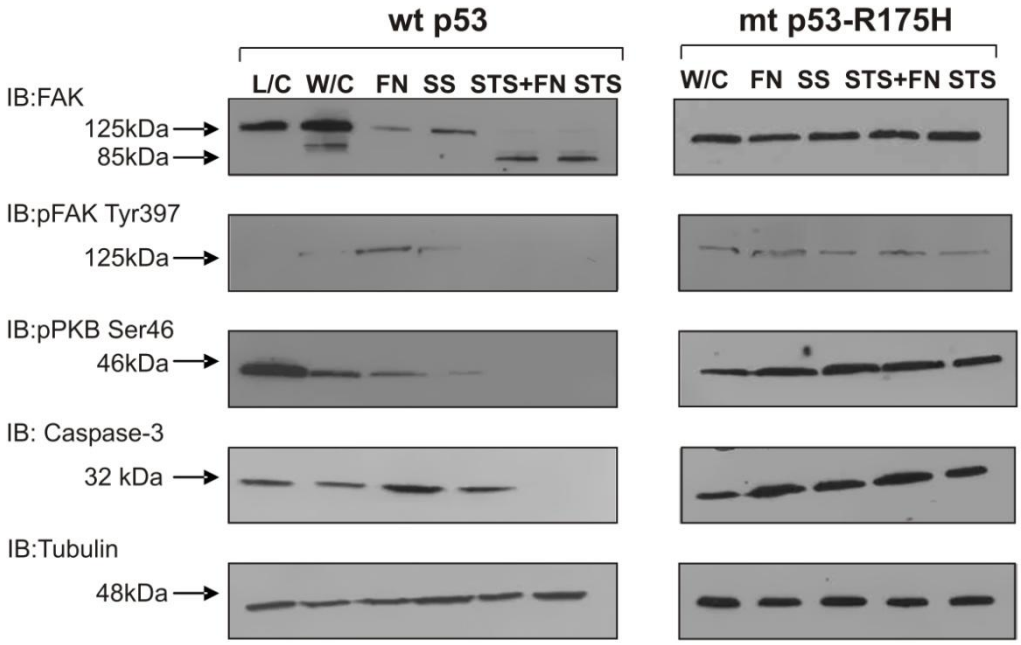

Figure 4.4: FN-dependent signals are independent of pFAKTyr397 and pPKBSer473 phosphorylation in HOSCC cell lines. Dephosphorylation of both pFAKTyr397 and pPKBSer473 accompanies FAK cleavage in the wt p53 WHCO6 cell line. pFAKTyr397 and pPKBSer473 were not influenced by STS/FN treatment in the mt p53-R175H SNO cell line. Tubulin was included as the loading control. A SNO loading control (L/C) is included in the first lane of each WHCO6 immunoblot to allow for comparison.

4.4 Discussion

As loss of anchorage dependence is pivotal to the metastastic progression of tumours, characterization of cell adhesion events is critical to enhance the understanding of anoikis-related signalling. In the anchorage-dependent HOSCC cell lines, survival signals transduced via the ECM were assessed by culturing the cells in the absence of serum and on tissue culture dishes coated with insoluble FN. The enhanced cell adhesion induced by FN/integrin engagement is attributed to increased activation of FAK by Tyr397 phosphorylation (Sonoda *et al*., 1999; Zhang *et al*., 2004 (a)). Consistent with previous reports in fibroblasts and epithelial tumours (Vitale *et al*., 1998; Zhang *et al*., 2004 (a)), FN increased Tyr397 phosphorylation (*Figure 4.1A*) and edge extension (*Figure 4.1B*) in the representative WHCO6 cell line.

FAK cleavage corresponded to caspase-3 activation in the wt p53 cell lines, whilst, the mt p53 cell lines were resistant to STS-mediated detachment (*See Figures 3.9B & 3.10*). Moreover, the mt p53-R175H cell line maintained integrin β1-activated FAK post STS treatment (*Figure 3.11*). Thus, making use of this unique model of moderately-differentiated oesophageal carcinoma cell lines, we examined whether FN-mediated signalling protected the wt p53 and detachment-resistant mt p53 cell lines from apoptotic death, as assessed by cell detachment. Notably, FN significantly reduced STS-mediated detachment ($p < 0.05$) in three of the wt p53 cell lines (WHCO1, WHCO3 and WHCO6), whilst cell detachment was not influenced in the mt p53 and caspase-3-null cell lines (*Figure 4.2*). Although FAK cleavage corresponded to increased cell detachment and caspase-3 activation (*Figure 3.10)*, FN did not offer protection to FAK cleavage in the wt p53 cell lines (*Figure 4.3*). Hence, as the apoptotic ladder was detected in both attached and detached cells (*Figure 3.9A*), these data suggest that caspase activation, and consequently FAK cleavage, are not influenced by cell detachment. This is the first documentation of ECM-dependent suppression of apoptotic stimuli in the highly metastatic HOSCC. Pertinently, the mt p53 cell lines were unaffected by FN-mediated survival signalling and the mt p53-R175H

cell line maintained FAK-dependent signalling post STS treatment (*Figure 4.4*). Thus, in combination with the observed resistance to STS-mediated detachment, these data corroborate an important role of persistent FAK activation in anoikis resistance.

Survival signals transduced via FN are attributed to activation of the PI3K cascade, and consequently, PKB Ser473 phosphorylation (Sonoda *et al*., 1999). However, contradictory reports indicate that FN-mediated survival signalling is cell-type dependent (Ilic *et al*., 1998; Zhang *et al*., 2004 (a)). Thus, as no significant difference in FAK cleavage was evident, we examined whether FN-treated cells maintained pFAKTyr397 and pPKBSer473 post STS treatment. The generation of FAK cleavage products in the region of 85kDa have been reported to repress FAK phosphorylation (Gervais *et al*., 1998) and, thus, reduce FAK-dependent survival signalling. Furthermore, dephosphorylation of FAK has been shown to occur rapidly post STS treatment (Beviligia *et al*., 2003; Lim *et al*., 2008). Consistent with these studies, in the representative wt p53 cell line (WHCO6), attenuation of FAK and PKB phosphorylation corresponded to FAK cleavage and caspase-3 activation (*Figure 4.4*). Hence, the cleavage of the C-terminal from FAK abrogates FAK and PKB activity in the wt p53 WHCO6 cell line. In contrast, in the detachment-resistant mt p53 cell line, STS induced oligonucleosomal cleavage was not accompanied by FAK cleavage or reduced FAKTyr397/PKBSer473 phosphorylation (*Figure 4.4*). Thus, although FN treatment significantly reduced STS-mediated detachment in three of the wt p53 HOSCC cell lines, no appreciable difference in FAK cleavage was observed. Furthermore, FAK cleavage was associated with abrogation of pFAKTyr397 and pPKBSer473 in the wt p53 WHCO6 cell line. Therefore, even though FN mediated-signals have been demonstrated to suppress apoptosis via PI3K-dependent PKB activation in other cell types (Sonoda *et al*., 1999; Zhang *et al*., 2003), seeding HOSCC cells onto FN prior to STS treatment did not maintain FAK or PKB phosphorylation. Accordingly, these observations point to an alternative survival role of FAK in the suppression of apoptotic stimuli.

In contrast, the absence of FAK cleavage corresponded to the maintenance of pFAKTyr397 and pPKBSer473 in the mt p53-R175H SNO cell line (*Figure 4.4*). Hence, these data indicate that the repressive effect that mt p53-R175H has been established to have on the FAK promoter (Golubovskaya *et al*., 2008 (a)), may be responsible for the constitutive phosphorylation and the maintenance of PKB-dependent survival signalling observed in the SNO cell line.

Sustained activation of FAK has been proposed to protect tumour cells from anoikis by repressing p53-dependent apoptosis (Ilic *et al*., 1998; Golubovskaya *e t al*., 2008 (a)). Thus, the lack of dependence on cell adhesion-dependent signalling in mt p53-R175H cell line supports the notion that mt p53-R175H is intimately involved in conferring growth resistance via a FAK-dependent mechanism. Consequently, to explore this possibility, the role of sustained activation of FAK on interplay between FAK and p53-mediated apoptosis forms the basis of the subsequent chapter.

Chapter 5

Interplay between p53 and FAK: impact of the mt p53-R175H 'loss of function' effect on FAK regulation

5.1 Introduction

Aberrant regulation of the p53-dependent apoptotic pathway is implicated as a major contributor to FAK-dependent anoikis resistance (Vitale *et al*., 1998; Golubovskaya *et al*., 2005). *In vitro*, overexpression of FAK abrogates p53-mediated apoptosis, as well as p53-dependent transcriptional activation of apoptotic genes (Golubovskaya *et al*., 2005; Golubovskaya *et al*., 2008 (a)). Pertinent to anoikis-related regulation, ECM activation of FAK reduces p53-dependent apoptosis (Ilic *et al*., 1998; Zhang *et al*., 2004 (a)), whilst FAK knockdown in combination with cisplatin treatment has been shown to trigger p53-mediated apoptosis (Lim *et al*., 2008). Furthermore, the apoptotic events triggered by FAK deactivation are accompanied by rapid dephosphorylation of the FAK autophosphorylation site, pFAKTyr397 (Beviligia *et al*., 2003). However, it is difficult to discern from the previous studies if cancer cells resist p53-mediated apoptosis due to downstream effects of FAK-dependent survival signaling, or whether FAK facilitates cell survival by direct inhibition of p53. The specific interaction between the FERM domain of FAK and N-terminal of p53 has been proposed to inhibit p53 activity by enhancing Mdm-2-dependent ubiquitination of p53 (Lim *et al*., 2008) or alternatively, inhibiting p53 transcriptional activity by binding to the p53 transactivation domain (Ilic *et al*., 1998; Zhang *et al*., 2004 (a)). Hence, in tumour cells overexpressing FAK, manipulation of the p53/FAK interaction may trigger p53-mediated apoptosis and thereby, enhance the apoptosis-inducing ability of chemotherapeutic reagents.

Recently, a direct correlation between FAK overexpression and mutant p53 has been demonstrated (Golubovskaya *et al*., 2009). p53 mutants differ in their ability to resist apoptotic stimuli. Specifically, the R175H "hot spot" mutant has been shown to be a potent inhibitor of apoptosis (Blandino *et al*., 1999; Tsang *et al*.,

2005; Golubovskaya *et al*., 2008 (a)). It has been suggested that the R175H mutation limits the flexibility of p53, thereby "locking" p53 into a more rigid conformation that reduces its DNA-binding capacity and possibly the ability to interact with other proteins (Aylon and Oren, 2007). This "loss of function" effect is attributed to reduced transcriptional upregulation of apoptotic intermediates, as the mutant is not resistant to ubiquitination (*Figure 5.1*; Shimizu *et al*., 2006).

Furthermore, in addition to the loss of transcriptional function, some p53 mutants exert a gain of function (GOF) effect and exhibit a selective advantage in carcinogenesis (*Figure 5.1*; Levine *et al*., 1991). GOF effects include enhanced cancer cell proliferation and increased tumourigenicity *in vivo*, suggesting that the GOF activity of mt p53 may play an important role in tumour progression. In mouse models, mutant p53 expression in lymphoblastic leukemia cells or murine fibroblasts resulted in greater tumourigenicity and tissue invasiveness as compared to p53-null cells (Dittmer *et al*., 1993; Hsiao *et al*., 1994). This GOF was attributed to altered patterns of gene expression as mt p53 has been found to upregulate the promoters of several genes, including multidrug resistance-1 (MDR-1) (Chin *et al*., 1992). In addition, mt p53 has been shown to downregulate proteins important to anoikis resistance, including caspase-3 (Tsang *et al*., 2005) and Fas (Zalcenstein *et al*., 2003).

Since most p53 DNA binding domain (DBD) mutants do not alter the tetramerization domain, mt p53 is able to heterotetramerize with wt p53 (Milner and Medcalf, 1991). Consequently, as the heterotetramerization of the conformational p53 mts with wt p53 converts the wt protein to an inactive, mutant conformation, p53 mutants exert dominant negative effects on co-expressed wt p53 (*Figure 5.1*; Ko and Prives, 1996; Willis *et al*., 2004). Therefore, akin to the LOF effect, in these mutants the dominant negative effect is attributed to the reduced transcriptional activation of p53 targets, as the wt/mt heterotetramer does not bind DNA with the same affinity as the wt p53 homotetramer (Chene, 1998; Nicholls *et al*., 2002). Furthermore, the ability of mutant p53 to inhibit wt p53

may be due to the mt p53 binding to components of the TFIID and TFIIH complexes (Wang *et al*., 1995). As a consequence, mutant p53 sequesters transcriptional cofactors necessary for wild-type p53 activity. Thus, the dominant negative effect of mutant p53 is reliant on the mutant p53 conformation, and consequently, the affinity of the mutant for p53 target sequences (Ko and Prives, 1996; Willis *et al*., 2004).

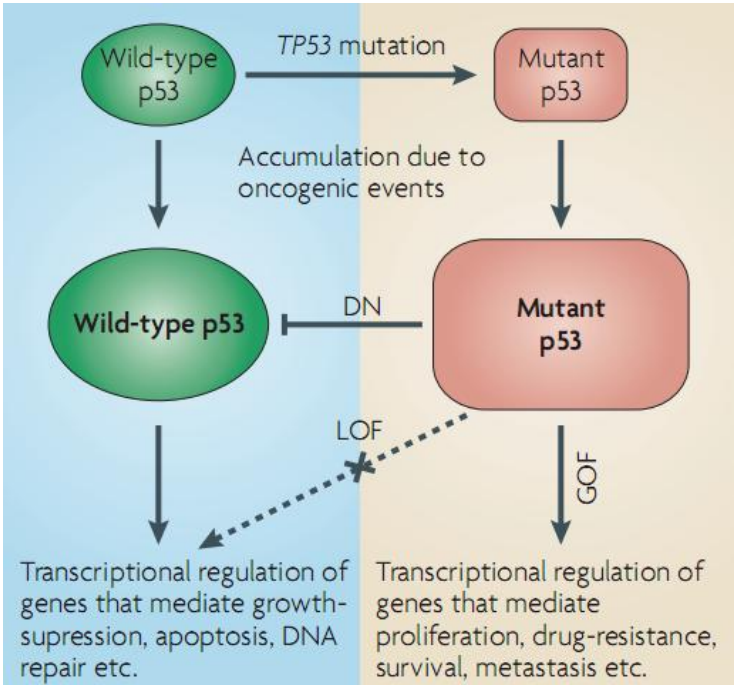

Figure 5.1: Diagrammatic summary of the impact of loss of p53 function. The phenotypic effects of p53 mutations can be classified as: 1) Mutations that abrogate the binding of p53 to its consensus DNA binding sequence. Consequently, due to "loss of function" these mutants abolish the transcriptional activity of p53. 2) Most missense mutations may produce a full-length mutant p53 capable of oligomerising with wt p53 to form a defective heterotetramer - these mutants exert a "dominant negative" function. 3) Several 'gain of function' mutations confer mutant p53 with new functions independent of wild-type p53. GOF = gain of function; DN = dominant negative; LOF = Loss of function © Brosh and Rotter, 2009

Importantly, one way in which the prevalent "hot spot" p53 mt-R175H exerts a LOF effect is by abolishing the ability of p53 to transcriptionally increase FAK expression (Golubovskaya *et al*., 2008 (a)). Pertinent to the loss of transcriptional regulation of FAK, we detail in the previous chapters that the mt p53-R175H cell line was resistant to STS-mediated FAK cleavage (*Figure 3.10*) and dephosphorylation (*Figure 4.4*). Moreover, ECM-mediated protection of apoptotic death is independent of PKB signalling in the HOSCC cell lines, indicating that the activation of FAK represses cell death via an alternative mechanism (*Figure 4.4*). Hence, in order to gain insight into the mechanism whereby the mt p53-R175H enhances FAK activity, we explored the influence of mt p53-R175H on interplay between FAK and p53.

5.2 Materials and Methods

5.2.1 Cell lines

As previously documented, see Chapter 2, Section 2.2.1

5.2.2 Antibodies

FAK, p53 and caspase-3 were specifically detected with a rabbit polyclonal antibody obtained from SantaCruz Technology. Monoclonal mouse anti-pFAK(Tyr397) (Millipore) was used to detect autophosphorylation of FAK. Polyclonal horseradish peroxidase (HRP)-bound anti-rabbit secondary antibody was used in (Separations, SA) and fluoroscine isothiocyanate (FITC)-conjugated anti-rabbit secondary antibody (Chappel, USA) were used in the immunoblot and immunofluorescence experiments respectively.

5.2.3 Protein estimation assay

As previously documented, see Chapter 2, Section 2.2.6

5.2.4 Immunoblot analysis

As previously documented see Chapter 2, Section 2.2.7

5.2.5 Indirect immunofluorescence

As previously documented, see Chapter 2, Section, 2.2.8

5.2.6 Co-immunoprecipitation

Cells were lysed in RIPA buffer (Appendix 1.3.2) for 30 min at 4 °C. The lysates containing 350 µg protein were incubated with 3 µl of anti-p53 (Santa Cruz Technology) at 4 °C overnight. 20 µl of protein G-Sepharose beads were added to each lysate at 4 °C for overnight. The supernatant was decanted and an equal volume (40 µl) of double lysis buffer (Appendix 1.3.1) was added to the pellet. The suspension was boiled for 5 min and centrifuged for 10 min at 12000 r.p.m in a Sorvall® MC 12 V centrifuge. Samples were resolved by SDS-PAGE and blotted onto nitrocellulose membranes (as above). Blots were incubated in anti-FAK to determine the relative association with p53.

5.2.7 Plasmids

The pCMV-Neo-Bam-p53 and pCMV-Neo-Bam-R175Hp53 plasmids (Appendix 5), containing the human full length p53 cDNA and R175H mutant p53 respectively, were kindly donated by Dr. Bert Vogelstein and Dr Moshe Oren from the Weizmann Institute of Science, Israel.

5.2.8 Preparation of competent cells for heat shock transformation

Competent cells were prepared according to the protocol outlined by Inoue *et al*., (1990). A colony of XL-1blue *E.coli* cells was inoculated in 50 ml of SOB^{HS} (Appendix 1.9.1). The cells were incubated at 18 °C, shaking at 180 r.p.m.. When the cells reached an Abs of 0.6 at 600nm, the cells were incubated on ice for 5 min and centrifuged at 2000 x *g* for 10 min. The pellet was resuspended in 15 ml of ice cold transformation buffer (TB) (Appendix 1.9.2). The cells were incubated on ice for 10 min, centrifuged at 8000 x *g* and resuspended in 4 ml of TB. DMSO (280 µl) was added and the cells were incubated on ice for 10 min. The cells (100 µl) were aliquoted into sterile Eppendorf tubes, placed in liquid nitrogen (10 sec) and stored at -70 °C.

5.2.9 Heat shock transformation of XL-1 blue *E.coli* cells

The heat shock transformation was performed according to the protocol outlined by Inoue *et al*. (1990). The competent cells prepared above were thawed on ice for 30 min. 30 ng of plasmid DNA (empty vector, wt p53 or mt p53-R175H) was added to the cells. The contents were mixed, placed on ice for 30 min and incubated at 42 °C for 90 sec. Cells were placed on ice and pre-warmed SOC (Appendix 1.9.3) medium (37 °C) was added. Cells were incubated at 37 °C for 40 min and 100 µl of the transformation mixture was inoculated on selective LA plate (1.8.1), which was incubated overnight at 37 °C.

5.2.10 Maxi-preparation to obtain adequate amount of purified plasmid

The Maxi-preparation kit (Qiagen), an alkaline based extraction procedure, was used to extract a sufficient amount (up to 500 µg) of purified plasmid from transformed competent cells. A single colony grown on selective LA plate was inoculated into 5 ml of LB (Appendix 1.8.2) containing 5% ampicillin. The

culture was incubated for 8 hr at 37 °C, shaking at 180 r.p.m.. Subsequently, 200 µl of the culture was inoculated into 100 ml of medium and incubated at 37 °C for 16 hr, shaking at 180 r.p.m.. The culture was centrifuged at 6000 x *g* (J2-21 rotor, Beckman JA-20) for 15 min at 4 °C. Once the pellet was resuspended in 10 ml of Buffer P1 and 10 ml of Buffer P2 respectively, the contents were mixed and incubated at TR for 5 min. Buffer 3 (10 ml) was added, contents were mixed immediately and incubated on ice for 20 min. The mixture was centrifuged at 20000 x *g* for 30 min at 4 °C. The supernatant was centrifuged at 20000 x *g* for 15 min at 4 °C. The supernatant was placed in a Qiagen-tip 500, which was previously preequilibrated (rinsed) with 10 ml of buffer QBT. The Qiagen-tip was rinsed twice with 30 ml of Buffer QC. The DNA was eluted with 15 ml of Buffer QF, mixed with 10.5 ml of isopropanol and centrifuged 15000 x *g* for 30 min at 4 °C. The resultant pellet was washed with 5 ml of 70% ethanol and centrifuged at 15000 x *g* for 10 min. Once the supernatant was removed, the pellet was allowed to dry for 10 min. DNA was resuspended in sterile dH_2O for 2 hr at 4 °C. The final DNA concentration in the sample was quantified with the Nanodrop® ND-1000 Spectrophotometer.

5.2.11 Restriction of plasmids from transformed *E.coli*

A reaction mixture (10 µl) containing 10 units (U) of BamHI (Amersham), 10 U of EcoRV (Amersham) and 1 µl buffer B (Amersham) was used to restrict either 15 µg of the pCMV-empty vector, pCMV-Neo-Bam-p53 or pCMV-Neo-Bam-R175Hp53 plasmids respectively. The resultant mixture was incubated at 37 °C for 3 hr. Restricted products (5 µl) and 250 ng of 1 Kb Plus DNA ladder™ (Gibco BRL) were each mixed with 5 µl of loading buffer (Appendix 1.11.1) and subject to 0.8% agarose gel electrophoreses (appendix 1.4.1) at constant voltage of 72V. Ethidium bromide (1%) was used to visualise the DNA under UV light.

5.2.12 Transfection of WHCO6 and SNO cell lines

The pCMV-Neo-Bam-p53 and pCMV-Neo-Bam-R175Hp53 plasmids were transfected into the H1299 and WHCO6 cell lines. A day prior to the transfection, 3 x 10^6 of the H1299 or WHCO6 cells were seeded onto a 60 mm tissue culture dish. Cells were maintained in 5 ml of tissue culture medium and 10% FCS at 37

°C. The transfection of the pCMV-Neo-Bam-p53 and pCMV-Neo-Bam-R175Hp53 plasmids was performed according to the manufacturer's instructions (Invitrogen). Transfection of the pCMV-Neo-Bam-R175Hp53 plasmid was performed at a 1:1 ratio of vector:Lipofectamine^{TM} 2000 (**referred to in text as low charge ratio**). With respect to the pCMV-Neo-Bam-p53 plasmid, transfections were performed at a 3:1 ratio of vector:Lipofectamine^{TM} 2000 (**referred to in text as high charge ratio**). Briefly, transfection reagent (7 µl) was placed in 200 µl of serum-free tissue culture medium. This was followed by the addition of 21 µg of the pCMV-Neo-Bam-p53 and 7 µg pCMV-Neo-Bam-R175Hp53 plasmids respectively, to form a mixture. After 15 min, the mixture was added drop wise to the tissue culture medium in the 6 cm dish containing the H1299 or WHCO6 cells. As a control, 7 µl of Lipofectamine^{TM} 2000 was mixed with, 7 µg/21 µg of the empty pCMV-Neo-Bam vector and 200 µl of medium for 15 min and added to a separate dish of cells.

5.2.13 Densitometry

Labworks TM Image Acquisition and Analysis software (Labworks version 4.5) was used for densitometric analysis to quantitatively determine the concentration level of protein in the western blots. When interpreting the transfection data, we considered a 1.2 fold increase (equivalent to 20 %), to be an appreciable change in FAK expression levels.

5.3 Results

5.3.1 The p53/FAK association is intact in HOSCC cell lines harbouring wt or mt p53-R175H

As the mt p53 cell lines were resistant to STS-mediated detachment and caspase-3 activation (*See Figure 3.9 & 3.10*), we examined whether the inhibitory p53/FAK interaction (Golubovskaya *et al*., 2005) was intact in moderately differentiated HOSCC cell lines harbouring wt p53 or mt p53-R175H, as well as the HT29 cell line harbouring the R273H DNA contact mutant. We clearly show by immunoprecipitation that FAK associates directly with wt and mt p53 (*Figure 5.2*). The p53/FAK interaction has been demonstrated to abrogate p53-dependent apoptosis (Golubovskaya *et al*., 2005; Lim *et al*., 2008).

5.3.2 STS induces nuclear accumulation of FAK in wt and mt p53-R175H cell lines

As staurosporine has been previously shown to enhance nuclear FAK (Lim *et al*., 2008), we examined whether apoptotic events that initiate oligonucleosomal cleavage, both with or without caspase-3 activation, influenced the nuclear localisation of FAK. The nuclear translocation of FAK has been shown to be a prerequisite for FAK-mediated inhibition of p53 (Lim *et al*., 2008). Due to the disruption of the nucleus during apoptotic events, analysis of the nuclear fraction became impractical. As FAK localisation has previously been demonstrated by fluorescence microscopy (Ossovskaya *et al*., 2008), STS-induced FAK nuclear translocation was detected by immunofluorescence in both the representative wt p53 cell line (WHCO6) and mt p53 cell line (SNO). Consequently, in both wt and mt p53 HOSCC cell lines, FAK accumulates in the nucleus (*Figure 5.3*) during cellular conditions that initiate oligonucleosomal cleavage (*See Figure 3.8A*).

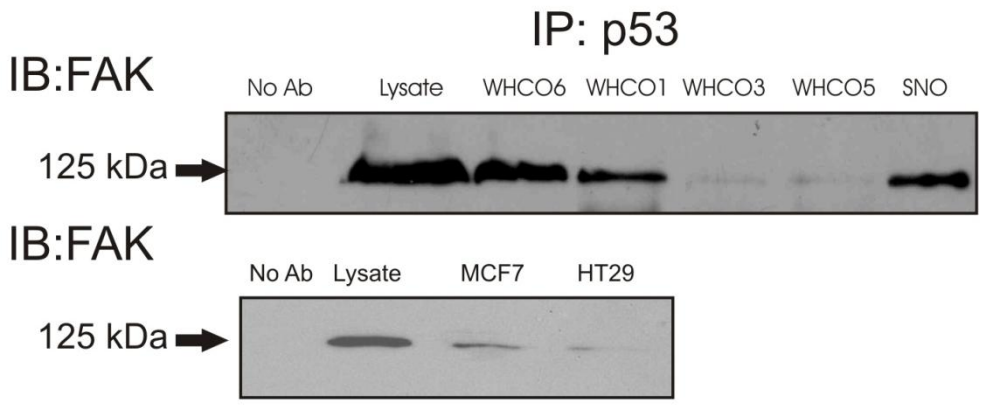

Figure 5.2: The p53/FAK association is independent of p53 mutational status. p53 was detected in complex with FAK in the wt p53, mt p53-R175H and mt p53-R273H cell lines. A whole cell lysate from the WHCO6 cell line was included for each immunoblot to demonstrate the specificity of the immunoprecipitation reaction. A negative control (Lysate + 2µl anti-p53 antibody) was included to demonstrate the specificity of the co-immunoprecipitation.

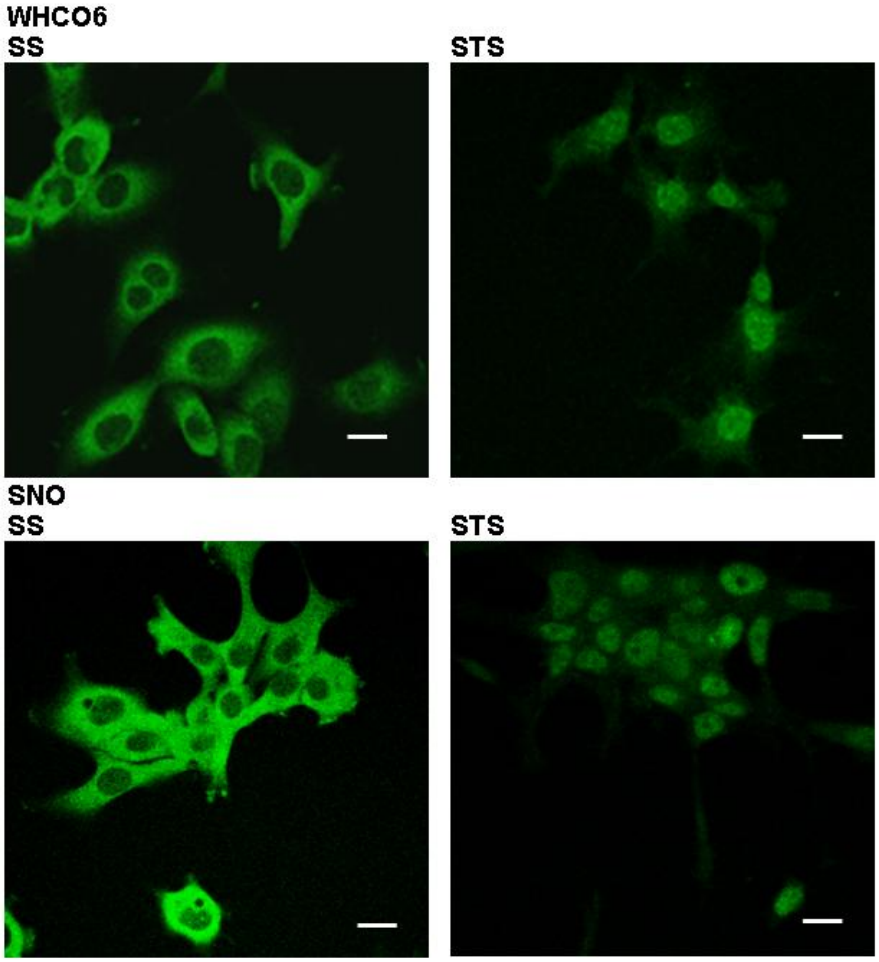

Figure 5.3: FAK accumulates in the nucleus in both wt and mt p53 cell lines post STS treatment. Nuclear localisation of FAK was observed post STS treatment in both wt and mt p53 cell lines, following immunofluorescent detection. Scale bar = 10µm; serum-free conditions (SS), 30nM STS (STS).

5.3.3 The p53/FAK association is independent of FAK Tyr397 phosphorylation

Since nuclear FAK has been shown to enhance the association between p53 and FAK (Lim *et al*., 2008), we examined whether p53 remained associated with FAK in the wt p53 (WHCO6) and mt p53 (SNO) cell lines. During STS-mediated apoptotic events, the p53/FAK interaction was maintained in both wt and mt p53 cell lines. Furthermore, p53 was detected in complex with the cleavage product of FAK (*Figure 5.4A*). The inhibitory effect of FAK on p53 is independent of FAK phosphorylation (Lim *et al*., 2008). Accordingly, STS-mediated dephosphorylation of FAK did not influence the p53/FAK association. Importantly, corresponding to the absence of FAK cleavage, FAK remained phosphorylated in the mt p53-R175H cell line post STS treatment (*Figure 5.4B*).

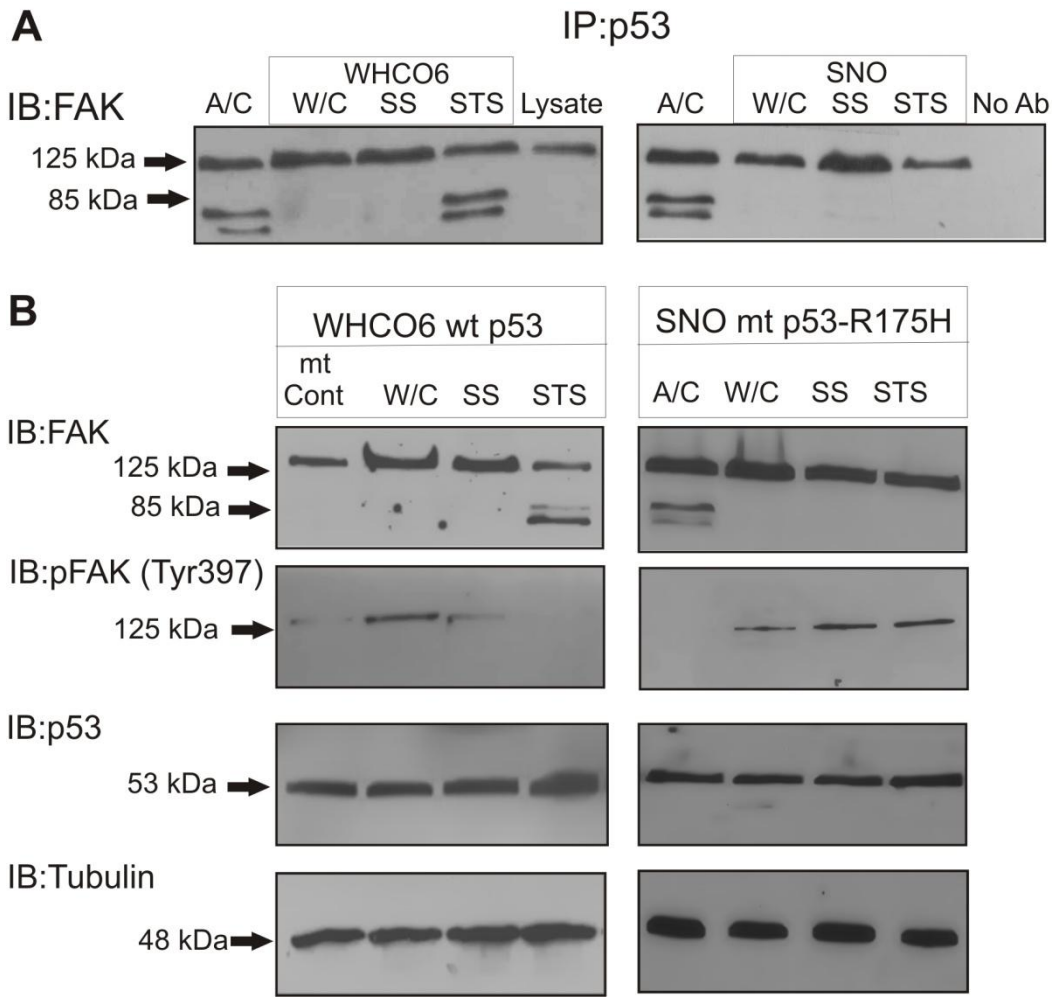

Figure 5.4: p53 associates with FAK independent of STS-mediated cleavage of FAK and Tyr397 phosphorylation. A) p53 was detected in complex with FAK in the wt p53 WHCO6 and mt p53-R175H SNO cells under: normal tissue culture conditions/ whole cell lysate from WHCO6 cell line (W/C), serum-free conditions (SS) and treated with 30 nM STS (STS). Notably, p53 was detected in complex with cleaved FAK post STS treatment in the wt p53 WHCO6 cell line B) STS-treatment results in FAK cleavage and dephosphorylation at Tyr397 in the wt p53 WHCO6 cell line, whilst FAK was not cleaved and pFAKTyr397 remained unchanged in mt p53-R175H SNO cell line. Mt cont = W/C control from p53-R175H cell line, APT cont = STS treated apoptotic control

5.3.4 Sequence analysis confirmed the integrity of pCMV-Neo-Bam-p53 and pCMV-Neo-Bam-R175Hp53 plasmids

We clearly demonstrate that the R175H mutation does not interfere with the ability of mt p53-R175H to associate with FAK (*Figure 5.2*). However, the detachment-resistant SNO cell line harbouring mt p53-R175H cell line was resistant to FAK cleavage, caspase-3 activation (*Figure 3.10*) and dephosphorylation of FAK (*Figure 4.4*). In response to stress stimuli, p53 accumulates in the nucleus and represses FAK gene transcription (Golubovskaya *et al*., 2005). As the R175H mutation abrogates the DNA binding ability of p53, mt p53-R175H is resistant to the transcriptional regulation of FAK (Golubovskaya *et al*., 2008 (a)). Hence, one possible way in which the mt p53-R175H cell line might evade caspase-dependent apoptosis is by upregulating the expression of the FAK protein. In this way, the anti-apoptotic ability of FAK would be enhanced, facilitating the evasion of anoikis-related death. This possibility was explored in transient transfection assays, employing plasmids encoding either wt or mt p53-R175H.

The integrity of the pCMV-Neo-Bam empty vector, pCMV-Neo-Bamp53 and pCMV-Neo-BamR175Hp53 plasmids was established by restriction digest (*Figure 5.5*), followed by sequence analysis (*Figure 5.6*). Restriction digest of the pCMV-Neo-Bam empty vector generated a linear plasmid (orange), double digest of the pCMV-Neo-Bamp53 vector generated a 1.8kb fragment (green), whilst, double digest of the pCMV-Neo-BamR175Hp53 vector generated a 1.3kb fragment (blue). Both the integrity of wt p53 (*Figure 5.6A*) and the R175H mutation located on exon 5 (*Figure 5.6B*) were confirmed by sequence analysis of a single colony.

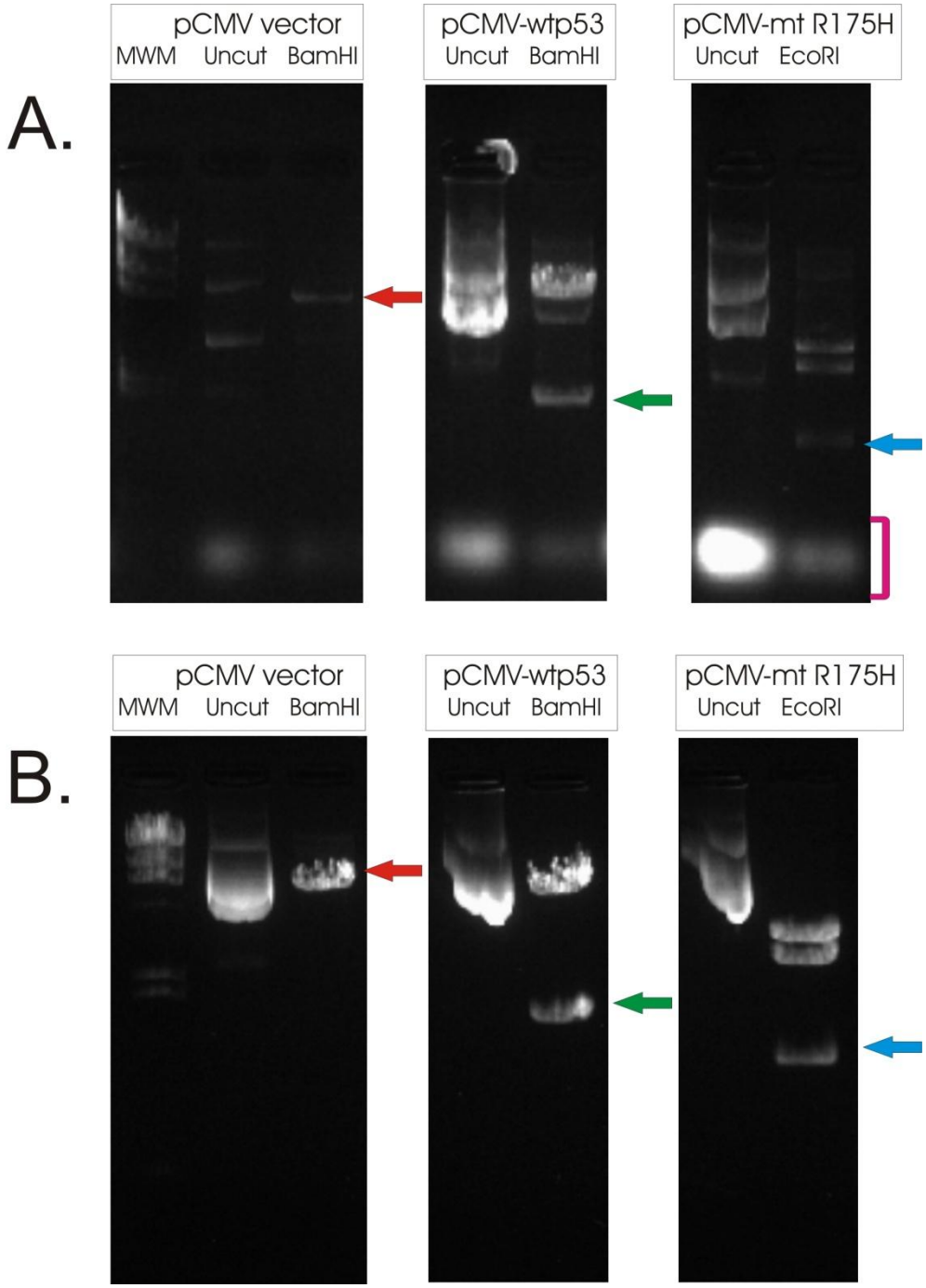

Figure 5.5: Restriction of the purified pCMV-Neo-Bam, pCMV-Neo-Bam-wtp53 and pCMV-Neo-Bam-R175H vectors. (a) An agarose gel separation of vectors extracted via (A) mini-prep and (B) maxi-prep. Single nick generated linear plasmid (orange); double digest generated 1.8kb fragment (green);

double digest generated 1.3kb fragment (blue); RNA degradation products (pink).

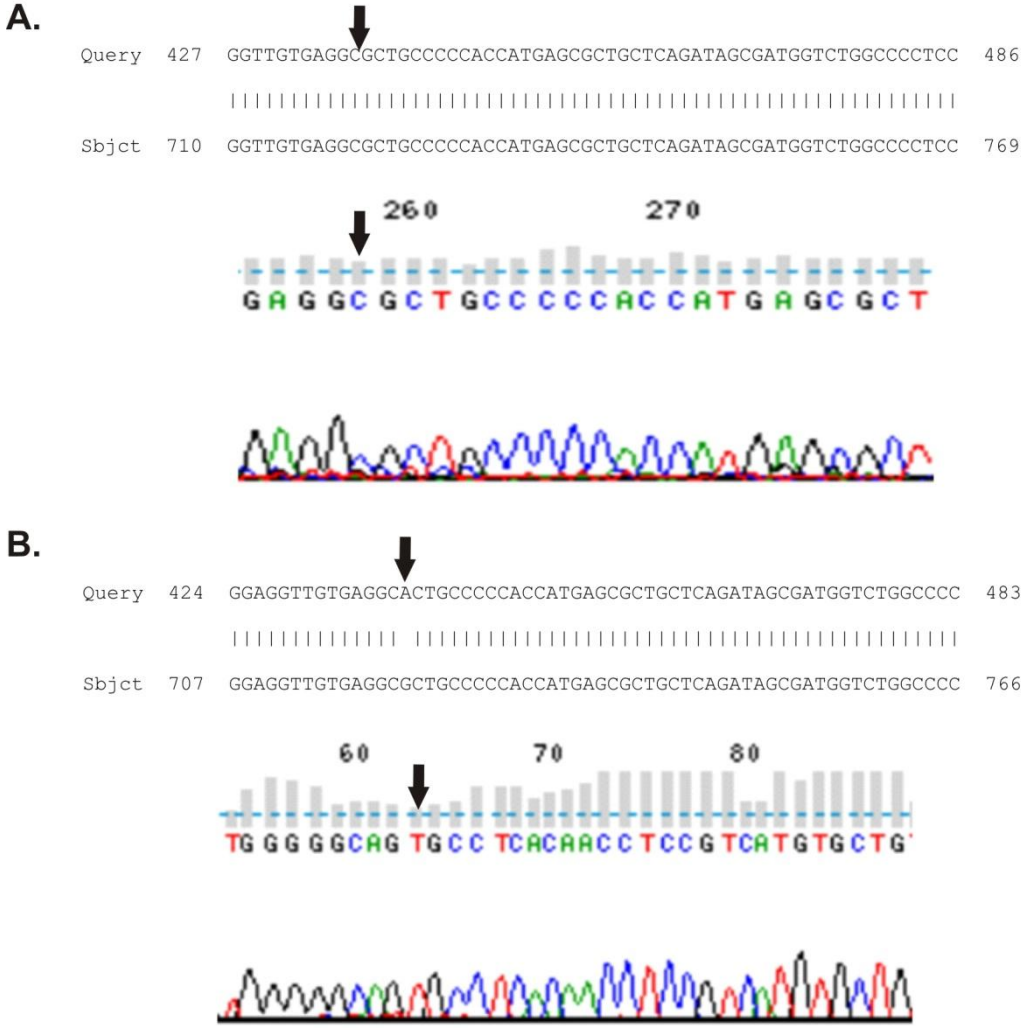

Figure 5.6: Sequence analysis of the wt p53 and mt p53-R175H pCMV-Neo-Bam vectors. A) wt p53 and B) the R175H mutation on exon 5 was confirmed by sequence analysis of a single colony of the pCMV-Neo-Bam-p53R175H and pCMV-Neo-Bam-p53 vectors respectively.

5.3.5 Overexpression of mt p53-R175H increased FAK expression

As all commercially available p53 antibodies recognize both wt and mt p53 (Chene, 1998), the p53-null H1299 cell line (*Figure 5.7*) was used to optimise transient transfection assays with vectors containing genes encoding wt p53 or mt p53-R175H. Lipofectamine is a cationic liposomic reagent widely used to introduce DNA encoding therapeutic proteins into cells (Azad and Rojanasakul, 2006). The overall positive charge of the Lipofectamine/DNA complex interacts with the negative charge of the plasma membrane and facilitates internalization of the complex into the cells by endocytosis (Azad and Rojanasakul, 2006). The charge ratio of the cationic species determines the cytotoxicity of cationic lipsomes, with a higher charge ratio being more toxic (Dokka *et al*., 2000; Lv *et al*., 2006). Previous transfection studies in the same series of HOSCC cell lines indicated that a low charge ratio of DNA: Lipofectamine2000 was well tolerated by the HOSCC cells (*See Materials and Methods 5.2.12*). In addition, p53 has previously been successfully transfected with Lipofectamine 2000 in the H1299 cell line under these conditions (Vikhanskaya *et al*., 2007).

Thus, the H1299 cell line was transiently transfected with vectors encoding genes for either wt p53 or mt p53-R175H. As mutant p53 does not activate expression of its negative regulator, MDM2 (Prives and Hall, 1999; Peng *et al*., 2001), it is more stable than wild-type p53. Consistent with these reports, only mt p53-R175H was detected post transfection in the H1299 cell line at the lower charge ratio of vector to transfectant (*Figure 5.8*). Although FAK expression decreased post mt p53-R175H transfection at 24hr, there was an appreciable increase of FAK expression (1.2 fold relative to empty vector control) post 48hr transfection.

5.3.6 Overexpression of wt p53 did not influence FAK expression

It is well established that the subset of cell death induced by cationic liposomes is primarily via apoptotic death pathways (Aramaki *et al*., 1999; Aramaki *et al*., 2000). Accordingly, the volume of Lipofectamine used in the previous transfection assay was sufficient to activate caspase-3 and therefore, apoptotic pathways (*Figure 5.8*). Thus, as wt p53 was not detected post transfection with the low charge ratio of vector to transfectant, the transient transfection assay for wt p53 was repeated with three-fold DNA to transfectant. Wt p53 was only detected in the H1299 cell line post 24hr of transfection. No appreciable change in FAK expression was evident post wt p53 transfection (*Figure 5.9*).

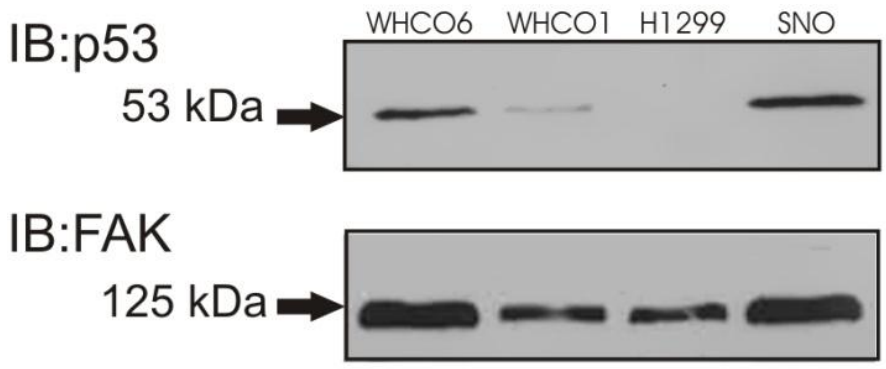

Figure 5.7: The p53-null H1299 non-small lung carcinoma cell line expresses FAK. Comparable FAK expression to the WHCO1 cell line was evident in the H1299 cell line. p53 was not detected by immunoblot in the H1299 cell line.

A.

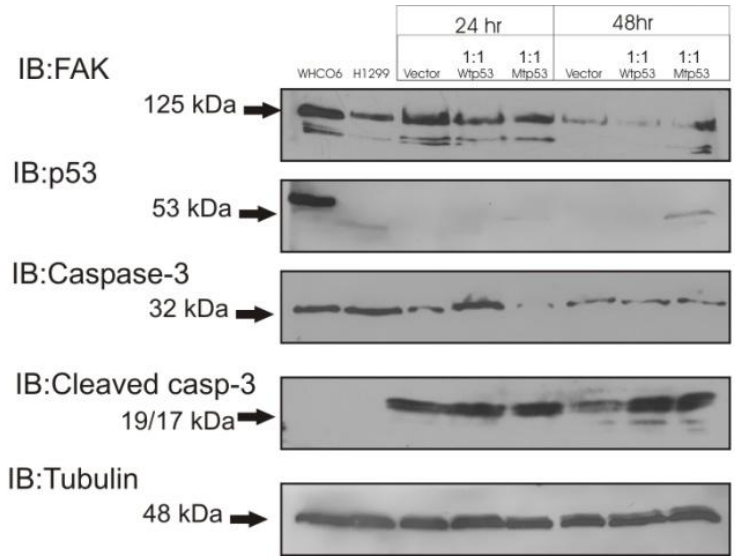

See next page for legend.

B.

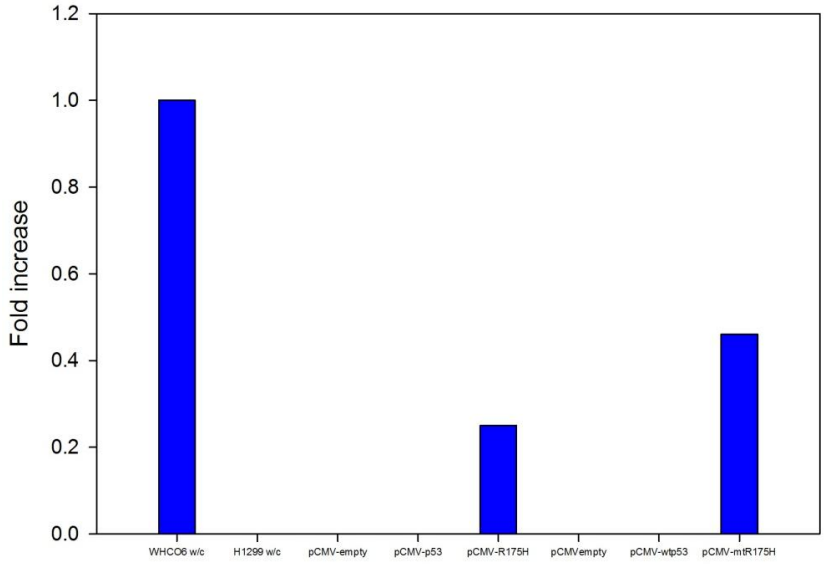

C.

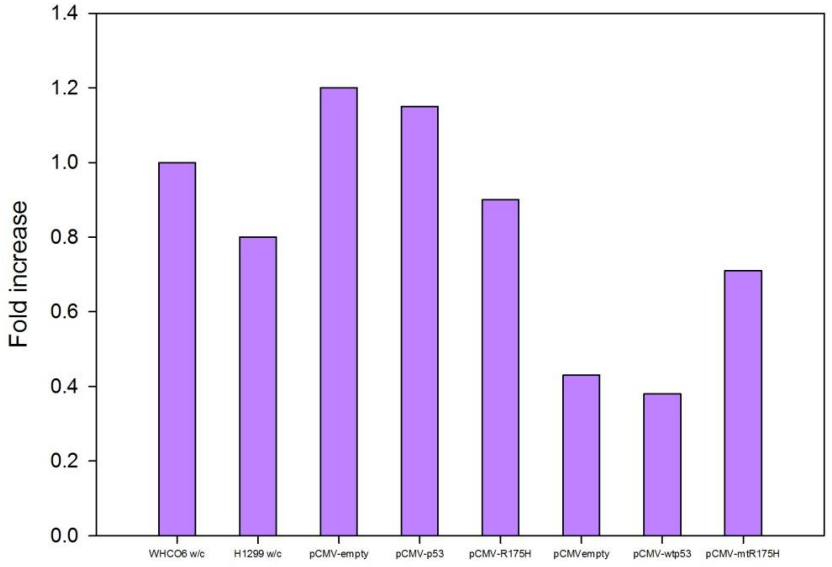

Figure 5.8: Overexpression of mt p53-R175H in the H1299 cell line increased FAK expression. A) Mt p53-R175H was detected in the H1299 cell line post transfection at the low charge ratio of DNA:Lipofectamine. Caspase-3 activation was detected in the pCMV-empty vector control. B&C) Densitometric analysis revealed that corresponding to the detection of (B) mt p53-R175H, (C) FAK expression increased 1.2 fold relative to the empty vector control, post 48hr transfection.

A.

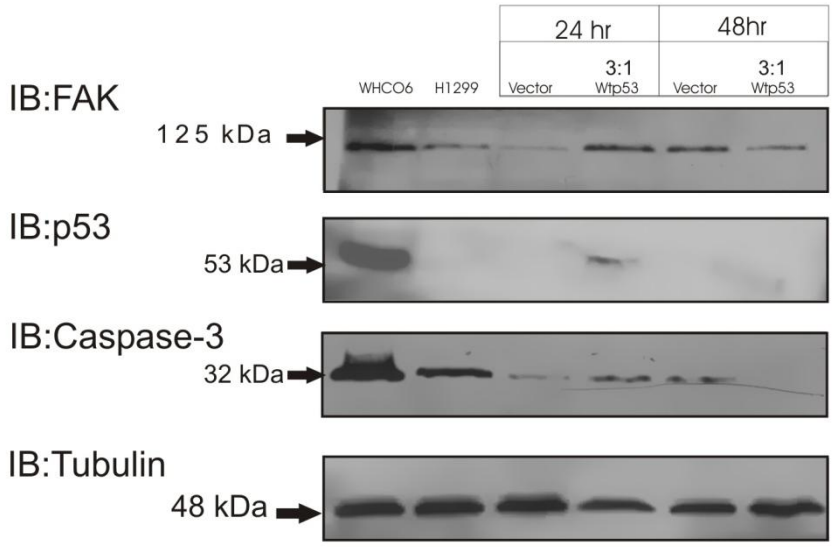

See next page for legend.

B.

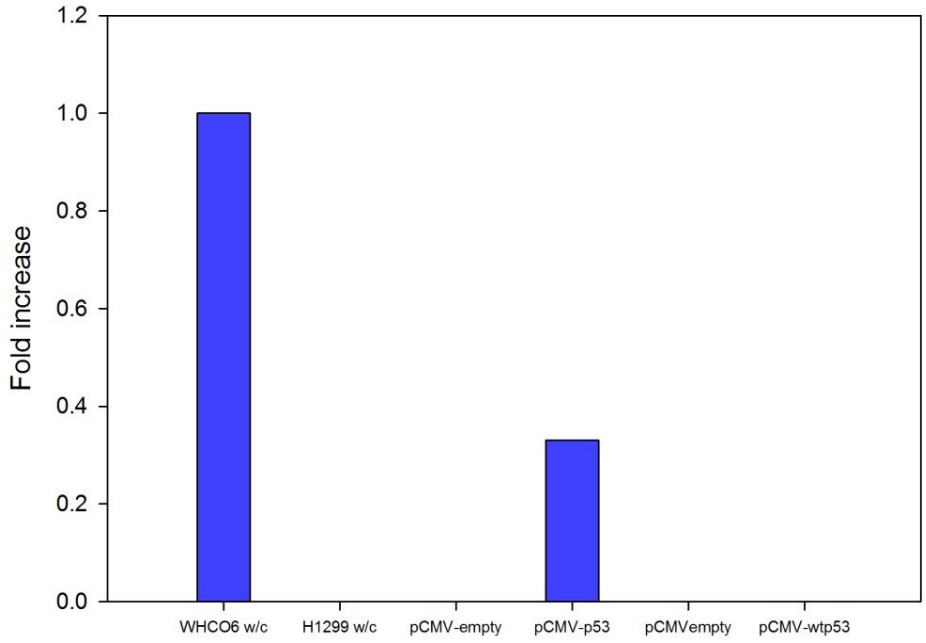

C.

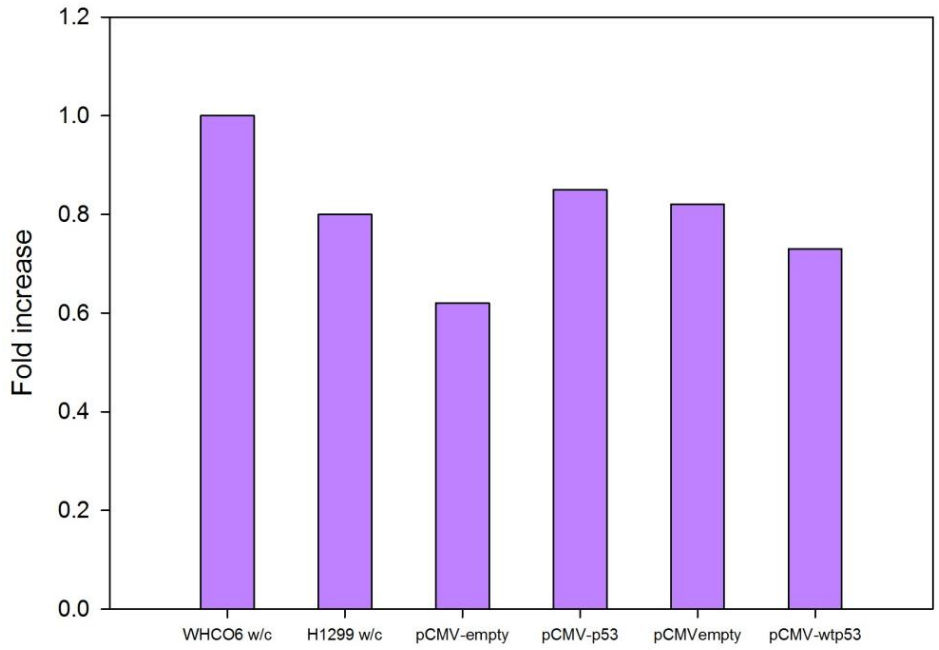

Figure 5.9: Overexpression of wt p53 does not repress FAK expression. A) Wt p53 expression was detected in the H1299 cell line after 24hr post transfection at the higher charge ratio of DNA to transfectant reagent. B) Densitometric analysis revealed that overexpression of (B) wt p53 did not repress (C) FAK expression.

5.3.7 mt p53-R175H does not protect wt p53 HOSCC cell line from STS-dependent FAK cleavage

As overexpression of mt p53-175H increased FAK expression in the H1299 cell line (*Figure 5.8*), we examined whether the previously described dominant negative effect of mt p53-R175H (Ko and Prives, 1996; Willis *et al*., 2004) was evident post STS treatment in the representative wt p53 WHCO6 cell line. WHCO6 cells were transiently transfected with mt p53-R175H for 24 hr, following treatment with STS for 24hr. Corresponding to previous transfection assays (*Figure 5.8*), the introduction of mt p53-R175H into the wt p53 WHCO6 cell line increased p53 expression 1.2 fold relative to the empty vector control (*Figure 5.10*). Although the mt p53-R175H did not oppose STS-mediated FAK cleavage, FAK expression in the mt p53-R175H/STS transfected cells was elevated 1.4 fold relative to the STS control (*Figure 5.10*).

A.

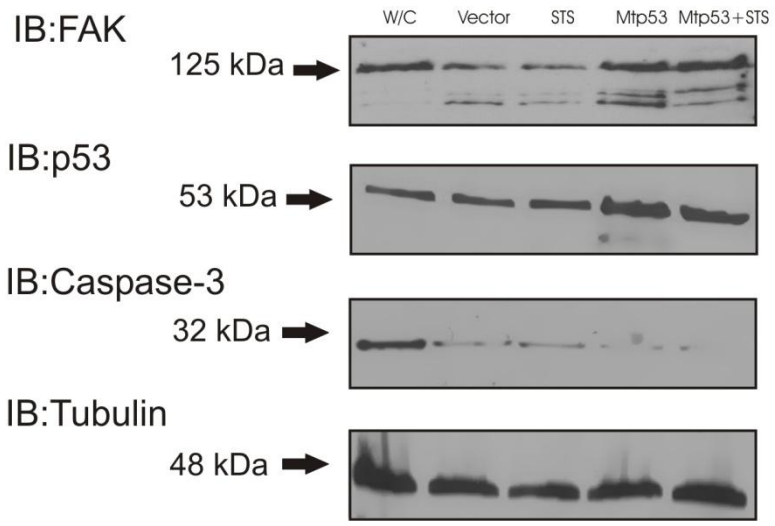

See next page for legend.

B.

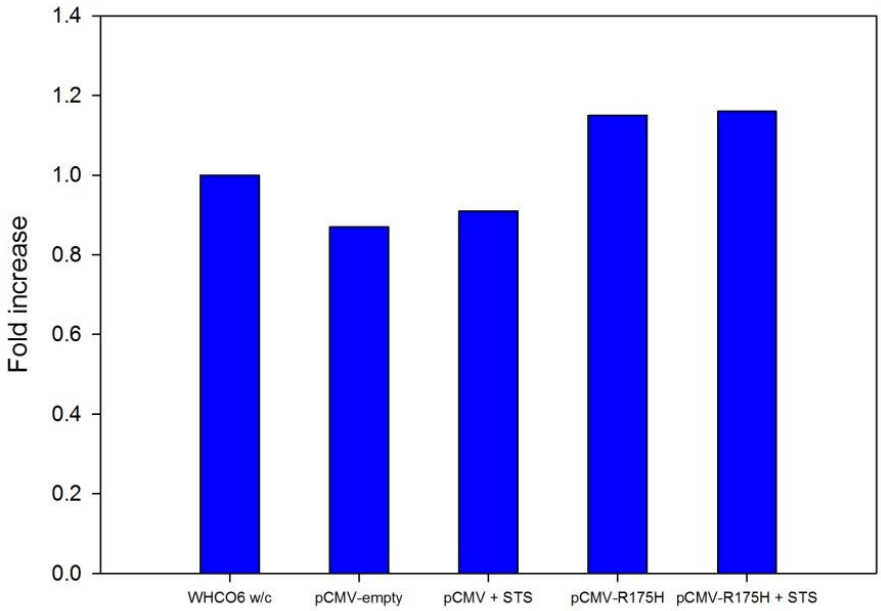

C.

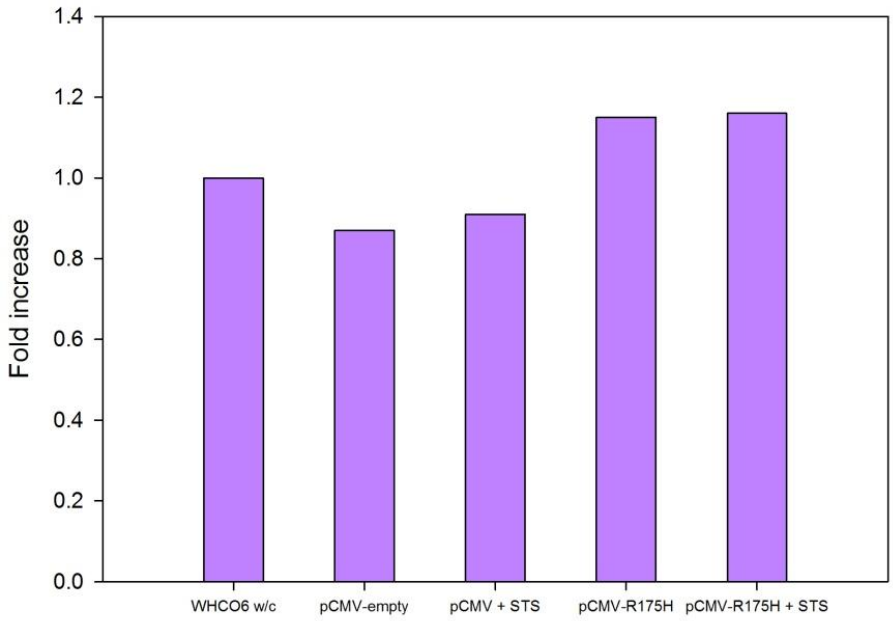

Figure 5.10: Mt p53-R175H does not protect wt p53 WHCO6 cell line from STS-mediated FAK cleavage. A) p53 expression increased post transfection with the pCMV-Neo-Bam-p53R175H vector in the mt p53-R175H cell line. FAK cleavage was not reduced by the overexpression of mt p53-R175H in the wt p53 cell line. B&C) Densitometric analysis revealed that increased (B) p53 expression corresponded to increased (C) FAK expression.

5.4 Discussion

An alternative survival role of FAK has recently been shown that involves its nuclear translocation and repression of p53-dependent apoptosis (Golubovskaya *et al*., 2005; Lim *et al*., 2008). However, this regulation has been exclusively demonstrated in cell lines harbouring wt p53. The "hot spot" p53 mt-R175H is proposed to confer resistance to apoptosis by repressing the FAK promoter (Golubovskaya *et al*., 2008 (a)). In addition, we have shown that the mt p53-R175H cell line displays altered FAK regulation (*Figure 3.10 & 4.4*). Thus in order to establish the role of mt p53-R175H on FAK regulation in oesophageal carcinoma, we compared interplay between p53 and FAK, in HOSCC cell lines expressing either wt or mt p53-R175H.

The p53/FAK association is mediated via interactions between the N-terminal of (amino acids 206–422) and seven amino acids located in the proline-rich region of p53 (Golubovskaya *et al*., 2008 (b)). Due to impaired flexibility, the conformational mt p53-R175H has reduced DNA-binding capacity (Aylon and Oren, 2007). However, the R175H did not influence the ability of p53 to associate with FAK (*Figure 5.2*). Furthermore, the proline-rich region of p53 that interacts with p53 contains the Pro/Arg72 polymorphism, which frequently changed to an arginine residue in different tumours. Hence, in addition to the R175H mutation, the Pro/Arg72 polymorphism, in the mt p53-R175H cell line did not affect the p53/FAK association. Moreover, during STS-mediated apoptotic events, the p53/FAK interaction was maintained in both wt and mt p53 cell lines (*Figure 5.3*). Consistent with previous reports, nuclear accumulation of FAK was detected in both wt and mt p53-R175H cell lines post STS treatment (*Figure 5.2;* Golubovskaya *et al*., 2008 (a); Ossovskaya *et al*., 2008). Since caspase-3 activation was not detected in the mt p53-R175H cell line, these results suggest that caspase-3 dependent events do not influence stress-induced FAK nuclear translocation. Although the association has been demonstrated to be enhanced post doxorubicin/staurosporine treatment (Lim *et al*., 2008), this is the first study to show that the association is maintained post caspase-3 activation and

independent of p53 mutational status. Importantly, these data reveal that the altered regulation of FAK and resistance to caspase activation in the mt p53-R175H cell line (*Figure 3.9 & 3.11*) is not due to the inability of mt p53-R175H to associate with FAK.

Mt p53-R175H is resistant to the transcriptional regulation of FAK (Golubovskaya *et al*., 2008 (a)). Emphasizing the importance of this LOF effect, we have established that the mt p53-R175H cell line was resistant to STS-mediated FAK cleavage (*Figure 3.9*) and dephosphorylation (*Figure 4.4*). Moreover, a direct correlation between overexpression of FAK and mutant p53 has been demonstrated in breast cancer (Golubovskaya *et al*., 2009). In agreement with this data, overexpression of mt p53-R175H in the p53-null H1299 cell line increased FAK expression post 48hr transfection (*Figure 5.8*). Furthermore, overexpression of wt p53 had no appreciable effect on FAK expression (*Figure 5.9*). Therefore, in addition to loss of transcriptional regulation of FAK, these data demonstrate that mt p53-R175H may enhance FAK expression, and as a consequence FAK-dependent signalling.

Several studies, in both mice and humans, have discovered cells expressing mutant p53 possess a carcinogenic advantage (Dittmer *et al*., 1993; Hsiao *et al*., 1994; Liu *et al*., 2000). These studies demonstrate that the p53 mutants disrupt normal p53 function, by reducing the activity of p53 tetramers. Importantly, the tetramerization of mt p53 with wt p53 reduces the ability of the p53 tetramer to bind the FAK promoter (Willis *et al*., 2004). Thus, as mt p53-R175H increased FAK expression in the p53-null H1299 cell line (*Figure 5.8*), we investigated whether the introduction of the mt p53-R175H into the wt p53 cell line was sufficient to abrogate FAK-dependent regulation. Notably, although overexpression of mt p53-R175H did not protect the wt p53 WHCO6 cell line from STS-mediated FAK cleavage, the introduction of mt p53-R175H increased FAK expression (*Figure 5.10*). Hence, these data emphasize that the mt p53-R175H exerts a dominant negative effect on endogenous wt p53.

Applicable to FAK activity, we show that FAK expression is related to Tyr397-phosphorylation (*Figure 2.4*). Thus, it is evident that by increasing the expression of FAK, the mt p53-R175H may have a profound influence on the regulation of anchorage-independent death, through enhanced FAK-dependent signalling. Moreover, the altered regulation of FAK-directed events in the mt p53-R175H cell line was not due to the inability of mt p53-R175H to associate with FAK (*See Figure 5.3*). However, the mt p53-R175H cell line was resistant to FAK dephosphorylation (*Figure 4.4 & 5.3*). Constitutive activation of FAK protects cells from anoikis-mediated activation of caspase-8 (Kurenova *et al*., 2004). Hence, the persistent activation of FAK observed in mt p53-R175H cell line may be facilitating resistance to detachment and caspase activation, through the suppression of the Fas-mediated death cascade. Therefore, to ascertain the full impact of mt p53-R175H in anoikis-related regulation, the investigation of the influence of FAK-dependent signalling on Fas-mediated death is detailed in the next chapter.

Chapter 6

Role of FAK activation in the suppression of Fas-mediated apoptosis in HOSCC cell lines

6.1 Introduction

In addition to repressing p53-dependent anoikis (Frisch *et al*., 1998; Golubovskaya *et al*., 2005), constitutive activation of FAK has also been reported to suppress Fas-mediated apoptosis (Kurenova *et al*., 2004; Kamarajan and Kapila, 2007). Substrate-deprived death was demonstrated to be accompanied by increased levels of Fas, FasL and enhanced formation of the DISC, whilst Fas attenuation by siRNA treatment rescues anoikis-mediated DISC formation (Ishida *et al*., 2003; Kamarajan *et al*., 2010). Moreover, an indirect link between Fas and FAK-mediated signaling via receptor interacting kinase (RIP) has been demonstrated (Kamarajan *et al.*, 2010). Hence, the suppression of Fas-mediated apoptosis by FAK-dependent signalling represents an important component of the regulation of anoikis-related events.

Fas expression was originally believed to be restricted to cells of the immune system, however, Fas is expressed in most adult tissues including liver, thymus, heart and ovary (Papoff *et al*., 1999; Siegel *et al*., 2000). Importantly, Fas and its associated ligand, FasL, have been shown to be constitutively expressed by normal human oesophageal mucosal cells (Gratas *et al*., 1998). Unlike Fas which is ubiquitously expressed, FasL is expression mainly restricted to activated T lymphocytes and natural killer cells (Krueger *et al*., 2003). In this way, the immune system utilises FasL as a powerful means to eliminate compromised cells. Consequently, transformed and infected cells are identified by FasL-bearing cells of the immune system and destroyed (Krueger *et al*., 2003). Clearly, this immune attack is dependent on the inherent capability of the target cell to enter apoptosis. Thus, the loss of control of these death pathways has dire consequences as compromised cells are permitting to continue proliferating.

In previous chapters we have shown, in the HOSCC cell line harbouring mt p53-R175H, FAK remained phosphorylated at Tyr397 under the same apoptotic conditions that four wt p53 cell lines displayed FAK cleavage and caspase-3 activation (*Figure 3.9 & 4.4*). The resultant cell death that accompanies reduced FAK activity has been attributed to reduced survival signaling via the PI3K-dependent signaling cascade (Sonoda *et al*., 1999). However, FN-mediated signals were independent of PKB-dependent signalling (*Figure 4.4*). In addition, the "hot-spot" mt p53-R175H exerts a dominant negative effect on wt p53, and enhances FAK expression (Golubovskaya *et al*., 2005). Consistent with these studies, overexpression of mt p53-R175H increased FAK expression (*Figure 5.8*). Therefore, as abrogation of FAK expression has been shown to be associated with enhanced caspase-8 activation and the induction of anoikis (Kurenova *et al*., 2004), we explored whether the persistent activation of FAK in the mt p53-R175H cell line was accompanied by the suppression Fas-mediated apoptosis. Uniquely, the novel complex between Fas and FAK identified in wt and mt p53-R175H cell lines provides unique insight into the association between sustained FAK activity and delayed Fas-mediated apoptosis. Hence, the data presented in this chapter strongly supports our earlier contention that, the "hot spot" mt p53-R175H may have a significant impact on the survival of tumor cells post cell detachment, by opposing the induction of FAK-dependent anoikis.

6.2 Materials and Methods

6.2.1 Cell lines

As previously documented, see Chapter 2, Section 2.2.1

6.2.2 RNA extraction

As previously documented, see Chapter 2, Section 2.2.2

6.2.3 Reverse transcription

As previously documented, see Chapter 2, Section 2.2.3

6.2.4 Antibodies

Fas and FasL were specifically detected with a rabbit polyclonal antibody obtained from SantaCruz Technology. Monoclonal mouse anti-pFAK(Tyr397) (Millipore) and anti-caspase8 (Cell Signalling Technology) was used to detect autophosphorylation of FAK and activation of caspase-8 respectively. Polyclonal horseradish peroxidase (HRP)-bound anti-rabbit secondary antibody was used in (Separations, SA) and fluoroscine isothiocyanate (FITC)-conjugated anti-rabbit secondary antibody (Chappel, USA) were used in the immunoblot and immunofluorescence experiments respectively.

6.2.5 Protein estimation assay

As previously documents, see Chapter 2, Section 2.2.6

6.2.6 Immunoblot analysis

20µg of protein per lane was resolved on a 10% SDS-PAGE and electro-blotted onto a nitrocellulose membrane (Sartorius). Nonspecific binding sites on the membrane were pre-blocked in blocking buffer for 1 hr. Blots were incubated with anti-Fas (1:650), anti-FasL (1:500) for 1hr or overnight with p-FAK(Tyr397) (1:500) or caspase-8 (1:500) in 1% BSA. Following incubation in HRP-conjugated secondary (1:5000) membranes were washed 6 times at 5 min intervals with PBS before being exposed to the SuperSignal West Pico Chemiluminescent working solution for 5 min. Blots were sealed in polyethylene

wrap and exposed to hyperfilm™ MP autoradiography film (Amersham, UK) for 10 min.

6.2.7 Indirect immunofluorescence

The visual determination of Fas and FasL was determined by indirect immunofluorescence. Cultured cells were fixed with 4% paraformaldehyde for 30 min and washed twice with PBS. Following permeabilisation with 0.25% Triton X-100 for 10 min, cells were rinsed twice with PBS and allowed to dry partially. Fixed cells were incubated with anti-Fas (1:100) or anti-FasL (1:100) antibodies respectively for 1hr. Following incubation with the anti-rabbit fluoroscine isothiocyanate-conjugated secondary antibody (1:250) for 1hr, Elvanol mounting agent was added to the wells and cells were viewed at 400 X magnification under a Zeiss LSM 410 confocal microscope (FITC excitation 490, emission 525).

6.2.8 Co-immunoprecipitation

Cells were lysed in RIPA buffer containing 50 mM Tris-HCl (pH 7.5), 150 mM NaCl, 0.5% deoxycholate, 0.5% Triton X-100, 0.05% STS, 1 mM PMSF and aprotinin, for 30 min at 4 °C. The lysates containing 350 µg protein were incubated with 3 µl of anti-integrin Fas (Santa Cruz Technology) at 4 °C for 6 hr. Then 20 µl of protein G-Sepharose beads were added to each lysate at 4 °C for overnight. The suspension was boiled for 5 min and centrifuged for 10 min at 12000 r.p.m. in a Sorvall® MC 12 V centrifuge. Samples were resolved by SDS-PAGE and blotted onto nitrocellulose membranes (as above). Blots were incubated in anti-FAK and anti-FasL to determine the relative association with Fas.

6.2.9 Densitometry

Labworks *TM* Image Acquisition and Analysis software (Labworks version 4.5) was used for densitometric analysis to quantitatively determine the concentration level of FasL, Fas and caspase-8 in the Western blots.

6.3 Results

6.3.1 HOSCC cell lines harbouring wt or mt p53-R175H express FasL

Fas-mediated apoptosis is initiated by the interaction of membrane-bound FasL, with its corresponding death receptor, Fas (O'Reilly *et al*., 2009). We have already established that the HOSCC cell lines express Fas (*Figure 2.9*). Therefore, in order to fully characterise the Fas death cascade we assessed whether the HOSCC series of cell lines express FasL. The 40kDa membrane-bound counterpart of FasL was detected in the HOSCC, HT29 and MCF7 cell lines (*Figure 6.1A*). Under standard tissue culture conditions, the WHCO1 cell line had the highest FasL expression. The lowest FasL expression was observed in the WHCO3 and WHCO6 cell lines, on average approximately 2 fold less than the WHCO1 cell line (*Figure 6.1B*).

6.3.2 Peri-nuclear localisation of FasL was observed in HOSCC cell lines

Consistent with previous reports in glycosylated proteins, distinct peri-nuclear localisation of FasL was observed in HOSCC cell lines, as well as the caspase-3 null MCF7 and mt p53-R273H HT29 control cell lines (*Figure 6.2*). Increased membrane expression of FasL has been proposed to enable oesophageal tumors to evade immune surveillance (Kozowski *et al*., 2007). Contrary to this observation, no distinct membrane localisation of FasL was observed in the HOSCC cell lines (*Figure 6.2*).

A.

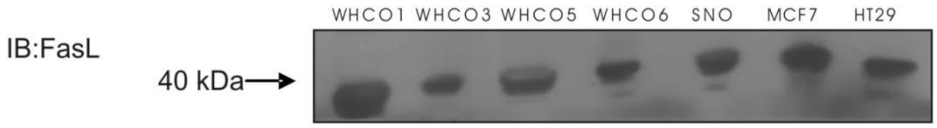

B.

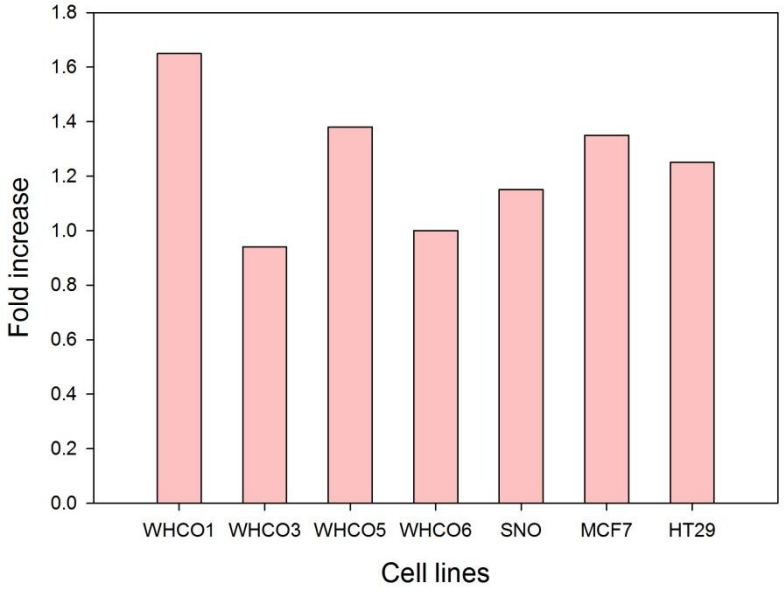

Figure 6.1: FasL is differentially expressed by the HOSCC, MCF-7 and HT29 cell lines under standard tissue culture conditions. (A) Western blot analysis of the cell lysates using a polyclonal antibody against FasL. The membrane-associated counterpart of FasL was detected at 40 kDa. (B) Densitometric analysis of the immunoblot was performed using Labworks™ Image Acquisition and Analysis software. The relative difference FasL was assessed across all of the HOSCC cell lines. Expression levels are relative to the maximum per 20µg of protein in the WHCO6 cell line. Note: the whole cell samples used to detect FAK in *Figure 2.3A* we were the same samples used to detect FasL, and therefore, the tubulin immunoblot also represents the loading control for the above immunoblot.

WHCO1

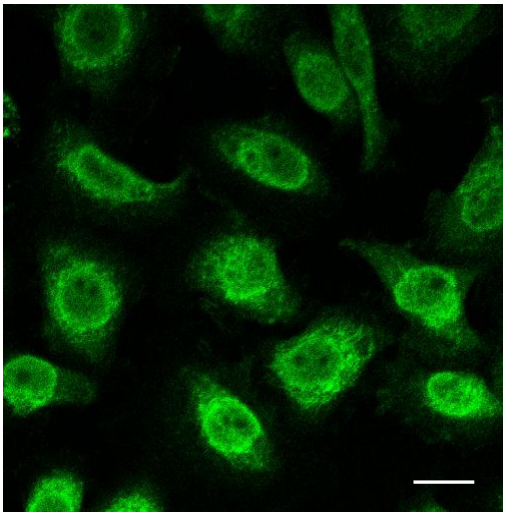

WHCO3

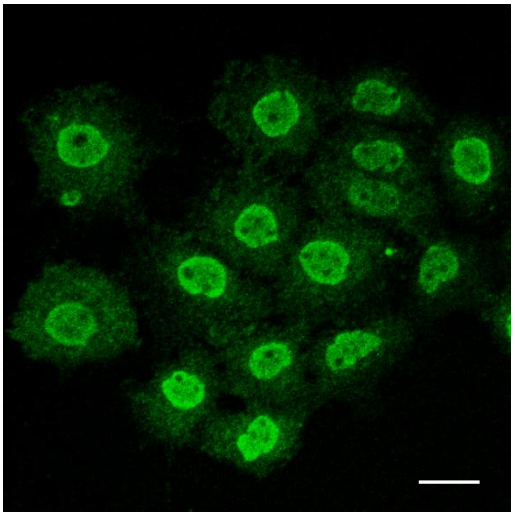

WHCO5

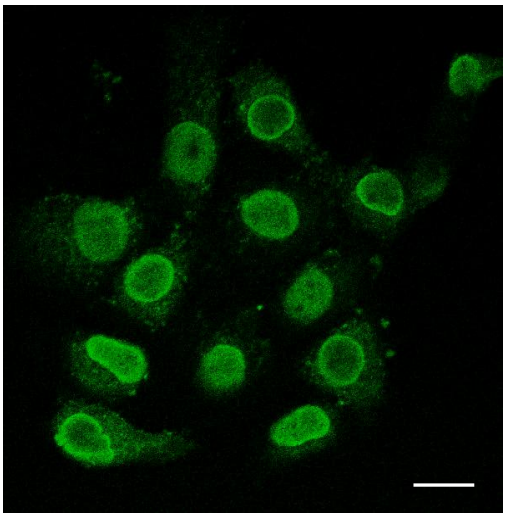

WHCO6

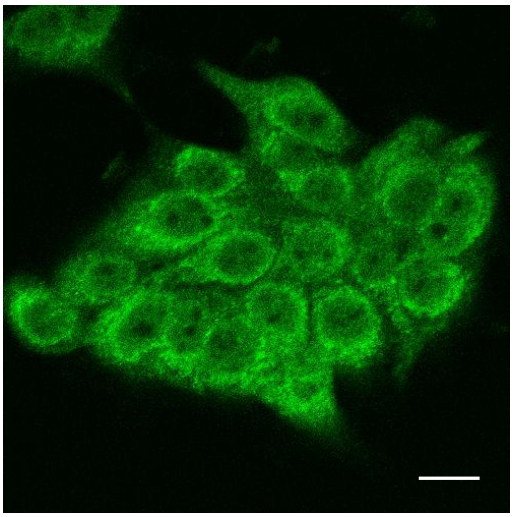

SNO

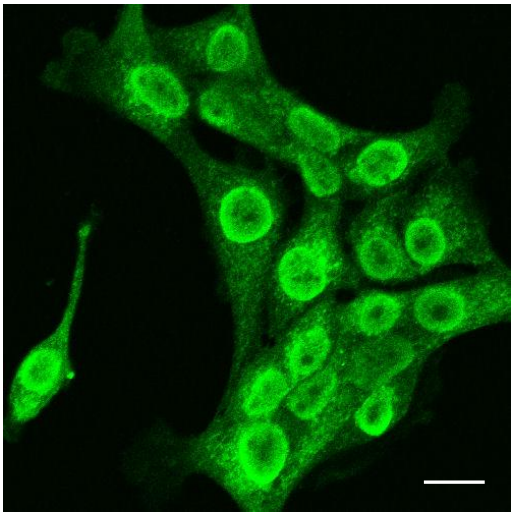

HT29

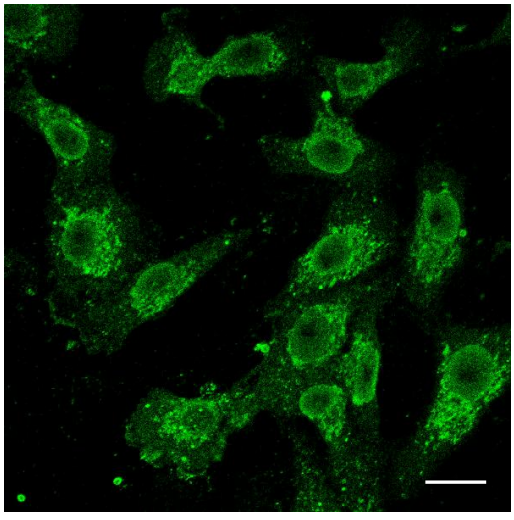

MCF7 Negative control

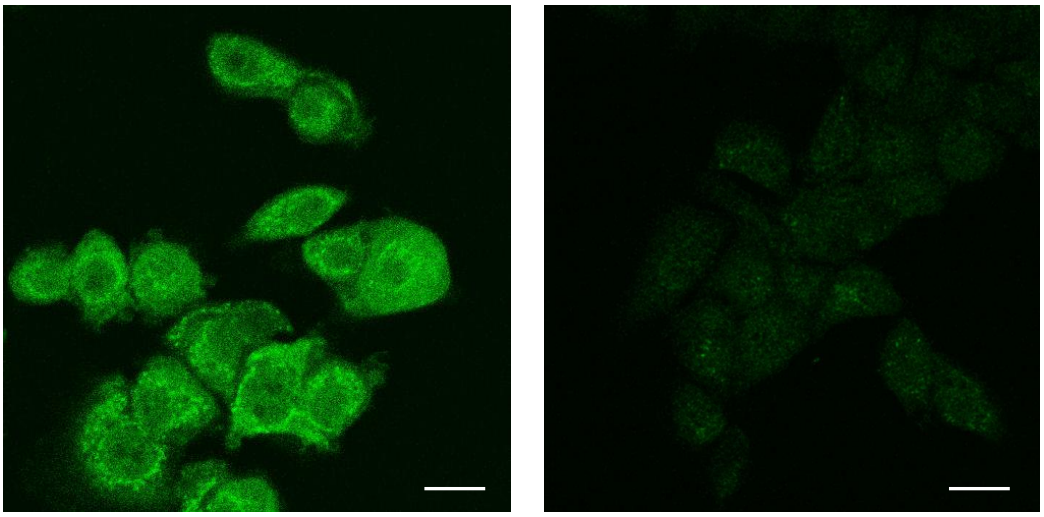

Figure 6.2: Peri-nuclear localisation of FasL was observed in the HOSCC cell lines. Under standard tissue culture condition, distinct peri-nuclear localisation of FasL is evident, with a smaller percentage being localised in the cytoplasm. Negligible diffuse staining was observed in the negative control (excluding anti-FasL antibody). Scale bar = 15μm

6.3.4 STS modulates Fas and FasL expression in wt p53 HOSCC cell lines

Fas and FasL have been shown to be upregulated following detachment from the ECM (Ishida *et al*., 2003; Kamarajan *et al*., 2010). In addition, p53 has been implicated in the regulation of Fas-mediated apoptosis, as wt p53 has been demonstrated to increase Fas membrane trafficking (Bennet *et al*., 1998). Furthermore, the "hot spot" mt p53-R175H and p53-R273H have been demonstrated to suppress Fas transcriptional upregulation (Zalcenstein *et al*., 2003). Therefore, the effect of STS-mediated apoptosis on Fas and FasL expression was assessed in both wt and mt p53 cell lines.

There was a distinct variation in Fas expression post STS treatment between wt and mt p53 cell lines. In the WHCO1, WHCO3 and WHCO6 cell lines the 52 kDa isoform increased post serum withdrawal (*Figure 6.3B*). The WHCO1 cell line exhibited a 2 fold increase in the 52 kDa subunit of Fas post serum withdrawal. Similarly in the WHCO3 and WHCO6 cell line, expression of the 52kDa subunit of Fas increased 2.4 and 1.6 fold respectively following serum withdrawal (*Figure 6.3B*). The partially glycosylated 48kDa subunit of Fas was still not detected in the WHCO3 cell line following treatment (*Figure 6.3C*). Alternatively, no change in Fas expression was evident post serum-withdrawal/STS treatment in the SNO or MCF7 cell lines. Consistent with previous reports in cell lines harbouring the mt p53-R273H (Zalcenstein *et al*., 2003), Fas was only detected post serum-withdrawal in the HT29 cell line (*Figure 6.3A*). Although serum-removal had an impact on Fas expression, no substantial difference in Fas expression was observed between untreated and STS-treated HOSCC, MCF7 or HT29 cells (*Figure 6.3B & C*).

FasL expression was upregulated post serum withdrawal in the WHCO3 and WHCO6 cell lines by 1.5 and 1.6 fold respectively (*Figure 6.3D*). While FasL expression remained unchanged in the MCF-7 cell line, FasL expression increased post STS treatment in the WHCO1, WHCO6, SNO and HT29 cell lines (*Figure 6.4D*).

A.

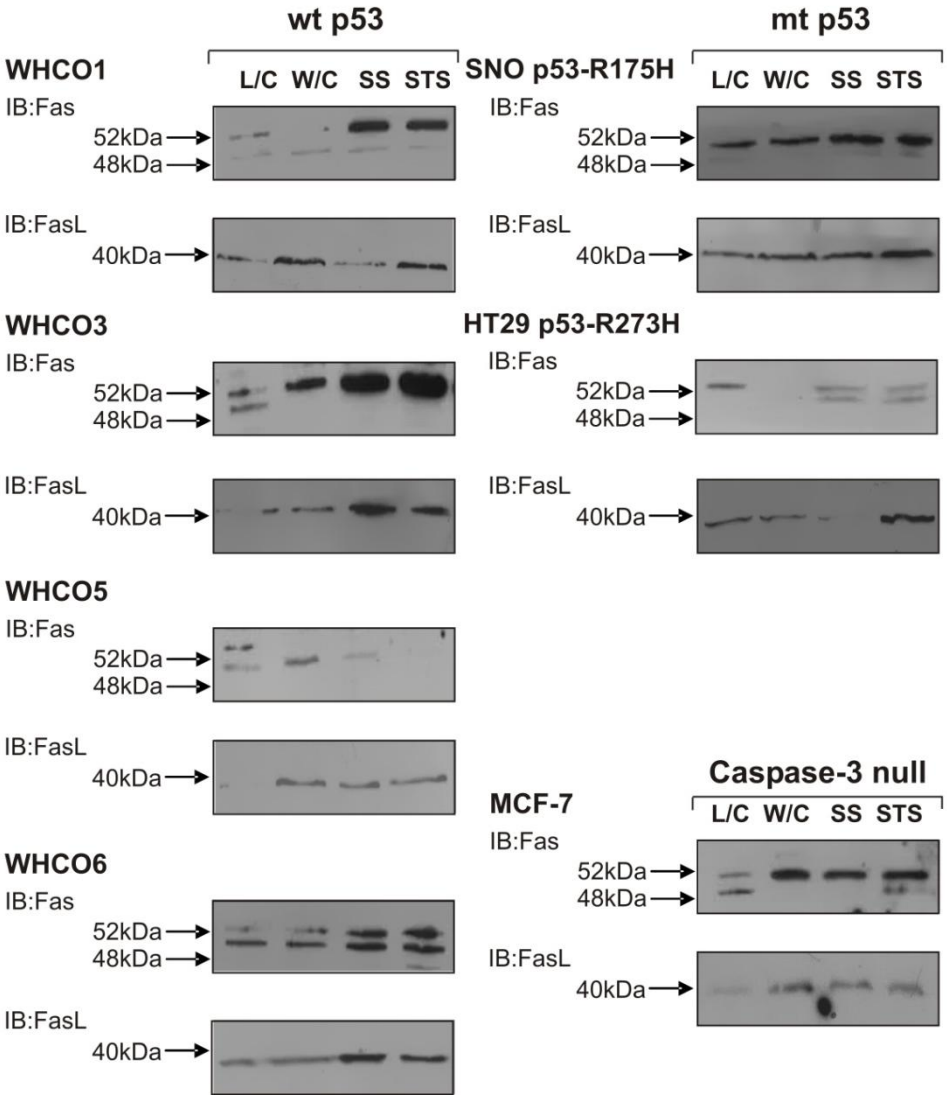

See next page for legend.

B.

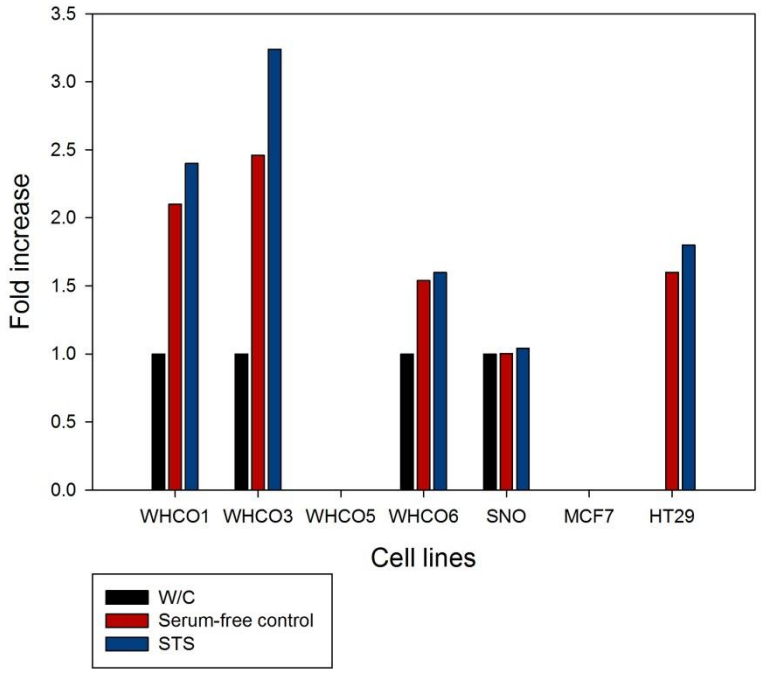
3.5
3.0
2.5
2.0
1.5
1.0
0.5
0.0
Fold increase
WHCO1
WHCO3
WHCO5
WHCO6
SNO
MCF7
HT29
Cell lines
W/C
Serum-free control
STS

C.

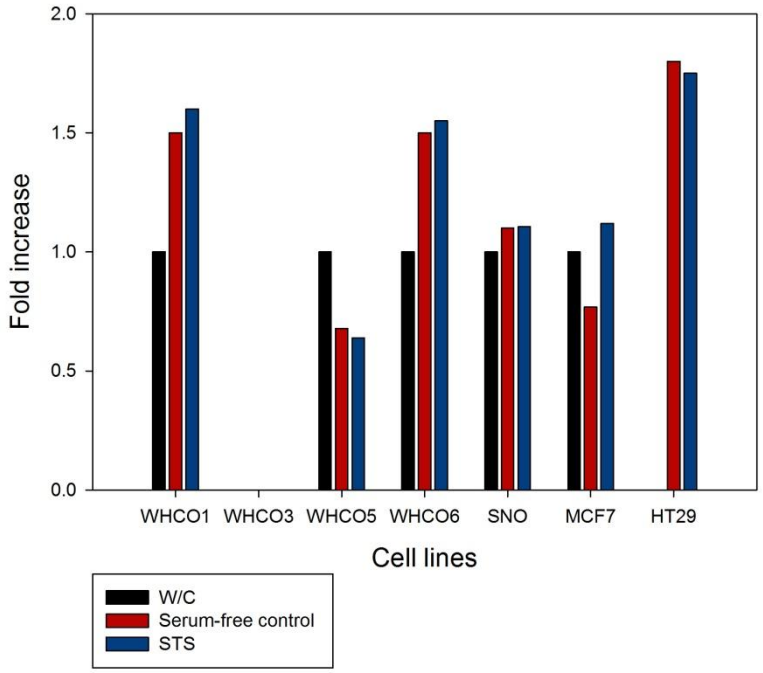
2.0
1.5
1.0
0.5
0.0
Fold increase
WHCO1
WHCO3
WHCO5
WHCO6
SNO
MCF7
HT29
Cell lines
W/C
Serum-free control
STS

D.

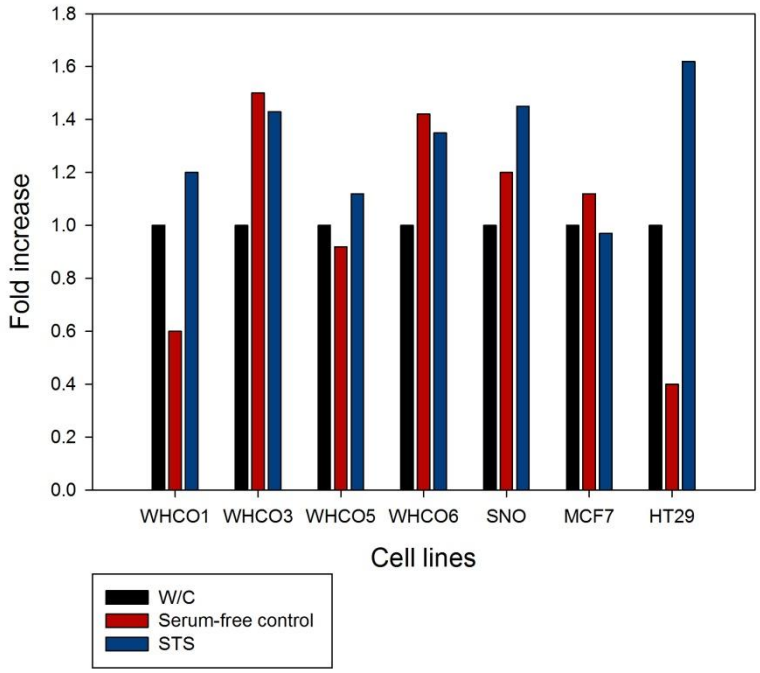

Figure 6.3: The expression of Fas and FasL is modulated post serum-withdrawal and STS-treatment in the HOSCC cell lines. A) The expression of the partially glycosylated 48 kDa and fully glycosylated 52kDa isoform of Fas was variable among the cell lines. The 48 kDa isoform was not detected in the WHCO3 and MCF-7 cell lines. B&C) With exception to the WHCO5 cell line, the fully glycosylated (B) 52 kDa isoform of Fas increased in the wt p53 cell lines (WHCO1, WHCO3 and WHCO6). The WHCO5 cell line does not express the 52 kDa isoform of Fas. Both the (C) 48 kDa and 52 kDa variants remained constant in the SNO cell line. In the HT29 cell line both the 48 kDa and 52 kDa isoforms were only detected post serum withdrawal. D) Densitometric analyses of FasL expression post serum-withdrawal revealed that the 40kDa counterpart of FasL increased post STS treatment in the WHCO1, SNO and HT29 cell lines. Note: a SNO loading control (L/C) was included in the first lane of each immunoblot to allow for densitometric comparison.

6.3.5 The HOSCC cell lines differentially express caspase-8

Fas-mediated anoikis converges on the activation of caspase-8 and -3, which cleave structural proteins, thereby dismantling sites of focal contact (Frisch *et al*., 1999; Mawji *et al*., 2007). Under standard tissue culture conditions, the expression of caspase-8 was relatively uniform across the HOSCC, as well as the HT29 and MCF7 control cell lines (*Figure 6.4*). The lowest caspase-8 expression was observed in the WHCO3 and WHCO6 cell lines, on average approximately 2 fold less than the WHCO1 cell line (*Figure 6.4B*).

A.

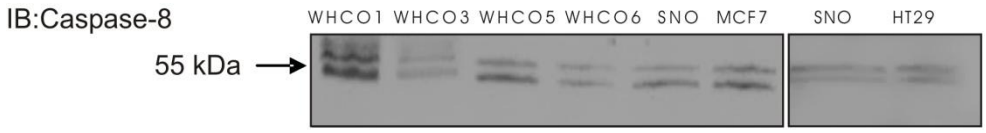

B.

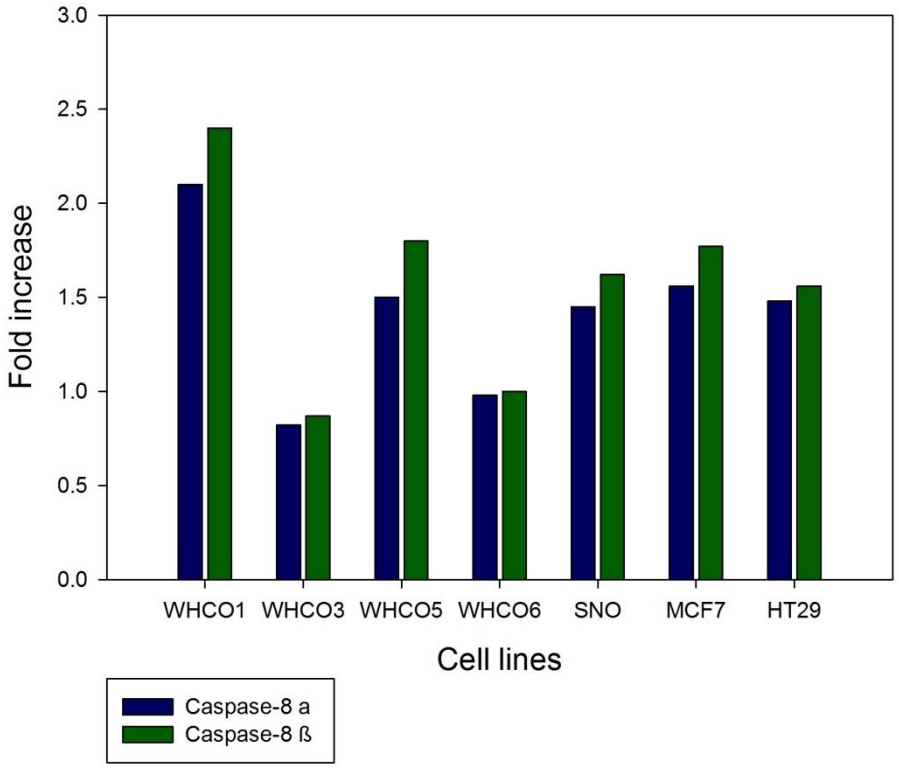

Figure 6.4: Caspase-8 is differentially expressed in the HOSCC, MCF-7 and HT29 cell lines under standard tissue culture conditions. A) Western blot analysis of the cell lysates using a polyclonal antibody against human caspase-8 that detected both caspase-8/α and -8/β isoforms. The highest level of caspase-8 expression was observed in the WHCO1 and WHCO5 cell lines. B) Densitometric analysis of the immunoblot was performed using Labworks™ Image Acquisition and Analysis software. Expression levels are relative to the maximum per 20µg of protein in the WHCO6 cell line. Note: the whole cell samples used to detect FAK in *Figure 2.3A* we were the same samples used to detect caspase-8, and therefore, the tubulin immunoblot also represents the loading control for the above immunoblot.

6.3.5 Sustained integrin β1-dependent signalling is accompanied by delayed Fas-mediated apoptosis in the mt p53-R175H cell line

We have clearly shown that the HOSCC cell line harbouring the mt p53-R175H was resistant to caspase-3 activation, FAK cleavage and dephosphorylation of FAK and PKB (*Figure 3.8 & 4.4*). Thus, we investigated whether the mt p53-R175H was resistant to Fas-mediated apoptosis as measured by caspase-8 and -3 activation. In comparison to the representative wt p53 WHCO6 cell line, the mt p53-R175H cell line was resistant to caspase-8 and -3 activation at 30 nM STS (*Figure 6.5A*). However, definitive FAK cleavage and caspase-8 and -3 activation was observed post treatment with 120 nM STS (*Figure 6.5A*). Aberrant β1 integrin-dependent signaling is associated with resistance to Fas-mediated anoikis (Estrugo *et al*., 2007). Although, the mt p53-R175H cell line maintains integrin β1-dependent signalling post 30 nM STS treatment (*Figure 3.11*), treatment with 120 nM STS resulted in FAK dephosphorylation (*Figure 6.5A*) and the abrogation of the integrin β1-FAK association (*Figure 6.5B*).

6.3.6 The novel complex identified between Fas and FAK is independent of p53-directed events.

The delay in Fas-mediated apoptotic death in the mt p53-R175H cell (*Figure 6.5A*) was accompanied by the maintenance of pFAKTyr397 and sustained integrin β1-activated FAK (*Figure 4.4 & 6.5B*), thus, implicating a role of FAK in directly regulating Fas-dependent apoptosis. Although an indirect link between FAK and Fas has been reported (Kamarajan *et al*., 2010), we identify a novel complex between Fas and FAK by immunoprecipitation in wt and mt p53-R175H cell lines (*Figure 6.6A*). The delay in caspase-8 activation observed in the mt p53-R175H cell line was accompanied by the maintenance of a Fas/FAK complex (*Figure 6.6A*). Moreover, the ligation of FasL to Fas was only detected post FAK cleavage and in the absence of the Fas/FAK complex (*Figure 6.6B & C*). As we have also shown that FAK interacts with p53, we assessed whether the Fas/FAK complex could be detected in the p53-null H1299 cell line. We clearly show by

immunoprecipitation the Fas/FAK complex in the p53-null H1299 cell line (*Figure 6.7*).

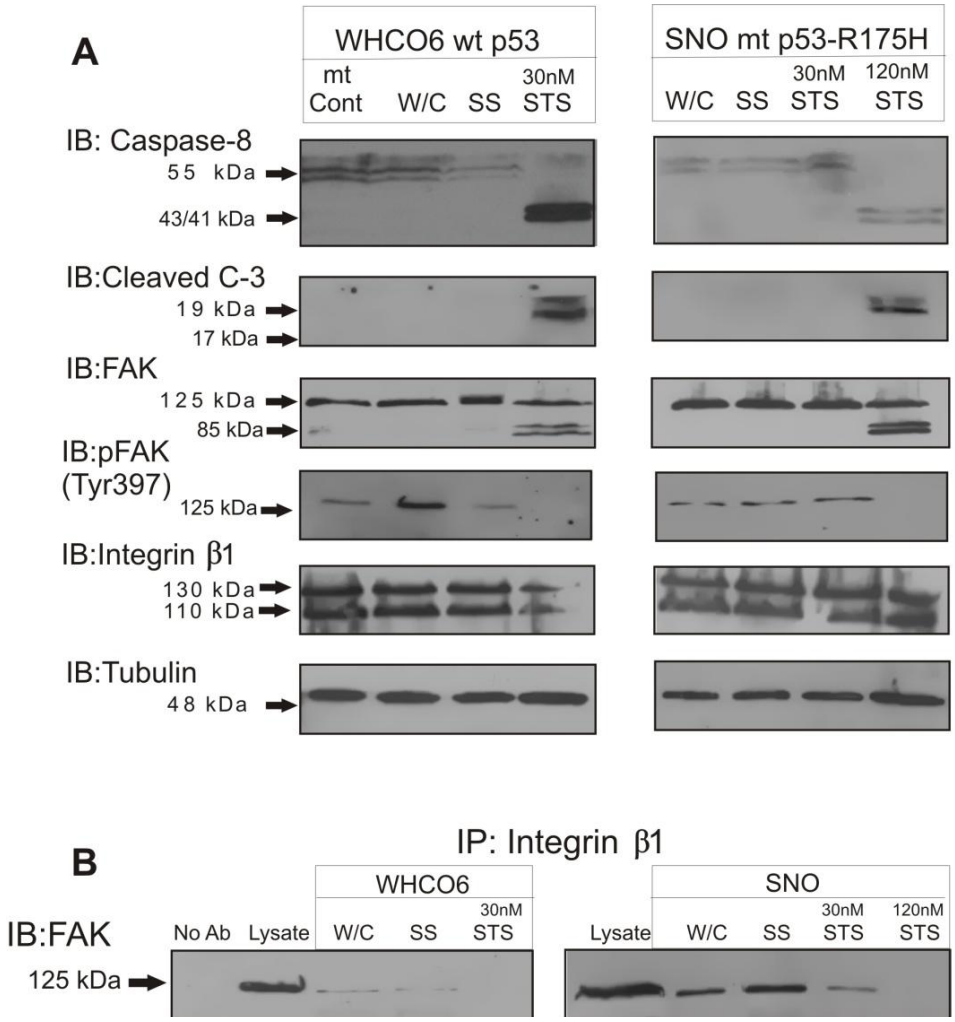

Figure 6.5: Sustained integrin β1-dependent signalling accompanies delayed Fas-mediated apoptosis in the mt p53-R175H cell line. A) The Fas-mediated apoptotic pathway is intact in the mt p53-R175H cell line. Caspase-3 and -8 were activated in a time course corresponding to FAK cleavage in the wt p53 WHCO6 cell line at 30nM STS. In contrast, activated caspase-3 and -8 was only detected post 120nM STS in the mt p53-R175H cell line. Caspase-8/α and -8/β and the processed intermediates of caspase-8 (p43/41) are indicated. B) The association between integrin β1 and FAK was detected in wt and mt p53-R175H cell lines. Abrogation of the integrin β1/FAK interaction was observed at 30nM STS and 120nM STS in the wt and mt p53-R175H cell lines respectively. Normal tissue culture conditions (W/C), serum-free conditions (SS).

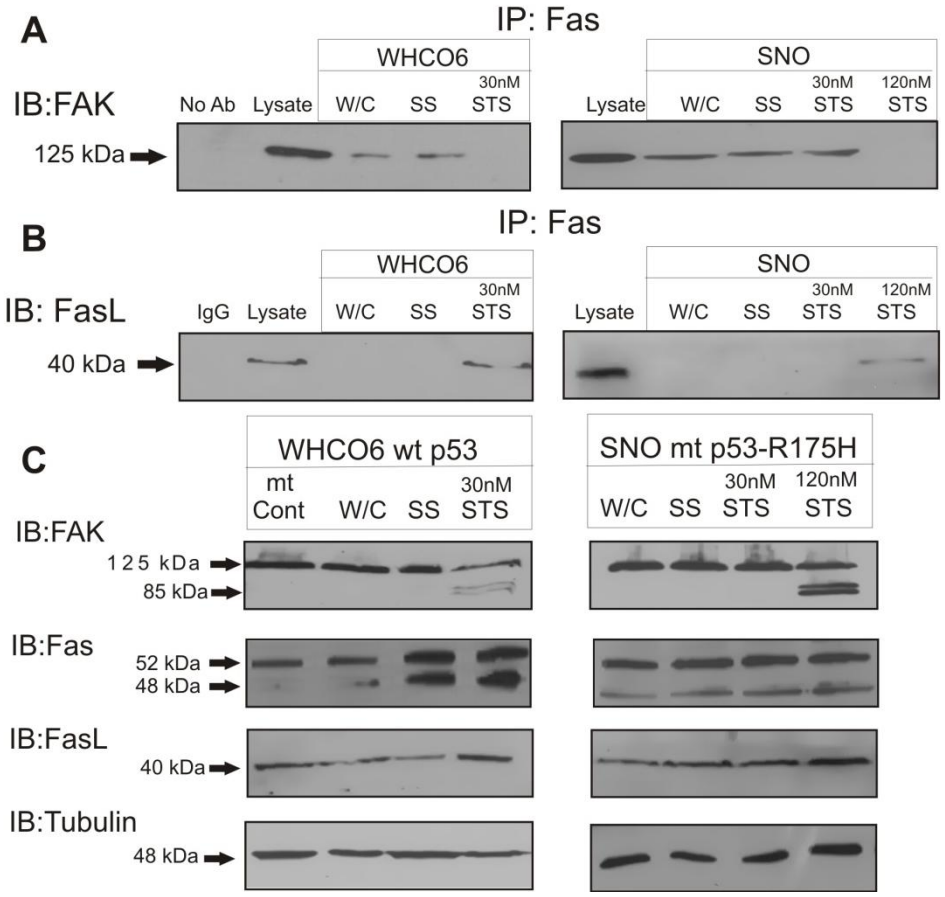

Figure 6.6: Delayed Fas-mediated apoptosis in the mt p53-R175H cell line is accompanied by the maintenance of a Fas/FAK complex A) The Fas/FAK complex, identified in the wt p53 WHCO6 and mt p53-R175H cell lines, decreased in a time course corresponding to the detection of the (B) FasL/Fas interaction. Note, the Fas/FAK complex was maintained at 30nM STS in the mt p53-R175H cell line. C) Immunoblot analysis of the supernatant fraction from the anti-Fas immunoprecipitates. Fas expression increased post serum-withdrawal in the wt p53 WHCO6 cell line, whilst Fas remained unchanged in the mt p53-R175H cell line. Mt cont =W/C control from mt p53-R175H cell line; normal tissue culture conditions (W/C); serum-free conditions (SS).

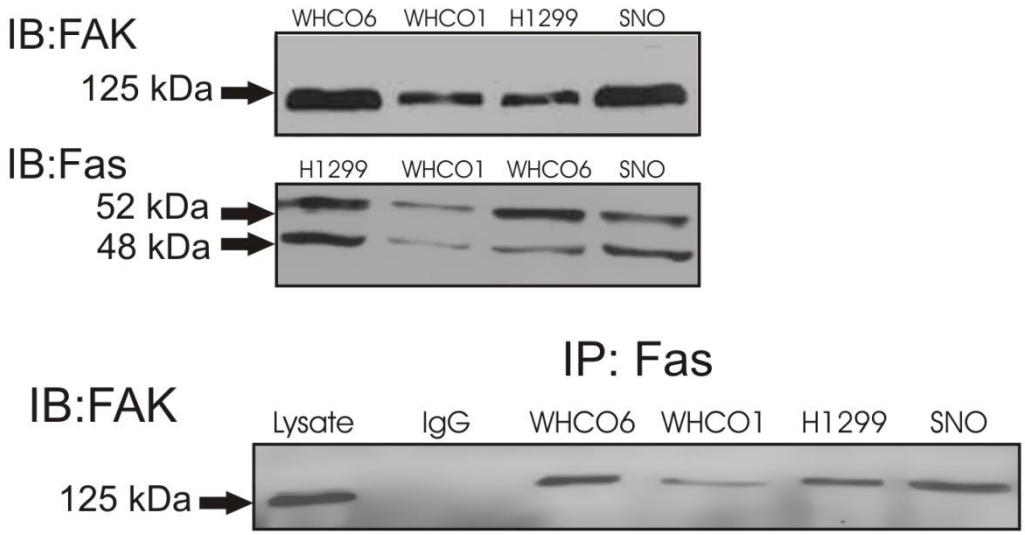

Figure 6.7: The Fas/FAK association is independent of p53-directed events. A) p53-independent regulation of FAK and Fas is evident in the p53-null H1299 cell line. B) The association between FAK and Fas was detected in the p53-null H1299 and HOSCC cell lines.

6.4 Discussion

The demonstration of a link between FAK-dependent signalling and the repression of Fas-mediated anoikis has heightened interest in the role of ECM-activated FAK in anchorage-dependent death (Kurenova *et* al., 2004; Kamarajan *et al*., 2010). In this regard, the squamous keratinocytes of the oesophagus presents a particularly insightful model as overexpression of FAK and reduced sensitivity to Fas-mediated death correlates with enhanced oesophageal tumour metastasis (Rigberg *et al*., 1999; Miyazaki *et al*., 2003). Although the ability of mutant p53 to resist apoptotic stimuli is well established, the R175H "hot-spot" p53 mutant is a potentially a potent inhibitor of anoikis, by abolishing the ability of p53 to transcriptional regulate Fas and FAK gene transcription (Zalcenstein *et al*., 2003; Golubovskaya *et al*., 2008 (a)). Pertinently, we have previously demonstrated resistance to staurosporine (STS)-mediated detachment and FAK Tyr397 dephosphorylation by a HOSCC cell line harboring mt p53-R175H (*Figure 3.9 & 3.10*). Thus, as these data implicate mt p53-R175H as being intimately involved in anoikis resistance, we made use of this unique model of HOSCC cell lines to analyze the influence of FAK-dependent signaling on Fas-mediated death.

Fas-mediated apoptosis is initiated by the interaction of membrane-bound FasL, with its corresponding death receptor, Fas (synonyms: Apo-1, CD95, and TNFRSF6) (Aoudjit and Vuori, 2001). Unlike Fas, which is ubiquitously expressed, FasL is predominantly expressed by activated T lymphocytes, as well as "immune privileged" tissues including the testes, ovary and retina (Krueger *et al*., 2003). Extending the demonstration of FasL protein expression in normal esophageal tissue (Bennet *et al*., 1999), we show HOSCC cell lines, harboring both wt p53 or mt p53-R175H to differentially express FasL (*Figure 6.1*). In addition, predominantly peri-nuclear localisation of FasL was observed (*Figure 6.2*). Thus, although HOSCC tumours are proposed to evade immune surveillance by increasing the FasL surface expression (Rigberg *et al*., 1999), no unusual

distribution of FasL was observed in this series of moderately differentiated tumours.

Substrate-deprived death was demonstrated to be accompanied by increased levels of Fas (Ishida *et al*., 2003). Unlike the mt p53-R273H cell line, Fas expression was not suppressed in the mt p53-175H cell line (*Figure 2.9*). Moreover, in contrast to the wt p53 cell lines, Fas expression was not altered by STS treatment in the mt p53-R175H cell line (*Figure 6.3B & C*). Therefore, the regulation of Fas expression in the mt p53-R175H cell line appears to be independent of p53-directed events. In addition, FasL levels have been demonstrated to be upregulated following detachment from the ECM (Ishida *et al*., 2003). In agreement with this report, an increase in FasL expression was evident post STS treatment in the WHCO1, WHCO6, SNO and HT29 cell lines (*Figure 6.3D*). However, as the mt p53 cell lines were resistant to STS-mediated detachment (*Figure 3.9*), no distinct relationship between the regulation of FasL expression and anoikis-related events is evident in the HOSCC cell lines.

Fas-mediated anoikis converges on the activation of caspase-8 and -3, which cleave structural proteins, thereby dismantling sites of focal contact (Frisch *et al*., 1999; Mawji *et al*., 2007). Despite similar expression and distribution of Fas and FasL to the wt p53 cell lines (*Figure 2.4 & 6.1*), the mt p53-R175H cell line was resistant to caspase-8 activation and, hence, Fas-mediated apoptosis at 30nM STS (*Figure 6.5A*). However, definitive FAK cleavage, and activation of caspase-8 and -3 was observed post treatment with 120nM STS in the mt p53-R175H cell line (*Figure 6.5A*). Therefore, although Fas-mediated caspase-8 activation was not evident at 30nM STS, Fas-mediated apoptosis was still induced by a stronger apoptotic stimulus. Thus, despite HOSCC being reported to be non-responsive to Fas-mediated apoptosis (Rigberg *et al*., 1999), the components of death receptor apoptotic pathway are intact in both wt and mt p53-R175H cell lines.

Survival signals transduced by FAK are eliminated by caspase-dependent cleavage of the C-terminal portion of FAK (Cooper *et al*., 2003). Accordingly,

STS-mediated events that result in the activation of caspase-8 and -3 were accompanied by the cleavage and dephosphorylation of FAK (*Figure 6.5A*). Pertinently, at low STS treatment concentrations, FAK-dependent signalling was maintained in the mt p53-R175H cell line. The direct interaction between the C-terminal of FAK with the cytoplasmic tail of the β integrin subunit facilitates the rapid Tyr397 autophosphorylation of FAK (Schaller *et al*., 1994). Correspondingly, the cleavage and resultant dephosphorylation of FAK corresponded to the attenuation of the integrin β1/FAK association (*Figure 6.5B*). Enhanced integrin β1-dependent signaling has been linked to resistance to Fas-mediated apoptotic death, as ligand bound β1 integrin inhibits procaspase-8 activity (Estrugo *et al*., 2007). Thus, the persistent integrin β1-dependent activation of FAK observed at low STS treatment concentrations may be responsible for the resistance to caspase-8 activation in the mt p53-R175H cell line.

An indirect link between FAK and Fas has been demonstrated to regulate Fas-dependent apoptosis (Kamarajan *et al*., 2010). However, the identification of a novel Fas/FAK complex reveals that FAK may be directly coordinating Fas-mediated death (*Figure 6.6A*). Intriguingly, despite the fact that we have previously identified an association between FAK and p53 in these HOSCC cell lines (*Figure 5.4*), the identification of the Fas/FAK complex in the p53-null H1299 cell line confirms the lack of dependence of this complex on p53-directed events (*Figure 6.7*). Moreover, whilst STS-mediated dephosphorylation of FAK did not influence the p53/FAK association, dephosphorylation of FAK was accompanied by the abrogation of the Fas/FAK complex. Importantly, caspase-8-related apoptotic events were accompanied by the abrogation of the Fas/FAK association (*Figure 6.5A and 6.6A*). Moreover, in the same anti-Fas immunoprecipitates, the ligation of FasL to Fas was only detected post FAK dephosphorylation and in the absence of the Fas/FAK complex (*Figure 6*.6B). Therefore, in addition to maintaining FAK-dependent survival signaling, sustained FAK activation may oppose anoikis by directly suppressing Fas-mediated apoptosis.

Thus, despite the fact that Fas-mediated apoptosis is delayed in the SNO cell line harbouring the conformational mt p53-R175H, the death receptor cascade is still inducible in wt and mt p53-R175H HOSCC cell lines co-expressing Fas and FasL. Notably, in the mt p53-R175H cell line, the delay in caspase-8 activation was accompanied by the maintenance of integrin β1-activated FAK and the Fas/FAK complex (*Figure 6.5)*. Accordingly, enhanced FAK activation may enable tumours to escape anoikis, by directly suppressing Fas-mediated apoptosis.

Chapter 7

General Discussion and Conclusion

Sustained FAK-dependent signalling underpins anoikis resistance in oesophageal carcinoma

7.1 p53 mutational status does not influence the expression of key anoikis-related intermediates in moderately differentiated HOSCC

In normal tissue, as a barrier to metastasis, loss of adhesion to the ECM induces anoikis via the p53- or Fas-mediated apoptotic pathways (Ilic *et al.*, 1998; Marconi *et al*., 2004; Mawji *et al*., 2007). Fundamental to anoikis-related regulation is FAK, a cell adhesion molecule that coordinates various signalling cascades at sites of cell contact (Zhang *et al*., 2004 (a); Lui *et al*., 2008). However, although enhanced expression and activation of FAK has been shown to repress anoikis (Kurenova *et al*., 2004; Lui *et al*., 2008; Kamarajan *et al*., 2010), the mechanism underlying anoikis resistance is poorly defined. Thus, the molecular analysis of interplay between FAK and the key apoptotic constituents is imperative, as it reveals the mechanism used by tumours to escape anoikis.

HOSCC is a highly prevalent cancer, particularly amongst the black population in the South African rural regions of the Transkei and Soweto (Isaacson, 2005). Since most patients present with advanced metastatic disease at time of diagnosis (Tew *et al*., 2005; Jemal *et al*., 2009), HOSCC would appear to be highly resistant to anoikis. Critically, metastatic oesophageal cancer occurs in over 50% of patients and remains incurable (Tew *et al*., 2005). Accordingly, characterization of the anoikis-related signalling in HOSCC may allow the design of therapeutics that restores anoikis sensitivity to tumours cells, thereby, preventing their metastatic progression. Hence, in this study, by examining the interaction of FAK

with key apoptotic regulators, we sought to understand the mechanism underlying anoikis resistance in HOSCC.

FAK has been implicated as the key intermediate in the acquisition of anoikis resistance, as constitutive activation through Tyr397 phosphorylation of FAK maintains cell adhesion-dependent signalling and, thereby, facilitates tumour cell survival post detachment (Owen *et al*., 1999; Wang, 2001; Webb *et al*., 2004). In this report, despite the five HOSCC cell lines being derived from moderately differentiated tumours, there was a distinct variation in FAK protein expression and Tyr397 phosphorylation levels across the cell lines (*Figure 2.3*). Overexpression of FAK and the enhanced expression of Tyr397-phosphorylated FAK are correlated with oesophageal tumorigenesis and metastasis (Ayaki *et al*., 2001; Miyazaki *et al*., 2003; Gabriel *et al*., 2006). Thus, the variation of FAK expression in the HOSCC cell lines indicates that the visual categorisation of oesophageal tumours may be a poor indication of molecular alterations that accompany oesophageal tumorigenesis – particularly in the moderately differentiated category. Consequently, in this study, the identification of similarities or disparities in anoikis-related signalling within this series of moderately differentiated HOSCC cell lines, may aid in refining this broad category. Specifically, the WHCO6 and SNO cell lines with elevated FAK expression relative to the other HOSCC cell lines (*See Figure 2.3*) pertinently facilitated the investigation of FAK-dependent signalling on anoikis-related events.

Although p53 mutants are well established to desensitize tumours to apoptotic stimuli (Blandino *et al*., 1999; Tsang *et al*., 2005), several studies point to mutant p53 as being intimately involved in FAK-dependent anoikis resistance (Zhang *et al*., 2004 (a); Golubovskaya *et al*., 2005; Golubovskaya *et al*., 2009). Mutations of the p53 gene are selected for in greater than 50% of all human cancers (Hollstein *et al*., 1991). The most common p53 mutations are single point mutations in the DNA-binding domain. These mutations lead to single amino acid changes that influence the sequence-specific binding or the conformation of

the mutant protein, abrogating its ability to induce the transcription of target genes. Of the three most common "hot-spot" p53 mutants (R175H, R248H, R273H), mt p53-R175H mutant is known to be the most severe conformational p53 mutant and a potent inhibitor of apoptosis by abolishing the transcriptional regulation of caspase-3, Fas and FAK (Tsang *et al*., 2003; Zalcenstein *et al*., 2003; Golubovskaya *et al*., 2008 (a)). Consequently, these studies suggest that by suppressing the expression of key anoikis-related intermediates, mt p53-R175H is potentially a potent inhibitor of anoikis.

In oesophageal tumours, loss of the tumour suppressor function of p53 is a frequent event in HOSCC progression (Xue *et al*., 2006). In particular, mt p53-R175H is associated with the metastatic progression of HOSCC (Wang *et al*., 2003). Furthermore, the sequence polymorphism in exon 4 at codon 72 that encodes for either a proline or arginine is a frequent occurrence in HOSCC patients (Vos *et al*., 2003). Consistent with these reports, sequence analysis of p53 in the series of moderately differentiated HOSCC cell lines revealed that the SNO cell line harbours the conformational mt p53-R175H and the Pro/Arg72 polymorphism was identified in both the WHCO1 and SNO cell lines (*Figure 3.2 & 3.3*). However, despite elevated expression of FAK and comparable p53 expression to the SNO cell line, the WHCO6 cell line harbours wt p53 (*Figure 2.3 & 2.7*). Moreover, Fas was differentially expressed by the wt and mt p53 HOSCC cell lines (*Figure 2.9*). Accordingly, in this series of moderately differentiated HOSCC cell lines, no distinct relationship between the level of expression of the anoikis-related intermediates and the mutational status of p53 is evident. However, a definite correlation between FAK overexpression and mt p53 has been demonstrated, whilst overexpression of FAK correlates with enhanced oesophageal tumorigenesis (Miyazaki *et al*., 2003; Golubovskaya *et al*., 2009). Therefore, due to the fact that mechanism underlying anoikis resistance in oesophageal carcinoma is unknown, the response of wt/mt p53 HOSCC cell lines to apoptotic stimuli was ascertained, to achieve an understanding of the significance of enhanced FAK-dependent signalling on cell death events.

7.2 mt p53-R175H cell line: a model for the investigation of FAK-dependent anoikis regulation

The initiation and execution of anoikis is mediated by the intrinsic and extrinsic apoptotic pathways, which converge on the activation of caspases, DNA fragmentation and cell death (Ilic *et al*., 1998; Mawji *et al*., 2007). Clearly, the integrity of these pathways is crucial for anoikis induction. Even though HOSCC is highly resistant to the anti-apoptotic ability of chemotherapeutic reagents (Leu *et al*., 2000), the data presented shows that oligonucleosomal cleavage was still inducible by the widely used apoptosis-inducing agent STS, in both wt and mt HOSCC cell lines (*Figure 3.8A*). Hence, the apoptotic pathway is intact in both wt and mt p53-R175H HOSCC cell lines. Thus far, no similar data was found in the literature that shows comparable oligonucleosomal cleavage between cancer cell lines endogenously expressing wt p53 or p53-R175H. Furthermore, we show that the p53-R175H cell line was resistant to STS-mediated detachment (*Figure 3.9*) and FAK dephosphorylation (*Figure 4.4*). As FAK has been previously shown to be rapidly dephosphorylated post STS treatment (Beviglia *et al*., 2003; Lim *et al*., 2008), this is the first report of a mt p53-R175H cell line that is resistant to both STS-induced FAK dephosphorylation and detachment.

Loss of cell-matrix contact in epithelial cells reduces integrin-mediated FAK survival signalling, thereby triggering anoikis (Frisch and Francis, 1994; Zhang *et al*., 2004 (a)). The direct interaction between the C-terminal of FAK with the cytoplasmic tail of the β subunit of the integrins facilitates the rapid autophosphorylation of FAK at Tyr397 (Schaller *et al*., 1994). Importantly, the cleavage of FAK induces the loss of integrin-associated FAK at sites of focal contact (Schaller *et al*., 1994; van Nimwegen and van der Water, 2007). Pertinently, we show that the FAK/integrin β1 association was maintained in the mt p53-R175H cell line post apoptotic stimuli (*Figure 3.11*). Hence, the mechanism whereby the mt p53-R175H confers resistance to apoptotic stimuli may rely on sustained integrin-activation of FAK. Importantly, these data demonstrate a unique relationship between loss of tumour suppressor function of

p53 and enhanced cell adhesion-mediated signalling. Consequently, the mt p53-R175H cell line represents a unique model for the investigation of FAK-dependent regulation of anoikis resistance in HOSCC, the intricacies of which may also pertain to other epithelial tumours. Specifically, this model permits the dissection of the influence of p53 mutational status on crosstalk between FAK- and the key apoptotic regulators, p53 and Fas.

7.3 ECM-activated FAK suppresses detachment: opposing role of mt p53-R175H

Cell-ECM connections profoundly regulate cell fate decisions as they suppress the proliferation of cells existing outside their appropriate environment (Badylak *et al*., 2009). Consequently, interactions between the ECM and the tumour cell are believed to be a major determinant in anoikis resistance (Zhang *et al*., 2004 (a); Kamarajan and Kapila, 2007). In an experimental setting, fibronectin/integrin β1 engagement has been demonstrated to be a potent inhibitor of anoikis via the activation of FAK-dependent survival signalling (Guan and Shalloway, 1992; Zhang *et al*., 2004 (a)). However, while these studies have demonstrated that increased activation of FAK is associated with the repression of apoptotic pathways and maintained cell survival in the absence of cell contact (Guan and Shalloway, 1992; Zhang *et al*., 2004 (a); Kamarajan and Kapila, 2007), the exact mechanism of this regulation is poorly understood. Thus, we explored the influence of FN-mediated activation of FAK on the suppression of apoptosis in wt and mt p53 cell lines. Intriguingly, while FN reduced STS-mediated detachment in the wt p53 HOSCC cell lines (WHCO1, WHCO3 and WHCO6), the mt p53 cell lines displayed a lack of dependence on FN-dependent signalling (*Figure 4.2*). Pertinently, as the mt p53-R175H cell line also displayed maintained integrin β1-activated FAK (*Figure 3.11*), loss of tumour suppressor function of p53 may be a critical factor that facilitates the anchorage-independent survival of oesophageal tumour cells.

Upon integrin-ECM engagement, FAK activate various signaling pathways involved in cell survival and proliferation (van Nimwegen and van der Water, 2007). Notably, Tyr397 phosphorylation of FAK recruits PI3K, leading to the activation of its downstream target protein kinase B (PKB/AKT) (Gilcrease, 2007). However, although the survival signals transduced by FN-integrin engagement via FAK are attributed to activation of the PI3K/PKB pathway (Sonoda *et al*., 1999; Dai *et al*., 2005), the protection to STS-mediated detachment demonstrated in the wt p53 cells lines was independent of PKB Ser473 phosphorylation (*Figure 4.4*). In contrast to the wt p53 cell line, both FAK- and PKB-mediated signalling were maintained in the mt p53-R175H cell line post STS treatment (*Figure 4.4*). Thus, these data reveal that the repressive effect that mt p53-R175H has been established to have on the FAK promoter (Golubovskaya *et al*., 2008 (a)), may be responsible for the maintenance of PKB-dependent survival signalling observed in the SNO cell line. Furthermore, as the maintenance of FAK-dependent signalling was accompanied by resistance to detachment (*Figure 3.9*), these data reaffirm the notion that enhanced FAK-dependent signalling facilitates the survival of tumour cells post detachment.

7.4 Impact of "loss of function" effect of mt p53-R175H on FAK regulation

Consequently, as the ECM-mediated protection of apoptotic death is independent of PKB signalling in the wt p53 HOSCC cell lines (*Figure 4.4*), the alternative survival role of FAK in the suppression of p53-dependent apoptosis was explored. In response to stress, the highly conserved nuclear export signal, IALKLGCLEI on the N-terminal domain of FAK facilitates the nuclear accumulation of FAK (Ossovskaya *et al*., 2008). The nuclear translocation of FAK has been demonstrated to enhance the association between FAK and p53 (Golubovskaya *et al*., 2005; Lim *et al*., 2008). Despite impaired flexibility (Aylon and Oren, 2007), the R175H mutation did not influence the ability of p53 to associate with FAK (*Figure 5.4*). Moreover, consistent with previous studies (Lim *et al*., 2008), nuclear FAK was detected in the wt and mt p53-R175H cell lines post STS

treatment (*Figure 5.3*). Thus, the altered regulation of FAK and resistance to caspase-3 activation in the mt p53-R175H cell line is not due to the inability of mt p53-R175H to associate with FAK.

Upon activation by stress stimuli, wt p53 has been demonstrated to bind to the FAK promoter and repress FAK expression (Golubovakaya *et al*., 2008). However, due to reduced DNA-binding capacity, mt p53-R175H does not bind the FAK promoter (Golubovakaya *et al*., 2008). Hence, one possible way in which mt p53-R175H SNO cell line might be evading caspase-dependent apoptosis is through the upregulation of FAK expression. In this way, the anti-apoptotic ability of FAK would be enhanced, facilitating the evasion of anoikis-related death. Accordingly, the overexpression of mt p53-R175H in a p53-null cell line increased FAK expression, whilst, wt p53 had no appreciable effect on FAK expression (*Figure 5.8 & 5.9*). Consequently, the loss of transcriptional regulation of FAK in tumours harbouring mt p53-R175H may be a critical event in FAK-dependent anoikis resistance.

As the dominant negative effect of mutant p53 leads to the inactivation of wt p53, mutation of one allele of p53 can result in loss of function. Importantly, the tetramerization of mt p53 with wt p53 reduces the ability of the p53 tetramer to bind the FAK promoter (Willis *et al*., 2004). Thus, due to the implication of this regulation in anoikis-related events, this possibility was explored by overexpressing mt p53-R175H in the representative wt p53 WHCO6 cell line, followed by the induction of apoptosis with STS. Although the mt p53-R175H did not protect the wt p53 WHCO6 cell line from STS-mediated FAK cleavage, the expression of FAK was elevated relative to the STS control (*Figure 5.10*). Thus, these data corroborate our earlier proposal that, through a 'loss of function' effect, mt p53-R175H may facilitate anoikis resistance, by enhancing FAK-dependent signalling.

7.5 Gene therapy: targeting anoikis-related intermediates

Although several intermediates are implicated in anoikis resistance, due to its central role in tumourigenesis, much attention as been focused on the role of p53 as a potential drug target (Buganim and Rotter, 2009). Consequently, numerous reports have documented the frequency and distribution of p53 mutants in various tumour types (Blandino *et al*., 1999; Zalcenstein *et al*., 2003; Wang *et al*., 2003; Vrba *et al*., 2008), allowing p53 mutants to be graded according to their "oncogenic power" (Buganim and Rotter, 2009). Aberrant p53 activity may be a result of deregulation of upstream effectors, or alternatively, p53 may be deleted or inactivated by viral infection. In these instances, targeting the upstream regulators of p53 or reintroduction of wt p53 represents the appropriate therapeutic approach. However, in the majority of tumours, there is a loss of p53 function due to mutation in the DNA binding domain of the protein (Petitjean *et al*., 2007). Consequently, studies that characterize the properties of these mt p53 proteins are imperative to the development of customized p53-based therapy.

At present, there are several approaches to p53-based therapy. In cases where p53 is intact, but its negative regulator Mdm2 is overexpressed, abrogating the p53/Mdm2 interaction represents a viable therapeutic approach. Consequently, peptides that target this association will restore wt p53 activity by preventing p53 degradation. By screening a diverse library of synthetic chemicals, one class of cis-imidazoline analogues (Nutlins), were shown to induce growth arrest and apoptosis by binding to p53 and disrupting the p53/Mdm2 association (Vassilev *et al*., 2004). Moreover, RITA (Reactivation of p53 and induction of Tumour cell Apoptosis) was also demonstrated to abrogate the p53/Mdm2 association by binding to the p53 transactivation site (Kojima *et al*., 2005; Tovar *et al*., 2006). Both compounds stabilize p53 by interfering with the p53/Mdm2 complex.

Alternatively, in tumours where p53 is absent due to an allelic deletion or truncation, wt p53 activity can be reestablished by introducing full-length p53 into the tumour cells. Adenoviral serotype 5-mediated infection of wt p53 is used to

forcibly deliver the p53 protein to the p53-null tumour cells. Of the numerous p53-based gene therapy products in clinical trials, Advexin (INGN 201, 2003) and ScH-58500 have shown the most promise as effective anti-cancer agents (Barnard, 2000). Importantly, the efficacy of these therapies is enhanced by chemotherapy.

Currently the most promising approach to p53-based therapy is to specifically target mutated p53 proteins, reverting mutated p53 proteins to a wt p53 conformation, thereby restoring wt p53 activity. Although this approach is highly ambitious, initial studies demonstrated that the DNA binding capacity of p53 can be restored. The PAb241 antibody against the carboxy-terminus of p53 or the presence of ME1, a mouse single chain Fv fragment (scFv) against the common epitope of mutant p53, can restore specific DNA-binding capability to several p53 mutants (Hansen *et al*., 1996; Orgad *et al*., 2005). In addition, suppressor mutations have been demonstrated to restore the mutant conformation to a wild-type conformation (Joerger *et al*., 2005; Suad *et al*., 2009). Hence, the relative flexibility of p53 has enabled the design of small molecules that alter the structure of mutated p53 to partially restore its DNA binding capacity. PRIMA-1 (P53 Reactivation and Induction of Massive Apoptosis) was identified following a screen for a library of low-molecular-weight compounds. By reestablishing DNA contact, PRIMA-1 was demonstrated to induce apoptosis in tumours harbouring mutated p53 (Rehman *et al*., 2005). However, as the mechanism of PRIMA-1 involves the restoration of p53/Hsp90 interactions, the efficacy of this molecule is limited to temperature sensitive p53 mutants (E285K, L194F, R280K). Therefore, PRIMA-1 does not significantly affect the "hot-spot" p53 mutants (R175H, R273H, R249S). Alternatively, a promising compound that restores wt p53 activity is P53R3. Moreover, studies show that P53R3 restores sequence specific DNA-binding of p53-R175H and p53-R273H (Weinmann *et al*., 2008). In addition, P53R3 was more effective than PRIMA-1 at reestablishing wt p53 activity. Importantly, by restoring mutationally destabilized p53, these compounds may reinstate p53-dependent transcriptional regulation of anoikis-dependent genes, including FAK and Fas.

7.6 Fas-mediated apoptosis is delayed in mt p53-R175H cell line: implication for chemotherapeutic intervention

Intriguingly, in addition to repressing p53-dependent anoikis (Frisch *et al*., 1998; Golubovskaya *et al*., 2005), FAK has also been implicated in the suppression of the death-receptor pathway (Kurenova *et al*., 2004; Kamarajan and Kapila, 2007). Moreover, enhanced integrin β1-dependent signaling has been linked to resistance to Fas-mediated apoptotic death, as ligand bound β1 integrin inhibits procaspase-8 activity (Estrugo *et al*., 2007). Thus, making use of the detachment-resistant mt p53-R175H cell line displaying persistent integrin β1-activated FAK, we explored the influence of sustained FAK activation on the Fas-mediated death cascade.

Cancer cells expressing membrane-bound FasL are proposed to evade immune attack by inducing apoptosis in Fas-sensitive lymphoid cells (Kozowski *et al*., 2007). Consequently, as increased membrane expression of FasL and reduced cell surface expression of Fas have been previously reported in oesophageal tumours, HOSCC would appear to be highly resistant to immune surveillance (Rigberg *et al*., 1999). Moreover, perturbations in Fas/FasL death cascade are pivotal to HOSCC tumour progression (Xue *et al*., 2006). Contrary to these reports, in this series of HOSCC cell lines, no aberrant localisation of Fas (*Figure 2.10*) or FasL (*Figure 6.2*) was observed. Furthermore, although Fas, FasL and caspase-8 have been demonstrated to be strongly downregulated at early stages during the development of HOSCC (Xue *et al*., 2006), all of the moderately differentiated HOSCC cell lines express the comparable levels of Fas, FasL and caspase-8. However, despite similar expression and distribution of Fas and FasL, caspase-8 activation was delayed in the mt p53-R175H cell line (*Figure 6.5A*). Moreover, although the mt p53-R175H cell line was resistant to caspase activation at low apoptotic stimuli, the cleavage and dephosphorylation of FAK was observed once the apoptotic stimulus was increased (*Figure 6.5A*). Survival signals transduced by FAK are eliminated by caspase-dependent cleavage of the C-terminal portion of FAK (Cooper *et al*., 2003). Correspondingly, the delay in caspase activation was accompanied by maintain integrin β1-activation of FAK.

Thus, as ligand bound β1 integrin inhibits procaspase-8 activity (Estrugo *et al*., 2007), the persistent integrin β1-dependent activation of FAK observed at low STS treatment concentrations may be responsible for the resistance to caspase-8 activation in the mt p53-R175H cell line.

Remarkably, due to sustained integrin β1-activated FAK and delayed Fas-mediated apoptosis, this data reveals that tumours harboring the mt p53-R175H may be more likely to escape the host's immune surveillance. In addition, despite HOSCC being reported to be non-responsive to Fas-mediated apoptosis (Rigberg *et al*., 1999), caspase-8 activation was detected in both wt and mt p53-R175H cell lines (*Figure 6.5A*). Importantly, this would suggest that although chemotherapeutics targeting the Fas-mediated death cascade may be a viable therapeutic approach in HOSCC, these reagents would be less effective in oesophageal tumors harboring mt p53-R175H.

7.7 FAK interacts with both key apoptotic regulators: sustained FAK-dependent signalling underpins anoikis resistance in HOSCC

Considerable evidence points to a crucial role of p53 and Fas in FAK-mediated repression of anoikis, however, the exact function of interplay between FAK and the key apoptotic constituents remains to be clarified (Kurenova *et al*., 2004; Golubovskaya *et al*., 2008 (a); Lim *et al*., 2008; Kamarajan *et al*., 2010). In particular, an indirect link between FAK and Fas has been demonstrated to regulate Fas-dependent apoptosis (Kamarajan *et al*., 2010). However, in this report, the identification of a novel Fas/FAK complex reveals that FAK may be directly coordinating Fas-mediated death (*Figure 3B*). Intriguingly, we have also identified an association between FAK and p53 in these HOSCC cell lines (*Figure 5.4*). Thus, FAK interacts with both key apoptotic regulators in both wt and mt p53-R175H cell lines. Importantly, while the p53/FAK interaction was not influenced by apoptotic events (*Figure 5.4*), the Fas/FAK complex was abrogated by STS treatment (*Figure 6.6A*). Significantly, the Fas/FAK complex was maintained at low STS treatment concentrations in the SNO cell line harbouring

the mt p53-R175H (*Figure 6.6A*). Thus, in addition to maintaining FAK-dependent survival signaling, sustained FAK activation may oppose anoikis by directly suppressing Fas-mediated apoptosis. Overexpression of FAK correlates with enhanced HOSCC progression (Miyazaki *et al*., 2003). Therefore, through interactions with both key apoptotic regulators, aberrant FAK activity would have an impact on both intrinsic and extrinsic death cascades. In addition, integrin-mediated activation of FAK enhances PKB-dependent survival signalling (Sonoda *et al*., 1999; Majumder and Sellers, 2005). Correspondingly, sustained PKB activation accompanied FAK phosphorylation in the detachment-resistant mt p53-R175H cell line (*Figure 4.4*). Therefore, collectively these data provide compelling evidence that strongly advocate aberrant regulation of FAK-dependent signalling as a critical factor underlying anoikis resistance.

7.8 Is FAK a possible chemopreventative target for HOSCC?

Based on its overexpression in HOSCC (Miyazaki *et al*., 2003) and known roles in opposing anoikis, FAK would appear to be a potential target for cancer therapy. Three novel kinase inhibitors of FAK, blocking FAKTyr397 autophosphorylation, were recently developed, one by Novartis, TAE226 (Golubovskaya *et al*., 2008 (c)) and another two by Pfizer, PF-573,228 and PF-562,271 (Roberts *et al*., 2008). TAE226 inhibited glioma and ovarian tumour growth *in vivo* (Golubovskaya *et al*., 2008 (c)). Although the efficacy of PF-573,228 on tumour growth *in vivo* has not been reported; it only inhibited motility and did not inhibit cell growth *in vitro*, whilst, PF-562,271 effectively blocked kinase activity of FAK and decreased tumour growth (Roberts *et al*., 2008). Although several kinase inhibitors are successful chemotherapeutic reagents, these inhibitors specifically target enzymes displaying deregulated tyrosine kinase activity due to mutation. However, multiple studies demonstrates that overexpression of FAK facilitates tumour progression (Miyazaki *et al*., 2003; Lark *et al*., 2005; Jiang *et al*., 2010). Thus, as there is no evidence that FAK is commonly mutated in cancer, the prospect that catalytic inhibitors of FAK would suppress cancer growth is poor.

A major concern with the use of FAK tyrosine kinase inhibitors is that FAK-dependent signalling is not solely regulated by tyrosine phosphorylation (Golubovskaya *et al*., 2005). Pertinently, the specific association between FAK and p53 is not dependent on Tyr397 phosphorylation (Lim *et al*., 2008). Accordingly, inhibition of FAK phosphorylation would not influence this association. Alternatively, a synthetic peptide containing the binding sites of p53 abrogated the p53/FAK association and reduced cancer cell viability in the MCF7 cell line (Golubovskaya *et al*., 2008 (a)). In contrast, the synthetic peptide did not significantly reduce growth in the normal mouse MEF and human MCF10A cells (Golubovskaya *et al*., 2008 (a)). The variation in response to the peptide has been attributed the difference in intracellular signalling between the normal and cancerous cells. Accordingly, cancer cells with 'overactivated' FAK are proposed to be more sensitive to the peptide (Golubovskaya *et al*., 2008 (a)). Hence, these results reported by Golubovskaya and colleagues suggest that therapeutics targeting the p53/FAK interaction may represent a far better alternative to FAK catalytic inhibitors.

Alternatively, the novel complex between FAK and Fas identified in this report was shown to be abrogated by STS-dependent events that resulted in FAK Tyr397 dephosphorylation (*Figure 6.6A*). As the molecular characterisation of this association is beyond the scope of this report, it is unknown whether an inhibition of FAK phosphorylation would selectively induce Fas-mediated apoptosis. However, as the Fas/FAK association is associated with delayed Fas-mediated apoptosis (*Figure 6.6A*), further studies that characterise this complex may facilitate the development of specific inhibitors that re-sensitise tumours to Fas-mediated apoptosis.

7.9 Conclusion

The acquisition of anoikis resistance is a critical step in metastasis, as it allows tumour cells to survive in the circulatory and lymphatic system, and colonise distant sites. However to date, the mechanism underlying resistance to anoikis remains cryptic. Thus, the molecular analysis of interplay between the major cell adhesion and apoptotic constituents is imperative, as it reveals the 'modus operandi' used by tumours to escape anoikis. Accordingly, details of this nature may allow the design of therapeutics that restores anoikis sensitivity to tumours cells, thereby, preventing their metastatic progression.

Although the mechanism underlying anoikis resistance in HOSCC is unknown, overexpression of FAK correlates with enhanced HOSCC progression (Miyazaki *et al*., 2003). In addition, constitutively active FAK, through Tyr397 autophosphorylation, rescues epithelial cells from anoikis (Owen *et al*., 1999; Wang, 2001; Webb *et al*., 2004). Therefore, critical to the characterization of anoikis-related regulation in oesophageal carcinoma, was the use of a HOSCC cell line harboring mt p53-R175H and displaying resistance to detachment and Tyr397 dephosphorylation of FAK.

The data presented highlight that, by interacting with both major apoptotic regulators, FAK is central to anoikis-related regulation. Moreover, through delayed Fas-mediated apoptotic events and maintained FAK phosphorylation, the "hot spot" mt p53-R175H may have a significant impact on the survival of tumor cells post cell detachment, by opposing the induction of anoikis. Hence, these results strongly support the contention that enhanced FAK-dependent signalling underpins anoikis resistance in HOSCC.

References

Aas, T., Børresen, A.L., Geisler, S., Smith-Sørensen, B., Johnsen, H., Varhaug, J.E., Akslen, L.A. and Lønning, P.E. (1996) Specific P53 mutations are associated with de novo resistance to doxorubicin in breast cancer patients. *Nat. Med.* **2**: 811-814.

Abiko, Y., Arai, J., Mitamura, T. and Kaku, T. (1997) Alteration of proto-oncogenes during apoptosis in the oral squamous cell carcinoma cell line, SAS, induced by staurosporine. *Cancer Lett.* **118**: 101-107.

Anselmi, C., Ettorre, A., Andreassi, M., Centini, M., Neri, P., and Di Stefano, A. (2002). *In vitro* induction of apoptosis vs. necrosis by widely used preservatives: 2-phenoxyethanol, a mixture of isothiazolinones, imidazolidinyl urea and 1, 2-pentanediol. *Biochem. Pharmacol.* **63**: 437-453.

Aoudjit, F. and Vuori, K. (2001) Matrix attachment regulates Fas-induced apoptosis in endothelial cells: A role for c-flip and implications for anoikis. *J. Cell. Biol.* **152**: 633-643.

Aramaki, Y., Takano, S. and Tsuchiya, S. (1999) Induction of apoptosis in macrophages by cationic liposomes. *FEBS Lett.* **460**: 472-476.

Aramaki, Y., Takano, S., Arima, H. and Tsuchiya, S. (2000) Induction of apoptosis in WEHI 231 cells by cationic liposomes. *Pharmacol. Res.* **17**: 515-520.

Attwell, S., Roskelley, C., Dedhar, S. (2000) The integrin-linked kinase (ILK) suppresses anoikis. *Oncogene* **19**: 3811-3815.

Ayaki, M., Komatsu, K., Mukai, M., Murata, K., Kameyama, M., Ishiguro, S., Miyoshi, J., Tatsuta, M. and Nakamura, H. (2001) Reduced expression of focal adhesion kinase in liver metastases compared with matched primary human colorectal adenocarcinomas. *Clin. Cancer Res.* **7**: 3106-3112.

Aylon, Y. and Oren, M. (2007) Living with p53, dying of p53. *Cell* **130**: 597-601.

Azad, N. and Rojanasakul, Y. (2006) Nanobiotechnology in drug delivery. Am J *Drug Deliv.* **4**: 79-88.

Badylak, S.F., Freytes, D.O., Gilbert, T.W., 2009. Extracellular matrix as a biological scaffold material: structure and function. *Acta Biomater.* **5**: 1-13.

Barnard, D.L. (2000) Technology evaluation: Sch-58500, *Canji. Curr. Opin. Mol. Ther.* **2**: 586-592.

Barnhart, B.C., Lee, J.C., Alappat, E.C., Peter, M.E. (2003). The death effector domain protein family. *Oncogene* **22**: 8634-8644.

Belmoktar, C.A, Hillion, J and Bendirdjian S.E. (2001) Staurosporine induces apoptosis through both caspases-dependent and caspases-independent mechanisms. *Oncogene*, **20**: 3354-3362.

Bennett, M., Macdonald, K., Chan, S.W., Luzio, J.P., Simari, R. and Weissberg, P. (1998) Cell surface trafficking of Fas: A rapid mechanism of p53-mediated apoptosis. *Science* **282**: 290-293.

Bennet, M.W., O'Connell, J., O'Sullivan, G.C., Roche, D., Brady, C., Collins, J.K. and Shanahan, F. (1999). Fas ligand and Fas receptor are coexpressed in normal human esophageal epithelium: a potential mechanism of apoptotic epithelial turnover. *Dis. Esophag*. **12**: 90-98.

Beviglia, L., Golubovskaya, V., Xu, L., Yang, X., Craven. R.J. and Cance, W.G. (2003) Focal adhesion kinase N-terminus in breast carcinoma cells induces rounding, detachment and apoptosis. *Biochem J.* **373**: 201-210.

Bey, E., Alexander, J., Whitcutt, J.N., Hunt, J.A. and Gear, J.H.S (1976) Carcinoma of the oesophagus in Africans: establishment of a continuously growing cell line from a tumour specimen. *In vitro* **12**: 107-114.

Bill, H., Knudsen, B., Moores, S.L., Muthuswamy, S.K., Rao, V.R., Brugge, J.S. and Miranti, C.K. (2004) Epidermal factor receptor-dependent regulation of

integrin-mediated signalling and cell cycle entry in epithelial cells. *Mol. Cell Biol*. **24**: 8586-8599.

Bird-Lieberman, E.L. and Fitzgerald, R.C. (2009) Early diagnosis of oesophageal cancer. *Br. J. Cancer*. **101**: 1-6. Review.

Blandino, G., Levine, A.J. and Oren, M. (1999) Mutant p53 gain of function: differential effects of different p53 mutants on resistance of cultured cells to chemotherapy. *Oncogene* **18**: 477-485.

Blott, E.J., Bossi, G., Clark, R., Zvelebil, M., Griffiths, G.M. (2001) Fas ligand is targeted to secretory lysosomes via a proline-rich domain in its cytoplasmic tail. *J. Cell Sci.* **114**: 2405-2416.

Bossi, G., Lapi, E., Strano, S., Rinaldo, C., Blandino, G. and Sacchi, A. (2006) Mutant p53 gain of function: reduction of tumor malignancy of human cancer cell lines through abrogation of mutant p53 expression. *Oncogene* **25**:304-309.

Bouillet, P. and O'Reilly L.A. (2009) CD05, BIM and T cell homeostasis. *Nat. Rev. Immunol.* **9**: 514-519

Bozzo, C., Sabbatini, M., Tiberio, R., Piffanelli, V., Santoro, C. and Cannas, M. (2006) Activation of caspase-8 triggers anoikis in human neuroblastoma cells. *Neurosci. Res.* **56:** 145-153.

Bradford, M. (1976) A rapid and sensitive method for the quantification of microgram quantities of protein utilising the principle of protein-dye binding. *Anal. Biochem.* **72:** 248-254.

Bramhall, S., Noack, N., Wu, M. and Loewenberg, J. (1969) A simple colorimetric method for determination of protein. *Anal. Biochem.* **31:** 146-148.

Brosh, R. and Rotter, V. (2009) When mutants gain new powers: news from the mutant p53 field. *Nat. Rev. Cancer* **9**: 701-13.

Brunet, A., Datta, S.R., Greenberg, M.E. (2001) Transcription-dependent and -independent control of neuronal survival by the PI3K-Akt signaling pathway. *Curr. Opin. Neurobiol.* **11**: 297-305.

Buganim, Y. and Rotter V. (2009) p53: balancing tumour suppression and implications for the clinic. *Eur. J. Cancer* **45**S: 217-234.

Buyru, N., Altinisik, J., Demokan, S. and Dalay, N. (2007) p53 genotypes and haplotypes associated with risk of breast cancer. *Cancer Det. Prev*. **31**: 207-213.

Buyru, N., Tigli, H. and Dalay, N. (2003) p53 codon 72 polymorphism in breast cancer. *Oncol. Rep.* **10**: 711-714.

Cahuzac, N., Baum, W., Kirkin, V., Conchonaud, F., Wawrezinieck, L., Marguet, D., Janssen, O., Zörnig, M. and Hueber, A.O. (2006) Fas ligand is localized to membrane rafts, where it displays increased cell death-inducing activity. *Blood* **107**: 2384-2391.

Calalb, M.B., Polte, T.R. and Hanks, S.K. (1995) Tyrosine phosphorylation of focal adhesion kinase at sites in the catalytic domain regulates kinase activity: a role for Src family kinases. *Mol.Cell Biol.* **15**: 954-963.

Cantley, L.C. (2002) The phosphoinositide 3-kinase pathway. *Science* **296**:1655-1657.

Cao, L., Han, L., Zhang, Z., Li, J., Qu, Z., Du, J., Liang, X., Liu, Y., Shi, S., Gao, L. and Sun, W. (2009) Involvement of anoikis-resistance in the metastasis of hepatoma cells. *Exp. Cell Res.* **315**: 1148-1156.

Ceccarelli, D.F., Song, H.K., Poy, F., Schaller, M.D. and Eck, M.J. (2006) Crystal structure of the FERM domain of focal adhesion kinase. *J. Biol. Chem.* **281**: 252-259.

Chaigne-Delalande, B., Moreau, J-F. and Legembre, P. (2008) Rewinding the Disc. Arc. Immunol. Ther. Exp. **56**: 9-14.

Chang, M.S., Lee, H.S., Lee, B.L., Kim, Y.T., Lee, J.S. and Kim, W.H. (2005) Differential protein expression between esophageal squamous cell carcinoma and dysplasia, and prognostic significance of protein markers. *Pathol. Res. Pract.* **201**: 417-425.

Chène, P. (1998) *In vitro* analysis of the dominant negative effect of p53 mutants. *J. Mol. Biol.* **14**: 205-209.

Chin, K.V., Ueda, K., Pastan, I. and Gottesman, M.M. (1992) .Modulation of activity of the promoter of the humanMDR1 gene by Ras and p53. *Science* **255**: 459-462.

Cho, Y., Gorina, S., Jeffrey, P.D. and Pavletich, N.P. (1994) Crystal structure of a p53 tumor suppressor-DNA complex: understanding tumorigenic mutations. *Science* **265:** 346-355.

Chua, B.T., Gallego-Ortega, D., Ramirez de Molina, A., Ullrich, A., Lacal, J.C. and Downward, J. (2009) Regulation of Akt(ser473) phosphorylation by choline kinase in breast carcinoma cells. *Mol. Cance*r. **8**: 131.

Cohen, G.M., Sun, X.M., Fearnhead, H., MacFarlane, M., Brown, D.G., Snowden, R.T. and Dinsdale, D. (1994) Formation of large molecular weight fragments of DNA is a key committed step of apoptosis in thymocytes. *J. Immunol.*, **153**: 507-516.

Cohen, L.A. and Guan, J.L. (2005). Mechanisms of focal adhesion kinase regulation. *Curr. Cancer. Drug Targets* **5:** 629-643.

Cohen, L.A. and Guan, J.L. (2005) Residues within the first subdomain of the FERM-like domain in focal adhesion kinase are important in its regulation. *J. Biol. Chem.* **280**: 8197-8207.

Collins JA, Schandi CA, Young KK, Vesely J, Willingham MC. (1997) Major DNA fragmentation is a late event in apoptosis. *J. Histochem. Cytochem.* **45**: 923-934.

Cooper, L.A., Shen, T.L. and Guan, J.L. (2003) Regulation of focal adhesion kinase by its amino-terminal domain through an autoinhibitory interaction. *Mol. Cell Biol.* **23**: 8030-8041.

Crowe, D.L. and Ohannessian, A. (2004) Recruitment of focal adhesion kinase and paxillin to β1 integrin promotes cancer cell migration via mitogen activated protein kinase activation. *BMC Cancer* **4**: 18-26.

Dai, R., Iwama, A., Wang, S. and Kapila, Y.L. (2005) Disease-associated fibronectin matrix fragments trigger anoikis of human primary ligament cells: p53 and c-myc are suppressed. *Apoptosis* **10**: 503-512.

Datta, S.R., Dudek. H, Tao, X., Masters, S., Fu, H., Gotoh, Y. and Greenberg, M.E.. (1997) Akt phosphorylation of BAD couples survival signals to the cell-intrinsic death machinery. *Cell* **91**: 231-241.

Datta, S.R., Brunet, A. and Greenberg, M.E. (1999). Cellular survival: a play in three Akts. *Genes Dev.* **13**:2905-2927.

De Arcangelis, A. and Georges-Labouesse, E.G. (2000). Integrin and ECM functions: roles in vertebrate development. *Trends Genet.* **16**: 389-395.

DeNardi, F.G. and Riddell, R. H. (1991) The normal esophagus. *Am. J. Surg. Pathol.* **15**: 296-309.

Díaz-Montero, C.M., Wygant, J.N. and McIntyre, B.W. (2006) PI3-K/Akt-mediated anoikis resistance of human osteosarcoma cells requires Src activation. *Eur. J. Cancer.* **42**:1491-1500.

Dittmer, D., Pati, S., Zambetti, G., Chu, S., Teresky, A.K., Moore, M., Finlay, C., Levine, A.J. (1993). Gain of function mutations in p53. *Nat. Genet.* **4**: 42-46.

Dokka, S., Toledo, D., Shi, X., Castranova, V. and Rojanasakul, Y. (2000) Oxygen radical-mediated pulmonary toxicity induced by some cationic liposomes. *Pharmacol. Res.* **17**: 521-525.

Dong, P., Tada, M., Hamada, J., Nakamura, A., Moriuchi, T. and Sakuragi, N. (2007) p53 dominant-negative mutant R273H promotes invasion and migration of human endometrial cancer HHUA cells. *Clin. Exp. Metastasis* **24**: 471-483.

Duronio, V. (2008) The life of a cell: Apoptosis regulation by the PI3K/PKB pathway. *Biochem. J.* **415**: 333-344.

Duxbury, M.S., Ito, H., Benoit, E., Zinner, M.J., Ashley, S.W. and Whang, E.E. (2003) RNA interference targeting focal adhesion kinase enhances pancreatic adenocarcinoma gemcitabine chemosensitivity. *Biochem. Biophys. Res. Commun.* **311**: 786-792.

Duxbury, M.S., Ito, H., Zinner, M.J. and Whang, E.E. (2004) Focal adhesion kinase gene silencing promotes anoikis and suppresses metastasis of human pancreatic adenocarcinoma cells. *Surgery* **135**: 55562-55582.

Enari, M., Sakahira, H., Yokoyama, H., Okawa, K., Iwamatsu, A. and Nagata, S. (1998) A caspase-activated DNase that degrades DNA during apoptosis, and its inhibitor ICAD. *Nature* **391**:43-50.

Engelman, J.A., Luo, J., Cantley, L.C. (2006) The evolution of phosphatidylinositol 3-kinases as regulators of growth and metabolism. *Nat. Rev. Genet.* 7: 606-619.

Espinosa, J.M. and Emerson, B.M. (2001) Transcriptional regulation by p53 through intrinsic DNA/chromatin binding and site-directed cofactor recruitment. *Mol. Cell.* **8**: 57-69.

Estrugo, D., Fischer, A., Hess, F., Scherthan, H., Belka, C. and Cordes, N. (2007) Ligand bound b1integrins inhibit procaspase-8 for mediating cell adhesion-mediated drug and radiation resistance in human leukemia cells. *PLoS ONE* **2**: e269.

Fidler, I.J. (2003). The pathogenesis of cancer metastasis: the 'seed and soil' hypothesis revisited. *Nat. Rev. Cancer* **3**: 453-458.

Frazier, M.W., He, X., Wang, J., Gu, Z., Cleveland, J.L. and Zambetti, G.P. (1998) Activation of c-*myc* Gene Expression by Tumor-Derived p53 Mutants Requires a Discrete C-Terminal Domain. *Mol. Cell Biol.* **18**: 3735-3743.

Frisch, S.M. (1999) Evidence for a function of death-receptor-related, death-domain-containing proteins in anoikis. *Curr. Biol.* **9:** 1047-1049.

Frisch, S.M. and Francis, H. (1994) Disruption of epithelial cell-matrix interactions induces apoptosis. *J. Cell. Biol.* **124**: 619-626.

Frisch, S.M. and Screaton, R.A. (2001) Anoikis mechanisms. *Curr. Opin. Cell Biol*. **13**: 555-562.

Frisch, S. M., Vuori, K., Ruoslahti, E. and Chan-Hui, P.Y. (1996) Control of adhesion-dependent cell survival by focal adhesion kinase. *J. Cell Biol.* **134**: 793-799.

Fukai, F., Mashimo, M., Akiyama, K., Goto, T., Tanuma, S., Katayama, T. (1998) Modulation of apoptotic cell death by extracellular matrix proteins and a fibronectin-derived anti-adhesive peptide. *Exp. Cell Res.* **242**:92-99.

Fulda, S. and Debatin, K-M. (2003) Death receptor signalling in cancer therapy. *Curr. Med. Chem.* **3**: 253-262.

Furuyama, K., Doi, R., Mori, T., Toyoda, E., Ito, D., Kami, K. (2006). Clinical significance of focal adhesion kinase in resectable pancreatic cancer. *World J. Surg.* **30**: 219-26.

Gabriel, B., zur Hausen, A., Stickeler, E., Dietz, C., Gitsch, G., Fischer, D.C., Bouda, J., Tempfer, C. and Hasenburg, A. (2006) Weak expression of focal adhesion kinase (pp125FAK) in patients with cervical cancer is associated with poor disease outcome. *Clin. Cancer Res.* **15**: 2476-2483.

Gamieldien, W., Victor, T.C., Mugwanya, D, Stepien, A., Gelderbrlom, W.C., Marasas, W.F.O., Geiger, D.H. and van Helden, P.D. (1998) p53 and p16/CDKN2 gene mutations in esophageal tumors from a high-incidence area in South Africa. *Int. J. Cancer* **78**: 544-549.

Gavrieli, Y., Sherman, Y. and Ben-Sasson, S.A. (1992) Identification of programmed cell death in *In situ* via specific labelling of nuclear DNA fragmentation. *J. Cell. Biol.* **119**: 493-501.

Gervais, F.G., Thornberry, N.A., Ruffolo, S.C., Nicholson, D.W. and Roy, S. (1998) Caspases cleave focal adhesion kinase during apoptosis to generate a FRNK-like polypeptide. *J. Biol. Chem.* **273**: 17102-17108.

Gilcrease, M.Z. (2007) Integrin signalling in epithelial cells. *Cancer Lett.* **247**: 1-25.

Golubovskaya, V.M., Conway-Dorsey, K., Edmiston, S.N., Tse, C.-K., Lark, A.A., Livasy, C.A., Moore, D., Millikan, R.C. and Cance, W.G. (2009) FAK overexpression and p53 mutations are highly correlated in human breast cancer. *Int. J. Cancer* **125**: 1735-1738.

Golubovskaya, V.M., Kaur, A. and Cance, W. (2004) Cloning and characterization of the promoter region of human focal adhesion kinase gene: nuclear factor kappa B and p53 binding sites. *Biochim. Biophys. Acta* **1678**: 111-125.

a. Golubovskaya, V.M., Finch, R., Kweh, F., Massoll, N.A., Campbell-Thompson, M., Wallace, M.R. and Cance, W.G. (2008) p53 regulates FAK expression in human tumour cells. *Mole. Carc*. **47**: 373-382.

b. Golubovskaya, V.M., Finch, R., Zheng, M., Kurenova, E.V. and Cance, W.G. (2008). The 7-amino-acid site in the proline-rich region of the N-terminal domain of p53 is involved in the interaction with FAK and is critical for p53 functioning. *Biochem. J.* **411**: 151-160.

c. Golubovskaya, V. M., Virnig, C. and Cance, W. G. (2008) TAE226-induced apoptosis in breast cancer cells with overexpressed Src or EGFR. *Mol. Carcinog*. **47**: 222-234.

Golubovskaya, V.M., Finch, R. and Cance, W.G. (2005) Direct interaction of the N-terminal domain of focal adhesion kinase with the N-terminal transactivation domain of p53. *J. Biol. Chem.* **280**: 25008-25021.

Gorgoulis, V.G., Vassiliou, L.V., Karakaidos, P., Zacharatos, P., Kotsinas, A., Liloglou, T., Venere, M., Ditullio, R.A., Jr., Kastrinakis, N.G., Levy, B., *et al*. (2005). Activation of the DNA damage checkpoint and genomic instability in human precancerous lesions. *Nature* **434**: 907-913.

Grace, M.P., Kim, K.H., True, L.D. and Fuchs, E. (1985) Keratin Expression in Normal Esophageal Epithelium and Squamous Cell Carcinoma of the Esophagus. *Cancer Res.* **45**: 841-46.

Gratas, C., Tohma, Y., Barnas, C., Taniere, P., Hainaut, P. and Ohgaki, H. (1998) Up-regulation of Fas (APO-1/CD95) ligand and down-regulation of Fas expression in human esophageal cancer. *Cancer Res*. **58**: 2057-2062.

Grossman, J. (2002) Molecular mechanisms of "detachment-induced apoptosis"- Anoikis. *Apoptosis*. **7**: 247-260.

Guan, J.L. and Shalloway, D. (1982) Regulation of focal adhesion-associated protein tyrosine kinase by both cellular adhesion and oncogenic transformation. *Nature* **358**: 690-692.

Gupta, G.P. and Massague, J. (2006) Cancer metastasis: building a framework, *Cell* **127**: 679-695.

Hanahan, D. and Weinberg, R.A. (2000) The hallmarks of cancer. **100**: 57-71.

Hansen, S., Midgley, C.A., Lane, D.P., Freeman, B.C., Morimoto, R.I. and Hupp, T.R. (1996) Modification of two distinct COOH-terminal domains is required for murine p53 activation by bacterial Hsp70. *J. Biol. Chem.* **271**: 30922-30928.

Harris, S.L. and Levine, A.J. (2005) The p53 pathway: positive and negative feedback loops. *Oncogene* **24**: 2899-2908.

Hollstein, M., Sidransky, D., Vogelstein. D. and Harris, C. C. (1991) p53 mutations in human cancers. *Science* **253**: 49-53.

Howlett, A.R., Bailey, N., Damsky, C., Petersen, O.W. and Bissell, M.J. (1995) Cellular growth and survival are mediated by beta 1 integrins in normal human breast epithelium but not in breast carcinoma. *J. Cell Sci.* **108**: 1945-1957.

Hresko, R.C. and Mueckler, M. (2005) mTOR.RICTOR is the Ser473 kinase for Akt/protein kinase B in 3T3-L1 adipocytes. *J. Biol. Chem.* **280**: 40406-40416.

Hsai, J., Yi, C., Chen, J., Hsu, S.S., Yang, S., Chuang, C., Wang, P. and Miaw. (2003). Prognostic significance of caspase-3 expression in primary resected eosophageal squamous cell carcinoma. *Eur. J. Surg. Oncol*. **29**: 44-48.

Hsiao, M., Low, J., Dorn, E., Ku, D., Pattengale, P., Yeargin, J. and Haas, M. (1994). Gain-of-function mutations of the p53 gene induce lymphohematopoietic metastatic potential and tissue invasiveness. *Am. J. Pathol.* **145**: 702-714.

Hughes, S.J., Nambu, Y., Soldes, O.S., Hamstra, D., Rehemtulla, A., Iannettoni, M.D., Orringer, M.B. and Beer, D.G. (1997) Fas/APO-1 (CD95) is not translocated to the cell membrane in esophageal adenocarcinoma. *Cancer Res.* **57**: 5571-5578.

Hynes, R.O. and Yamada, K.M. (1982) Fibronectins: Multifunctional modular glycoproteins. *J. Cell. Biol.* **95**: 369-377.

Hynes, R.O. and Zhao, Q. (2000) The evolution of cell adhesion. *J. Cell Biol.* **150**: F89-96.

Ichwan, S.J., Yamada, S., Sumrejkanchanakji, P., Irabhim-Auerkari, E., Eto, K. and Ikeda, M. A. (2006) Defect in Ser46 phosphorylation of p53 contributes to acquisition of p53 resistance in oral squamous cell carcinoma cells. *Oncogene* **25:** 1216-12124.

Ilic, D., Almeida, E.A.C., Schlaepfer, D.D., Dazin, P., Aizawa, S. and Damsky, C.H. (1998). Extracellular matrix survival signals transduced by focal adhesion kinase suppress p53-mediated apoptosis. *J. Cell Biol.* **143**: 547-560.

Ilic, D., Furuta, Y., Kanazawa, S., Takeda, N., Sobue, K., Nakatsuji, N., Nomura, S., Fukimoto, J., Okada, M., Yamamoto, T. and Aizawa, S. (1995) Reduced cell motility and enhanced focal adhesion contact formation in cells from FAK deficient mice. *Nature* **377**: 539-544.

Inaba, M., Tashiro, T., Kobayashi, T., Fujimoto, S., Sakurai, Y., Maruo, K., Ohnishi, Y., Ueyama, Y. and Nomura, T. (1986) Evaluation of response rates to various antitumor agents of human gastric tumors implanted in nude mouse. *Jpn. J . Cancer Res.* **77**: 190-6.

INGN 201 (2003) Ad-p53, Ad5CMV-p53, Adenoviral p53, INGN 101, p53 genetherapy - Introgen, RPR/INGN 201. *BioDrugs.* **17**: 216-22.

Inoue, H., Nojima, H. and Okayama, H. (1990) High efficiency transformation of Escherichia coli with plasmids. *Gene.* **30**: 23-8.

Isaacson C, (2005). The change of the staple diet of black South Africans from sorghum to maize (corn) is the cause of the epidemic of squamous carcinoma of the oesophagus. *Med. Hypothesis* **64**: 658-60.

Ishida, K., Nagahara, H., Kogiso, T., Aso, T., Hayashi, N.and Akaike, T. (2003) Cell adhesion aside from integrin system can abrogate anoikis in rat liver cells by down-regulation of FasL expression, not by activation of PI-3K/Akt and ERK signalling pathway. *Biochem. Biophys. Res. Commun.* **300**: 201-208.

Iwakuma, T. and Lozano, G. (2003) MDM2, an introduction. *Mol. Cancer Res.* **1**: 993-1000.

Jänicke, R.U., Sprengart, M.L., Wati, M.R. and Porter, A.G. (1998). Caspase-3 is required for DNA fragmentation and morphological changes associated with apoptosis. *J. Biol. Chem*. **273**: 9357-9360.

Jemal, A., Siegel, R., Ward, E., Hao, Y., Xu, J. and Thun, M.J. (2009) Cancer statistics, 2009. *CA Cancer J. Clin.* **59**: 225-249.

Jiang, H., Liu, L., Ye, J., Liu, H., Xing, S. and Wu, Y. (2010) Focal adhesion kinase serves as a marker of cervical lymph node metastasis and is a potential therapeutic target in tongue cancer. *J. Cancer Res. Clin. Oncol.* **136**: 1295-1302.

Jiang, X. and Wang, X. (2000) Cytochrome c promotes caspase-9 activation by inducing nucleotide binding to Apaf-1. *J. Biol. Chem.* **275**: 31199-31203.

Jin, Z., and El-Deiry, W.S. (2005) Overview of cell death signalling pathways. *Cancer Biol. Therapy*. 4**2:** 139-163.

Joerger, A.C., Ang, H.C., Veprintsev, D.B., Blair, C.M. and Fersht, A.R. (2005) Structures of p53 cancer mutants and mechanism of rescue by second-site suppressor mutations. *J. Biol. Chem.* **280**: 16030-16071.

Kaeser, M.D. and Iggo, R.D. (2004) Promoter-specific p53-dependent histone acetylation following DNA damage. *Oncogene* **23**: 4007-4013.

Kamarajan, P. and Kapila, Y.L. (2007). An altered fibronectin matrix induces anoikis of human squamous cell carcinoma cells by suppressing integrin alpha v levels and phosphorylation of FAK and ERK. *Apoptosis* **12**: 2221-2231.

Kamarajan, P., Bunek, J., Lin, Y., Nunez, G. and Kapila, Y.L. (2010) Receptor-interacting protein (RIP), shuttles between cell death and survival signaling pathways. *Mol. Biol. Cell* **21**: 481-488.

Kantak, S.S. and Kramer, R.H. (1998). E-cadherin regulates anchorage-independent growth and survival in oral squamous cell carcinoma. *J. Biol. Chem.* **273**: 16953-16961.

Katada, N., Hinder, R.A., Smyrk, T.C., Hirabayashi, N., Perdikis, G., Lund, R.J., Woodward, T. and Klingler, P.J. (1997) Apoptosis is inhibited early in the dysplasia-carcinoma sequence of Barrett esophagus. *Arch Surg.* **132**: 728-33.

Kaufman, S.H. and Hengartner, M.O. (2001) Programmed cell death: alive and well in the new millennium. *Trends Cell Biol.* **11**: 526-524.

Kayagaki, N., Kawasaki, A., Ebata, T., Ohmoto, H., Ikeda, S., Inoue, S., Yoshino, K., Okumura, K. and Yagita, H. (1995) Metalloproteinase-mediated release of human Fas ligand. *J. Exp. Med*. **182**: 1777-1783.

Kerr, J.F.K., Wylliew, A.H. and Currie, A.R. (1972) Apoptosis, a basic biological phenomena with wider implications in tissue kinetics. *Brit. J. Cancer* **26**: 239-245.

Kivinen, K., Kallajoki, M. and Taimen, P. (2005). Caspase-3 is required in the apoptotic disintegration of the nuclear matrix. *Exp. Cell Res.* **311**: 62-73.

Knippschild, U., Oren, M. & Deppert, W. (1996) Abrogation of wild-type p53 mediated growth-inhibition by nuclear exclusion. *Oncogene* **12**:1755-1765.

Ko, L.J. and Prives, C. (1996) p53: puzzle and paradigm. *Genes Dev.* **1**: 1054-1072.

Ko, C.L., Yang, C.Y., Chung, C.Y., Wen, M.C., Hsu, C.P., Miaw, J. and Hsia, J.Y. (2010) Lack of Fas-pathway gene mutations in primary resected esophageal squamous cell carcinoma. *Chang Gung Med. J.* **33**: 145-151.

Kojima, K., Konopleva, M., Samudio, I.J., Shikami, M., Cabreira-Hansen, M., McQueen, T., Ruvolo, V., Tsao, T., Zeng, Z., Vassilev, L.T. and Andreeff, M. (2005) MDM2 antagonists induce p53-dependent apoptosis in AML: implications for leukemia therapy. *Blood* **106**: 3150-3159.

Kozowski, M., Kowalczuk, O., Sulewska, A., Dziêgielewski, P., Lapuc, G. Laudañski, W., Nikliñska, W., Chyczewski, L., Nikliński, J. and Laudañski, J. (2007) Serum soluble Fas ligand (sFasL) in patients with primary squamous cell carcinoma of the esophagus. *Folia. Histochem. Cytobiol.* **45**: 199-204.

Krueger A., Fas S. C., Baumann, S. and Krammer, P. H. (2003) The role of CD95 in the regulation of peripheral T-cell apoptosis. *Immunol. Rev.* **193:** 58-69.

Kupferman, M.E., Patel, V., Sriuranpong, V., Amornphimoltham, P., Jasser, S.A., Mandal, M., Zhou, G., Wang, J., Coombes, K., Multani, A., Pathak, S., Gutkind, J.S. and Myers, J.N. (2007) Molecular analysis of anoikis resistance in oral cavity squamous cell carcinoma. *Oral Oncol.* **43**: 440-454.

Kurenova, E., Xu, L-H., Yang, X., Baldwin, A.S., Craven, R.J., Hanks, S.K., Liu, Z-G. and Cance, W.G. (2004) Focal adhesion kinase suppresses apoptosis by binding to the death domain of receptor-interacting protein. *Mol. Cell Biol.* **24**: 4361-4371.

Kurihara, A., Nagoshi, H., Yabuki, M., Okuyama, R., Obinata, M. and Ikawa, S. (2007) Ser46 phosphorylation of p53 is not always sufficient to induce apoptosis: multiple mechanism of regulation of p53-dependent apoptosis. *Genes to Cells* **12**: 853-861.

Laemmli, U.K. (1970). Cleavage of structured proteins during the assembly of the head bacteriophage P4. *Nature (Lond.)* **227**: 680-685.

Lark, A.L., Livasy, C.A., Dressler, L., Moore, D.T., Millikan, R.C., Geradts, J., Iacocca, M., Cowan, D., Little, D., Craven, R.J. and Cance, W. (2005) High focal adhesion kinase expression in invasive breast carcinomas is associated with an aggressive phenotype. *Mod. Pathol.* **18**: 1289-1294.

Lee, S.H., Shin, M.S., Park, W.S., Kim, S.Y., Kim, H.S., Han, J.Y., Park, G.S., Dong, S.M., Pi, J.H., Kim, C.S., Kim, S.H., Lee, J.Y. and Yoo, N.J. (1999) Alterations of Fas (APO-1/CD95) gene in nonsmall cell lung cancer. *Oncogene* **18**: 3754-3760.

Lee, J.W. and Juliano, R.L. (2000) Alpha5beta1 integrin protects intestinal epithelial cells from apoptosis through a phosphatidylinositol 3-kinase and protein kinase B-dependent pathway. *Mol. Biol. Cell* **11**: 1973-1987.

Legembre, P., Daburon, S., Moreau, P., Moreau, J.F. and Taupin, J.L. (2006) Modulation of Fas-mediated apoptosis by lipid rafts in T lymphocytes. *J. Immunol.* **176**: 716-720.

Lerut, T. (1999). Treatment of oesophageal cancer. *Chest* **116**: 463S-465S.

Leu, C-M., Chungming, C. and Hu, C-P. (2000) Epidermal growth factor (EGF) suppresses staurosporine-induced apoptosis by inducing mcl-1 via the mitogen-activated protein kinase pathway. *Oncogene* **19**: 1665-1675.

Levkau, B., Herren, B., Koyama, H., Ross, R. and Raines, E.W. (1998) Caspase-mediated cleavage of focal adhesion kinase pp125FAK and disassembly of focal adhesions in human endothelial cell apoptosis. *J. Exp. Med.* **187**: 579-586.

Levine, A.J., Momand, J. and Finlay, C.A. (1991). The p53 tumour suppressor gene. *Nature* **351**: 453-456.

Li, L., Tang, J., Jia, L. and Li, P. (2004). Mutations of p53 gene exons 4-8 in human eosphageal cancer. *World J. Gast.* **11**: 2998-3001.

Li, P., Nijhawan, K., Budihardjo, I., Srinivasula, S.M., Ahmad, M., Alnemri, E.S. and Wang, X. (1997) Cytochrome c and dATP-dependent formation of Apaf-1/caspases-9 complex initiates an apoptotic protease cascade. *Cell* **89**: 175-184.

Lim, S-T., Chen, X.L., Lim, Y., Hanson, D.A., Vo, T-T., Howerton, K., Larocque, N., Fisher, S.J., Schlaepfer, D.D. and Ilic, D. (2008) Nuclear FAK promotes cell proliferation and survival through FERM-enhanced p53 degradation. *Mol. Cell* **29**: 9-22.

Lin, D-C, Du, X-L. and Wang, M-R. (2009) Protein alterations in ESCC and clinical implications: a review. *Dis Esophagus* **22**: 9-20.

Lin-Lee, Y.C., Tatebe, S., Savaraj, N., Ishikawa, T., Tien Kuo, M. (2001) Differential sensitivities of the MRP gene family and gamma-glutamylcysteine synthetase to prooxidants in human colorectal carcinoma cell lines with different p53 status. *Biochem Pharmacol.* **61**: 555-563.

Lobo, M. and Zachary, I. (2000) Nuclear localization and apoptotic regulation of an amino-terminal domain focal adhesion kinase fragment in endothelial cells. *Biochem. Biophys. Res. Commun.* **276**: 1068–1074.

Liu, W., Ahmad, S.A., Reinmuth, N., Shaheen, R.M., Jung, Y.D., Fan, F. and Ellis, L.M. (2000) Endothelial cell survival and apoptosis in the tumor vasculature. *Apoptosis* **5**: 323-328.

Liu, Z., Li, H., Derouet, M., Berezkin, A., Sasazuki, T., Shirasawa, S. and Rosen, K. (2006) Oncogenic Ras inhibits anoikis of intestinal epithelial cells by preventing the release of a mitochondrial pro-apoptotic protein Omi/HtrA2 into the cytoplasm, *J. Biol. Chem.* **281:**14738-14747.

Liu, G., Meng, X., Jin, Y., Bai, J., Zhao, Y., Cui, X., Chen, F. and Fu, S. (2008) Inhibitory role of focal adhesion kinase on anoikis in the lung cancer cell A549. *Cell Biol. Int.* **32**: 663-670.

Luo, M. and Guan, J-L. (2010) Focal adhesion kinase: A prominent determinant in breast cancer initiation, progression and metastasis. *Cancer Lett.* **289**: 127-139.

Lv, H., Zhang, S., Wang, B., Cui, S. and Yan, J. (2006) Toxicity of cationic lipids and cationic polymers in gene delivery. *J. Control Release* **114**: 100-109.

Mahidhara, R.S., De Oliveira, P.E.Q., Kohout, J., Beer, D.G., Lin, J., Watkins, S.C., Robbins, P.D. and Hughes, S.J. (2004) Altered trafficking of Fas and subsequent resistance to Fas-mediated apoptosis occurs by a wild-type p53 independent mechanism in esophageal adenocarcinoma. *J. Surg. Res.* **123**: 302-311.

Majumder, P.K. and Sellers, W.R. (2005) Akt-regulated pathways in prostate cancer. *Oncogene* **24**: 7465-7474.

Marconi, A., Atzei, P., Panza, C., Fila, C., Tiberio, R., Truzzi, F., Wachter, T., Leverkus, M. and Pincelli C. (2004) FLICE/caspase-8 activation triggers anoikis induced by beta1-integrin blockade in human keratinocytes, *J. Cell Sci.* **117**: 5815-5823.

Martin, S.J. and Green, D.R. (1995) Protease activation during apoptosis: death by a thousand cuts? *Cell* **82**: 349-352.

Martin, K.H., Boerner, S.A. and Parsons, J.T. (2002) Regulation of focal adhesion targeting and inhibitory functions of the FAK related protein FRNK using a novel estrogen receptor "switch". *Cell Motil Cytoskeleton.* **51**: 76-88.

Mawji, I.A., Simpson, C.D., Gronda, M., Williams, M.A., Hurren, R., Henderson, C.J., Datti, A., Wrana, J.L. and Schimmer, A.D. (2007) A chemical screen identifies anisomycin as an anoikis sensitizer that functions by decreasing FLIP protein synthesis, *Cancer Res.* **67**: 8307-15.

Mawji, I.A., Simpson, C.D., Hurren, R., Gronda, M., Williams, M.A., Filmus, J., Jonkman, J., Da Costa, R.S., Wilson, B.C., Thomas, M.P., Reed, J.C., Glinsky, G.V. and Schimmer, A.D. (2007) Critical role for Fas-associated death domain-like interleukin-1-converting enzyme-like inhibitory protein in anoikis resistance and distant tumor formation. *J. Natl. Cancer Inst.* **99**: 811-822.

McCabe, M.L. and Dlamini, Z. (2005) The molecular mechanisms of oesophageal cancer. *Int. Immunopharm.* **5**: 1113-1130.

McKeague, A.L., Wilson, D.J. and Nelson, J. (2003) Staurosporine-induced apoptosis and hydrogen peroxide-induced necrosis in two human breast cell lines. *Br. J. Cancer*. **88**: 125-131.

McLean, G.W., Brown, K., Arbuckle, M.I., Wyke, A.W., Pikkarainen, T., Ruoslahti, E. and Frame, M.C. (2001) Decreased focal adhesion kinase suppresses papilloma formation during experimental mouse skin carcinogenesis. *Cancer Res.* **61**: 8385-8389.

McLean, G.W., Komiyama, N.H., Serrels, B., Asano, H., Reynolds, L., Conti, F., Hodivala-Dilke, K., Metzger, D., Chambon, P., Grant, S.G. and Frame, M.C. (2004) Specific deletion of focal adhesion kinase suppresses tumor formation and blocks malignant progression. *Genes Dev.* **18**: 2998-3003.

Meredith, J.E. Jr, Fazeli, B. and Schwartz, M.A. (1993) The extracellular matrix as a cell survival factor. *Mol. Biol. Cell* **4**: 953-961.

Middeler, G., Zerf, D., Jenovai, S., Thu È lig, A., Tschodrich-Ro Ètter, M., Kubitscheck, U. & Peters, R. (1997) The tumor suppressor p53 is subject to both nuclear import and export, and both are fast, energy-dependent and lectin-inhibited. *Oncogene* **14**: 1407-1417.

Miller, S.E. and Veale, R.B. (2001) Environmental modulation of alpha(v), alpha(2) and beta(1) integrin subunit expression in human oesophageal squamous cell carcinomas. *Cell Biol. Int.* **25**: 61-9.

Milner. J. and Medcalf, E.A. (1991) Cotranslation of activated mutant p53 with wild type drives the wild-type p53 protein into the mutant conformation. *Cell* **65**: 765-774.

Mitra, S.K., Hanson, D.A., and Schlaepfer, D.D. (2005). Focal adhesion kinase: in command and control of cell motility. Nat. Rev. Mol. Cell Biol. **6**: 56-68.

Mitra, S.K. and Schlaepfer, D.D. (2006) Integrin-regulated FAK-Src signaling in normal and cancer cells. *Curr. Opin. Cell Biol.* **18**: 516-23.

Miyashita, T. and Reed, J.C. (1995) Tumor suppressor p53 is a direct transcriptional activator of the human Bax gene. *Cell* **80**: 293-299.

Miyazaki, T., Kato, H., Nakajima, M., Sohda, M., Fukai, Y., Masuda, N., Manda, R., Fukuchi, M., Tsukada, K. and Kuwano, H. (2003) FAK overexpression is correlated with tumour invasiveness and lymph node metastasis in oesophageal squamous cell carcinoma. *Br. J. Cancer* **89**: 140-145.

Moll, U.M., Ostermeyer, A.G., Haladay, R., Winkfield, B., Frazier, M. and Zambetti, G. (1996) Cytoplasmic sequestration of wild-type p53 protein impairs the G1 checkpoint after DNA damage. *Mol. Cell. Biol.* **16:** 1126-1137.

Montesano, R., Hollstein, M. and Hainaut, P. (1996) Genetic alterations in esophageal cancer and their relevance to etiology and pathogenesis: a review. *Int. J. Cancer* **69**: 25-235.

Mooney, L.M., Al-Sakkaf, K.A., Brown, B.L. and Dobson, P.R.M. (2002) Apoptotic mechanisms in T47D and MCF-7 human breast cancer cells. *Brit. J. Cancer* **87:** 909-917.

Muller, M., Wilder, S., Bannasch, D., Israeli, D., Lehlbach, K., Li-Weber, M., Friedman, S.L., Galle, P.R., Stremmel, W., Oren, M. and Krammer, P.H. (1998) p53 activates the CD95 (APO-1/Fas) gene in response to DNA damage by anticancer drugs. *J. Exp. Med.* **188**: 2033-2045.

Munsch, D., Watanabe-Fukunaga, R., Bourdon, J. C., *et al.* (2000) Human and mouse Fas (APO-1/CD95) death receptor genes each contain a p53-responsive element that is activated by p53 mutants unable to induce apoptosis. *J. Biol. Chem.* **275:** 3867-3872.

Muppidi, J.R. and Siegel, R.M. (2004) Ligand-independent redistribution of Fas (CD95) into lipid rafts mediates clonotypic T cell death. *Nat. Immunol.* **5**: 182-9.
Nagaprashantha, L.D., Vatsyayan, R., Lelsani, P.C., Awasthi, S., Singhal, S.S. (2010) The sensors and regulators of cell-matrix surveillance in anoikis resistance of tumors. *Int. J. Cancer.* [Epub ahead of print]
Nagata, S. (1999) Fas ligand-induced apoptosis. *Annu. Rev. Genet.* **33**: 29-55.
Nagata, S. and Goldstein, P. (1999) The Fas death factor. *Science* **267**: 1449-1456.
Nicholls, C.D., McLure, K.G., Shields, M.A., Lee, P.W. (2002). Biogenesis of p53 involves cotranslational dimerization of monomers and posttranslational dimerization of dimers. Implications on the dominant negative effect. *J. Biol. Chem.* **12**: 12937-12945.
Nicholson, D.W., Ali, A., Thornberry, N.A., Vaillancourt, J.P., Ding, C.K., Gallant, M., Gareau, Y., Griffin, P.R., Labelle, M., Lazebnik, Y.A., Munday, N.A., Raju, S.M., Smulson, M.E., Yamin, T.T., Yu, V.L. and Miller, D.K. (1995) Identification and inhibiton of ICE/ CED-3 nessessary for mammalian apoptosis. *Nature* **276**: 37-43.
Oda, K., Arakawa, H., Tanaka, T., Matsuda, K., Tanikawa, C., Mori, T., Nishimori, H., Tamai, K., Tokino, T., Nakamura, Y. and Taya, Y. (2000) p53AIP1, a potential mediator of p53-dependent apoptosis, and its regulation by Ser-46-phosphorylated p53. *Cell* **102**: 849-62.
Ogretmen, B. and Safa, A.R. (1997) Expression of the mutated p53 tumor suppressor protein and its molecular and biochemical characterization in multidrug resistant MCF-7/Adr human breast cancer cells. *Oncogene* **14**: 499-506.
Oktay, M.H., Oktay, K., Hamele-Bena, D., Buyuk, A., Koss, L.G. (2003) Focal adhesion kinase as a marker of malignant phenotype in breast and cervical carcinomas. *Hum. Pathol.* **34**: 240-245
Orford, K., Orford, C.C. and Byers, S.W. (1999) Exogenous expression of beta-catenin regulates contact inhibition, anchorage independent growth, anoikis, and radiation-induced cell cycle arrest. *J. Cell Biol.* **146**: 855-68.
Orgad, S., Goldfinger, N., Cohen, G., Rotter, V. and Solomon, B. (2005) Single chain antibody against the common epitope of mutant p53 restores wild-type activity to mutant p53 protein. *FEBS Lett.* **579**: 5609-5615.
Ossovskaya, V., Limb, S-T., Otac, N., Schlaepfer, D.D. and Ilic D. (2008) FAK nuclear export signal sequences. *FEBS Lett.* **582**: 2402-2406.
Owen, J. D., Ruest, P. J., Fry, D. W. and Hanks, S. K. (1999) Induced focal adhesion kinase (FAK) expression in FAK-null cells enhances cell spreading and migration requiring both auto- and activation loop phosphorylation sites and inhibits adhesion-dependent tyrosine phosphorylation of Pyk2. *Mol. Cell. Biol.* **19**: 4806-4818.
Owen-Schaub, L.B., Zhang, W., Cusack, J.C., Angelo, L.S., Santee, S.M., Fujiwara, T., Roth, J.A., Deisseroth, A.B., Zhang, W.W. and Kruzel, E. (1995). Wild-type human p53 and a temperature-sensitive mutant induce Fas/APO-1 expression. *Mol. Cell Biol.* **15**: 3032-3040.
Papoff, G., Hausler, P., Eramo, A., Pagano, M.G., Di Leve, G., Signore, A., Ruberti, G. (1999). Identification and characterization of a ligand-independent oligomerization domain in the extracellular region of the CD95 death receptor. *J. Biol. Chem.* **274**: 38241-38250.
Parsons, J.T. (2003). Focal adhesion kinase: the first ten years. *J. Cell Science* **116**: 1409-1416.
Pavletich, N.P., Chambers, K.A. and Pabo, C.O. (1993) The DNA-binding domain of p53 contains the four conserved regions and the major mutation hot spots. *Genes. Dev.* **7**: 2556-2564.

Peled, A., Zipori, D. and Rotter, V. (1996) Cooperation between p53-dependent and p53-independent apoptotic pathways in myeloid cells. *Cancer Res.* **56**: 2148-2156.

Peng, Y., Chen, L., Li, C., Lu, W., Agrawal, S. and Chen, J. (2001) Stabilization of the MDM2 oncoprotein by mutant p53. *J. Biol. Chem.* **276** :6874-6878.

Persad, S., Attwell, S., Gray, V., Mawji, N., Deng, J.T., Leung, D., Yan, J., Sanghera, J., Walsh, M.P. and Dedhar, S. (2001) Regulation of protein kinaseB/Akt-serine 473 phosphorylation by integrin-linked kinase: Critical roles for kinase activity and amino acids arginine 211 and serine 343. *J. Biol. Chem.* **276**: 27462-27469.

Peter, M.E. and Krammer, P.H. (2003) The CD95 (APO-1/Fas) DISC and beyond. *Cell Death Differ.* **10**: 26-35.

Petitjean, A., Mathe, E., Kato, S., Ishioka, C., Tavtigian, S.V., Hainaut, P. and Olivier, M. (2007) Impact of mutant p53 functional properties on TP53 mutation patterns and tumor phenotype: lessons from recent developments in the IARC TP53 database. *Hum Mutat.* **28:** 622-629.

Pickens, A. and Orringer, M. (2003). Geographical distribution and racial disparsity in esophageal cancer. *Ann. Thorac. Surg.* **76**: 1367-1369.

Pim, D. and Banks, L. (2004) p53 polymorphic variants at codon 72 exert different effects on cell cycle progression. *Int. J. Cancer* **108**: 196-199.

Prives, C. and Hall, P.A. (1999) The p53 pathway. *J. Pathol.* **187**: 112-126.

Puiu, L., Petrakou, E., Apostolidou, A., Athanassiadou, A., Psiouri, L., Papachatzopoulou, A., Gorgoulis, V.G., Kotsinas, A., Tzoracoeleftherakis, E., Maniatis, G.M. and Voutsinas, G. (2003) Lack of Fas (APO-1/CD95) gene structural alterations or transcript variant ratio changes in breast cancer. *Cancer Lett.* **194**: 91-97.

Qiao, L., Koutsos, M., Tsai, L.L., Kozoni, V., Guzman, J., Shiff, S.J. and Rigas, B. (1996) Staurosporine inhibits the proliferation, alters the cell cycle distribution and induces apoptosis in HT-29 human colon adenocarcinoma cells. *Cancer Lett.* **107**: 83-89.

Recher, C., Ysebaert, L., Beyne-Rauzy, O., Mansat-De Mas, V., Ruidavets, J.B., Cariven, P. (2004). Expression of focal adhesion kinase in acute myeloid leukemia is associated with enhanced blast migration, increased cellularity, and poor prognosis. *Cancer Res.* **64**: 3191-3197.

Rehman, A., Chahal, M.S., Tang, X., Bruce, J.E., Pommier, Y. and Daoud, S.S. (2005) Proteomic identification of heat shock protein 90 as a candidate target for p53 mutation reactivation by PRIMA-1 in breast cancer cells. *Breast Cancer Res.* **7**: R765-74.

Riedl, S.J. and Shi, J. (2004) Molecular mechanisms of caspases regulation during apoptosis. *Nature* **5**: 987-996.

Rigberg, D.A., Centeno, J., Kim, F.S., Ke, B., Swenson, K., Maggard, M. and McFadden, D.W. (1999) Irradiation-induced up-regulation of Fas in esophageal squamous cell carcinoma is not accompanied by Fas Ligand-Mediated apoptosis. *J. Surg. Oncol.* **71:** 91-96.

Robert, V., Michel, P., Flaman, J.M., Chiron, A., Martin, C., Charbonnier, F., Paillot, B. and Frebourg, T. (2000) High frequency in esophageal cancers of p53 alterations inactivating the regulation of genes involved in cell cycle and apoptosis. *Carcinogenesis.* **21**: 563-5.

Roberts, W. G., Ung, E., Whalen, P., Cooper, B., Hulford, C., Autry, C., Richter, D., Emerson, E., Lin, J., Kath, J., Coleman, K., Yao, L., Martinez-Alsina, L., Lorenzen, M., Berliner, M., Luzzio, M., Patel, N., Schmitt, E., LaGreca, S., Jani, J., Wessel, M., Marr, E., Griffor, M. and Vajdos, F. (2008) Antitumor activity and pharmacology of a selective focal adhesion kinase inhibitor, PF-562,271. *Cancer Res.* **68**: 1935-44.

Robinson, K.M., Haffejee, A.A. and Angorn, I.B. (1982) Tissue culture of tumour biopsies in oesophageal carcinoma and correlations with prognosis. *S. Afr. J. Surg.* **20**: 245-52.

Rodier, F., Campisi, J. and Bhaumik, D. (2007) Two faces of p53: aging and tumor suppression. *Nucleic Acids Res.* **35**: 7475-7484.

Rotter, V., Abutbul, H. & Ben-Ze'ev, A. (1983) p53 transformation-related protein accumulates in the nucleus of transformed fibroblasts in association with the chromatin and is found in the cytoplasm of non-transformed fibroblasts. *EMBO J.* **2**: 1041-1047.

Ryan, J.J., Prochownik, E., Gottlieb, C.A., Apel, I.J., Merino, R., Nun Äez, G. and Clarke, M.F. (1994) c-myc and bcl-2 modulate p53 function by altering p53 subcellular trafficking during the cell cycle. *PNAS* **91**: 5878-5882.

Rytomaa, M. and Martins, L.M. and Downward J. (1999) Involvement of FADD and caspase-8 signalling in detachment-induced apoptosis, *Curr. Biol.* **9**: 1043-1046.

Rytomaa, M., Lehmann, K. and Downward, J. (2000) Matrix detachment induces caspase-dependent cytochrome c release from mitochondria: inhibition by PKB/Akt but not Raf signalling, *Oncogene* **19**: 4461–4468.

Sanders, M.A. and Basson, M.D. (2000) Collagen IV-dependent ERK activation in human Caco-2 intestinal epithelial cells requires focal adhesion kinase. *J. Biol. Chem.* **275**: 38040-38047.

Sarbassov, D.D., Ali, S.M., Sengupta, S., Sheen, J.H., Hsu, P.P., Bagley, A.F., Markhard, A.L., Sabatini, D.M. (2006) Prolonged rapamycin treatment inhibits mTORC2 assembly and Akt/PKB. *Mol. Cell* **22**: 159-168.

Sarbassov, D.D., Guertin, D.A., Ali, S.M. and Sabatini, D.M. (2005) Phosphorylation and regulation of Akt/PKB by the rictor-mTOR complex. *Science* **307**: 1098-1101.

Scaffidi, C., Fulda, S., Srinivasan, A., Friesen, C., Li, F., Tomaselli, K.J., Debatin, K.M., Krammer, P.H. and Peter, M.E. (1998). Two CD95 (APO-1/Fas) signaling pathways. *EMBO J.* **17**: 1675-1687.

Schaller, M. D., Borgman, C. A., Cobb, B. S., Vines, R. R., Reynolds, A. B., and Parsons, J. T. (1992) pp125FAK a structurally distinctive protein tyrosine kinase associated with focal adhesions. *PNAS* **89**: 5192-5196.

Schaller, M. D., Hildebrand, J. D., Shannon, J. D., Fox, J. W., Vines, R. R. and Parsons, J. T. (1994) Autophosphorylation of the focal adhesion kinase, pp125FAK, directs SH2- dependent binding of pp60src. *Mol. Cell. Biol.* **14**: 1680-1688.

Schaller, M. D., Otey, C. A., Hildebrand, J. D. and Parsons, J. T. (1995) Focal adhesion kinase and paxillin bind to peptides mimicking beta integrin cytoplasmic domains. *J. Cell Biol.* **130**: 1181-1187.

Schaller, M. D., Hildebrand, J. D., Shannon, J. D., Fox, J. W., Vines, R. R. and Parsons, J. T. (1994) Autophosphorylation of the focal adhesion kinase, pp125FAK, directs SH2-dependent binding of pp60src. *Mol. Cell. Biol.* **14**: 1680-1688.

Sheard, M.A., Vojtesek, B., Janakova, L., Kovarik, J. and Zaloudik, J. (2000) Up-regulation of Fas (CD95) in human p53wild-type cancer cells treated with ionizing radiation. *Int. J. Cancer.* **73**: 757-762.

Schlaepfer, D.D., Hanks, S.K., Hunter, T., van der G.P. (1994) Integrin mediated signal transduction linked to Ras pathway by GRB2 binding to focal adhesion kinase. *Nature* **372**: 786–791.

Schneider, G.B., Kurago, Z., Zaharias, R., Gruman, L.M., Schaller, M.D., and Hendrix, M.J.C. (2002). Elevated focal adhesion kinase expression facilitates oral tumor cell invasion. *Cancer* **95:** 2508-2515.

Shapiro, L., Fannon, A.M., Kwong, P.D., Thompson, A., Lehmann, M.S., Grübel, G., Legrand, J.F., Als-Nielsen, J., Colman, D.R., Hendrickson, W.A. (1995). Structural basis of cell-cell adhesion by cadherins. *Nature* **374**: 327-337.

Shaulsky, G., Ben-Ze'ev, A. and Rotter, V. (1990) Subcellular distribution of the p53 protein during the cell cycle of Balb/c 3T3 cells. *Oncogene* **5**: 1707-1711.

Shibakita, M., Tachibana, M., Dhar, D.K, Ohno, S., Kubota, H.Y., Kinugasa S., Masunaga, R. and Nagasue, N. (2000) Spontaneous apoptosis in advanced eosophageal carcinoma: its relation to Fas expression. *Clinical Cancer Res.* **6**: 4755-4759.

Sieg, D.J., Hauck, C.R., Ilic, D., Klingbeil, C.K., Schaefer, E., Damsky, C.H. and Schlaepfer, D.D. (2000) FAK integrates growth-factor and integrin signals to promote cell migration. *Nat. Cell Biol*. **2**: 249-256.

Siegel, R.M., Frederiksen, J.K., Zacharias, D.A., Chan, F.K., Johnson, M., Lynch, D., Tsien, R.Y. and Lenardo, M.J. (2000) Fas preassociation required for apoptosis signaling and dominant inhibition by pathogenic mutations. *Science.* **288**: 2354-2357.

Siesser, P.M.F. and Hanks, S.K. (2006) The signaling and biological Implications of FAK Overexpression in Cancer. *Clin. Cancer Res.* **12**: 3233-3237.

Sigal, A. and Rotter, V. (2000) Oncogenic mutations of the p53 tumor suppressor: the demons of the guardian of the genome. *Cancer Res.* **60**: 6788-6793.

Simons, K. and Ikonen, E. (1997). Functional rafts in cell membranes. *Nature* **387**: 569-572.

Simpson, C.D., Anyiwe, K. and Schimmer, A.D. (2008) Anoikis resistance and tumor metastasis. *Cancer Lett.* **272**: 177-185.

Singer, S.J. and Nicolson, G.L. (1972). The fluid mosaic model of the structure of cell membranes. *Science* **175**: 720-731.

Shimizu, H., Saliba, D., Wallace, M., Finlan, L., Langridge-Smith, P.R.R. and Hupp, T.R. (2006) Destabilizing missense mutations in the tumour suppressor protein p53 enhance its ubiquitination *in vitro* and *in vivo*. *Biochem. J.* **397:** 355-367.

Shin, M.S., Kim, H.S. and Lee, S.H. (2002) Alterations of Fas-pathway genes associated with nodal metastasis in non-small cell lung cancer. *Oncogene* **21**: 4129-4136.

Sonoda, Y., Watanabe, S., Matsumoto, Y., Aizu-Yokota, E. and Kasahara, T. (1999) FAK is the upstream signal protein of the phosphatidylinositol 3-kinase-Akt survival pathway in hydrogen peroxide-induced apoptosis of a human glioblastoma cell line. *J. Biol. Chem.* **274**: 10566–10570.

Stennicke, H.R. and Salvesen, G.S. (1998) Properties of the caspases. *Biochim. Biophys. Acta.* **1387**: 17-31.

Stoner, G.D. and Gupta, A. (2001) Etiology and chemoprevention of esophageal squamous cell carcinoma. *Carcinogenesis* **22**: 1737-1746.

Stupack, D.G., Puente, X.S., Boutsaboualoy, S., Storgard, C.M. and Cheresh, D.A. (2001) Apoptosis of adherent cells by recruitment of caspase-8 to unligated integrins, *J. Cell Biol.* **155**: 459-470.

Suad, O., Rozenberg, H., Brosh, R., Diskin-Posner, Y., Kessler, N., Shimon, L.J., Frolow, F., Liran, A., Rotter, V. and Shakked, Z. (2009) Structural basis of restoring sequence-specific DNA binding and transactivation to mutant p53 by suppressor mutations. *J. Mol. Biol.* **385**: 249-265.

Suzuki, S. and Takahashi, K. (1999) Reduced substratum adhesion and decreased expressions of 1 and 4 integrins in human breast cancer cells with a property of anchorage-independent growth. *Int. J. Oncol.* **14**: 897-904.

Tamaoki, T., Nomoto, H., Takahashi, I., Kato, Y., Morimoto, M. and Tomita, F. (1986) Staurosporine, a potent inhibitor of phospholipids/ Ca^{++} dependent protein kinase. *Biochem. Biophys. Res. Com.* **135**: 397-402.

Takeichi, M., Inuzuka, H., Shimamura, K., Matsunaga, M. and Nose, A. (1990) Cadherin-mediated cell-cell adhesion and neurogenesis. *Neurosci. Res. Suppl.* **13**: S92-96.

Takikita, M., Hu, N., Shou, J.Z., Wang, Q.H., Giffen, C., Taylor, P.R. and Hewitt, S.M. (2009) Biomarkers of apoptosis and survival in esophageal squamous cell carcinoma. *BMC Cancer* **9**: 310.

Tanel, A. and Averill-Bates, D.A. (2007) Activation of the death receptor pathway of apoptosis by the aldehyde acrolein. *Free Radical Biol. Med.* **42**: 798-810.

Tew, W.P., Kelsen, D.P. and Ilson, D.H. (2005) Targeted therapies for esophageal cancer. *Oncologist* **10**: 590-601.

Thamilselvan, V., Craig, D. H., and Basson, M. D. (2007) FAK association with multiple signal proteins mediates pressure-induced colon cancer cell adhesion via a Src-dependent PI3K/Akt pathway. *FASEB J.* **21**:1730-1741.

Thompson, R., Tovar, C., Yang, H., Carvajal, D., Vu, B.T., Xu, Q., Wahl, G.M., Heimbrook, D.C. and Vassilev, L.T. (2004) Phosphorylation of p53 on key serine residues is dispensable for transcriptional activation and apoptosis. *J. Biol. Chem.* **17:** 53015-53022.

Toker, A. and Cantley L. C. (1997) Signalling through the lipid products of phosphoinositide-3-OH kinase. *Nature* **387**: 673-676.

Tovar, C., Rosinski, J., Filipovic, Z., Higgins, B., Kolinsky, K., Hilton, H., Zhao, X., Vu, B.T., Qing, W., Packman, K., Myklebost, O., Heimbrook, D.C. and Vassilev, L.T. (2006) Small-molecule MDM2 antagonists reveal aberrant p53 signaling in cancer: implications for therapy. *Proc. Natl. Acad. Sci. U S A.* **103**: 1888-1893.

Tsang, W., Ho, F.Y.F., Fung, K., Kong, S. and Kwok, T. (2005) p53-R175H mutant gains new function in regulation of doxorubicin-induced apoptosis. *Int. J. Cancer* **114**: 331-336.

Van Aken, E., De Wever, O., Correia da Rocha, A.S. and Mareel, M. (2001) Defective E-cadherin/catenin complexes in human cancer. *Virchows Arch.* **439**: 725-751.

Van Nimwegen, M.J. and van der Water, B. (2007) Focal adhesion kinase: A potential target in cancer therapy. *Biochem. Pharmacol.* **73**: 597-609.

Van Oijen, M.G.C.T. and Slootweg, P.J. (2000) Gain-of-function mutations in the tumor suppressor gene p53. *Clin. Cancer Res.* **6**: 2138-2145.

Veale, R. and Thornley, A. (1989). Increased single class low-affinity EGF receptors expressed by human oesophageal squamous carcinoma cell lines. *S. Afr. Med. J. Sci.*, **85:** 375-379.

Vassilev, L.T., Vu, B.T., Graves, B., Carvajal, D., Podlaski, F., Filipovic, Z., Kong, N., Kammlott, U., Lukacs, C., Klein, C., Fotouhi, N. and Liu, E.A. (2004) *In vivo* activation of the p53 pathway by small-molecule antagonists of MDM2. *Science* **303**: 844-848.

Vikhanskaya, F., Toh, W.H., Dulloo, I., Wu, Q., Boominathan, L., Ng, H.H., Vousden, K.H. and Sabapathy, K. p73 supports cellular growth through c-Jun-dependent AP-1 transactivation. *Nat. Cell Biol.* **9**: 698-705.

Vitale, M., Di Matola, T., Fenzi, G. Illario, M. and Rossi, G. (1998) Fibronectin is required to prevent thyroid cell apoptosis through an integrin-mediated adhesion mechanism. *J. Clin. Endocrinol. Metab.* **83**: 3673-3680.

Vitale, M., Di Matola, T., Bifulco, M., Casamassima, A., Fenzi, G. and Rossi, G. (1999) Apoptosis induced by denied adhesion to extracellular matrix (anoikis) in thyroid epithelial cells is p53 dependent but fails to correlate with modulation of p53 expression. *FEBS Lett.* **462**: 57-60.

Vogelstein, B., Lane, D. and Levine, A.J. (2000) Surfing the p53 network. *Nature* **408:** 307-310.

Vos, M., Adams, C.H., Victor, T.C. and van Helden, P.D. (2003) Polymorphisms and mutations found in the regions flanking exon 5 to 8 of the TP53 gene in a poalation at high risk for esophageal cancer in South Africa. *Cancer Genet. Cytogenet.* **140**: 23-30.

Vousden, K.H. (2002) Activation of the p53 tumor suppressor protein. *Biochim. Biophys. Acta* **1602**: 47-59.

Vrba, L, Junk, D.J., Novak, P. and Futscher, B.W. (2008) p53 induces distinct epigenetic states at its direct target promoters. *BMC Gen.* **9**: 486-498.

Walczak, H. and Krammer, P.H. (2000) The CD95 (APO-1/Fas) and the TRAIL (APO-2L) apoptosis systems. *Exp. Cell Res.* **256***:* 58-66.

Watanabe-Fukunaga, R., C. I. Brannan, N. Itoh, S. Yonehara, N. G. Copeland, N. A. Jenkins. and S. Nacata. (1992). The cDNA structure expression, and chromosomal assignment of the mouse Fas antigen, *J. Immunol.* **148**:1274-1279.

Watermann, D.O., Gabriel, B., Jäger, M., Orlowska-Volk, M., Hasenburg, A., zur Hausen, A., Gitsch, G., Stickeler, E. (2005) Specific induction of pp125 focal adhesion kinase in human breast cancer. *Br. J. Cancer*. **19**: 694-698.

Wang, X.W., Yeh, H., Schaeffer, L., Roy, R., Moncollin, V., Egly, J.M., Wang, Z., Freidberg, E.C., Evans, M.K., Taffe, B.G. (1995) p53 modulation of TFIIH-associated nucleotide excision repair activity. *Nat. Genet.* **10**:188-95.

Wang, X. (2001) The expanding role of mitochondria in apoptosis. *Genes Dev.* **15**: 2922-2933.

Wang, L.D., Zheng, S., Zheng, Z.Y., Casson, A.G. (2003) Primary adenocarcinomas of lower esophagus, esophagogastric junction and gastric cardia: in special reference to China. *World J. Gastroenterol.* **9**: 1156-1164.

Webb, D.J., Donais, K., Whitmore, L.A., Thomas, S.M., Turner, C.E., Parsons, J.T., Horwitz, A.F. (2004) FAK-Src signalling through paxillin, ERK and MLCK regulates adhesion disassembly. *Nat. Cell Biol.* **6**: 154-161.

Wei, M.C., Zong, W.X., Cheng, E.H., Lindsten, T., Panoutsakopoulou, V., Ross, A.J., Roth, K.A., MacGregor, G.R., Thompson, C.B. and Korsmeyer, S.J. (2001) Proapoptotic BAX and BAK: a requisite gateway to mitochondrial dysfunction and death, *Science* **292**: 727-730.

Weigelt, B., Hu, Z., He, X., Livasy, C., Carey, L.A., Ewend, M.G., Glas, A.M., Perou, C.M. and Van't Veer, L.J. (2005) Molecular portraits and 70-gene prognosis signature are preserved throughout the metastatic process of breast cancer. *Cancer Res.* **65**: 9155-9158.

Weinmann, L., Wischhusen, J., Demma, M.J., Naumann, U., Roth, P., Dasmahapatra, B. and Weller, M. (2008) A novel p53 rescue compound induces p53-dependent growth arrest and sensitises glioma cells to Apo2L/TRAIL-induced apoptosis. *Cell Death Differ.* **15**: 718-729.

Wen, L.P., Fahrni, J.A., Troie, S., Guan, J.L., Orth, K. and Rosen, G.D. (1997) Cleavage of focal adhesion kinase by caspases during apoptosis. *J. Biol. Chem.* **272**: 26056–26061.

Westhoff, M.A. and Fulda, S. (2009) Adhesion-mediated apoptosis resistance in cancer. *Drug Resist. Updat.* **12**:127-36.

Whitney, G. S., Chan, P. Y., Blake, J., Cosand, W. L., Neubauer, M. G., Aruffo, A., and Kanner, S. B. (1993) Human T and B lymphocytes express a structurally conserved focal adhesion kinase, pp125FAK. *DNA Cell Biol.* **12**: 823-830.

Willis, A., Jung, E.J., Wakefield, T. and Chen, X. (2004) Mutant p53 exerts a dominant negative effect by preventing wild-type p53 from binding to the promoter of its target genes. *Oncogene* **23**: 2330-2338.

Willis, S.N., Chen, L., Dewson, G., Wei, A., Naik, E., Fletcher, J.I., Adams, J.M. and Huang, D.C. (2005) Proapoptotic Bak is sequestered by Mcl-1 and Bcl-XL, but not Bcl-2, until displaced by BH3-only proteins, *Genes Dev.* **19**: 1294-1305.

Xia, Z., Dickens, M., Raingeaud, J., Davis, R.J. and Greenberg, M.E. (1995) Opposing effects of ERK and JNK-p38 MAP kinases on apoptosis. *Science* **270**: 1326-1331.

Xue, L-Y., Hu, N., Song, Y-M., Zou, S-M., Shou, J-Z., Qian, L-X., Ren, L-Q., Lin, D-M., Tong, T., He, Z-G., Zhan, Q., Taylor, P.R. and Lu, N. (2006) Tissue microarray analysis reveals a tight correlation between protein expression pattern and progression of oesophageal squamous cell carcinoma. *BMC Cancer* **6**: 296-311.

Yagi, T. and Takeichi, M. (2000) Cadherin superfamily genes: functions, genomic organization, and neurologic diversity. *Genes Dev.* **14**: 1169-1180.

Yamagishi, N., Ishihara, K., Saito, Y. and Hatayama, T. (2006). Hsp105 family proteins suppress staurosporine-induced apoptosis by inhibiting the translocation of Bax to mitochondria in HeLa cells. *Exp. Cell Res.* **312**: 3215-3223.

Yang, W., Zhang, Y., Tian, X., Ning, T. and Ke, Y. (2008) p53 codon 72 polymorphism and the risk of esophageal squamous cell carcinoma. *Mol. Carc.* **47**: 100-104.

Yang, X., Pater, A. and Tang, S.C. (1999) Differential Expression of Antiapoptotic Gene BAG-1 in Human Breast Normal and Cancer Cell Lines and Tissues. *Oncogene* **18**: 4546-4553.

Zalcenstein, A., Stambolsky, P., Weisz, L., Muller, M., Wallach, D., Goncharov, T.M., Krammer, P.H., Rotter, V. and Oren, M. (2003) Mutant p53 gain of function: repression of CD95 (Fas/APO1) gene expression be tumor-associated p53 mutants. *Oncogene* **22**: 5667-5676.

Zhang, Z., Vuori, K., Reed, J.C. and Ruoslahti, E. (1995) The alpha 5 beta 1 integrin supports survival of cells on fibronectin and upregulates Bcl-2 expression. *PNAS* **92**: 6161-6165.

a. Zhang, X.D., Gillespie, S.K. and Hersey, P. (2004) Staurosporine induces apoptosis of melanoma by both caspase-dependent and –independent apoptotic pathways. *Mol. Cancer Ther.* **3:** 187- 197.

b. Zhang, Y., Lu, H., Dazin, P and Kapila, Y. (2004) Squamous cell carcinoma cell aggregates escape suspension-induced p53-mediated apoptosis. Fibronectin and integrin alpha v mediate survival signals through focal adhesion kinase. *J. Biol. Chem.* **279**: 48342-48349.

Zhang, H.L., Chen, L.Q., Liu, R.L., Shi, Y.T., He, M., Meng, X.L., Bai, S.X. and Ping, Y.M. (2010) The number of lymph node metastases influences survival and International Union Against Cancer tumor-node-metastasis classification for esophageal squamous cell carcinoma. *Dis Esophagus.* **23**: 53-58.

Zhou, M., Gu, L., Yeager, A. M., *et al.* (1998) Sensitivity to Fas mediated apoptosis in pediatric acute lymphoblastic leukaemia is associated with a mutant p53 phenotype and absence of Bcl-2 expression. *Leukemia* **12:** 1756-1763.

Zimmerman, K. C., Bonzon, C. and Green, D.R. (2001) The machinery of programmed cell death. *Pharmacol. Therapeut.* **92**: 57-70.

APPENDICES

Appendix 1

1.1 Tissue culture

1.1.1 DMEM medium solution

1.37 %	DMEM
0.37 %	Sodium bicarbonate
2 %	Penicillin/Streptomycin solution (Penicillin: 500 U/ml; Streptomycin: 0.5 %)

Make up to final volume with dH_2O

1.1.2 Hams F12 medium solution

1.07 %	Hams F12 medium
0.118 %	Sodium bicarbonate
2 %	Penicillin/Streptomycin solution (Penicillin: 500 U/ml; Streptomycin: 0.5 %)

Make up to final volume with dH_2O

MIX:

3 volumes DMEM medium solution

1 volume Hams F12 medium solution

Filter sterilize

Store at 4°C

1.1.3 Phosphate buffer saline (1x)

136.9 mM	Sodium chloride
2.68 mM	Potassium chloride
10.1 mM	Disodium hydrogen phosphate dodecahydrate
1.76 mM	Potassium dihydrogen phosphate

Adjust pH between 7.2 to 7.3

Make up to final volume with dH_2O

Sterilise for 20 min at 151 lbq

Store at 4 °C

1.1.4 Trypsin:Ethylenediaminetetra-acetic acid (EDTA) solution

1.1.4a Trypsin solution

0.01 %	Trypsin

Make up to final volume with PBS

1.1.4b EDTA solution

0.004 %	EDTA

Make up to final volume with PBS

MIX:

50 %	Trypsin solution
50 %	EDTA solution

Store at 4 °C

1.2 Protein estimation

1.2.1 Coomassie Blue solution (0.25 %)

0.25 %	Coomassie brilliant blue powder
50 %	Methanol
10 %	Glacial acetic acid

Make up to final volume with dH_2O

1.2.2 Destaining solution

12 %	Glacial acetic acid
10 %	Methanol

Make up to final volume with dH_2O

1.2.3 Elution solution

66 %	Methanol
1 %	Ammonia

Make up to final volume with dH_2O

1.2.4 Example of standard curve (protein estimation)

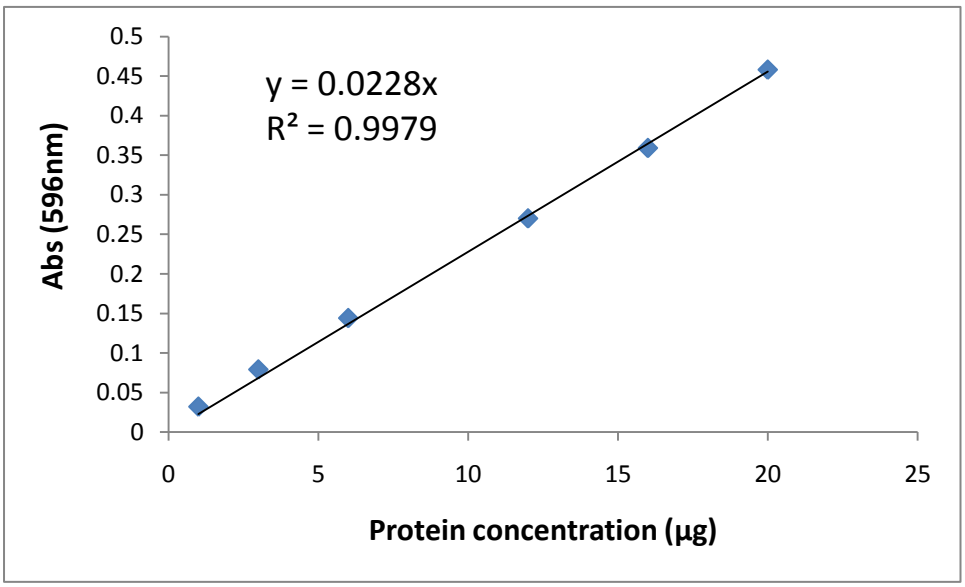

Figure A: Example of a protein estimation standard curve. The specific BSA standards, at varying concentrations, in µg, (x-axis) and their respective absorbance value at 596 nm (y-axis) were used to create the curve. The equation of the curve was used to calculate the unknown protein concentration in a given sample. R^2 = linear regression.

1.3 Sample preparation

1.3.1 Double lysis buffer

123.8 mM	Tris-HCl, pH 6.8
4 %	SDS
20 %	glycerol
10 %	β-mercaptoethanol

Make up to final volume with dH_2O

Store at 4 °C

1.3.2. RIPA buffer

50 mM	Tris-HCl (pH 7.5)
150 mM	NaCl
0.5 %	Deoxycholate
0.5 %	Triton X-100
0.05 %	SDS
1 mM	PMSF and aprotinin

Make up to final volume with dH_2O

Store at 4 °C

1.4 Electrophoresis

1.4.1 Agarose Gel (1 %)

0.3 g Agarose

Make up to 30 ml with TAE buffer (1×)

Heat until agarose dissolves

Pour gel and add:

1.5 µl EtBr

Allow gel to set for approximately 40 minutes

1.4.2 TAE Buffer (20×)

1.6 M Tris

0.8 M $NaAc.3H_2O$

40 M EDTA $Na2.2H_2O$

Adjust pH to 7.2.

Make up to 1000 ml with dH_2O

1.4.1 Separating gel

10 %	Acrylamide
0.1 %	NN’-methylenebisacrylamide
375 mM	Tris-HCl, pH 8.8
0.2 %	SDS

Make up to final volume with dH_2O

Just before use add:

1 mM	Ammonium persulphate
0.25 %	N,N,N’N’-tetramethylenediamine (TEMED)

1.4.2 Stacking gel

10 %	Acrylamide
0.1 %	NN’-methylenebisacrylamide
125 mM	Tris-HCl, pH 6.8
0.2 %	SDS

Make up to final volume with dH_2O

Just before use add:

1 mM	Ammonium persulphate
0.25 %	TEMED

1.4.3 Tracking dye

0.001 %	Bromophenol blue
50 %	Glycerol

Make up to final volume in dH_2O

Store at -20 °C

1.4.5 Running buffer

3.74 mM	SDS
25 mM	Tris pH 8.3
192.5 mM	Glycine

Make up to final volume with dH_2O

1.4.6 Destain solution

10 %	Acetic acid
10 %	Methanol

Make up to final volume with dH_2O

1.5 Western Blot

1.5.1 Transfer buffer

25 mM	Tris pH 8.3
1.41 %	Glycine
20 %	Methanol

Make up to final volume with dH_2O

Store at 4 °C

1.5.2 Blocking solution

50 mM	Tris-HCl, pH 7.8
2 mM	Calcium chloride dihydrate
5 %	non-fat milk powder
0.01 %	anti-foam
0.05 %	Triton-X 100

Make up to final volume with dH_2O

Store at 4 °C

1.5.3 SuperSignal West Pico Chemiluminescent Substrate kit

Before use MIX:

50 %	Luminol/Enhancer solution
50 %	Stable peroxide buffer

Store in the dark

1.5.4 Developer

6.4 M	Metol
0.6 M	Sodium sulphite (anhydrous)
80 mM	Hydroquinine
0.45 mM	Sodium carbonate (anhydrous)
34 mM	Potassium bromide

Make up to final volume with dH_2O

Store in the dark

1.5.5 Fixer

0.8 M	Sodium trisulphate
0.2 M	Sodium metasulphite

Make up to final volume with dH_2O

Store in the dark

1.6 Indirect immunofluorescence and confocal microscopy

1.6.1 Paraformalderhyde (4 %)

Solution A

0.14 M Sodium dihydrogen orthophosphate (anhydrous)

Make up to final volume with dH_2O

Solution B

0.63 M Sodium hydroxide

Make up to final volume with dH_2O

DISSOLVE:

4 % paraformalderhyde in

83% Solution A

17% Solution B

Make up to final volume

Heat to approximately 80 °C

Stir until solution is clear

Allow solution to cool

Adjust pH between 7.2 to 7.3

Filter and store solution at 4 °C

1.7 TUNEL assay reagents

1.7.1 Blocking solution

3 % H_2O_2

Make up to final volume with methanol

1.7.2 Permeabilisation solution

0.1 % Triton X-100

Make up to final volume with 0.1 % sodium citrate solution

1.7.3 DAB substrate solution

1 % DAB

Make up to final volume with dH_2O

Add 3-5 drops 10 N HCl until solution turns brown in colour

Store at -20 °C

1.7.3a DAB peroxide substrate working solution

0.05 % DAB substrate solution

0.015 % H_2O_2

Make up to final volume with PBS

Store at 4 °C

1.8 Competent cells preparation for electroporation

1.8.1 Luria agar plate

1 %	Sodium chloride
0.5 %	Yeast extract
1 %	Tryptone
1.5 %	Agar

Make up to final volume with dH_2O
Sterilise for 20 min at 151 lbq
Wait for solution to cool
Pour 25 ml of solution in separate petri-dishes
Allow 10 min for liquid agar in petri-dishes to set
Seal petri-dishes with parafilm
Store at 4 °C

1.8.2 Luria broth

1 %	Sodium chloride
0.5 %	Yeast extract
1 %	Tryptone

Make up to final volume with dH_2O
Sterilise for 20 min at 151 lbq
Store at 4 °C

1.9 Preparation of competent cells for heat shock transformation

1.9.1 SOB

2 % Tryptone
0.5 % Yeast extract
8.6 mM Sodium chloride
Sterilise for 20 min at 151 lbq
ADD:
2.5 mM Potassium chloride
10 mM Magnesium sulphate
0.5 mM Sodium hydroxide
Make up to final volume with dH_2O
Store at 4 °C

1.9.2 Transformation buffer (TB)

10 mM Pipes
15 mM Calcium Chloride
250 mM Potassium Chloride
Adjust pH to 6.7
Add Manganese chloride to a final concentration of 55 mM
Make up to final volume with dH_2O
Filter sterilize
Store at 4 °C

1.9.3 SOC medium

ADD:

2 % Glucose to SOB

Make up to final volume with dH_2O

Sterilise for 20 min at 151 lbq

Store at 4 °C

1.10 Mini-prep DNA plasmid extraction

1.10.1 Solution A

50 mM	Glucose
25 mM	Tris-HCl, pH 8.0
10 mM	EDTA

Make up to final volume with dH_2O

1.10.2 Solution B

0.8 %	Sodium hydroxide
1 %	SDS

Make up to final volume with dH_2O

1.10.3 Solution C

25 %	glacial acetic acid

Make up to final volume with dH_2O

Adjust pH to 4.8 with KOH

1.10.4 Mini-prep procedure (Sambrook *et al*., 1989)

- Innoculate a single colony in 5 ml of liquid broth supplemented with 0.02 % Ampicillin
- Place 1 ml of culture into Eppendorf tube
- Centrifuge Eppendorf at RT at 8000 x *g*, for 30 sec
- Discard supernatant
- Resuspend cells in 100 µl of solution A
- Add 200 µl of solution B
- Leave Eppendorf at RT for 5 min
- Add 150 µl of solution C
- Vortex briefly and incubate on ice for 5 min
- Centrifuge Eppendorf at 6000 x *g* for 20 min at 4 °C.
- Transfer supernatant into new Eppendorf tube
- Leave Eppendorf tube at RT for 5 min
- Add 230 µl of isopropanol and mix by inversion of Eppendorf tube
- Centrifuge Eppendorf at 8000 x *g* for 5 min
- Discard supernatant and dry pellet
- Add 180 µl of 99.99% ethanol and mix by inversion of Eppendorf tube
- Spin Eppendorf in centrifuge at 8000 x *g* for 1 min
- Discard supernatant and dry pellet for 15 min at 37 °C
- Add 40 µl of sterile dH_2O
- Incubate at 4 °C for 3 hours

1.11 Restriction of plasmids

1.11.1 Loading buffer

Tris-Acetate-EDTA (TAE) 20X

1 M	Tris pH 7.2
0.5 M	Sodium acetate
25.5 mM	EDTA

Make up final volume in dH_2O

Sterilise for 20 min at 151 lbq

MIX:

50 %	2X TAE (10 % of 20X TAE; Make to final volume with dH_2O)
50 %	glycerol
0.001 %	Bromophenol blue

Store at -20 °C

Appendix 2

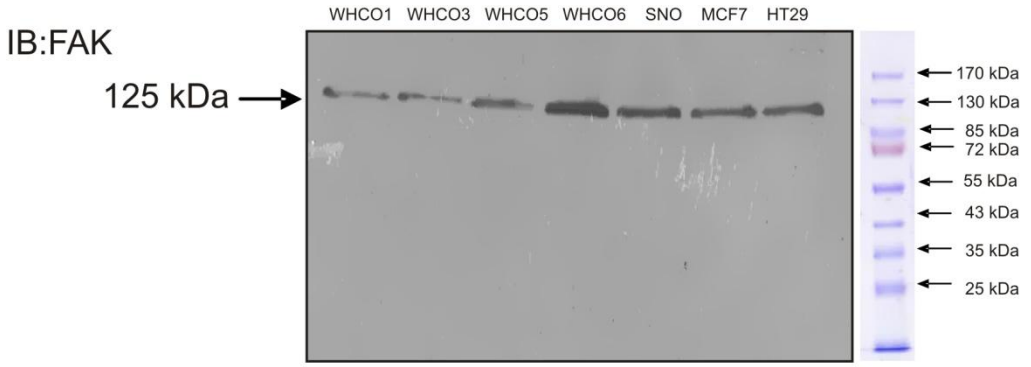

Figure B: Western blot analysis of FAK using a full gel. An entire 10% SDS-PAGE gel was electro-transferred onto nitrocellulose and probed with an anti-FAK antibody. FAK was specifically detected at 125 kDa. Non-specific binding of the anti-FAK antibody is not evident.

Appendix 3

3.1 FAK sequence trace

Chromatogram Details CO5FAKFW

Chromatogram Details

Label:	CO5FAKFW	**Format:**	ABIF
Folder:	090319061809	**Plate Label:**	23032009A1–A12
Sample Name:	27931	**Sample ID:**	27931
Instr. Model:	3100	**Instr. Name:**	3130XL–19238–017
Run Start:	2009–03–23 11:24:43	**Run Stop:**	2009–03–23 13:26:54
Lane:	3	**# Lanes:**	16
Spacing:	13.87	**Signal Strs:**	A=30,C=13,G=23,T=21
Mobility:	KB_3130_POP7_BDTv3.mob	**Matrix:**	n/a
Comment:	<ID:27931>480 bp		

Quality Graph

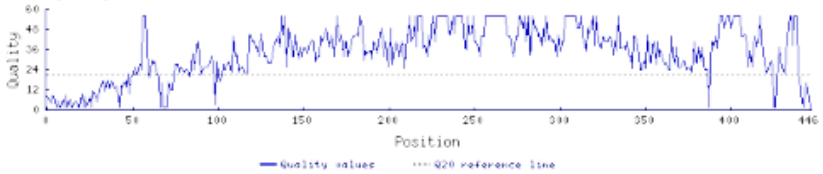

Read Length 447 b **Trimmed Length** 378 b (pos. 70–447) **Q20** 373 b

Sequence

Previous Revision:	n/a	**Current Revision:**	1	**Next Revision:**	n/a	**Latest Revision:**	1

Links: View Revision History

>CO5FAKFW CHROMAT_ID=77362

~~atctmcyycmawtyycacyscmgmtcswgaggagctcaactggatcaaagtggatatggga~~ 60
~~gtctcamgyy~~sygagggagaagtatgagcttgctcaccccccagaggagtggaaatatgaa 120
ttgagaattcgttattgccaaaaggatttctaaaccagttactgaagataagccaact 180
ttgaattttcttctatcaacaggtgaagagcgattatatgttagagatagctgatcaagtg 240
gaccaggaaattgctttgaagttgggttgtctagaaatacggcgatcatactgggagatg 300
cggggcaatgcactagaaaagaagtctaactatgaagtattagaaaaagatgttggttta 360
aagcgatttttcctaagagttactgrattctgtcaaggccaaaacactaagaaaactg 420
atccammaaacatttagacaatyatam

~~acgt~~ trimmed region(s)

Chromatogram Details CO5FAKFW

Chromatogram Trace

Label:	CO5FAKFW	**Sample Name:**	27931	**Lane:**	3
Format:	ABIF	**Sig Strs:**	A=30,C=13,G=23,T=21	**# Lanes:**	16
Source:	23032009A1–A12	**Start:**	2009–03–23 11:24:43	**Stop:**	2009–03–23 13:26:54
Comment:	<ID:27931>480 bp				

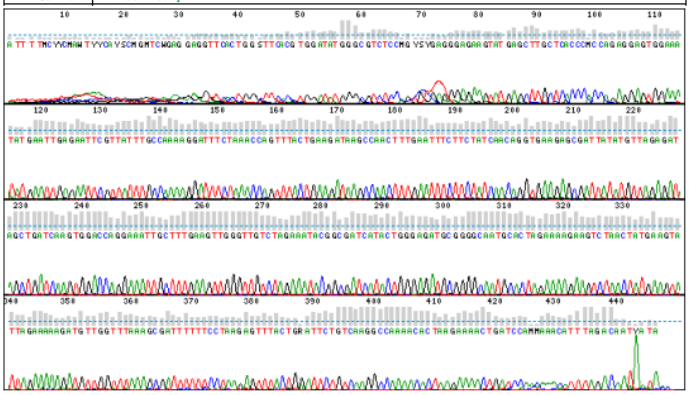

3.2 p53 sequence traces

Chromatogram Details Exon4CO1FW

Chromatogram Details

Label:	Exon4CO1FW	**Format:**	ABIF
Folder:	081030083448	**Plate Label:**	05112008A1–A12
Sample Name:	20933	**Sample ID:**	20933
Instr. Model:	3100	**Instr. Name:**	3130XL–19238–017
Run Start:	2008–11–05 12:03:58	**Run Stop:**	2008–11–05 14:06:23
Lane:	10	**# Lanes:**	16
Spacing:	14.17	**Signal Strs:**	A=136,C=160,G=181,T=110
Mobility:	KB_3130_POP7_BDTv3.mob	**Matrix:**	n/a
Comment:	<ID:20933>360 bp		

Quality Graph

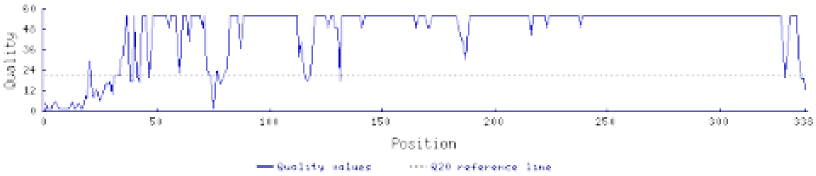

Read Length 339 b **Trimmed Length** 311 b (pos. 29–339) **Q20** 293 b

Sequence

Previous Revision:	n/a	**Current Revision:**	1	**Next Revision:**	n/a	**Latest Revision:**	1

Links: View Revision History

>Exon4CO1FW CHROMAT_ID=63361

~~grrrttwwrkkraskcyygtccttgcgt~~ccagcaatggatgatttgatgctgtccccgga 60
cgatattgaacaatgyttcactgaagacccaggtccagatgaagctcccagaatgccaga 120
ggctgctccccscgtggcccctgcaccagcagctcctacaccggcggcccctgcaccagc 180
cccctcctggcccctgtcatcttctgtcccttcccagaaaacctaccagggcagctacgg 240
tttccgtctgggcttcttgcattctgggacagccaagtctgtgacttgcacggtcagttg 300
ccctgaggggctggcttccatgagacttcaatgcctggc

~~acgt~~ trimmed region(s)

Chromatogram Details Exon4CO1FW

Chromatogram Trace

Label:	Exon4CO1FW	**Sample Name:**	20933	**Lane:**	10
Format:	ABIF	**Sig Strs:**	A=136,C=160,G=181,T=110	**# Lanes:**	16
Source:	05112008A1–A12	**Start:**	2008–11–05 12:03:58	**Stop:**	2008–11–05 14:06:23
Comment:	<ID:20933>360 bp				

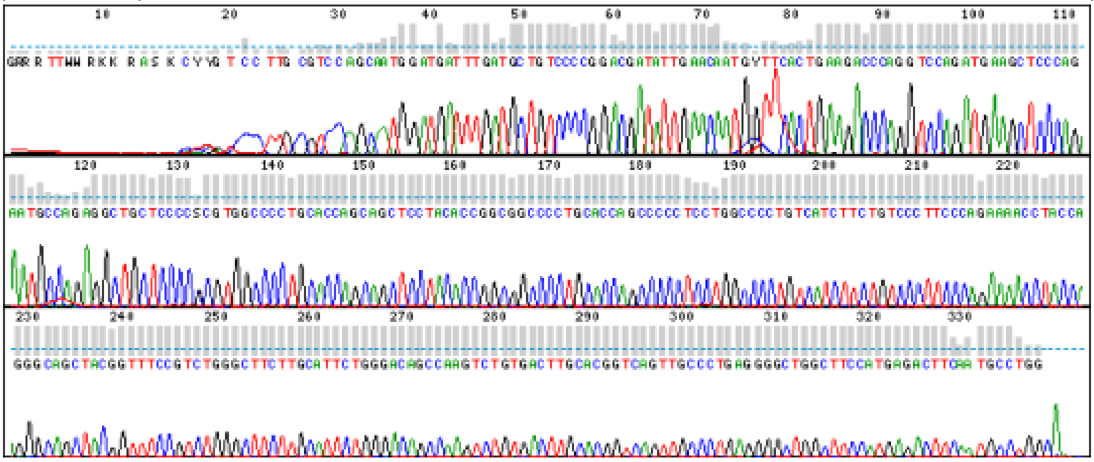

Chromatogram Details SNO_p53-Exon4-R

Chromatogram Details

Label:	SNO_p53-Exon4-R	**Format:**	ABIF
Folder:	081113071703	**Plate Label:**	12112008A1-A12
Sample Name:	21473	**Sample ID:**	21473
Instr. Model:	3100	**Instr. Name:**	3130XL-19238-017
Run Start:	2008-11-13 13:07:11	**Run Stop:**	2008-11-13 15:09:21
Lane:	3	**# Lanes:**	16
Spacing:	13.01	**Signal Strs:**	A=71,C=51,G=103,T=38
Mobility:	KB_3130_POP7_BDTv3.mob	**Matrix:**	n/a
Comment:	<ID:21473>		

Quality Graph

Read Length 336 b **Trimmed Length** 303 b (pos. 34-336) **Q20** 294 b

Sequence

Previous Revision:	n/a	**Current Revision:**	1	**Next Revision:**	n/a	**Latest Revision:**	1

Links: View Revision History

>SNO_p53-Exon4-R CHROMAT_ID=65475

~~aygkcmarggmamrvgmaccgtgmrrgtcacc~~agacttggctgtcccagaatgcaagaag 60
cccagacggaaaccgtwgctgccctggtaggtttctgggaagggacagaagatgacagg 120
ggccaggagggggctggtgcagggggccgccggtgtaggagctgctggtgcagggccacg 180
sgggggacagcctctggcattctgggagcttcatctggacctgggtcttcagtgaaccat 240
tgttccaatatcgtccgggggacagcatcaaatcatccattgcttgggacggcaagggggac 300
tgtagatgggtgaaaagagcagtcagaggaccagga

~~acgt~~ trimmed region(s)

Chromatogram Details SNO_p53-Exon4-R

Chromatogram Trace

Label:	SNO_p53-Exon4-R	**Sample Name:**	21473	**Lane:**	3
Format:	ABIF	**Sig Strs:**	A=71,C=51,G=103,T=38	**# Lanes:**	16
Source:	12112008A1-A12	**Start:**	2008-11-13 13:07:11	**Stop:**	2008-11-13 15:09:21
Comment:	<ID:21473>				

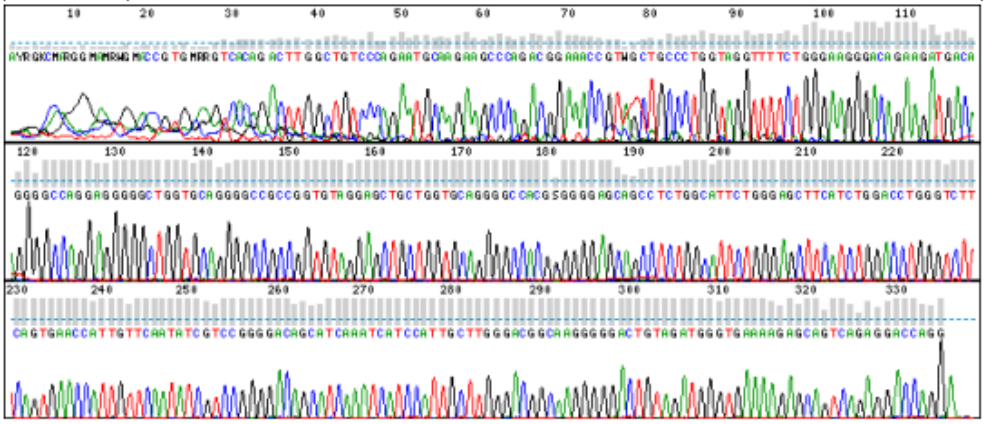

Chromatogram Details SN_p53-Exon5-Fw

Chromatogram Details

Label:	SN_p53-Exon5-Fw	**Format:**	ABIF
Folder:	081113071703	**Plate Label:**	12112008A1-A12
Sample Name:	21474	**Sample ID:**	21474
Instr. Model:	3100	**Instr. Name:**	3130XL-19238-017
Run Start:	2008-11-13 13:07:11	**Run Stop:**	2008-11-13 15:09:21
Lane:	5	**#Lanes:**	16
Spacing:	12.79	**Signal Strs:**	A=79,C=94,G=115,T=62
Mobility:	KB_3130_POP7_BDTv3.mob	**Matrix:**	n/a
Comment:	<ID:21474>		

Quality Graph

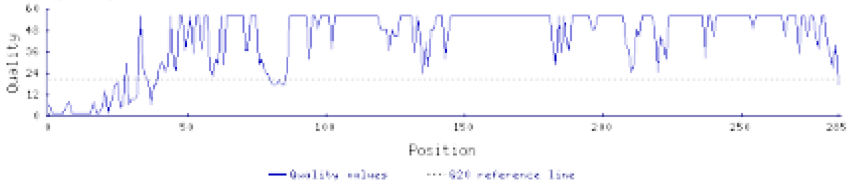

Read Length 286 b **Trimmed Length** 260 b (pos. 27-286) **Q20** 243 b

Sequence

Previous Revision:	n/a	**Current Revision:**	1	**Next Revision:**	n/a	**Latest Revision:**	1

Links: View Revision History

>SN_p53-Exon5-Fw CHROMAT_ID=65479

~~arwkwwttwrrrrrrrarmgtktctg~~tgctgactttcactctgtctccttcctcttccta 60
cagtactcccctgccctcaacaagatgttttgccaactggccaagacctgccctgtgcag 120
ctgtgggttgattccacacccccgcccggcacccgcgtccgcgccatggccatctacaag 180
cagtcacagcacatgacggaggttgtgaggcactgcccccaccatgagcgctgctcagat 240
agcgatggtgagcagctggggctggagagacgacagggctggttga

~~acgt~~ trimmed region(s)

Chromatogram Details SN_p53-Exon5-Fw

Chromatogram Trace

Label:	SN_p53-Exon5-Fw	**Sample Name:**	21474	**Lane:**	5
Format:	ABIF	**Sig Strs:**	A=79,C=94,G=115,T=62	**# Lanes:**	16
Source:	12112008A1-A12	**Start:**	2008-11-13 13:07:11	**Stop:**	2008-11-13 15:09:21
Comment:	<ID:21474>				

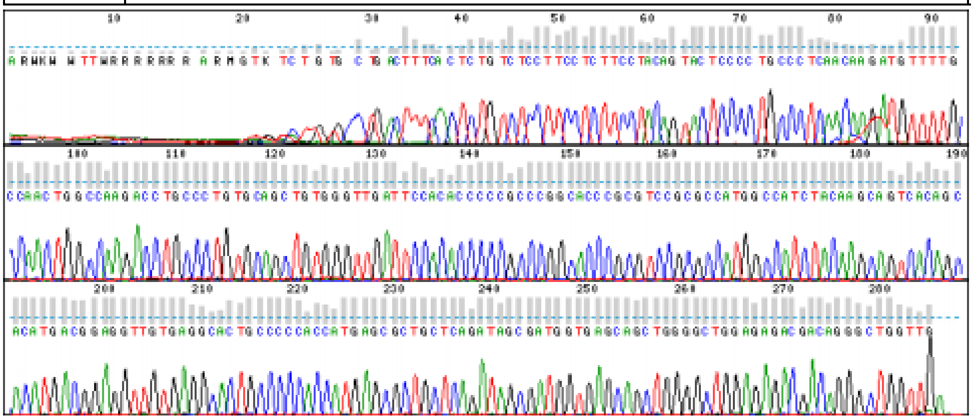

Appendix 4

4.1 Statistical results of TUNEL assay

Table 1: Paired t test analysis of apoptotic nuclei in STS-treated cells

	WHCO1		WHCO3		WHCO5		WHCO6		SNO		MCF7		HT29	
Treatment	SS	STS	SS	STS	SS	STS	SS	STS	SS	STS	SS	STS	SS	STS
Mean	**1.333**	**27.333**	**1.667**	**28.000**	**2.000**	**20.000**	**0.333**	**24.333**	**0.333**	**89.000**	**1.000**	**54.000**	**1.000**	**70.667**
SD	0.577	3.590	1.155	3.606	1.000	4.359	0.577	3.055	0.577	4.000	1.000	7.810	1.000	15.177
SEM	0.333	6.692	0.667	2.082	0.577	2.517	0.333	1.764	0.333	2.309	0.577	4.509	0.577	8.762

	WHCO1	WHCO3	WHCO5	WHCO6	SNO	MCF7	HT29
T	-3.881	-12.047	-6.971	-13.37	-13.314	-13.858	-7.934
P	0.018	<0.001	0.002	<0.001	<0.001	<0.001	0.001

*Indicates significant difference ($p < 0.05$)

4.2 Statistical results of cell detachment assay

Table 2: Paired t test analysis of the effect of STS cell detachment

	WHCO1		**WHCO3**		**WHCO5**		**WHCO6**		**SNO**		**MCF7**		**HT29**	
	SS	STS	SS	STS	SS	STS	SS	STS	SS	STS	SS	STS	SS	STS
Mean	**2.667**	**47.333**	**1.667**	**86.333**	**3.333**	**77.667**	**2.333**	**51.000**	**2.667**	**27.667**	**3.333**	**32.333**	**1.333**	**23.000**
SD	2.082	6.110	2.082	6.658	1.528	3.055	1.528	4.583	1.528	4.509	2.082	4.041	0.577	4.359
SEM	1.202	3.528	1.202	3.844	0.882	1.764	0.882	2.646	0.882	2.603	1.202	2.333	0.333	2.517

	WHCO1	WHCO3	WHCO5	WHCO6	SNO	MCF7	HT29
t	-11.985	-21.021	-37.694	-17.45	-10.186	-11.049	-8.535
P	<0.001	<0.001	<0.001	<0.001	<0.001	<0.001	0.001

*Indicates significant difference (p <0.05)

4.3 Statistical results of effect of FN on cell detachment

Table 3: One way ANOVA analysis of the effect of FN on STS-mediated cell detachment

Comparison	WHCO1	WHCO3	WHCO5	WHCO6	SNO	MCF7	HT29
30nM STS vs. FN	<0.001	<0.001	<0.001	<0.001	<0.001	<0.001	<0.001
30nM STS vs. Serum-free c	<0.001	<0.001	<0.001	<0.001	<0.001	<0.001	<0.001
FN + 30nM STS vs. FN	<0.001	<0.001	<0.001	<0.001	<0.001	<0.001	<0.001
FN + 30nM ST vs. Serum-free c	<0.001	<0.001	<0.001	<0.001	<0.001	<0.001	<0.001
30nM STS vs. FN + 30nM STS	<0.001	<0.001	0.035	0.019	0.085	0.07	0.052
Serum-free control vs. FN	0.032	0.011	0.477	0.903	0.768	0.927	0.715

*Indicates significant difference ($p < 0.05$)

4.3.1 WHCO1

One Way Repeated Measures Analysis of Variance

Normality Test (Shapiro-Wilk) Passed (P = 0.540)

Equal Variance Test: Passed (P = 0.901)

Treatment Name	N	Missing	Mean	Std Dev	SEM
Serum-free control	3	0	5.667	1.528	0.882
FN	3	0	11.667	2.082	1.202
FN + 30nM STS	3	0	24.667	3.786	2.186
30nM STS	3	0	39.667	2.082	1.202

Source of Variation	DF	SS	MS	F	P
Between Subjects	2	8.667	4.333		
Between Treatments	3	2048.250	682.750	97.536	<0.001
Residual	6	42.000	7.000		
Total	11	2098.917			

The differences in the mean values among the treatment groups are greater than would be expected by chance; there is a statistically significant difference (P = <0.001). To isolate the group or groups that differ from the others use a multiple comparison procedure.

Power of performed test with alpha = 0.050: 1.000

All Pairwise Multiple Comparison Procedures (Holm-Sidak method):
Overall significance level = 0.05

Comparisons for factor:

Comparison	Diff of Means	t	Unadjusted P	Critical Level
30nM STS vs. Serum-free c	34.000	15.739	<0.001	0.009
30nM STS vs. FN	28.000	12.961	<0.001	0.010
FN + 30nM ST vs. Serum-free c	19.000	8.795	<0.001	0.013
30nM STS vs. FN + 30nM STS	15.000	6.944	<0.001	0.017
FN + 30nM STS vs. FN	13.000	6.018	<0.001	0.025
FN vs. Serum-free control	6.000	2.777	0.032	0.050

Comparison	Significant?
30nM STS vs. Serum-free c	Yes
30nM STS vs. FN	Yes
FN + 30nM ST vs. Serum-free c	Yes
30nM STS vs. FN + 30nM STS	Yes
FN + 30nM STS vs. FN	Yes
FN vs. Serum-free control	Yes

4.3.2 WHCO3

One Way Repeated Measures Analysis of Variance

Normality Test (Shapiro-Wilk) Passed (P = 0.883)

Equal Variance Test: Passed (P = 0.795)

Treatment Name	N	Missing	Mean	Std Dev	SEM
Serum-free control	3	0	7.667	2.517	1.453
FN	3	0	20.667	5.132	2.963
FN + 30nM STS	3	0	61.333	5.132	2.963
30nM STS	3	0	88.000	4.000	2.309

Source of Variation	DF	SS	MS	F	P
Between Subjects	2	34.667	17.333		
Between Treatments	3	12300.917	4100.306	213.311	<0.001
Residual	6	115.333	19.222		
Total	11	12450.917			

The differences in the mean values among the treatment groups are greater than would be expected by chance; there is a statistically significant difference (P = <0.001). To isolate the group or groups that differ from the others use a multiple comparison procedure.

Power of performed test with alpha = 0.050: 1.000

All Pairwise Multiple Comparison Procedures (Holm-Sidak method):
Overall significance level = 0.05

Comparisons for factor:

Comparison	Diff of Means	t	Unadjusted P	Critical Level
30nM STS vs. Serum-free c	80.333	22.441	<0.001	0.009
30nM STS vs. FN	67.333	18.809	<0.001	0.010
FN + 30nM ST vs. Serum-free c	53.667	14.992	<0.001	0.013
FN + 30nM STS vs. FN	40.667	11.360	<0.001	0.017
30nM STS vs. FN + 30nM STS	26.667	7.449	<0.001	0.025
FN vs. Serum-free control	13.000	3.632	0.011	0.050

Comparison	Significant?
30nM STS vs. Serum-free c	Yes
30nM STS vs. FN	Yes
FN + 30nM ST vs. Serum-free c	Yes
FN + 30nM STS vs. FN	Yes
30nM STS vs. FN + 30nM STS	Yes
FN vs. Serum-free control	Yes

4.3.3 WHCO5

One Way Repeated Measures Analysis of Variance

Normality Test (Shapiro-Wilk) Passed (P = 0.898)

Equal Variance Test: Passed (P = 0.319)

Treatment Name	N	Missing	Mean	Std Dev	SEM
Serum-free control	3	0	6.333	3.215	1.856
FN	3	0	8.667	2.517	1.453
FN + 30nM STS	3	0	68.000	2.646	1.528
30nM STS	3	0	76.333	6.658	3.844

Source of Variation	DF	SS	MS	F	P
Between Subjects	2	50.667	25.333		
Between Treatments	3	12657.667	4219.222	296.664	<0.001
Residual	6	85.333	14.222		
Total	11	12793.667			

The differences in the mean values among the treatment groups are greater than would be expected by chance; there is a statistically significant difference (P = <0.001). To isolate the group or groups that differ from the others use a multiple comparison procedure.

Power of performed test with alpha = 0.050: 1.000

All Pairwise Multiple Comparison Procedures (Holm-Sidak method):
Overall significance level = 0.05

Comparisons for factor:

Comparison	Diff of Means	t	Unadjusted P	Critical Level
30nM STS vs. Serum-free c	70.000	22.733	<0.001	0.009
30nM STS vs. FN	67.667	21.975	<0.001	0.010
FN + 30nM ST vs. Serum-free c	61.667	20.027	<0.001	0.013
FN + 30nM STS vs. FN	59.333	19.269	<0.001	0.017
30nM STS vs. FN + 30nM STS	8.333	2.706	0.035	0.025
FN vs. Serum-free control	2.333	0.758	0.477	0.050

Comparison	Significant?
30nM STS vs. Serum-free c	Yes
30nM STS vs. FN	Yes
FN + 30nM ST vs. Serum-free c	Yes
FN + 30nM STS vs. FN	Yes
30nM STS vs. FN + 30nM STS	No
FN vs. Serum-free control	No

4.3.4 WHCO6

One Way Repeated Measures Analysis of Variance

Normality Test (Shapiro-Wilk) Passed (P = 0.959)

Equal Variance Test: Passed (P = 0.103)

Treatment Name	N	Missing	Mean	Std Dev	SEM
Serum-free control	3	0	3.667	2.082	1.202
FN	3	0	4.333	3.055	1.764
FN + 30nM STS	3	0	48.333	10.066	5.812
30nM STS	3	0	65.000	3.606	2.082

Source of Variation	DF	SS	MS	F	P
Between Subjects	2	10.667	5.333		
Between Treatments	3	8738.667	2912.889	71.239	<0.001
Residual	6	245.333	40.889		
Total	11	8994.667			

The differences in the mean values among the treatment groups are greater than would be expected by chance; there is a statistically significant difference (P = <0.001). To isolate the group or groups that differ from the others use a multiple comparison procedure.

Power of performed test with alpha = 0.050: 1.000

All Pairwise Multiple Comparison Procedures (Holm-Sidak method):
Overall significance level = 0.05

Comparisons for factor:

Comparison	Diff of Means	t	Unadjusted P	Critical Level
30nM STS vs. Serum-free c	61.333	11.747	<0.001	0.009
30nM STS vs. FN	60.667	11.620	<0.001	0.010
FN + 30nM ST vs. Serum-free c	44.667	8.555	<0.001	0.013
FN + 30nM STS vs. FN	44.000	8.427	<0.001	0.017
30nM STS vs. FN + 30nM STS	16.667	3.192	0.019	0.025
FN vs. Serum-free control	0.667	0.128	0.903	0.050

Comparison	Significant?
30nM STS vs. Serum-free c	Yes
30nM STS vs. FN	Yes
FN + 30nM ST vs. Serum-free c	Yes
FN + 30nM STS vs. FN	Yes
30nM STS vs. FN + 30nM STS	Yes
FN vs. Serum-free control	No

4.3.5 SNO

One Way Repeated Measures Analysis of Variance

Data source: Data 1 in Notebook7

Normality Test (Shapiro-Wilk) Passed (P = 0.677)

Equal Variance Test: Passed (P = 0.374)

Treatment Name	N	Missing	Mean	Std Dev	SEM
Serum-free control	3	0	3.000	1.000	0.577
FN	3	0	2.000	1.000	0.577
FN + 30nM STS	3	0	47.333	7.767	4.485
30nM STS	3	0	54.000	2.000	1.155

Source of Variation	DF	SS	MS	F	P
Between Subjects	2	38.167	19.083		
Between Treatments	3	7028.250	2342.750	148.746	<0.001
Residual	6	94.500	15.750		
Total	11	7160.917			

The differences in the mean values among the treatment groups are greater than would be expected by chance; there is a statistically significant difference (P = <0.001). To isolate the group or groups that differ from the others use a multiple comparison procedure.

Power of performed test with alpha = 0.050: 1.000

All Pairwise Multiple Comparison Procedures (Holm-Sidak method):
Overall significance level = 0.05

Comparisons for factor:

Comparison	Diff of Means	t	Unadjusted P	Critical Level
30nM STS vs. FN	52.000	16.048	<0.001	0.009
30nM STS vs. Serum-free c	51.000	15.739	<0.001	0.010
FN + 30nM STS vs. FN	45.333	13.990	<0.001	0.013
FN + 30nM ST vs. Serum-free c	44.333	13.682	<0.001	0.017
30nM STS vs. FN + 30nM STS	6.667	2.057	0.085	0.025
Serum-free control vs. FN	1.000	0.309	0.768	0.050

Comparison	Significant?
30nM STS vs. FN	Yes
30nM STS vs. Serum-free c	Yes
FN + 30nM STS vs. FN	Yes
FN + 30nM ST vs. Serum-free c	Yes
30nM STS vs. FN + 30nM STS	No
Serum-free control vs. FN	No

4.3.6 MCF7

One Way Repeated Measures Analysis of Variance

Normality Test (Shapiro-Wilk) Passed (P = 0.778)

Equal Variance Test: Passed (P = 0.488)

Treatment Name	N	Missing	Mean	Std Dev	SEM
Serum-free control	3	0	4.000	1.000	0.577
FN	3	0	4.333	2.082	1.202
FN + 30nM STS	3	0	30.000	2.000	1.155
30nM STS	3	0	37.667	7.371	4.256

Source of Variation	DF	SS	MS	F	P
Between Subjects	2	18.500	9.250		
Between Treatments	3	2728.667	909.556	50.144	<0.001
Residual	6	108.833	18.139		
Total	11	2856.000			

The differences in the mean values among the treatment groups are greater than would be expected by chance; there is a statistically significant difference (P = <0.001). To isolate the group or groups that differ from the others use a multiple comparison procedure.

Power of performed test with alpha = 0.050: 1.000

All Pairwise Multiple Comparison Procedures (Holm-Sidak method):
Overall significance level = 0.05

Comparisons for factor:

Comparison	Diff of Means	t	Unadjusted P	Critical Level
30nM STS vs. Serum-free c	33.667	9.681	<0.001	0.009
30nM STS vs. FN	33.333	9.586	<0.001	0.010
FN + 30nM ST vs. Serum-free c	26.000	7.477	<0.001	0.013
FN + 30nM STS vs. FN	25.667	7.381	<0.001	0.017
30nM STS vs. FN + 30nM STS	7.667	2.205	0.070	0.025
FN vs. Serum-free control	0.333	0.0959	0.927	0.050

Comparison	Significant?
30nM STS vs. Serum-free c	Yes
30nM STS vs. FN	Yes
FN + 30nM ST vs. Serum-free c	Yes
FN + 30nM STS vs. FN	Yes
30nM STS vs. FN + 30nM STS	No
FN vs. Serum-free control	No

4.3.7 HT29

One Way Repeated Measures Analysis of Variance

Normality Test (Shapiro-Wilk) Passed (P = 0.352)

Equal Variance Test: Passed (P = 0.149)

Treatment Name	N	Missing	Mean	Std Dev	SEM
Serum-free control	3	0	3.000	1.000	0.577
FN	3	0	2.000	1.000	0.577
FN + 30nM STS	3	0	23.000	4.583	2.646
30nM STS	3	0	29.333	3.055	1.764

Source of Variation	DF	SS	MS	F	P
Between Subjects	2	3.167	1.583		
Between Treatments	3	1742.000	580.667	56.650	<0.001
Residual	6	61.500	10.250		
Total	11	1806.667			

The differences in the mean values among the treatment groups are greater than would be expected by chance; there is a statistically significant difference (P = <0.001). To isolate the group or groups that differ from the others use a multiple comparison procedure.

Power of performed test with alpha = 0.050: 1.000

All Pairwise Multiple Comparison Procedures (Holm-Sidak method):
Overall significance level = 0.05

Comparisons for factor:

Comparison	Diff of Means	t	Unadjusted P	Critical Level
30nM STS vs. FN	27.333	10.456	<0.001	0.009
30nM STS vs. Serum-free c	26.333	10.074	<0.001	0.010
FN + 30nM STS vs. FN	21.000	8.033	<0.001	0.013
FN + 30nM ST vs. Serum-free c	20.000	7.651	<0.001	0.017
30nM STS vs. FN + 30nM STS	6.333	2.423	0.052	0.025
Serum-free control vs. FN	1.000	0.383	0.715	0.050

Comparison	Significant?
30nM STS vs. FN	Yes
30nM STS vs. Serum-free c	Yes
FN + 30nM STS vs. FN	Yes
FN + 30nM ST vs. Serum-free c	Yes
30nM STS vs. FN + 30nM STS	No
Serum-free control vs. FN No	No

Appendix 5

Information Sheet # p53-1

Plasmid	Tube color
wt	clear
V143A	green
R175H	blue
R248W	yellow
R249S	orange
R273H	purple

Reference: Baker, S.J., Markowitz, S., Fearon, E.R., Willson, J.K.V., and Vogelstein, B. Suppression of human colorectal carcinoma cell growth by wild-type p53. *Science* 249: 912-915, 1990.

All inserts can be excised with Bam HI, yielding 1.8 kb fragments, except R175G and R273H, which can be excised with Eco RI, yielding 1.3 kb fragments